The cross-sectional characteristics of glacial valleys and their spatial variability

Rebecca J Coles

PhD

Geography Department

University of Sheffield

Feb 2014

Acknowledgments

Many thanks go to my supervisors, Chris Clark for his infinite wisdom and Felix Ng for his Matlab wizardry. Also to Steve Wise for his input which contributed to Chapter 7. In addition, thanks goes to the University of Sheffield for awarding this PhD a University Studentship, the Geography Department and staff, particularly Peter Bragg for coming to my aid during computer related crises. To James; probably the only person who never doubted me. My family (Mum, Dad and Nick) for encouraging me down an academic path. And finally, to the many cafes of Sheffield, especially the Rude Shipyard and Number 9, who tolerated me buying a single coffee and spending the entire day occupying a table.

Abstract

Glacial valleys are fundamental large-scale geomorphological landscape features that dissect mountain ranges. Their cross-sectional shape is recognised as distinct from fluvial valleys. They develop into the typical glacial 'U-shaped' valley as a consequence of the intensity and duration to which the valley has been exposed to glacial processes. Factors in such 'U' development have been related to climate, lithology and tectonic settings.

This thesis presents a semi-automated GIS-based method for systematically measuring valley cross-sections over large areas such as across mountain divides and small mountain ranges like the Pyrenees. When compared to the traditional hand-drawn transect method the semi-automated method produced an equivalent of 857,781 transects; a 1,000 fold increase in data previously reported. Descriptive statistics are provided on cross-sectional area, form ratio and a measure of the tendency to a parabolic form (*b*-value) for 21,412 valleys sampled from Patagonia, the Southern Alps, New Zealand and the Pyrenees.

By measuring the actual shape and size of valley cross-sections in large quantities and relating the data to proxies for ice residence time and flux, as well as landscape characteristics such as valley floor slope, climatic effects, tectonic uplift and lithology, insights into glacial processes and valley development were gained. To further understand how relationships varied spatially, Geographical Weighted Regression (a local scale statistical technique) was used in the sample areas. Results show that more intense and prolonged glaciation yields large, wide parabolic valley cross-sections, in contrast to predominant paradigm of valley deepening. A major finding was a link between valley cross-sectional widening and the flattening of the valley longitudinal profile.

Table of Contents

List of Figures

List of Tables

1. Introduction

1.1. Introduction

Mountain landscapes are a result of tectonic uplift and erosional processes. Before the realisation that erosion unloads mountains and therefore contributes itself to uplift, tectonics and erosion were largely viewed separately, as different disciplines. It was thought that initially uplift took place which is followed by downwearing due to glacial, fluvial and hillslope erosional processes (Davis, 1899). The type of erosional process or combination of erosional processes and their intensity is dependent on climate conditions (i.e. rainfall intensity; presence of stabilising vegetation; glacial verses fluvial regimes). With changes in climate, shifts in erosional processes occur.

Current research has shown that uplift, erosion and climate are intrinsically linked. Examples of this include the hypothesis that increased erosion can change climate by accelerating uplift and mountain range height, disrupting weather patterns creating cooler, stormier conditions (Molnar & England, 1990). Mountain ranges can also deflect westerly circulation patterns (Manabe & Terpstra, 1974) and dictate monsoon patterns and intensity (Kutzbach *et al.*, 1993). In addition, chemical weathering has been attributed to global CO_2 drawdown and is therefore a control on climate (Kump *et al.*, 2000).

In the notion that uplift, climate and erosion took place in isolation, erosional processes were thought to have fluctuated between glacially dominated and fluvially dominated regimes (i.e. transitions between glaciations and interglaciations) due to Milankovitch Cycles; variations in the Earth's orbit. The more recent coupled view sees a more complex and interactive system where uplift, climate and erosion exist as a linked system with feedback mechanisms (this has been modelled by Braun *et al.*, 1999; Tomkin & Braun, 2002; Brocklehurst & Whipple, 2006; Egholm *et al.*, 2009). However, conclusions on feedback mechanisms are contradictory. For example research on the influence of erosion to uplift has proposed that greater erosion increases relief due to isostatic uplift (Molnar & England, 1990), however the 'glacial buzzsaw' theory indicates that glacial erosion limits relief (Brozović *et al.*, 1997). Whilst Macgregor *et al.* (2000), through modelling, discovered a "self-defeating" mechanism, whereby, glacial erosion

lowers the relief and hence accumulation area reducing net mass balance and the opportunity for glaciers to form.

Given the interactions mentioned above it is clear that landscapes do not evolve in the old Davisian sequence portrayed in the “geographical cycle”; tectonic uplift followed by erosion (Davis, 1899). The complex interactions between climate, uplift and erosion form the landscapes that are observed on Earth today. Feedbacks ensure that the landscape itself influences how it continues to evolve. A clue to a landscape’s evolution is the morphology of the landscape which is left behind. This is a signature of the processes which formed it and the geology which resisted these processes. Interpretation of this signature is key to unlocking the mechanisms which influence landscape evolution and the timescales involved.

1.2. Glacial landscape morphology

There are a number of ways in which the above topic can be tackled. These include numerical modelling (e.g. Braun & Sambridge, 1997) and measuring rates of uplift and downwearing (Cosmogenic isotope analysis (e.g. Fabel *et al.*, 2004) and thermochronology (e.g.Ehlers & Farley, 2003)). Another approach is using process-based studies to derive empirical and theoretical relationships. For example, erosion rates by glacial abrasion were reviewed by Hallet (1979) and used in models, such as Harbor (1992), on valley shape development. Another way to assess erosional processes, as well as erosion rates, and the approach used in this thesis, is the exploitation of landscape shape, which has a long history of investigation (e.g. McGee, 1883; Svensson, 1959). Glacial features left behind, as imprints on the landscape, can indicate past ice extent and the intensity of glaciations, and may provide an opportunity to understand the processes which created them from the examination of landscape form. By studying glacial geomorphology advances have been made in the understanding of glacial processes.

1.3. The V to U-Shaped valley paradigm

As long ago as in the 1880s geomorphologists thought to use valley shape as an indicator of the processes which operated (McGee, 1883; , 1894). It has been intuitively

known and accepted by glacial geomorphologists whether a valley has been glaciated based on its size and shape (Figure 1.1). This inference on the nature of the processes from the observed valley shape is a significant connection. But are fluvial and glacial valleys really different and how strong is the connection between process and shape?

Figure 1.1 Glencoe in the Scottish Highlands showing distinct glacial characteristics, such as a broad and deep U-valley form with truncated spurs, hanging valleys and a steeped longitudinal profile.

Valleys are generally categorised into two simple forms, the V-shape of fluvial valleys and a distinctive U-shape of glacially eroded valleys. It is important to note that despite geomorphologists making clear distinctions between glacial and fluvial valleys, although it is possible to observe a valley under predominately fluvial processes, a glacial valley is only generally observed after deglaciation and therefore subject to fluvial, as well as periglacial and hillslope processes. Consequently, it is not generally possible to observe a glacial valley under entirely glacial processes, as the valley is already evolving back to a fluvial form. Despite this, the imprint of an intensive or prolonged glacial episode remains marked for a substantial geological timescale. It is proposed that alpine glaciers generally exploit existing valleys created by fluvial processes, progressively modifying the valley shape into a U. The process of altering valleys to a more glacial form gives an indication of the intensity and timescale the landscape has undergone glaciation, as well

as the geological resistance to glacial erosion. Harbor (1992) modelled the evolution of the U-shaped valley from a V-shape showing that ice had the ability to rapidly modify the valley shape and enhance valley depth. Seddick *et al.* (2009) replicated these results but questioned whether all the processes are correctly constrained in the model as valley widening does not occur, yet it is clearly evident in certain landscapes (much wider and shallower glacial valleys), particularly towards the poles, and despite efforts to recreate these conditions the model fails to reproduce this landscape scenario.

A further advancement in modelling includes projects to model the evolution of whole landscapes (i.e. mountain chains) over time by incorporating the many processes which form landscapes. These landscape evolution models have helped to increase the understanding of how landscapes change over long timescales (e.g. Kooi & Beaumont, 1994). Not until more recently were glacial processes incorporated into such models and mountain ranges recreated in a modelling environment (Braun *et al.*, 1999). These alpine landscape evolution models have given insight into how a cycle of glaciations can impact a landscape (Tomkin & Braun, 2002). In order to verify whether the model outputs are valid interpretations it is important that they are compared to real landscapes. Currently few model outputs have been calibrated or tested against glacial landscapes observed around the globe today. There are a couple of notable expectations (Brocklehurst & Whipple, 2006; Egholm *et al.*, 2009). One study calibrated valley longitudinal profiles to modelled profiles in the Sierra Nevada mountains, USA (Brocklehurst & Whipple, 2006), whilst a second used a comparison of global hypsometric data to test a modelled landscape with real landscapes found around the globe (Egholm *et al.*, 2009). However these studies remain the exception. An explanation for this is that there is a lack of an accessible geomorphological dataset or method for analysing geomorphology over large areas which is efficient to apply. So, as yet, many landscape evolution models remain untested.

As one of the largest scale glacial features, together with cirques, arêtes and horns, U-shaped valleys are a fundamental relief characteristic in mountain ranges, controlling the evacuation of ice, and are evidence of huge amounts of material being exhumed, which has been shown to contribute to isostatic uplift. Their size and shape is a signature of glaciation and therefore, an indicator of the landscape's history. U-shape valleys, with their unique form, could therefore provide a geomorphological test for model outputs. If large-scale features such as U-shaped valleys can be accurately recreated by landscape evolution modelling, the combination of process physics in the

model could be concluded to be plausible, and the model outputs and outcomes would become a more reliable source for understanding the development of landscapes over long timescales. For this to happen, landscape evolution models must be rigorously tested against real landscapes, without this their true potential cannot be realised.

If it is true that valley shape records the process of erosion, and its intensity and duration, then the final valley shape we find today should contain this erosional history. Because mountain ranges and glaciations have core areas and a periphery, there should be a pattern of spatial variability. As we move away from the centre of the mountain range, valleys should change from U-shaped to V-shaped.

1.4. Valley cross-sectional profile

Although U-shaped valleys have a longitudinal profile which is distinct from a fluvial valley, the cross-sectional profile not only gives the landform its name but is easily observed (Figure 1.2). Attempts to define the cross-sectional profile started when Davis (1916) described its form as a catenary curve and then mathematically by Svensson (1959) who thought that a parabola was the best approximation. Other morphmetric studies have been used to classify the U-Shaped valley cross-profile, notable by Graf (1970) who emphasised the importance of form ratio (depth / width) as a measure.

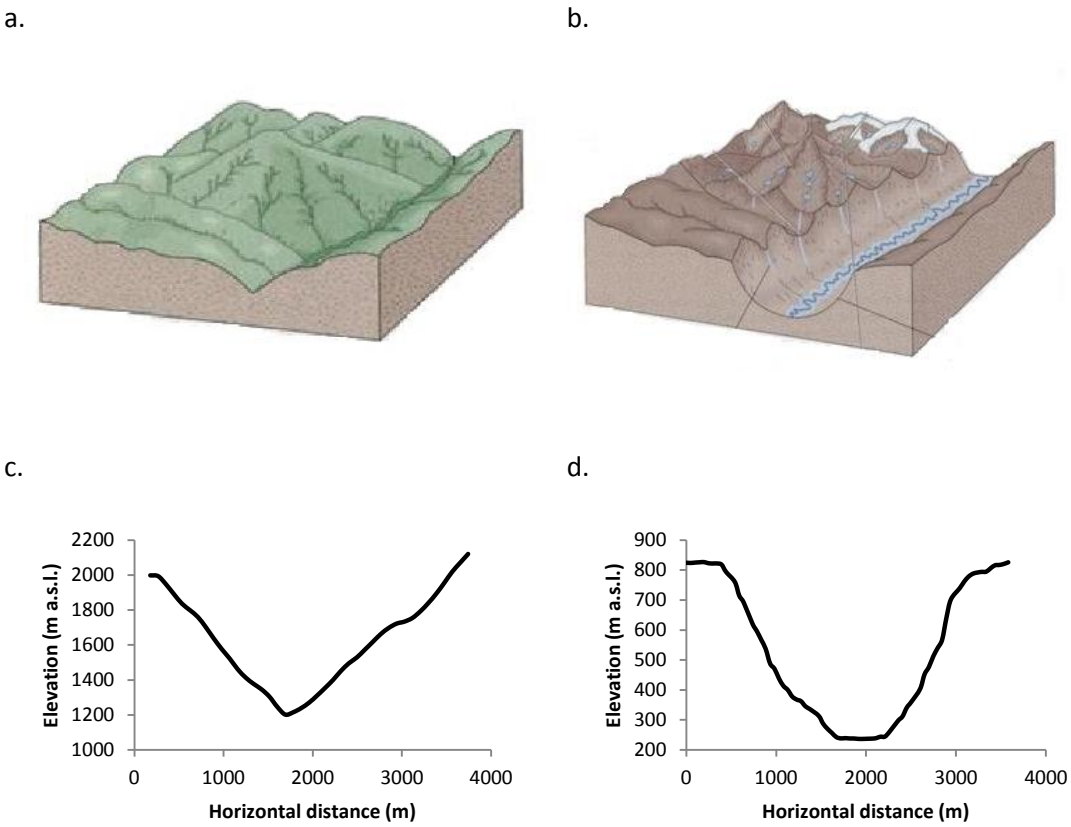

Figure 1.2 Illustrations of an idealised fluvial landscape (a) and an idealised recently deglaciated landscape (b). Cross-sectional profiles of a real V-shaped valley (c) found in fluvial landscapes and a real U-shaped valley (d) associated with glacial landscapes.

1.5. Advances in technology and availability of data

The method for measuring the cross-sectional profile of a U-shaped valley has not developed since the first cross-profiles were studied. It involves little more than extracting elevations at set points along individual transects. Developments in Geographical Information Systems (GIS) in recent years and the greater availability of Digital Elevation Models (DEMs) has created an opportunity to take a much needed step in the analysis of large-scale geomorphology and particularly valley cross-sections. Advances in computation power and the ability of software to handle large quantities of data mean that the technology has the capability to analyse many valleys; potentially whole mountain ranges. The wide accessibility of free DEM data is now a powerful resource.

1.6. Summary

As one of the largest features of a glacial landscape, U-shaped valleys are important in determining landscape history and exhumation rates and consequently isostatic uplift. U-shaped valleys are therefore integral to the evolution of a landscape and the Earth system as a whole. Advances in technology and the availability of data have presented the opportunity to examine glacial valley cross-sections over large areas and explore spatial variability in valley shape and size.

1.7. Research Aim

The aim of this thesis is to take a new data-rich approach to investigate the cross-sectional size and shape characteristics of glacial valleys and assess their spatial variability. A key aim is to derive and use a means of assessing valley shape continuously along valleys rather than sampling selected cross-sections. The main purpose is to quantify valley shape to assist comparison with simulations of Landscape Evolution Modelling and seek underlying controls.

To explore controls on valley morphology it is possible to take several approaches. One approach is to model the evolution of a landscape. The advantage here is that the drivers which control the change of the modelled landscape are known and can be systemically altered in line with the desired experiments, thus enabling comparisons to be made, e.g. the effect of two different lithologies on valley form. However, it is difficult to know whether the experiment outcomes represent the true complexity of real world landscape scenarios; whether process formulations are sufficient to capture real world behaviour and if all the important feedbacks which exist have been incorporated. Other approaches involve the study of real landscapes to deduce the processes which they have undergone. The morphology of a landscape can give clues to this. However, as often is the case when dealing with the real world, complex interactions mean that it is often difficult to isolate controlling variables. For example, when selecting two areas to make comparisons between lithology there may also be an inadvertent difference of climate as well. Then there is also the question of scale. When investigating valley cross-sections, the study of single valleys enables possible controls on erosion to be scrutinised in detail, e.g. lithological data on rock hardness and joint spacing collected in the field. Although the data collected in such studies might be of a

high quality, it is only feasible to conduct such studies over a limited sample area and it is still impossible to entirely constrain conditions unlike in modelling. Another approach using real landscapes is to take a broader-brush approach, where many hundreds of valleys are analysed over whole mountain ranges, enabling a large dataset to be collected. This approach is used in this thesis. By doing so it is hoped that common themes may become evident through the large volumes of data. When analysing a landscape characteristic, such as valley cross-section morphology across large areas, it becomes even more difficult to select sample areas which fit experimental criteria where results can be interpreted and compared. It is therefore important that any interpretations are carefully considered in the context of the mountain environments used in the experiment.

Detailed thesis objectives are outlined in Section 3.6 after the thesis motivations and founding concepts are defined.

1.8. Thesis Outline

This thesis consists of nine chapters which are divided into three principle sections:

Section A (Chapter 1 and 2) – Understanding of the research niche.

Section A includes the current chapter, **Chapter 1**, which introduces theories on the impact of large-scale geomorphology on the Earth system and highlights the inadequate research in U-shaped valleys to date. **Chapter 2** analyses in detail the developments in research in this area by reviewing the literature, and gaps in the research are discussed.

Section B (Chapters 3, 4 and 5) – Tackling the research gap.

Section B deals with the specifics of how this thesis produces results which contribute to the understanding of the V to U-shaped valley paradigm. In **Chapter 3** a strategy for the thesis is outlined. **Chapter 4**, details the semi-automated method developed for analysing valley cross-sectional profiles. The study areas the method is applied to are described and justified in **Chapter 5**.

Section C (Chapter 6, 7, 8 and 9) – Results and their implication.

Section C analyses the dataset created by the method detailed in **Chapter 4** when it is applied to the sample areas (**Chapter 5**). In Chapter 6 the results from entire sample

areas are analysed. Results are then analysed for spatial variability and patterns in **Chapter 7**. Finally, **Chapters 8 and 9** comprise the discussion of the results and conclusions drawn from them. The implications of the results are discussed and avenues for further research are suggested.

1. Introduction

2. A review of assessment and understanding of glacial valley cross-sectional shape

2.1. Introduction

This chapter reviews the relevant research on glacial valley cross-sectional shape to date. When glacial valley form is referred to here it is solely concerning valley cross-section shape and size. The chapter begins by looking at the initial observations of glacial valleys and the recognition that they might develop to an idealised form. It progresses onto research which has mathematically described valley shape and summarises the extent to which valley cross profiles have been assessed. A section touches on glacial erosion process theory in order to contextualise the modelling of individual valleys and whole landscapes in the form of landscape evolution models. Advances in data collection and manipulation are reviewed and related to specific use in the measurement of valleys. Throughout each section the literature is tackled in broadly chronological order. Finally, gaps in current research are identified and the possibility to resolve them using further advances in technology are highlighted.

2.2. Concept and basis for glacial valleys having a distinct cross-sectional shape

2.2.1. The beginnings of glacial geomorphology

It was Louis Agassiz in 1837 who first proposed that ice had been more extensive in the past. He achieved this advance in glaciological understanding through identifying depositional glacial phenomena and geomorphology, such as erratics and moraines. It was not until much later that the ability for glaciers to erode the landscape which they occupied was recognized (Ramsay, 1859, cited in Harbor, 1989). Making a bold statement, Ramsay (1859, cited in Harbor, 1989) declared “that all glaciers must deepen their bed by erosion.” He identified that glaciers had the ability to “scoop” out depressions which, once deglaciation occurred, formed lakes such as Llyn Ogwen in

Snowdonia (Ramsay, 1859, cited in Harbor, 1989). As an interest in glacial geomorphology gathered pace it was not long before the distinct shape of glacial valley cross profiles was chronicled. Campbell (1865) had a unique approach in describing landforms, using letters in the alphabet to explain geomorphology and depicted a glacial valley as a U. But McGee (1883, 1894) was the first to compare differences between the cross-sectional shape of fluvial and glacial valleys. He described glacial valleys as being "U-shaped rather than V-shaped in cross-profile". Incredibly, within the same document, McGee (1894) set out to give process explanations for the U-shape through erosion laws and ice flow knowledge. This was met with much scepticism from the growing glacial geomorphological research community (Harbor, 1989). In the subsequent years much debate centred on the degree to which glaciers altered valleys by erosion, with the majority of geomorphologists, including McGee, believing that glaciers modified fluvial valleys and there was little vertical erosion (Harbor, 1989). The description of a U-shaped valley did not gain further attention until Davis (1916) described the cross-sectional valley shape as a catenary curve. And much later still, Svensson (1959) proposed cross-sectional valley shape was best described mathematically as a parabola. Figure 2.1 shows three real valleys with catenary, parabola and U-shape curves. Observations show that all curves can be observed in valley forms.

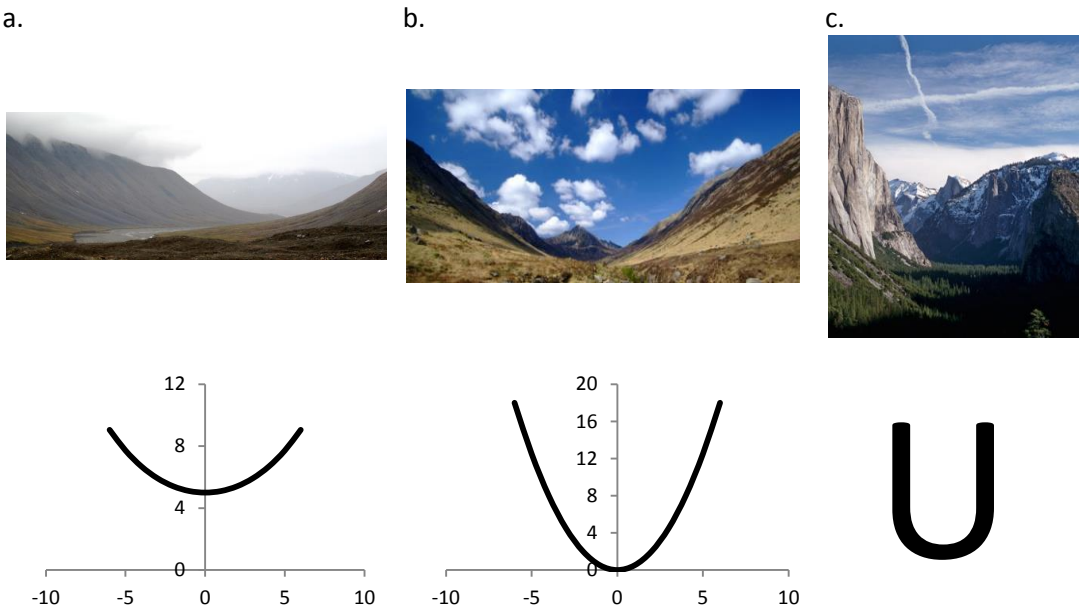

Figure 2.1 (a) Shows a valley in Svalbard and below a catenary curve with the equation $y = \mathrm{acosh}\left(\frac{x}{a}\right)$, where the *a* constant is given a value of 5. (b) shows the Glen Rosa valley on Arran, Scotland. It appears to show a parabolic form illustrated in the graph below it which depicts the power-law curve $y = ax^b$, where the a coefficient has a value of 0.5 and the *b*-value is 2. Finally (c) shows Yosemite valley, California, USA and below the photograph is the letter U which matches the valley form.

2.2.2. 'U-shaped' description still prevails

Initial valley descriptions were derived purely from observations rather than measurements. Subsequent analysis of valley cross-sections involved quantifying valley profiles to one of the 'U-shapes' described in Figure 2.1. This was often in locations along a glacial valley where the U-shape was best represented. Any process theory regarding valley cross profiles attempted to recreate the U-shape rather than the U-shape concept being underpinned by process theory. Despite Davis (1916) and Svensson's (1959) definitions of a glacial valley cross-section most modern day descriptions still refer to the U-shape of glaciated valleys. No doubt the continued use of this term is due to it being easy to visualise and relate to observed valleys. It is a concept which has stood for over 100 years, becoming deeply entrenched in glacial geomorphology and assumed as given. Recently, research has worked towards recreating a U-shaped valley through process theory and relating outcomes to real landscape forms adopted by glaciated valleys has been done with varying success. It seems long overdue that the glacial valley cross-section is re-examined in order to see whether this is an accurate interpretation of valley form. Analysis of spatial variability

can also be examined to give insight into glacial processes and the timescales in which they operate.

The cross-sectional valley form has been used to infer valley evolution. The transition from a fluvial V-form to a more U-shape occurs over glacial cycles and a well-developed U-shape is thought to be a result of a prolonged and/or intense glaciation (Harbor, 1992). In combination with the evolution of valley cross-profiles, studies on the development of the valley longitudinal profile have looked at the change of a graded fluvial valley to a typical glacial valley which, characteristically, has a steep valley headwall whilst the valley flattens downstream (MacGregor *et al.*, 2000). An intensely glaciated valley cannot only have a flattened valley profile but can in fact erode below the base level to create an overdeepened valley floor (Shoemaker, 1986).

Overdeepenings are steps in the valley longitudinal profile. They are a unique feature of glacial valleys as fluvial processes do not have the ability to erode below the base level (Swift et al. 2008, Shoemaker, 1986). They are found where glacial erosion is intense, for example at ice convergences (Hall & Glasser, 2003, Shoemaker, 1986, Jamieson et al. 2008). Shoemaker (1986) found that overdeepenings have not only been associated with converging flow but also with where the ice subsequently diverges. Fjords are a geomorphological manifestation of overdeepenings as sunken valleys. Swift *et al.* (2008) found in East Greenland that overdeepenings were connected to lithology. Highly resistance lithology was associated overdeepenings and this was attributed to the valleys, which had deep narrow cross-sections, not being an efficient form for ice flow. Whilst valleys in less resistant lithologies having wide, relatively shallow valley cross profiles, which is most effective for the evacuation of ice and therefore were less likely to erode below their base levels.

Is it really true that glacial valleys are U-shaped? And if so, what does variation in cross-sectional valley measures tell us about glaciations and glacial processes?

2.3. Descriptors of valley shape

2.3.1. The Power-law equation

Svensson's (1959) description of valley cross-sections as parabolic was part of a wider movement which aimed to quantify geomorphology and developed into a discipline known as geomorphometry. Geomorphometry can be divided into two categories, specific and general (Evans, 1972), the former addressing specific landforms and the latter evaluating the continuous land surface. The investigation of cross-sectional valley profiles falls into the specific category of geomorphometry.

Svensson (1959) suggested that the form of a valley cross profile followed a parabolic curve. This idea was determined by measurements taken from three cross-sections in the Lapporten valley, Norway. The cross-section measurements were then averaged to give two results, one for the left-hand side of the valley and one for the right. A power-law equation was used (Svensson, 1959):

$$y = ax^b \quad [2.1]$$

where the *x* is the horizontal direction and the *y* the vertical direction. To determine the *a* coefficient and *b* exponent the power law can be transformed into its logarithmic form so that a least squared linear regression can be fitted to the empirical data.

$$ln\, y = ln\, a + b\, ln\, x \quad [2.2]$$

The *a* coefficient indicates the breadth of the valley floor whilst the *b* exponent, commonly called the *b*-value, determines whether the valley has a parabolic form by signifying the steepness of the valley sides. It is therefore the *b*-value which is often thought of as the extent of glacial erosion on a valley. In numerical terms a *b*-value of 1 indicates a perfect V-shape (Figure 2.2) whilst values greater than 1 a concave-upwards curve (Figure 2.3) and values less than 1 a convex-upwards curve (Wheeler, 1984). Values close to 2 indicate the parabolic form thought to be adopted by a glaciated valley (Figure 2.3).

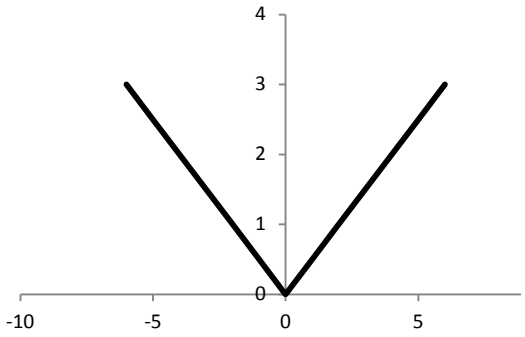

Figure 2.2 The power law where the *b*-value is 1. This is used to represent a fluvial "V-shaped" valley.

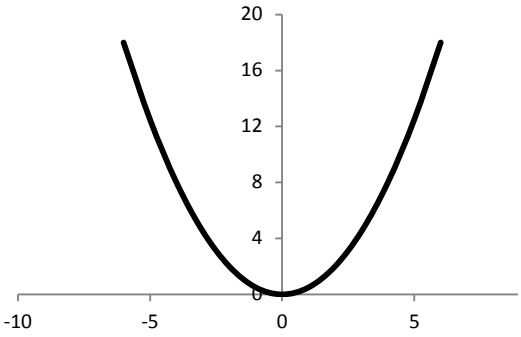

Figure 2.3 The power-law curve with a *b*-value of 2. Svensson (1959) used this to represent a glacial "U-shaped" valley.

2.3.2. Power-law limitations

Criticisms of the power-law equation are based around three main problems, these are summarised by Pattyn and Van Huele (1998) as;

1. The curve is only fitted to each side of the valley individually because negative x-values cannot be used. Therefore the complete valley cross-section is not fully considered (Wheeler, 1984; Harbor, 1992).
2. The datum problem relates to the curve being forced to pass through the origin of the coordinate system (i.e. x=0, y=0) as negative y-values cannot be used (Wheeler, 1984).
3. Logarithmic transformation bias occurs, in that the best fit curve is biased to favour points close to the origin of the coordinate system (Harbor, 1992).

An additional concern has been expressed regarding the fit of the parabolic curve in that it may be influenced by fill at the valley bottom (Wheeler, 1984; Harbor, 1992).

2.3.3. The datum problem

As stated above, both negative x and y-values cannot be used in the power-law equation. This is overcome for the x-axis by fitting a power curve to each side of the valley. However, regarding the y axis, the power curve is forced through the origin (the present day valley floor). There as two concerns with using the origin for the y-values. The first concerns the values chosen for the y-axis, and consequently where the zero-

datum (i.e. x=0, y=0) is located (Wheeler, 1984), and whether the present day valley floor (Svensson, 1959; Graf, 1970) or sea-level is used as the zero-datum (Doornkamp & King, 1971). Testing showed large discrepancies in *b*-values depending on whether local valley relief (i.e. present day valley floors) or elevation above sea-level is used for the coordinate system (Wheeler, 1984; James, 1996), leading Wheeler (1984) to suggest the quadratic equation is used as an alternative:

$$Y = a + bX + cX^2 \quad [2.3]$$

The advantage of using this curve is that the complete cross-section can be evaluated, rather than individual valley sides. This, combined with the fact that it is not significantly constrained in either direction, as the curve can extend below the valley bottom, therefore means the datum problem is not of such a concern.

Using a quadratic solution also overcomes the secondary concern that the present day valley floor used as the zero-datum in many power-law calculations is influenced by post-glacial depositional fill, which raises and flattens the valley floor (Wheeler, 1984). As a consequence the derived *b*-values may be exaggerated due to the greater curvature of the power curve where it is forced through an artificially high datum point (Wheeler, 1984). The quadratic equation allows for the extrapolation of the valley floor and sides beneath glacial deposits at the bottom of the valley (Wheeler, 1984).

However, when using the quadratic equation, interpretation of the coefficients is not as straightforward as with the power-law (Pattyn & Decleir, 1995). In addition, a major drawback to this approach is the assumption that the curve is parabolic (Harbor, 1992; Pattyn & Decleir, 1995). Analysis using the power-law shows that many valleys are not parabolic (Svensson, 1959; Graf, 1970; Doornkamp & King, 1971; Aniya & Welch, 1981; Hirano & Aniya, 1988). As an alternative to the quadratic equation but still circumventing the datum problem Aniya and Welch (1981) used different datum points, repeating the power-law for each in order to fine the *a* and *b* coefficients which had the best fit. A drawback of this trial and error method is that it is time consuming.

2.3.4. Power-law logarithmic transformation bias

Harbor and Wheeler (1992) argue that the logarithmic transformation of the power-law equation is of much greater concern than the datum problem. The transformation creates a bias to fitting of the curve to the data points closest to the centre of the valley.

This is not only a problem in its own right as regression coefficients are biased to the few data points near the centre of the valley, but these data points are more likely to be influenced by glacial deposition, which alter the valley's originally eroded form. A solution to this is to consider each profile separately and remove data points close to the valley centre (James, 1996) or to use a correction factor when restoring the logarithmic transformation to the power-law (Jansson, 1985).

2.3.5. The general power-law

To resolve the limitations of the power-law, Pattyn and Van Huele (1998) and Pattyn and Decleir (1995) proposed the general power-law. The general power-law eliminates the logarithmic transformation bias and minimises the error between the empirical data and the curve. The general power-law is given by:

$$y - y_0 = a\,|x - x_0|^b \qquad [2.4]$$

where y_0, x_0 are the coordinates of the origin of the cross-profile. The solution is found through the logarithmic general least-squares adjustment. Their tests showed high sensitivity of the power-law to origin coordinates whilst the general power-law was able to consistently resolve the datum problem. Another advantage of this equation is that it can handle whole valley profiles instead of tackling individual valley sides. Although the reported test results appear convincing, the only valley cross profile used to test this equation was very symmetrical in form and it is questionable whether such results could be achieved on commonly observed asymmetrical valleys.

Despite the criticisms of the power-law (Wheeler, 1984; Harbor, 1992; Pattyn & Van Huele, 1998) and the various alternatives suggested (Aniya & Welch, 1981; James, 1996; Pattyn & Van Huele, 1998) the power-law (Svensson, 1959) initially suggested is still the most utilised solution in quantifying cross-sectional valley shape.

2.3.6. Form ratio

Graf (1970) noted that the power-law equation only describes the curve of the valley and, in fact, two valleys could have exactly the same regression model but still have two very different forms. This is due to the power-law equation describing an endless curve. It is therefore important to use an additional measure in conjunction with *b*-values to

describe valley morphology. Graf (1970) proposed that form ratio (the ratio of valley depth to valley top width) should also be used to constrain valley form. Initially suggested for fluvial valley morphology (Morisawa, 1968 p. 111), it needed no adaption for glacial valleys. Form ratio is a simple ratio equation:

$$FR = {}^{D}/_{W} \quad [2.5]$$

where *FR* is form ratio, *D* is valley depth and *W* is valley top width. The power-law equation tackles each side of the valley individually; it is half the valley width measured from the centre of the valley to the valley side, but the form ratio uses the width of the valley from valley top to valley top. Therefore the valley width used in the form ratio equation is double the width used in the power-law. Form ratio cannot be used in isolation as it is unable to represent the degree of curvature of a profile or the valley size (Graf, 1970).

2.3.7. Cross-sectional area

A much less used valley measure is the cross-sectional area of valley profiles. It is a simple measure of the area inside a valley (Haynes, 1972) and indicates the amount of material eroded (Phillips, 2009). As it has been suggested that glaciers have the ability to exhume more material than fluvial systems (e.g. Harbor & Warburton, 1993; e.g. Clayton, 1996; Naylor & Gabet, 2007) it is fair to assume that glacial valleys might be greater in size. Haynes (1972) and Augustinus (1992b) used this measure in studies comparing catchment areas with outlet troughs finding that there was a positive relationship between the two variables. In an investigation to use valley form as a means of distinguishing between glacial and fluvial valleys Phillips (2009) found cross-sectional area to be a more powerful discriminator than *b*-values or form ratio.

2.3.8. Relationship between b-values and form ratio

Glacial erosional processes alter valley shape, changing a pre-existing V-shaped fluvial valley into a U-shape. The timescales involved in changing a landscape are dependent on the intensity of glacial processes and its resistance to erosion. Therefore it is a justified assumption that valley morphology can give clues to the amount of glacial erosion a valley has undergone. Research has linked valley shape and size to process intensity.

Penck (1905, cited in Graf, 1970) stated that a valley cross-sectional area is proportional to the amount of ice flowing through it, whilst Graf (1970) thought that glacial valleys developed into a parabolic form and become deeper and relatively more narrow with time. A parabolic form (*b*-value close to 2) is suggested to be the ideal glacial valley shape and a mature glacial valley will have a *b*-value of 2 whilst less well-developed glacial valleys a *b*-value less than 2 (Figure 2.4).

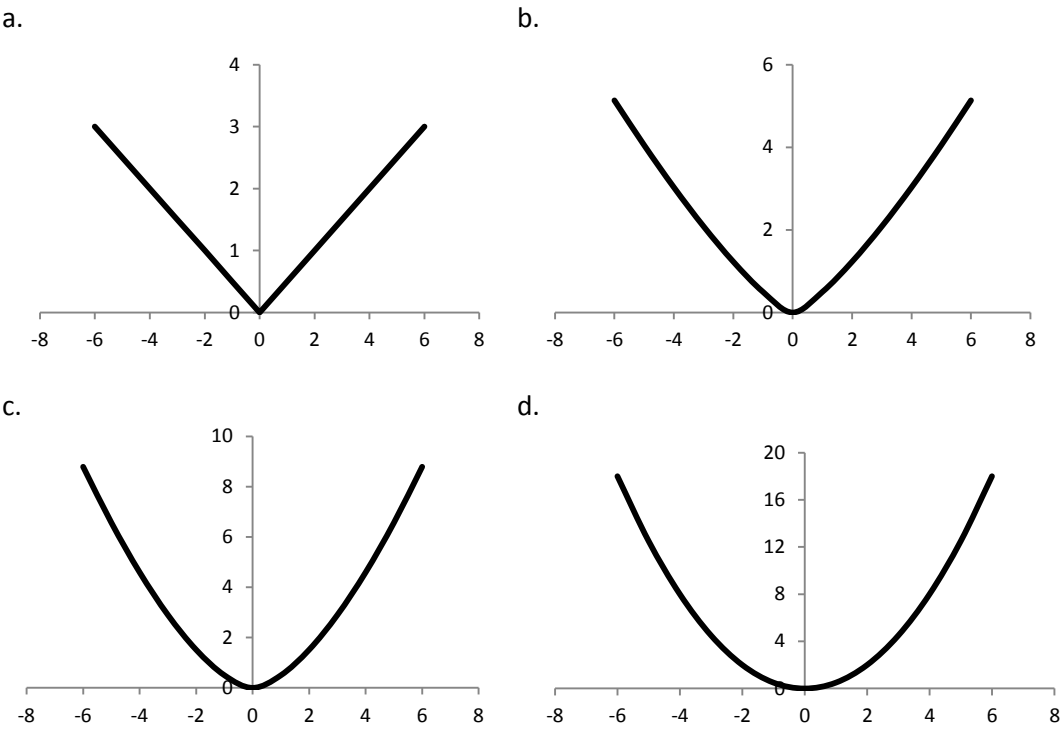

Figure 2.4 Shows how the parabolic curve changes as the *b*-value is increased. As the *b*-value increases from the value of 1 to 2 the curve becomes more convex and indicates a more mature glacial cross-section. (a) shows a *b*-value of 1 and has a form ratio of 0.3, (b) a *b*-value 1.3 with a form ratio of 0.4, (c) a *b*-value 1.6 with a form ratio of 0.7 and finally, (d) a *b*-value 2 with a form ratio of 1.5. Throughout, the *a* coefficient is kept constant at 0.5 for all the curves.

Although it has been suggested that valleys become deeper and relatively narrower (higher form ratio) with an increasing parabolic form (Graf, 1970), Hirano and Aniya (1988) found that the relationship between *b*-values and form ratio did not always follow this relationship. When comparing *b*-values and form ratio of several different studies (Graf, 1970; Doornkamp & King, 1971; Aniya & Welch, 1981; Aniya & Naruse, 1985 cited in Hirano & Aniya, 1988) it is evident that different relationships exist. Deep narrow valleys, where form ratio and *b*-value have a positive relationship with evolution,

occur in a 'Rocky Mountain' type of glacially eroded landscapes. Whilst wider and relatively shallower valleys were observed in a 'Patagonia-Antarctica' type landscape and show form ratio decreasing as *b*-values increase with valley development (Figure 2.5 and 2.6). These two types of glacial responses indicate that alpine (Rocky Mountain type) mountains develop by deepening whilst Patagonia-Antarctica regions develop valleys through widening, therefore suggesting different erosion focuses (Pattyn & Decleir, 1995) (Figure 2.6). Observed landscapes, such as those in Figure 2.1, are testament to these different glacial valley types. It is also suggested that the 'Rocky Mountain' and 'Patagonia-Antarctica' type valleys may not only exist in separate areas but can coexist in the same mountain range such as the Tian Shan Mountains, China (Li *et al.*, 2001b). Brook *et al.* (2004b) go on to suggest that the different profile types are due to geology rather than regime type, where low rock mass strength geologies form wider valleys compared to areas of higher rock mass strength where deeper, narrower valleys were observed.

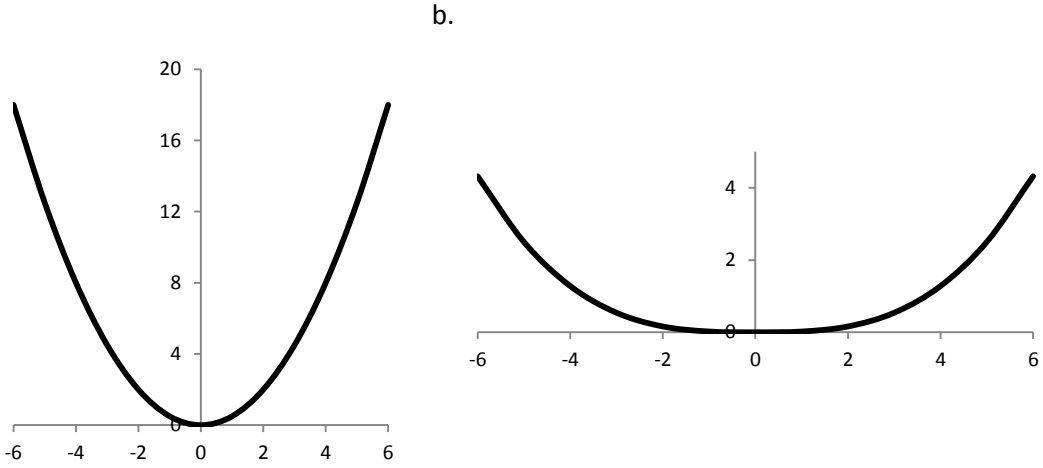

Figure 2.5 (a) Shows a Rocky Mountain type glacial valley. It has a deep narrow valley form with an *a* coefficient of 0.5, a *b*-value of 2 and a form ratio of 1.5. (b) Shows a Patagonia-Antarctica type glacial valley. This valley is wide and relatively shallow. It has an *a* coefficient of 0.02, a *b*-value of 3 and a form ratio of 0.36.

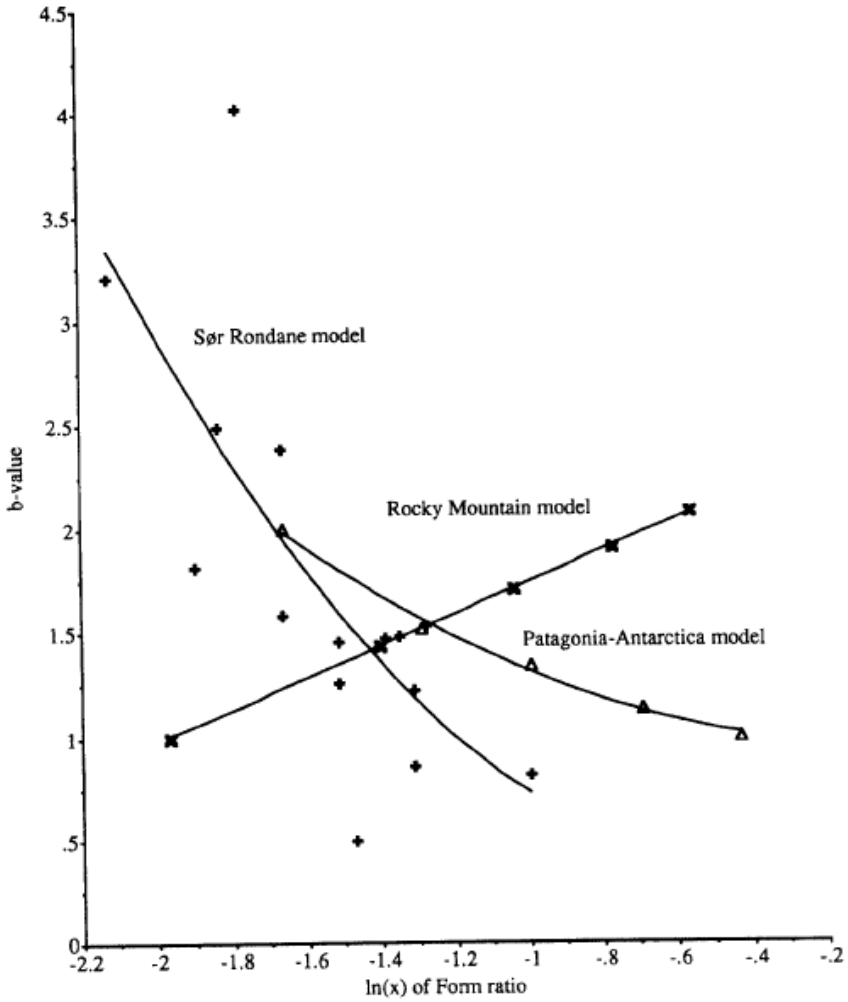

Figure 2.6 A form ratio-*b*-value diagram showing Pattyn and Decleir's (1995) results of the Sør Rondane, Antarctica which are compared with Hirano and Aniya's (1988) Rocky Mountain and Patagonia-Antarctica models. The Patagonia-Antarctica model shows that as valleys develop the *b*-value increases whilst the form ratio decreases. For the Rocky Mountain model both the *b*-value and form ratio increase.

2.3.9. Other measures of valley shape

Other measures used when analysing glacial landscapes include 'specific geometry' used to define valley cross-sections like valley width and depth (Evans, 1972). Using such absolute measures give a true sense of valley size and scale and enables comparisons. Measures of hypsometry are also often used, especially when comparing fluvial and glacial landscapes across large areas. Hypsometry is classified as 'general geometry' as it is possible to incorporate the terrain characteristics of an entire landscape (Evans, 1972). Measures include the hypsometric curve (the area-altitude relationship) and the hypsometric integral (the area beneath the curve which relates to the percentage of

total relief to cumulative percentage area). Hypsometry has been used to compare with models (Egholm, 2009, Brocklehurst & Whipple, 2006)

Testing all glacial landscape measures is beyond the scope of this thesis, however Phillips (2009) reviewed the geometry of valleys for both specific and general measures and investigated in some detail measures of valley cross-section area, power-law functions, form ratio, grain and texture, stream order, drainage density, ruggedness number, ridge density, peak density and hypsometry. Comparisons were made as to how well these measures perform when discriminating between fluvial and glacial landscapes. It was found that valley cross-sectional area was the best discriminator and hence its inclusion as a measure in this thesis. Form ratio and the power-law function *b*-value have also been included as a large proportion of the valley cross-section literature uses these values and this aids comparisons to be made.

2.4. Inconsistencies in cross profile technique

Cross-sectional valley profile data is predominately collected by drawing transects across valleys portrayed on topographic maps. This technique is time consuming and subjective meaning that results can be questionable. For example, some profiles have been taken from ridge top to ridge top (Montgomery, 2002) (Figure 2.7a) whilst other researchers took profiles from valley trimlines (Graf, 1970; Pattyn & Decleir, 1995; Li *et al.*, 2001b) (Figure 2.7b). This difference in measurement technique could alter the power-curve and consequently the *b*-value, as well as the form ratio, and therefore comparisons between these studies cannot be made. Inconsistencies in how transects were drawn and the measures derived present serious problems when comparing the results from various papers. The angle at which transects are drawn across the valley is rarely mentioned in the literature, as it is assumed that the profile is taken perpendicular to the valley. However, valleys are often not uniform, making the transect method subjective and open to differing interpretation of where the line should be drawn (Figure 2.7c). It seems that transects are often carefully chosen to best represent the U form of a glacial valley, therefore eliminating any areas of the valley which do not conform to a U-shape and biasing our view of the prevalence of the U-shaped valley form. Amerson *et al.* (2008) acknowledge these difficulties and, as such, avoids valley confluences and 'irregularities in form or grossly unequal subtending ridge elevation' when selecting valley sites.

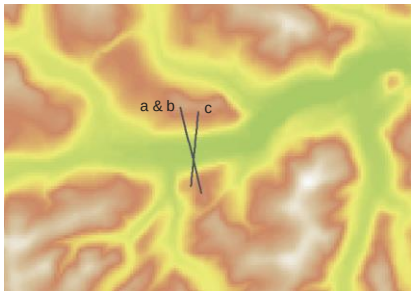

a.

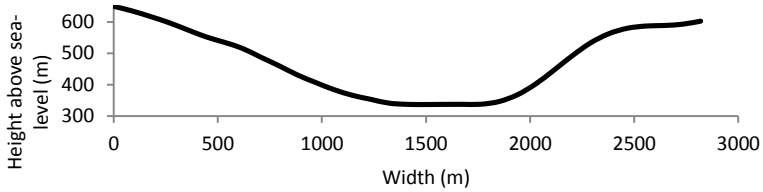

Left-hand *b*-value = 1.35 Right-hand *b*-value = 1.33 Form Ratio = 0.11

b.

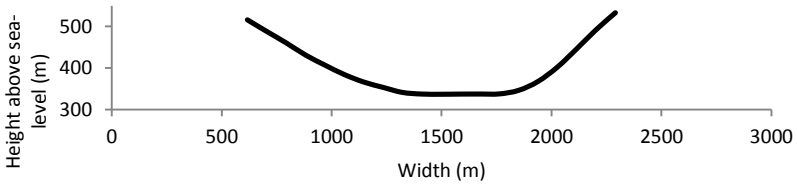

Left-hand *b*-value = 1.9 Right-hand *b*-value = 2.86 Form Ratio = 0.12

c.

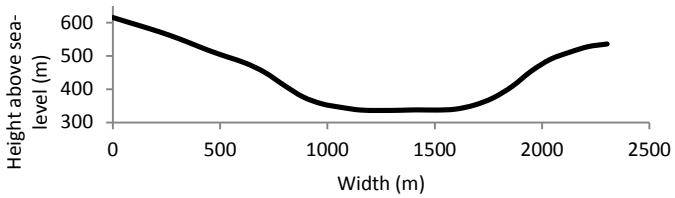

Left-hand *b*-value = 1.24 Right-hand *b*-value = 2.04 Form Ratio = 0.12

Figure 2.7 Transects drawn across a valley in the Cairngorms, Scotland, show the inconsistencies which can arise from the individually selected profile method. Profile (a) shows the initial profile drawn across the valley from valley top to valley top. It has similar *b*-values, of 1.35 and 1.33, for each side of the valley, and a form ratio of 0.11. Profile (b) has the same orientation as profile (a) but instead spans the valley from the break in slope to the opposite break in slope. It has far higher *b*-values for each side of the valley as the steepness of the valley sides are not tempered by a levelling off at the valley tops. It has a similar form ratio of 0.12. Profile (c) shows a transect which has a slightly different orientation to profile (a). This change in orientation changes the valley profile shape so that the resultant *b*-values differ from profile (a). In fact The left-hand valley side has a far smaller *b*-value whilst the right-hand side exhibits a far larger *b*-value. It has a similar form ratio of 0.12.

2.5. Extent of the quantitative basis for cross-sectional valley shape

It has already been alluded to that relatively few cross-valley profiles have been used to develop quantitative measures of valleys; Svensson (1959), for example, averaged just three valley profiles in one single valley to justify the power-law equation. To gauge the quantity of cross-sectional valleys analysed Table 2.1 summarises all research to date of valley cross-sectional profiles. All studies reported here measured elements of the cross-sectional valley profiles, and apart from the studies indicated, the studies obtained measurements for *b*-values and form ratios and used the transect technique.

Table 2.1 Summary of entire cross-sectional valley profile research with measurements taken.

Study Area	**Number of profiles**	**Reference**	**Measures derived**				
			***b*-value**	**Form ratio**	**Cross-sectional area**	**Width**	**Depth**
Tian Shan Mountains, China	49	Li *et al.* (2001a) and used in Li *et al.* (2001b)	√	√			
Tian Shan Mountains, China	an additional 7	Li *et al.* (2001b)	√				√
Beartooth Mountains, Wyoming and Montana, USA	60	Graf (1970)	√	√		√	√
North Wales, Yorkshire and the Lake District, UK	4	Doornkamp and King (1971)	√	√			
Southern Alps, New Zealand	At least 45	Augustinus (1992a)	√	√			
Athabaska Glacier, Alberta, Canada	8	Kaneasewich (1963)					√
Victoria Valley System, Antarctica	13	Aniya and Welch (1981)	√				√
Two Thumb Range, Southern Alps, New Zealand	111	Brook *et al.* (2006) and used in Brook *et al.* (2008)	√			√	√
Two Thumb Range, Southern Alps, New Zealand	same profiles as above	Brook *et al.* (2008)	√	√		√	√
Banff, Canada	Approx 6	Hirano and Aniya (1988)	√	√			
Lapporten, Norway	3	Svensson (1959)	√				
Central Sør Rondane Mountains, East Antarctica	18	Pattyn and Decleir (1995)	√	√		√	√

Study Area	Number of profiles	Reference	Measures derived				
			b-value	Form ratio	Cross-sectional area	Width	Depth
Sierra Nevada, USA	7	James (1996), one profile (Tenaya Canyon) used in Pattyn and Van Huele (1998)	√				
Antarctica and Patagonia	6	Aniya and Naruse (1985), unpublished, cited in Hirano and Anyia (1988)	√	√			
Glen Rosa, Isle of Arran, Scotland, UK	3	Wheeler (1984)	√				
Scotland and Iceland	At least 60	Brook *et al.* (2004b)	√	√			
The Sukkertoppen Ice Cap, East Greenland	19	Haynes (1972)			√		
British Columbia, Canada	33	Roberts and Rood (1984)				√	√
Fjordland, New Zealand	33	Augustinus (1992b)			√	√	√
West coast, Scotland, UK	34	Brook *et al.* (2003)					√
Central Idaho, USA	At least 21 fluvial and 25 glaciated	Amerson *et al.* (2008)			√	√	√
Olympic mountains, USA	131 (54 fully glaciated, 42 partially glaciated and 35 unglaciated)	Montgomery (2002)			√	√	√

Table 2.1 shows that in the literature 696 profiles have been measured using the transect method, 531 of the profiles obtain measurements for form ratio and *b*-values, whilst 165 gained values for width, depth, cross-sectional area or all three. This gives context of the current research and its basis; both the amount of profiles investigated and the regions from which these profiles have been taken. The current sample size is in the 100s for which research studies have based the understanding U-shaped forms of glacial valleys. It is suspected however that the wide acceptance of the U-shaped glacial valley form comes from personal observations in the mountains (Figure 2.1) rather than just the quantitative basis reported here.

2.6. Glacial process studies and valley shape

Glacial valleys are eroded by a combination of mechanisms; these include abrasion (polishing and striating), plucking (quarrying), crushing (fracturing) and meltwater erosion including chemical dissolution. Together, in some combination, they create the distinct shape of glacial valleys but the relative importance of each process is under regular discussion. This section provides an overview of the processes involved in glacial erosion relevant to valley shape.

The process of erosion can be generalised into three stages. Firstly, the rock failure, where fragments are loosened from the bed. Secondly, evacuation, which is where these fragments are moved from their original position, and finally, transportation of the fragments via entrainment in the ice, water or in subglacially deforming layers (Bennett, 1990). For the erosion of hard beds two distinct processes are traditionally cited; abrasion and plucking.

Abrasion is the wearing down and smoothing of the glacier bed by sediment entrained in the sliding ice of the glacier itself. It can encompass the process of polishing, the reduction of the roughness to a rock surface and striating, effectively the scratching of the bedrock. Boulton (1974) observed striating beneath the Breiðamerkurjökull glacier, southeast Iceland. The fragment creating the striation on the bedrock was associated with the smaller fragments of crushed debris and suggested that this fine debris provided sediment which is needed for a more polishing type of abrasion. Abrasion rates are attributed to the effective force of the sediment as it is pushed along the bed. This is known as the basal contact pressure. Two views were developed with regard to contact pressure of a particle in contact with the glacier bed. The first view is that contact pressure is directly related to the effective normal pressure which is a function of normal pressure produced by the weight of the overlying ice (Boulton *et al.*, 1974). The second quite different view is that basal water pressure to buoy up the ice preventing contact pressure and instead erosion occurs by viscous drag on the particle which controls the movement of the rock fragment and depends on particle properties and ice velocity normal to the bed (Hallet, 1979). High effective normal pressures therefore occur when the ice is thick and the basal wa

ter pressure is low. It is altered when obstacles impede ice flow. The Boulton (1974) model also takes into account that as effective normal pressure increases the friction between the rock fragment and the bed increases resulting in the slowing of

transportation of the particle and thus erosion. The ice deforms around the particle and continues a faster rate of flow. In this model it is possible for friction to become so great that lodgement of the particle can occur.

In contrast the Hallet (1979) model assumes that the contact pressure between a rock fragment and the bed is independent of the effective normal pressure as the particle is encased in ice and essentially floating within it. Instead, the contact pressure is a function of the rate at which the ice flows towards the bed, forcing any particle in contact with the bed. This type of ice flow is dependent on the rate of basal melting and the presence of extending glacier flow.

More recent work on glacial abrasion models include research by Iverson (1990, 1991) who highlights the importance of including fragment rotation into erosion models, as rock fragments have longer life spans as erosive tools if rotation occurs. Iverson's (1990) laboratory experiments strongly support Hallet's (1970) model, highlighting the importance of downward ice flow velocity.

Abrasion rates have also been connected with rock type. The amount of sediment which is delivered to the bed and resistance of both the sediment and the bed and the difference between the two contribute to the overall erosion rate (Hallet, 1979). The greatest erosion will take place where the rock fragments are highly resistant whilst the bedrock is relatively soft lithology (Bennet and Glasser, 2009). Abrasion produces fine-grained sediment by the grinding down of the glacier bed (Bennett, 1990). The influence of lithology on erosion will be discussed later on in this chapter.

In contrast plucking, also termed quarrying, is the failure, evacuation and transportation of larger blocks (Bennett, 1990). Unlike abrasion which has a smoothing effect, plucking maintains bed roughness and therefore influences sliding speed and stability of temperate glaciers (Hallet, 1996). Ice can exploit pre-existing joints in the bedrock to cause the failure of blocks (Bennett, 1990). Following this ice combined with water at the ice bed interface can remove sediment fragments produced by abrasion and plucking from the bed (Boulton *et al.*, 1974). In order for this to occur the ice must first be moving with enough tractive force to transport entrained material (Boulton *et al.*, 1974). The existence of cavities at the ice-bed interface, which generate pressure induced temperature fluctuations and are where freeze/thaw conditions occur and therefore rock failure (Röthlisberger & Iken, 1981). An optimum cavity size was identified and attributed to the close interaction with basal meltwater pressures (Hallet,

1996). Both plastic flow and the regelation of meltwater contribute to material being incorporated into the glacier ice (Boulton *et al.*, 1974). Once the material is in motion with the ice it is able to erode the glacier bed further via abrasion, as previously discussed.

As abrasion and plucking work in opposition, one smoothing the bed whilst the other roughening it, respectively, the process which prevails has been attributed to landscape and glacier characteristics (such as ice thickness, velocity and water pressure (Iverson, 1991)) and bedrock properties.

Water at the ice/bed interface is integral to both the sliding velocity and the contact ice has with the bed, both of which affect erosion rates. When water pressure is high sliding can increase whilst the effective normal pressure of the ice against the bed decreases, separating the ice from the bed and therefore reducing the amount of abrasion (Iverson, 1991) which can take place. However, increased water pressure increases sliding and therefore increases erosion and in conjunction can aid the removal of loosened rock fragments (Iverson, 1991). Iverson (1991) found that the optimum subglacial conditions for plucking involved fluctuations in water pressure where decreased water pressure would create conditions of high effective normal pressure which, in turn, would shift the weight of the ice on to the rock irregularities creating increased stresses on the rock causing the growth of pre-existing cracks approximately parallel to the compressive principle stress. Removal of blocks could then take place once water pressure increases again.

In northwest Scotland bedrock properties were investigated by Krabbendam and Glasser (2011). They found that Torridon's soft, thick bedded and widely jointed sandstone was predisposed to being abraded whilst the hard, thin bedded and narrow joints Cambrian quartzite had been eroded predominately by glacial plucking. Concluding that a lithology with a combination of hard rock with thick bedding planes and wide jointing is the most resistant to glacial erosion, such as igneous and metaigneous rocks like granite and orthogneisses (Krabbendam and Glasser, 2011), whilst the converse is true for soft, thin bedded and narrow jointed lithologies, such as shales, certain chalks and deeply weathered bedrock transitional to regolith (Figure 2.8) (Krabbendam and Glasser, 2011).

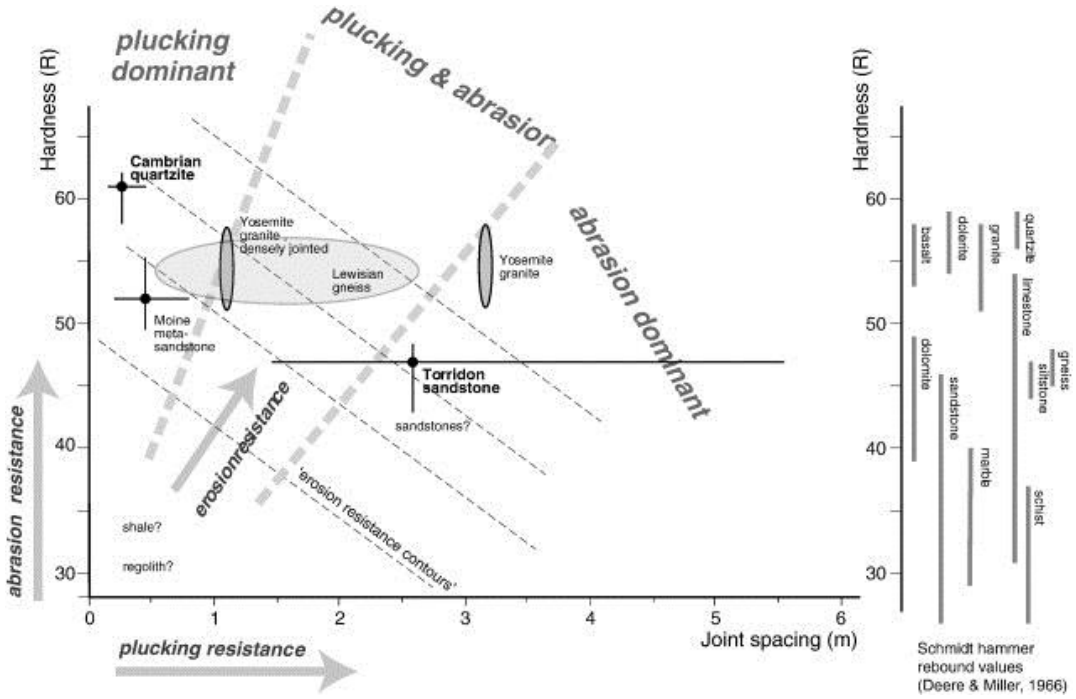

Figure 2.8 A schematic diagram showing the relationship between joint spacing and hardness (Krabbendam and Glasser, 2011). It shows the relative positions of Cambrian quartzite and Torridon sandstone with other rock types and relates this to the dominant erosional process; abrasion or plucking.

Although it has been suggested that plucking is capable of more erosion over abrasion (Briner and Swanson, 1998, Duhnforth et al. 2010) Krabbendam and Glasser (2011) argue that this might not be the case as this conclusion was made from research on hard lithologies such as granite (Johns, 1993, Duhnforth, 2010) and gabbro (Briner and Swanson, 1998). In the case of soft lithologies such as Torridon sandstone it is suggested that abrasion is just as effective as plucking (Krabbendam and Glasser, 2011).

An additional erosional process is that of crushing, also called fracturing. It is caused by the downward force of the combined mass of the ice and the sediment entrained in it. It is this force of sediment in the ice pressing against the bedrock which causes crushing type erosion. In contrast to abrasion this force does not increase with ice velocity (Sugden & John, 1976). Evidence of crushing is found in the form of chatter marks, crescentric gouges and lunate marks (Franzén & Olvmo, 1991).

In warm-based glaciers meltwater exists at the ice-bed interface in subglacial channels, as well as a film of water. As previously alluded to, meltwater can combine with other processes and contribute to rock failure, evacuation and transportation of material. In general the more meltwater which is available the more erosion can occur. The

presence of water also enables freeze-thaw to occur which can loosen and dislodge material. In addition another erosional process which can occur when water is present is chemical dissolution which particular rock types, i.e. limestone, are more prone to.

To understand these *individual* processes, modelling has been undertaken (e.g. Boulton *et al.*, 1974; Hallet, 1979; Roberts & Rood, 1984; Hallet, 1996). However modelling of processes often takes place in isolation of other processes and it is known that many glacial landforms are formed by a combination of multiple erosional mechanisms and the feedbacks which operate between them. For example, roches montonnées, are formed where abrasion occurs on the stoss slope and plucking on the lee slope of the landform (Figure 2.9). Plucking of material ensures that there is a constant supply of sediment entrained in the ice bed to abrade the exposed stoss slope of the next roche montonnée (Bennett, 1990; Iverson, 1995; Hallet, 1996). Without this sediment abrasion could not occur as ice alone cannot abrade bedrock. Such feedbacks are likely to exist in glacial valley formation.

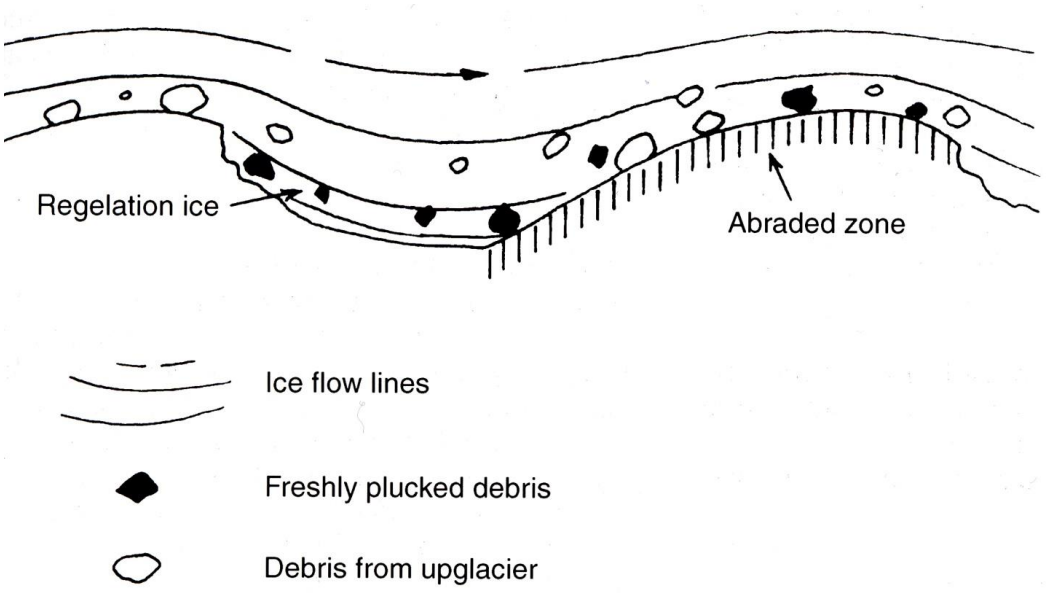

Figure 2.9 A series of roche moutonees showing a feedback mechanism where plucked material contributes to abrasion of the stoss slope of the landform (Bennett, 1990; Iverson, 1995; modified from Hallet, 1996)

Process studies have generally relied on the interpretation of the resulting geomorphology rather than direct observations at the ice-bed interface, with a few exceptions (e.g. Iverson *et al.*, 2007), Boulton, 1974, Cohen et al. 2005, Anderson et al. 1982), and in the laboratory with experiments (Iverson, 1990 and 1991, Lister et al. 1968 and Mathews, 1979). Research has mostly focused on understanding micro-scale and meso-scale landforms, such as striations and roche montonnées and very few have tried to relate the processes to macro-scale erosional landforms, such as cirques and glacial troughs, which are created by a combination of many erosional processes. It has not been until recently that modelling has developed to account for trough and mountain scale landforms and feedbacks between individual processes have barely started.

2.7. Early phase modelling addresses valley shape

2.7.1. Modelling glacial valley development

Research progressed from the modelling of individual glacial processes (e.g. abrasion) to attempts to model the development of glacial valleys for both cross-sectional (Harbor, 1992) and longitudinal form (MacGregor *et al.*, 2000) in order to replicate the evolution of a valley. It was recognised by Matthes (1930 cited in Harbor, 1992) that in order for a valley to evolve from a V to a U-shape, widening part way up the valley sides needed to occur. It was thought that the U-shape adopted by glacial valleys is due to the form being the most efficient for ice flow (Hirano & Aniya, 1988; Flint *et al.*, 1994). Problems with early models were that they were mainly conceptually based using ice flow and erosion mechanisms and only partly incorporated process knowledge (e.g. Nye & Martin, 1967; Johnson, 1970; Boulton *et al.*, 1974; Roberts & Rood, 1984). They also relied on the end form whilst attempting to deduce intermediate stages of development (Johnson, 1970; Boulton *et al.*, 1974; Roberts & Rood, 1984). By developing iterative models the stages of landform development can be analysed (Oerlemans, 1989). The combination of advances in numerical ice flow models (e.g. Reynaud, 1973), as well as the process-models previously discussed, advanced process-based models.

Harbor (1992) took a different tact, using a finite-element model for ice flow through a valley cross-section to gain insight into the understanding of valley transformation from a V-shape to a U-shape and enabling initial time estimates to be made by calibrating the model to realistic rates of erosion.

In the Harbor (1992) model, erosion is scaled with sliding velocity (Figure 2.10), as this formulation best represents the abrasion law proposed by Hallet (1979). It assumes that if other erosional mechanisms are operating then they also follow this velocity-scaling and does not attempt to incorporate individual processes, such as plucking or meltwater erosion or any feedbacks between processes. Research using this model finds that ice initially concentrates erosion laterally, changing the V-shape to a U-shape and once this is achieved the ice incises vertically. This creates deep narrow U-shaped valleys. Seddick *et al.* (2005) improve the model by incorporating a sliding law which is dependent on effective pressure and therefore taking into consideration lateral drag from the glacier side walls, as well as basal-stress. Despite these adjustments the model results replicate those produced in the Harbor (1992) model outputs. However, Seddick *et al.* (2009) questioned whether the model output is representative for all glacial valleys as the model only produces deep, narrow, 'Rocky Mountain' or alpine type valleys. It does not replicate very wide valleys, described as 'Patagonia-Antarctica' type valleys, which are observed in empirical studies of valley cross-section.

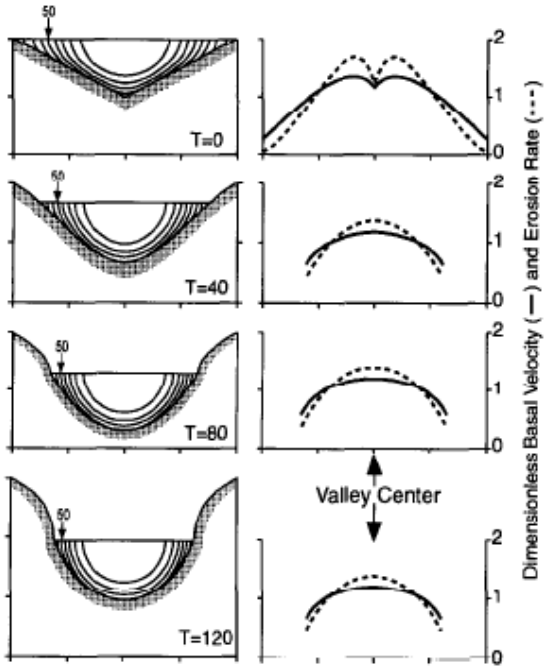

Figure 2.10 Harbor's (1992) model results showing how erosion is scaled with basal velocity squared. Progressive time steps (T) in valley cross-section evolution show the development of a "U-shape".

2.7.2. Whole landscape approach

Classical landscape evolution models were conceptual and concentrated on downwearing and slope retreat (Davis, 1899; King, 1953; Hack, 1960; Penck, 1972). After the mid-twentieth century there was a lull in landscape evolution investigations as research concentrated on the process-modelling previously discussed. It wasn't until much more recently that an interest in landscape evolution modelling has been revived. With the advent of more computational power it has become a realistic ambition to numerically model how landscapes change over time. Rather than incorporating all the process-models which had been developed, landscape evolution modellers tend to use diffusion-type equations to represent the combination of the effects of hillslope and fluvial processes.

Although fluvial and uplift scenarios in landscape evolution models are now well established, glacial components have only recently been included in these models (e.g. Braun *et al.*, 1999). Braun *et al*. (1999) adapted a landscape evolution model developed by Braun and Sambridge (1997) combining fluvial, hillslope and glacial processes in order to conduct experiments with glacial landscapes. In the model the shallow-ice approximation (Knap *et al.*, 1996) was used for computing ice flow velocity, despite the research recognising its limitations but it was thought justified. It has since been acknowledged that the shallow-ice approximation performs badly in complex topography such as alpine mountains. As with Harbor's (1992) model, glacial erosion was simply scaled with sliding velocity. The parameterisation used in the models are substitutes for modelling individual processes and representing all known process physics; they are a necessary compromise. A second concern is that few models have been calibrated or tested against real landscapes, with some notable exceptions (e.g. Brocklehurst & Whipple, 2006; Egholm *et al.*, 2009)

Landscape evolution models have produced some interesting results. Insights from the Braun *et al.* (1999) modelling experiment can be summarised as:

1. Glacial landscapes could hold larger ice volumes than fluvial ones, meaning that the form of the landscape is a great influence on its ability to retain ice.
2. Glaciers can erode drainage divides unlike fluvial processes.
3. Glacial erosion reached a steady state after several glaciations, despite increases in ice volume and increased uplift. This is due to uplift creating areas where ice was frozen to the bed. Ice that is not sliding cannot erode meaning that the

model maintains a constant area of sliding ice and explaining the steady state of erosion. Therefore erosion cannot necessarily keep pace with uplift.

4. Large pulses of erosion occur as glaciations finish as a consequence of fluvial processes excavating glacial deposits, as well as striving to adjust landscapes to their preferred form.

A subsequent study by Tomkin and Braun (2002) using the same model also presented some interesting results. Again, these can be summarised as:

1. Glaciers concentrate erosion near peaks, thus reducing elevation.
2. During glaciations, fluvial erosion downstream is reduced. This is because river sediment loads are artificially increased by sediment in glacial meltwater, preventing fluvial erosion, supporting evidence of this in the field (Whipple & Tucker, 1999).
3. Where frozen-bed conditions prevail, near peaks, higher relief is produced.
4. Although isostatic uplift occurs due to greater erosion during glaciations, it does not significantly increase relief or result in greater peak elevation. Therefore the model experiments contradict Molnar and England's (1990) assertion that relief production can largely be a consequence of glacial erosion.

The conclusions reached from glacial landscape evolution modelling, such as those summarised above, demonstrate how modelling can be a powerful tool at this level. However, without verifying or calibrating model behaviour it is difficult to trust experimental results fully. One way of doing this is to relate modelled morphology with empirical glacial geomorphological studies.

Brocklehurst and Whipple (2006) used observed fluvial drainage area and downstream distance relationships with longitudinal profiles to calibrate a fluvial landscape evolution model. Real glacial longitudinal profiles could then be compared to modelled fluvial longitudinal profiles for the same landscapes, as if they had not been glaciated. By using this method the degree to which observed landscapes had been modified by glaciations could be analysed (Brocklehurst & Whipple, 2006). Results from this study showed that a different response to glacial erosion was evident between valleys in small and large catchment areas. In small catchment areas glaciated valleys have undergone erosion of both the valley floors and ridgelines so there is no increase in relief. Erosion is also concentrated above the mean Quaternary Equilibrium Line Altitude (ELA). Widening without incision, observed at lower elevations of small catchment area valleys, was

attributed to short residence times where only the first stages of valley development (Harbor, 1992) had taken place. Larger drainage area valleys dramatically modify both longitudinal profiles and cross-sections, even below the mean Quaternary ELA. It is suggested that this could be due to a larger accumulation area, greater shading of the valley floor, longer residence time, as well as the influence of a shallower longitudinal slope and differing subglacial drainage conditions (Brocklehurst & Whipple, 2006).

An alternative approach is to use real landscapes to verify the model outputs. One study which has taken this approach used the global hypsometric landscape signature to compare with the results of a glacial landscape evolution model applied to an initially fluvially dominated landscape; the Sierra Nevada, Spain (Egholm *et al.*, 2009). This modelling experiment shows support for the glacial buzzsaw theory (Brozović *et al.*, 1997).

Glacial valleys are one of the fundamental landscape features; as such landscape evolution models should accurately constrain this landscape characteristic. Calibrating or testing model results with empirical glacial geomorphology, is a useful approach. Quantification of real landscapes must be developed in order for such comparisons to be made.

2.8. Revolution in DEM availability permits a new quantification of *U-ness* and exploration of variability across whole mountain ranges

Digital Elevation Models (DEMs) are datasets comprising an array of pixels with elevation values and which can have various spatial resolutions. Over recent years, free availability of DEMs over the internet have given geomorphologists an opportunity to study areas around the globe. Obvious advantages of this approach include accessing remote regions and covering large areas.

Investigating DEMs with powerful Geographical Information System (GIS) software means that analysis can be automated or semi-automated increasing efficiency and the quantity of data output. In glacial geomorphology GIS has been used for a variety of reasons from assimilation of multi-source and multi-scale data when combining different studies, identification of spatial and temporal relationships and using these

findings to verify or calibrate numerical ice sheet models (Napieralski *et al.*, 2007). For valley cross-sectional analysis DEMs have been used in GIS software to analyse transects (Montgomery, 2002; Amerson *et al.*, 2008; Phillips, 2009) rather than using contour maps (Roberts & Rood, 1984; Hirano & Aniya, 1988; Augustinus, 1992b; Li *et al.*, 2001a; Li *et al.*, 2001b; Brook *et al.*, 2006), however the opportunity to develop valley cross-sectional analysis beyond the transect technique has not yet been realised.

A notable exception to the above was Phillips' (2009) work which developed a method for finding the average U-shape of whole valley sections. Effectively this method is the equivalent of deriving and averaging many thousands of transects for a valley. The whole valley shape is being sampled, which increases the sample size and avoids the difficulty of whether a transect is representative. In his work Phillips (2009) sampled 150 25km² DEMs, of which 75 represented fluvial landscapes and 75 glacial landscapes, effectively a sampling hundreds of thousands of transects. This research aimed to find geometry values which gave the best distinction between fluvial and glacial valleys using DEMs and GIS techniques. For the study areas both general and specific geomorphmetry measures were analysed with the aim to find the best descriptor of glacial and fluvial landscapes. Of the wide ranging techniques attempted specific measures of cross-sectional valley shape were deemed to show an excellent distinction between valleys. Particularly successful measures included valley width and depth and the most successful was the valley cross-sectional area (Phillips, 2009). Interestingly, the *b*-value of the average valley profile was not found to be successful (Phillips, 2009). This is curious given that existing literature argues that the *b*-value is able to define valley shape and, therefore, the process which created it.

2.9. Summary

Technological advances in DEM availability and resolution, as well as the ability for GIS software to handle and manipulate large volumes of data, has presented the opportunity to develop techniques for analysing glacial valley cross-sectional profiles using a more automated method than the previously used transect technique. This thesis exploits this opportunity, whilst developing Phillips' (2009) average valley technique further, making it more user friendly and able to handle large study areas. In these study areas, which can include whole mountain ranges such as the Pyrenees or span mountain divides of larger mountain ranges such as the southern Andes, measures

of valley shape and size can be quantified and spatial variability explored. It is anticipated that such an approach should provide a firmer quantitative basis for assessing glacial valley shape and create a basis for calibrating or testing landscape evolution models.

3. Thesis strategy

3.1. Introduction

This chapter outlines how the thesis tackles the research aim of investigating variability in valley cross-sectional characteristics. It considers how valley cross-sections are expected to change across mountain ranges and through time. A major component of the research was to devise a practical methodological approach for investigating valley cross-sectional variability. This is discussed and techniques and quantitative measures for valley cross-sections are evaluated. From intuitive expectations of how valley cross-sections might vary a range of hypotheses and objectives are outlined.

3.2. Measures of cross-sectional valley form

In order to quantify the cross-section of U-shaped valleys, and thus the degree of shaping, specific measures which represent the valley cross-sectional form must be chosen. The *b*-value of a parabolic equation has been shown to represent the degree to which a valley has been altered from a fluvial V-shape to a glacial U-shape (Svensson, 1959). Graf (1970) employed the form ratio measure to constrain the relationship between valley width and depth. The relationship between the *b*-value and form ratio also can be investigated. Hirano and Aniya (1988) suggest that this relationship indicates the type of glacial valley, either 'Rocky Mountain', in the case of valleys which become deeper with increased *b*-values, or 'Patagonia-Antarctica', where larger *b*-values are found as valleys become wider relative to depth (Hirano & Aniya, 1988). Form ratio and *b*-values do not, however, describe valley size. Phillips (2009) found that the cross-sectional area, a descriptor of valley size, was actually the best discriminator between fluvial and glacial valleys, due to glacial valleys being larger than fluvial valleys.

Together, it is argued *b*-value, form ratio, *b*-value/form ratio relationship and cross-sectional area, provide good measures of glacial valleys. Throughout this thesis the informal term *U-ness* will be used to describe these profile cross-sectional measures and to what extent a valley approaches that of the idealised U-shape believed to arise from glacial erosion.

3.3. Expectations

3.3.1 Ice residence time

Perhaps the length of ice occupation in a landscape can be indicated by the degree to which glacial landforms have developed, such as the extent of *U-ness* in valleys. Whilst many reconstructions of ice sheets focus on the maximum ice extent, it is the case that from an erosion point of view, the length of time ice has been in existence is key to the development of glacial landforms (Porter, 1989). Such residence time is a consequence of climate. Colder conditions, which result in a lower snowline altitude and, therefore, a greater ice accumulation zone (Egholm *et al.*, 2009), create more prolonged periods where ice is in existence. Greater ice residence times enable more glacial erosion to take place (Harbor, 1992) and therefore more glacially distinct landforms develop. As a result, glacial valleys should show signs of greater *U-ness* in landscapes which have been subject to longer ice residence times. This assumes that glacial erosion increases with ice residence time. Proportional responses have been successfully employed in other research (e.g. Brook *et al.*, 2006), where space was used as a proxy for time (as it was known that more northerly valleys had undergone greater glaciations than southerly ones) to determine the role of glaciations in the evolution of valley cross-sections.

In addition to regional climate, temperature gradients arising from elevation influence ice residence time. High elevations have cooler conditions which allow ice accumulation. Consequently the highest elevations can maintain the most favourable conditions for ice occupation and therefore have the greatest ice residence times. The highest elevations in a mountain range are found at the mountain divide, and lower elevations towards the mountain range periphery. Ice residence time is therefore greatest at the divide and decreases with distance away from the divide. Where valley form is concerned, the expectation is that greatest *U-ness* is found where there has been greatest ice residence time, at the highest elevations (Figure 3.1) and closest to the divide (Figure 3.2 and 3.3). Therefore elevation and distance from the divide are used as proxies for ice residence time in this thesis. Such a proxy is used because direct measurements of ice residence time are usually unavailable.

There are examples of similar proxy use in various earlier studies of glacial landscapes. Brook *et al.* (2006) used distance from the divide as a proxy to understand the development of U-shaped valleys. They found that where ice occupancy was greatest,

near the divide, so were glacially distinct valleys. By identifying the spatial variability in glacial valley cross-sections insights into valley evolution can be gained.

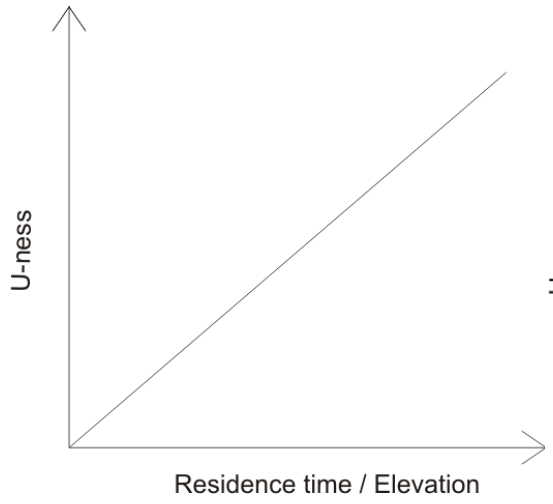

Figure 3.1 *U-ness* should increase with increased ice residence time. Ice residence time is greatest at the highest elevations where conditions for ice occupation are most favourable.

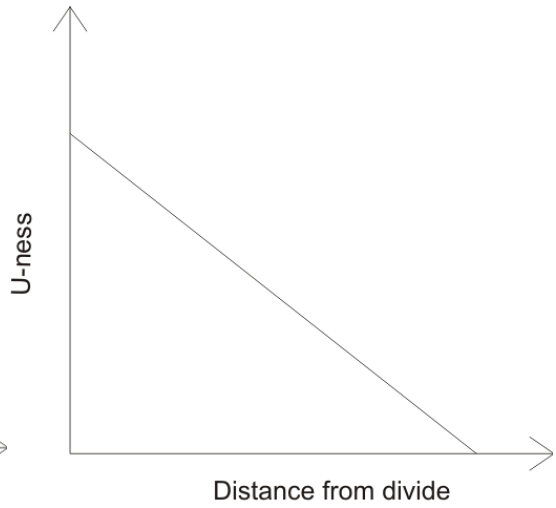

Figure 3.2 As distance from the divide increases *U-ness* should decrease. This is because the highest elevations are found at the divide and therefore the greatest ice residence time.

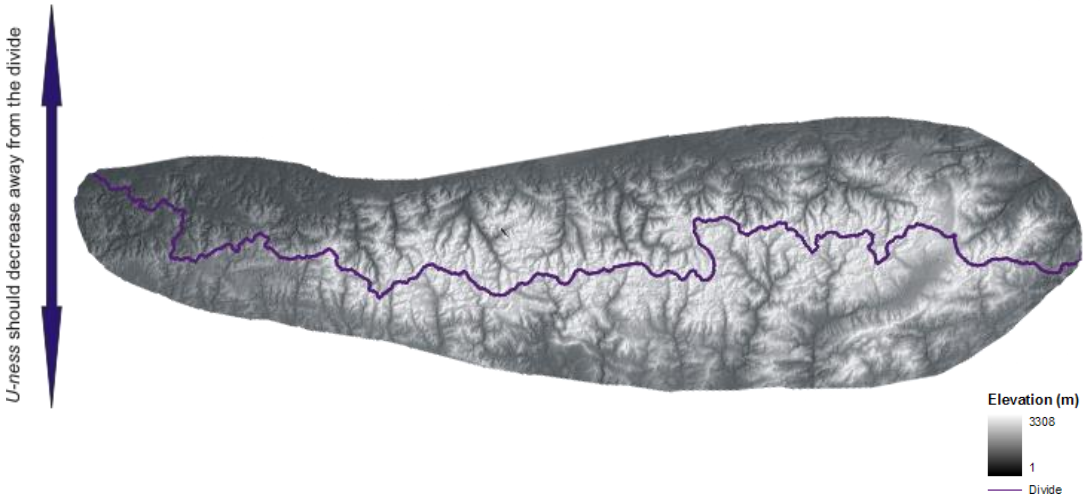

Figure 3.3 A DEM of the Pyrenees with the mountain divide shown. *U-ness* should decrease away from this divide as the landscape has had less glacial influence.

3.3.2 Ice Flux

Ice flux is the amount of ice which moves through any specific location per unit of time. The movement of ice occurs both by internal deformation and sliding at the ice/bed interface. Where sliding occurs so does erosion and the intensity of erosion is widely thought to have a positive relationship with sliding velocity. Past modelling experiments, for example, have often scaled erosion with sliding velocity (e.g. Harbor, 1992). In addition, effective normal pressure, influenced mainly by ice mass, has been demonstrated to have a more complex relationship with erosion rates (Boulton *et al.*, 1974). For example fluctuations in water pressure have been shown to be more effective for plucking-type erosion than constant effective normal pressure (Iverson, 1991). Taking both ice mass and velocity into consideration, despite some complexity regarding effective normal pressure, it is generally assumed that as ice flux increases so does the erosion rate (Figure 3.4). Within a glacier the greatest ice flux is found beneath the Equilibrium Line Altitude (ELA) (Hallet *et al.*, 1996), where the accumulation zone becomes the ablation zone (Figure 3.5) and the glacier cross-section and velocity are at their maximum. It is at the ELA, therefore, that the maximum erosion rate is expected and consequently *U-ness* should be greatest. However, this is complicated by the fact that the ELA moves as the glacier advances and retreats and is therefore not a fixed location. The average ELA is the location where the greatest ice flux has occurred throughout all glacial periods. It is at this location of the average ELA that the greatest cumulative erosion should have taken place and therefore where the greatest *U-ness* is expected.

Hallet *at al.* (1996) proposed that ice flux scaled with catchment area. A range of studies have used this concept to interpret valley morphology. Studies have analysed the relationship between catchment area and valley cross-section finding a positive relationship with various measures of valley size, such as valley cross-sectional area, valley width and depth (Haynes, 1972; Roberts & Rood, 1984; Augustinus, 1992b; Montgomery, 2002; Brook *et al.*, 2003; Amerson *et al.*, 2008). These studies indicate that as catchment area increases so do measures of valley cross-section due to their potential for greater ice flux. These studies therefore suggest that catchment area is a suitable proxy for ice flux and as such catchment area will be used as a proxy for ice flux in this thesis.

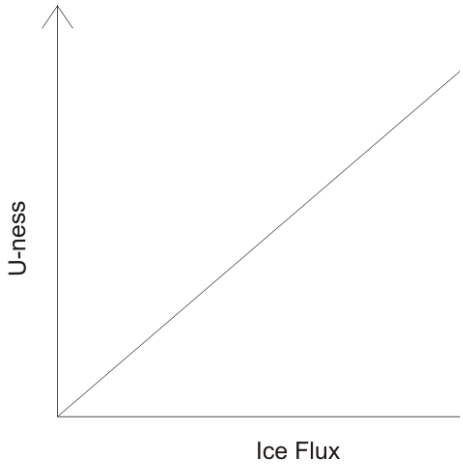

Figure 3.4 As ice flux increases so should *U-ness*.

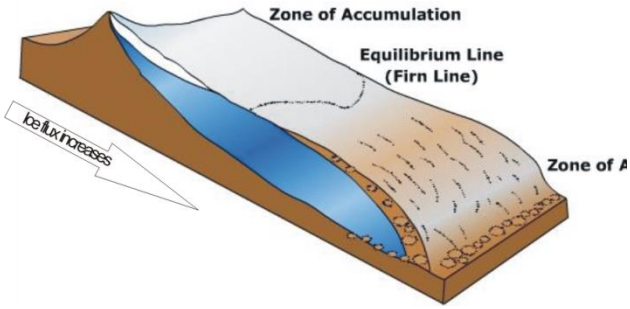

Figure 3.5 Unlike residence time ice flux increases down valley to a maximum at the ELA.

3.3.2.1 Residence time / ice flux confounding problem

The expectations outlined above, where greatest *U-ness* is expected at locations of longest residence time (highest elevations), whilst also at the point of greatest ice flux which increases down glacier towards the average Equilibrium Line Altitude (ELA), clearly work against each other. The problem to where greatest *U-ness* is found is caused by the residence time and ice flux expectation being in opposition which will influence the spatial distribution of *U-ness*. Taking this complication into consideration the greatest *U-ness* values are anticipated to be found somewhere between the highest elevation and the average ELA location (Figure 3.6).

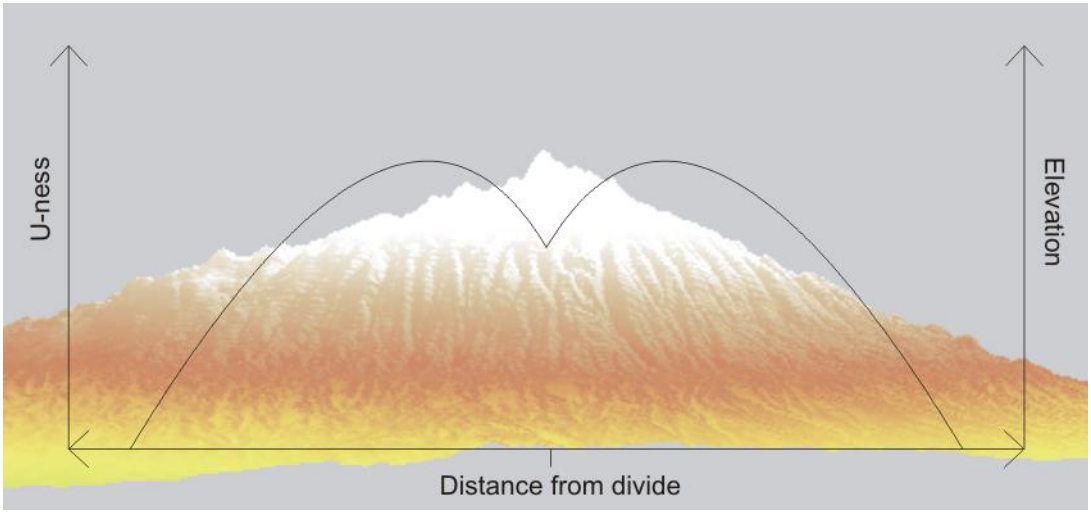

Figure 3.6 Due to residence time being greatest at the highest elevations whilst ice flux is greatest at the average ELA position, the interaction between these two factors might result in the greatest *U-ness* occurring part way down a valley and not at the highest elevation, mountain divide or average ELA position.

3.3.3 Lithology

Increased intensity of erosion from greater ice flux or residence time could be enhanced if the lithology of the bed is less resistant to erosion. It is therefore initially assumed that glacial valleys will develop more rapidly in weak than in highly resistant lithology (Figure 3.7). A secondary consideration is one highlighted by Augustinus (1992a) and Brook *et al.* (2004a) which states that valley cross-sections adopt different forms due to how resistant the bedrock lithology. Deep narrow valleys form in highly resistant lithology whilst wide, relatively shallow, valleys occur in less resistant lithology. Such contrasts in form ratio, combined with form ratio relationship with *b*-values, have been identified as a Rocky Mountain and Patagonia-Antarctica type valley respectively (Hirano & Aniya, 1988) (Figure 3.8). In order to test hypotheses with regards to lithology the sample areas chosen should reflect a range of different bedrock resistance to glacial erosion.

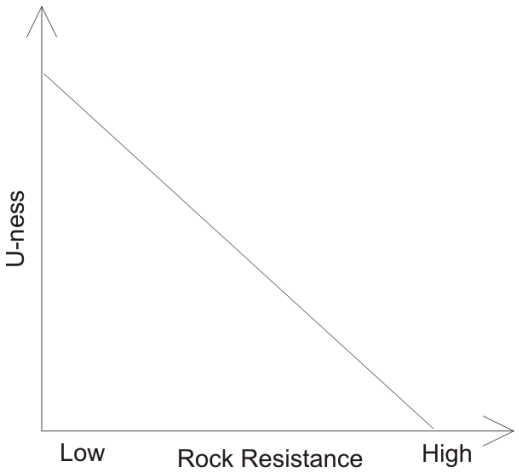

Figure 3.7 Valleys with low resistance to erosion should display greater *U-ness* measures than valleys found in highly resistant lithologies.

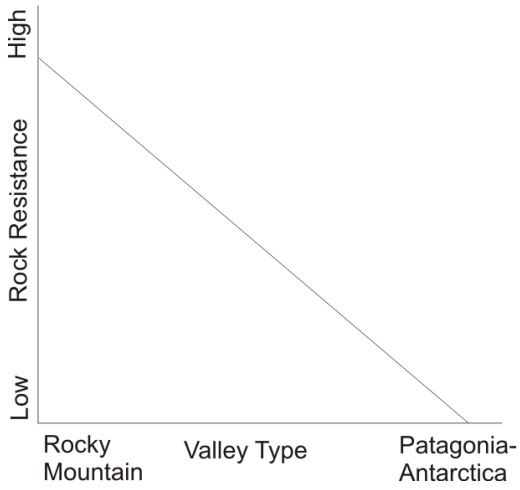

Figure 3.8 The impact of lithology is illustrated with highly resistant rock conforming to a Rocky Mountain valley type, whilst low resistant geology tends to a Patagonia-Antarctica valley shape (Augustinus, 1992a; Brook *et al.*, 2004b).

3.3.4 Tectonic Uplift

A further impact on glacial landforms, such as U-shaped valleys, is the tectonic uplift rate during glaciations of a region. It has been proposed that as uplift increases so does fluvial erosion (Burbank *et al.*, 1996). This is due to attempts by fluvial processes to gain base level equilibrium by rapidly incising the enhanced longitudinal valley floor slopes. Glacial erosion rates should increase due to increased accumulation areas contributing to greater ice flux (Brozović *et al.*, 1997) and field data of sediment exhumed from glacial basins of differing sizes (Hallet, Hunter and Bogen, 1996). Large glacial basins show high sediment yields (Hallet, Hunter and Bogen, 1996). U-shaped valleys should reach a classic glacial form more quickly in areas of high uplift as glacial erosion is enhanced by active tectonic uplift (Figure 3.9). Consequently it is important that areas which experienced intense tectonic uplift during glaciations are included in the sample areas and compared to tectonically stable areas.

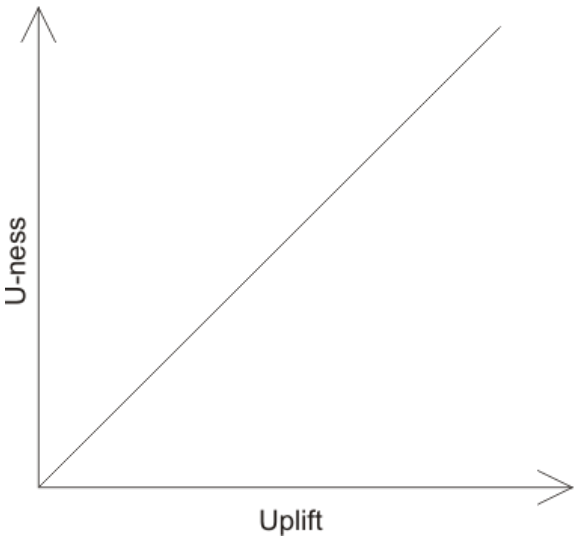

Figure 3.9 As uplift increases so does erosion and therefore *U-ness*.

3.4. Method

The individually selected transect method, used by the majority of valley cross-section studies, is not used here due to its subjectiveness and limitation with regard to sample sizes. Instead, the method adopted is the Phillips (2009) average valley profile method. It is favoured as it eliminates any bias of drawing transects, encompasses the whole valley rather than just giving a snap shot of the valley and has the potential for semi-automating analysis over large areas. Currently the method has been used on areas of 25km². For the method to be used in this thesis it needed to be developed to cope with larger areas so that it is possible to analyse whole mountain ranges. Once this is achieved the method can become a powerful tool in understanding glacial valley morphology and spatial variability. The existing method also currently uses a separate piece of software; LandMapR© toolkit by LandMapper Environmental Solutions, for some of the stages of data processing. To make the method more user-friendly an improvement would be to integrate it entirely into one piece of software, such as ArcGIS. Shuttle Radar Topography Mission (SRTM) DEMs are freely available via internet downloads giving 90 m resolution data for most of the globe. These DEMs can provide the data needed to analyse carefully selected study areas in ArcGIS.

3.5. Research Aim

The aim of this thesis is to take a new data-rich approach to investigate the cross-sectional size and shape characteristics of glacial valleys and assess their spatial variability. A key aim is to derive and use a means of assessing valley shape continuously along valleys rather than sampling selected cross-sections. The main purpose is to quantify valley shape to assist comparison with simulations of Landscape Evolution Modelling and seek underlying controls.

3.6. Thesis Objectives

1. **To develop a pragmatic whole valley means of cross-valley assessment which permits measurement at the mountain range scale.**

   Phillips (2009) started development of a method which used the concept of an average valley profile whereby an average cross-sectional profile was extracted from valley sections rather than individual profiles. One of the advantages of this method is that it enables the processing of large volumes of data on a semi-automated basis. In order to carry out experiments using any average cross-section method within this thesis suitable sample areas are selected.

2. **From the average valley cross-sections extracted from landscapes by the method mentioned above, determine values for valley shape and size and their spatial variability across mountain ranges.**

   Together with the spatial variation of valley measures greater understanding of valley development and the processes which contribute to valley form can be inferred.

   Landscape EM modellers need to check to see if their models produce landscapes that resemble those found in Nature. This is difficult to achieve because if any particular area is chosen, whilst the resulting landscape is known, the initial conditions with which to start the numerical experiment are not known. For example, what was the starting landscape and its geology and climate over hundreds and thousands of years? Rather, the empirical data/model comparison is probably best achieved by asking whether the LEM produce valleys of the appropriate scale, dimension and variations spatially. The dataset in this thesis will produce a large dataset (10,000s) of valley cross-sections in an accessible format for comparison with modelled valleys.

3. **It is logical to suppose that ice flux and residence time work against each other. Is this the case or is there a primary control?**

   Whilst a confounding problem has been widely suggested (e.g. Porter, 1989), attempts to investigate and quantify it are limited. In this thesis the confounding effect of ice flux and residence time on valley morphology will be explored.

4. **How consistent is valley form within sample areas, valley systems and between adjacent valleys? Or do small localised differences have a strong influence on valley morphology?**

   Given similar overall conditions; climate, tectonics, glacial intensity and lithology, how similar are adjacent valley morphologies? How much do local effects influence valley morphology, such as slight differences in aspect? Or are these negligible?

5. **Interpret the valley cross-section morphology dataset in the context of previous literature. Does the dataset support current thoughts on landscape evolution and can it be explained by current process understanding?**

   Is it really possible that valleys can be defined by the processes that they have undergone? Can fluvial or glacial valleys simply be defined by a V or U cross-profile form? And therefore is it justified to use the transition between the V to U forms as a continuum to deduce landscape evolution timescales?

   The glacial valley morphology literature accepts a parabolic valley form to be the idealised glacial valley, but how frequent is its occurrence in real landscapes? Are there any particular valley measures which perform best at discriminating between fluvial and glacial valleys?

6. **Do landscapes with more favourable conditions for glacial erosion show a more mature valley morphology?**

   Are greater *U-ness* measures found with greater latitudes? Does the orientation of the mountain range affect *U-ness*? Does uplift affect the glacial valley form? And how does geology impact on the valley cross-section morphology?

7. **The valley cross-section is one element of the valley morphology. Is there a link between the cross-profile evolution of valleys with its longitudinal profile?**

   It is widely acknowledged that the cross-profiles of valleys tend towards a parabolic form with glaciation whilst the longitudinal profile flattens when evolving from a fluvial valley form. Previous research has dealt with the cross-section and longitudinal profiles independently. In this thesis understanding of

the cross-sectional evolution of glacial valleys will be linked to the longitudinal valley development.

3.7. Summary

Using process knowledge, modelling and the geomorphological literature, hypotheses of expected outcomes have been developed to direct the research in this thesis and to develop the thesis objectives. By simplifying and separating out ideas which influence valley development these thoughts can be tested. The objectives support the overall aim which is to investigate the cross-sectional size and shape characteristics of glacial valleys and their spatial variability.

4. Method for measuring cross-section profiles of whole valley segments

4.1. Introduction

The method detailed in this chapter was developed to overcome the problems presented by the transect method used to date. It utilises advances in Geographical Information System (GIS) software and the wider availability of Digital Elevation Models (DEMs) to develop a method which can assess valley shape of large areas. In this method, GIS is used to measure valley profiles using a semi-automated approach and then analyse the results spatially in order to assess spatial variability and infer valley development.

Beyond mapping techniques the full potential of GIS has not been exploited by glacial geomorphologists (Napieralski *et al.*, 2007). In this chapter the use of GIS tools and GIS spatial analysis capabilities are integrated into a method which quantifies valley cross-section shape, size and variability. It is an example of the potential advances which are possible in glacial geomorphology if the full suite of GIS tools are used effectively.

4.2. Traditional methods for assessing valley cross profile shape

The cross-sectional profiles of valleys, and particularly the striking difference between fluvial and glacial valleys, have been studied for over a century (e.g. Davis, 1906). Fluvial valleys have commonly been associated with a 'V' shaped cross-sectional profile whilst glacial valleys a 'U' shape. Svensson (1959) suggested the parabola as an appropriate mathematical representation of a glacial valley cross-section. Through numerical modelling, Harbor (1992) showed how a valley develops into a U-shape. Further to this, observations of spatial changes in the U-shape of a valley have informed the timescales

involved in valley development, and relationships with climate, tectonics and topographic evolution (e.g. Graf, 1970; e.g. Brook *et al.*, 2008).

Traditionally valley cross-sectional profiles have been examined by drawing individual transects across a valley using a map with elevation denoted by contour lines (e.g. Doornkamp & King, 1971), and more recently using DEMs (e.g. Brook *et al.*, 2008). The transect method of examining valley cross-sections is both time consuming and subject to errors due to the subjective nature in which the transects are drawn. Transects are a snap shot of the whole valley and only small samples can be collected. It is possible that transects are selected to best represent a 'U' form. They are not representative of the valley as a whole. This thesis will investigate a whole valley approach to seek an alternative dataset. Individually selected transects do have some limitations and are sensitive to several factors which influence the result. These are identified as:

1. Transects are drawn to bisect contour lines but this can be difficult where a valley bends.
2. The arbitrary nature of where profiles are drawn, this may not be representative of the whole valley or area of interest.
3. Only small areas can be analysed, mainly due to the time consuming nature of this method. Small sample sizes may not show a good representation of a landscape.
4. Tributaries complicate where transects can be drawn.
5. It is difficult to determine exact position of the valley top and therefore where a transect should start and end.
6. It is a discrete sampling method.

Today there is widely available elevation data in the form of DEMs, and GIS provide the software capable of analysing this data. However, despite these technological developments, no automated process of analysing valley cross-sectional profiles over large areas (whole mountain ranges) has been developed. Many researchers are still using the individually selected transect method. Figure 4.1 demonstrates some of the problems with the transect method. Three transects are drawn at slightly different orientations across a valley. Although these profiles appear fairly similar the *b*-values show considerable different values, ranging from 1.24 to 1.37 for the left-hand side of the valley and, more significantly, 1.33 to 2.04 on the right-hand side. This is probably not only due to the orientation to which the transect bisects the valley, producing

slightly different cross valley shapes, but also due to the difficulty in defining the start and finish points of the transect. It also may reflect the sensitivity of the fitting of the power-law curve to the data. The final transect shows the problems which arise when a tributary disrupts the cross-sectional profile of a transect.

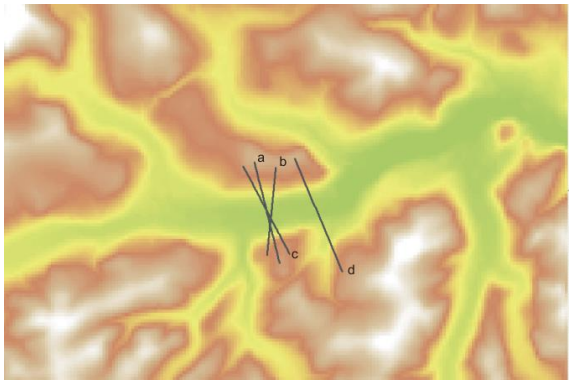

a.

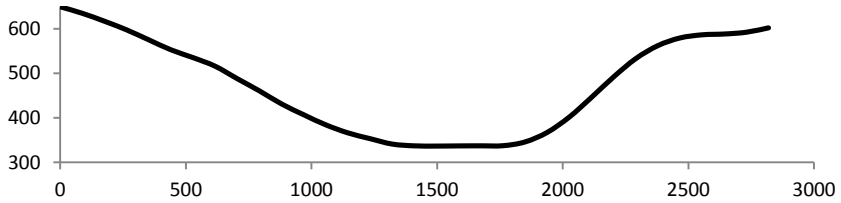

Left-hand *b*-value = 1.35 Right-hand *b*-value = 1.33

b.

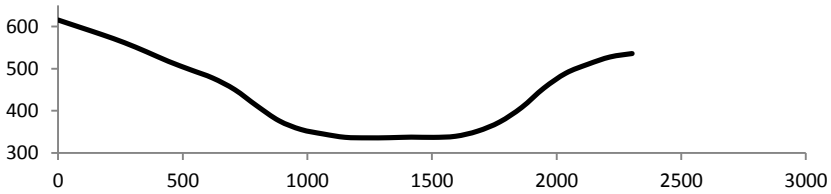

Left-hand *b*-value = 1.24 Right-hand *b*-value = 2.04

c.

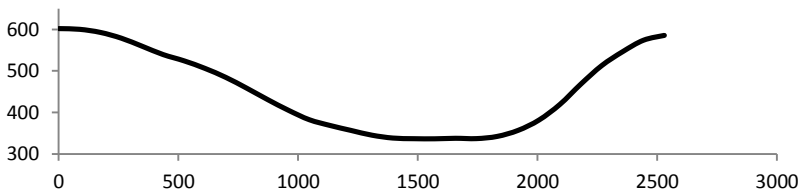

Left-hand *b*-value = 1.37 Right-hand *b*-value = 1.88

d.

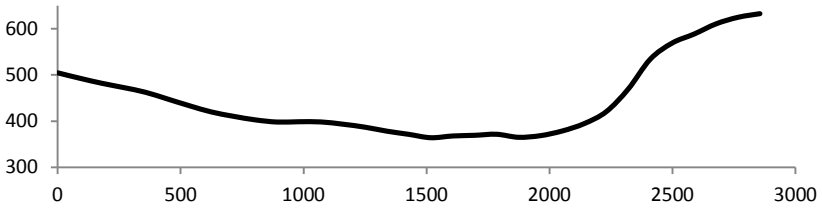

Left-hand *b*-value = 1.44 Right-hand *b*-value = 2.08

Figure 4.1 Transects drawn across a valley in the Cairngorms, Scotland, show the inconsistencies which can arise from the individually selected profile method. Profiles a – c show how profile orientation can alter results especially for valley *b*-values. Profile d demonstrates how the presence of a tributary can disrupt the valley profile making it difficult to draw transects which are representative of valleys with many tributaries.

4.3. Conceptual basis for method

4.3.1 Phillips method

Phillips (2009) began to tackle the problem described in Section 4.2, developing a semi-automated method to distinguish between fluvial and glacial derived valleys. He used GIS to analyse landscape geomorphology from DEMs. The average cross-profile method used ArcGIS and LandMapR software to modify a DEM. It generated a framework for sampling valley dimensions enabling the selection of valley statistics to be consistently sampled across different valley scales and shapes. This method produces average cross-sectional profiles which are generated for areas where the sampling framework is applied. It was demonstrated that this method worked well for the sample areas selected, producing an average cross-sectional profile for each sample area (i.e. whole valleys in a DEM). However, there are several practical problems with this method:

4.5.1.1 The LandMapR element of the method is not integrated into ArcGIS making the method less efficient. An additional concern is that the processes undertaken in LandMapR are concealed and therefore difficult to fully understand.

4.5.1.2 Average cross-sectional profiles are only realised for the entire sample areas or groups of valleys, such as stream order groups, rather than individual valleys. Therefore the spatial variability of a sample area cannot be analysed.

4.5.1.3 The method is computationally intensive, only allowing for relatively small sample areas to be analysed.

If these obstacles are overcome the average cross-sectional profile method conceived by Phillips (2009) could be a powerful tool for understanding the spatial variability of valley cross-sections.

4.3.2 Fundamental concepts

One approach would be to devise a method which automatically draws thousands of transects across valleys (Figure 4.2) in order to extract cross-sectional profiles but the orientation and position of transects is of a concern (as discussed in Section 4.2). Instead, the landscape is manipulated based on the Phillips (2009) average valley profile method (Figure 4.3), so that an average profile for whole valleys can be found.

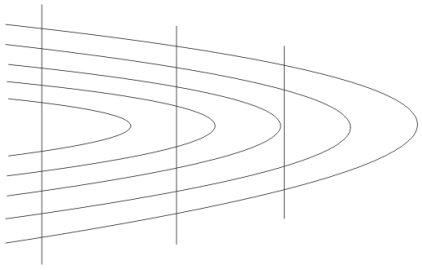

Figure 4.2 The traditional method of generating valley cross-sectional profiles. Here three transects have been drawn across a valley giving a discrete snapshot of valley shape and size.

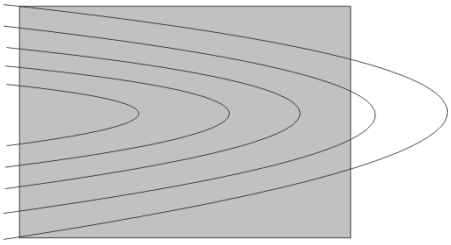

Figure 4.3 Greyed area shows the area which is used to find the average valley cross-sectional profile. This represents an infinite amount of transects and represents a continuous measurement of the whole valley.

Because valleys differ in scale, it is important that a sampling technique for extracting valley profiles (i.e. width and height or x and y values) is not biased by this. If values were taken at 10 m intervals from the valley centre then a bias would occur, under sampling small valleys (Figure 4.4) and oversampling large valleys (Figure 4.5). Therefore the method devised by Phillips (2009) used values at the location on the valley side at a percentage above the valley floor which resolved the sampling bias problem.

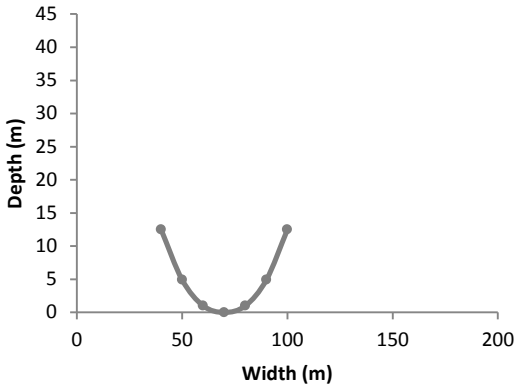

Figure 4.4 A small valley is under sampled if width and height measurements are taken at 10 m intervals from the valley centre.

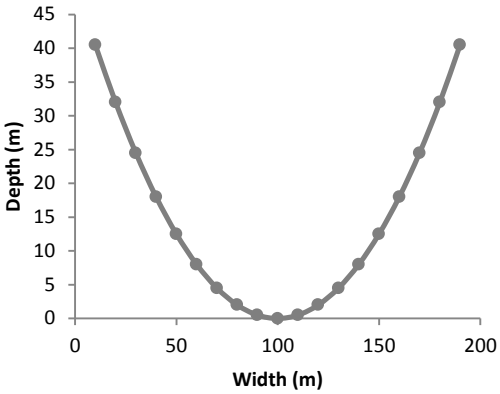

Figure 4.5 Whilst a large valley is over sampled if the same sampling method was used as in Figure 4.4.

To derive an average height and width at set percentage intervals above a valley floor the valley must be 'de-trended' (Figure 4.6 and 4.7). Valley size and shape is of interest in this thesis, yet valleys have a trend which is a longitudinal profile which slopes downstream. Within GIS the longitudinal profile of valleys needs to be de-trended so that the average values for valley width and height can be measured at regular percentage positions above the valley floor. To obtain a individually selected transect of a valley is not a problem as the values are found at discrete points (Figure 4.8), however if an average profile of a valley is desired then de-trending needs to occur (Figure 4.9).

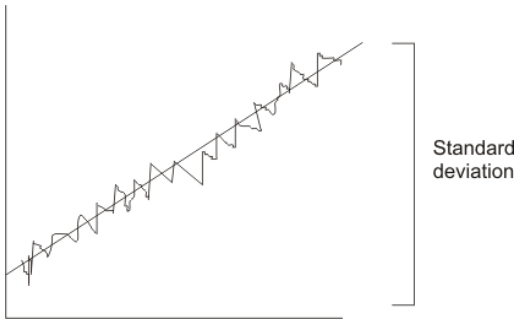

Figure 4.6 An example of rising trend where there is also variation. This could be temperature or the width or height of a valley at a specific percentage height above the valley floor.

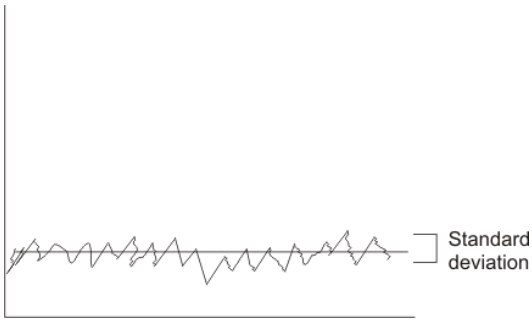

Figure 4.7 The same data as in Figure 4.6 but de-trended, therefore only showing the variation.

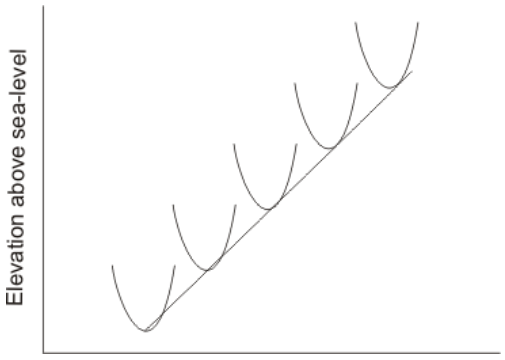

Figure 4.8 A typical valley with a downstream sloping longitudinal profile. Taking measurements for valley width and height at set percentage values above the valley floor would be difficult without drawing many transcects manually.

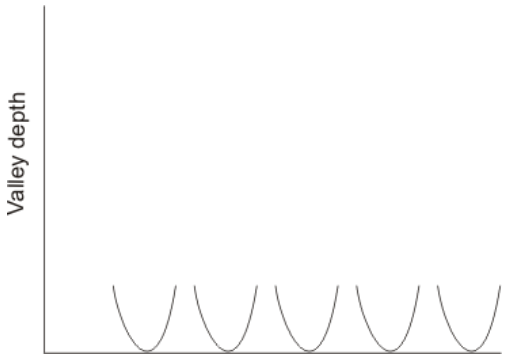

Figure 4.9 The valley in Figure 4.8 but de-trended. Now is far simpler to find an average value for the valley width and height at set points up the valley sides.

To de-trend valleys, so that a sampling framework can be created to sample valley dimensions at fixed positions on valley sides, the landscape must be manipulated. The result of this manipulation is that all the valley bottoms lay at zero whilst the ridges and peaks are assigned a value of 100. Once the landscape has been manipulated to form a surface known as the Normalised Elevation Model (NEM), the sampling framework can be extracted from it (Figure 4.10 and 4.11). The sampling framework is in the form of 'contours' at 10 unit intervals. Effectively, these 'contours' are the percentage slope position of the valley sides at 10% intervals above the valley floor.

a.

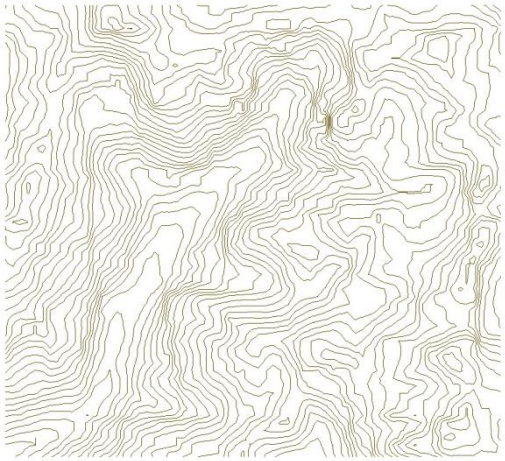

b.

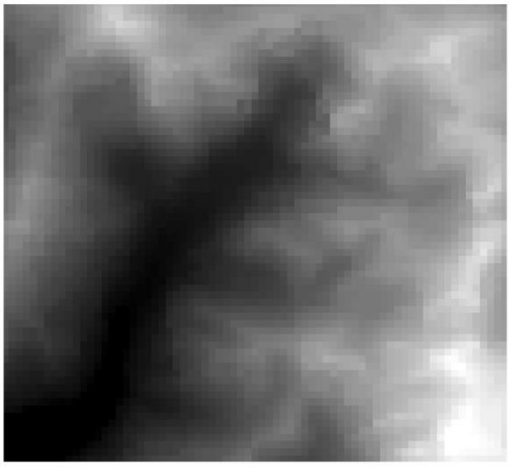

Figure 4.10 A DEM (b) with contours (a) at 20m intervals showing valley systems.

a.

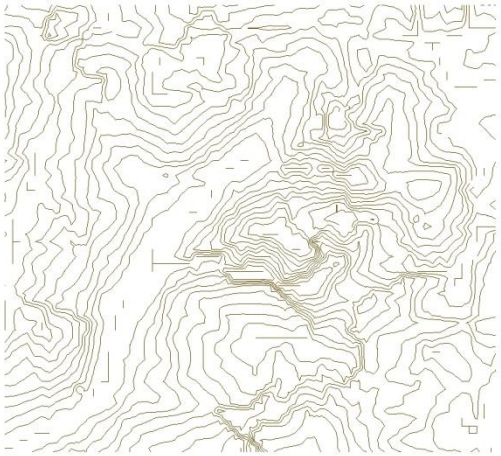

b.

Figure 4.11 The same area as in Figure 4.10, where the valley floors are manipulated to zero and the ridges at 100. The 'contours' shown are at 10 unit intervals above the valley floor (a). These equate to the valley slope positions at 10% intervals. The flattening of the valley longitudinal profiles can be seen (b).

For each sample area a local relief map (valley side height above local valley floor), as well as a map denoting distance from valley centre is derived. Using the sampling framework, values of local relief and distance from valley centre can then be found for each of the percentage slope positions (Figure 4.12 and 4.13).

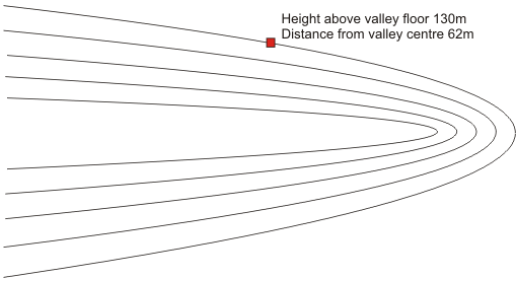

Figure 4.12 Sampling framework (% contours) showing a single data position for valley height and width values.

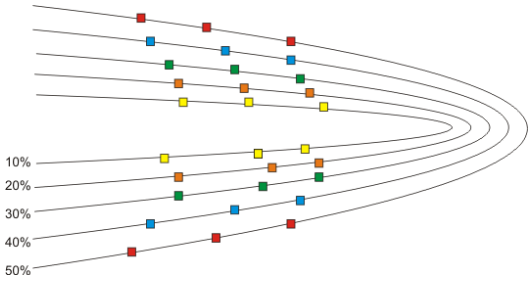

Figure 4.13 An example of six data points on each percentage sampling framework slope position. The values for valley height and width can be extracted at these points. These values can then be averaged to generate an average valley cross-sectional profile. In reality many more data points contribute to the average cross-sectional profile. The amount is dependent on the resolution of the original DEM.

In contrast to the transect method, where discrete profiles are found, the average profile creates an average cross-sectional profile by taking many local height and width values at each percentage slope position within a defined area. As both sides of the valley are used when averaging height and width values, a single valley profile is created. For the purposes of visual completeness this can be reflected across the y-axis to create a symmetrical valley cross-sectional profile. Figure 4.14 shows an average profile plotted with profiles of the same valley derived from the individually selected transect method.

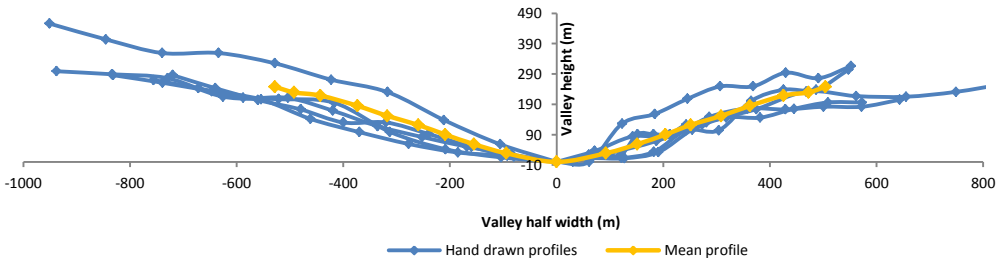

Figure 4.14 Six individually selected profiles of a 2nd order valley on Mt Kenya and the average profile derived for the same valley segment (this is derived from the new method and not merely the average of the individually selected profiles). The average profile is symmetrical as the method averages both sides of the valley; the method also has a smoothing affect when compared to the individually selected profiles. The average profile lies in amongst the individually selected profiles taken from the same valley visually confirming that the method does create a sensible average profile of the valley.

4.4. Overview of method

The method developed incorporates several stages which can be divided into four distinct data processing groups. Two of the stages, deriving valley segment profiles and deriving proxies, involve manipulation and analysis of DEMs within ArcGIS. The initial stage is deriving the mean valley segment profiles whereby valleys are divided into defined segments and then the values for the mean valley profile for that segment are found. From the defined valley segments proxies for ice residence time and flux can be found by a relatively simple process in ArcGIS. Proxies for the ice residence time and flux include the mean valley segment elevation and a value which represents the catchment area for the valley segment, respectively. The mean valley segment profile values, as well as the values for ice residence and flux proxies, are exported from ArcGIS into Excel and the next stage where measures representing *U-ness* are derived. Here a form ratio value can be found directly for each mean profile but for values representing cross-sectional area and *b*-values the mean valley profile values are required to be exported into Matlab where many profiles can be analysed at once. The cross-sectional area and *b*-value results from Matlab are returned to the dataset in Excel and relationships with the ice proxy values observed. Finally the completed dataset in Excel is returned to ArcGIS where spatial analysis can be undertaken. Figure 4.15 shows graphically the stages described above in a flow diagram. The method will be explained in this chapter with the aid of this flow diagram.

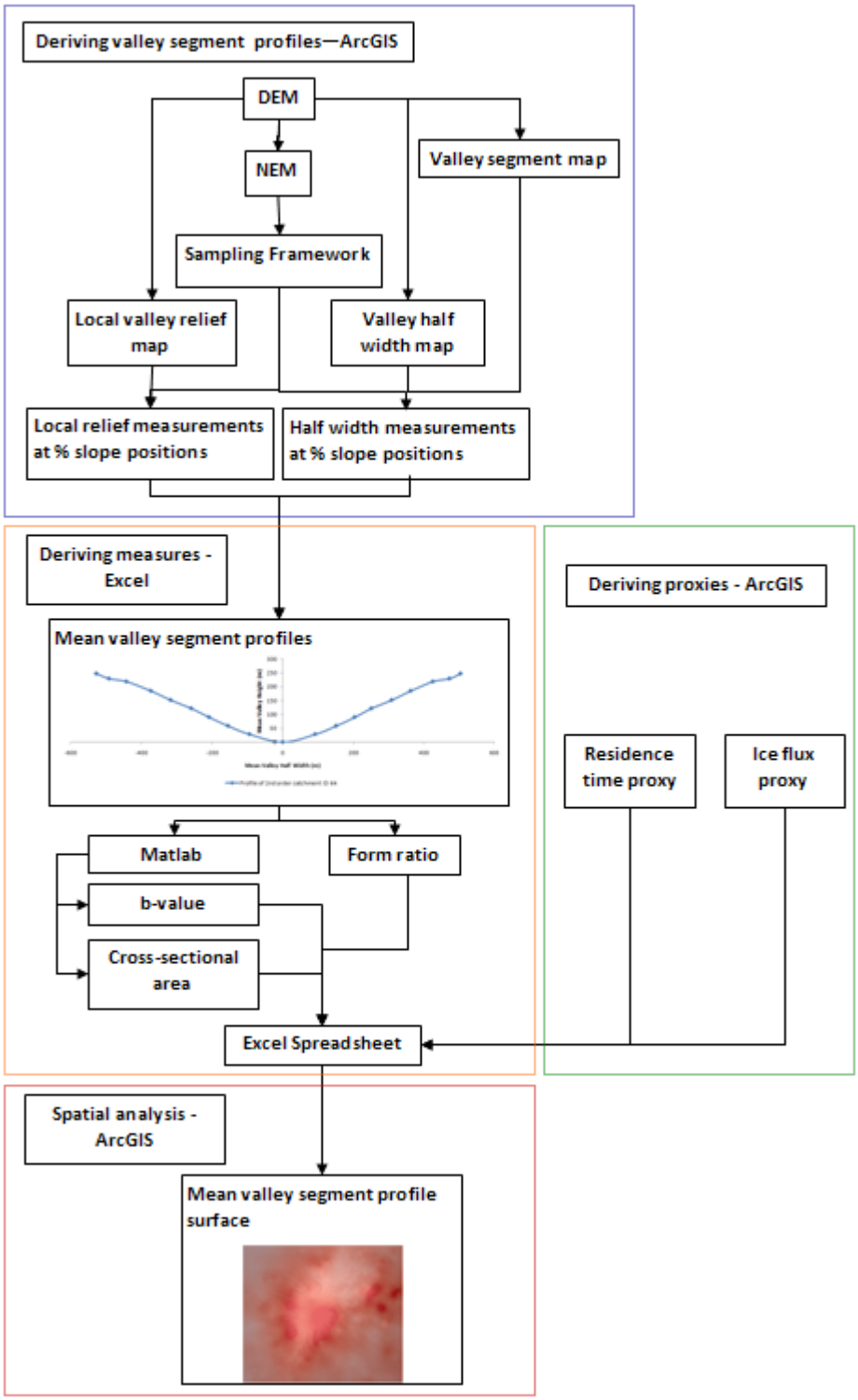

Figure 4.15 The stages undertaken in the average valley cross-sectional profile method. There are four key stages, 1) Deriving mean valley segment profiles in ArcGIS, 2) deriving proxy measures for ice flux and residence time in ArcGIS , 3)deriving measures of *U-ness* of these mean valley segments which is carried out in Excel and Matlab and finally 4) the returning of all the collated data to ArcGIS where spatial analysis can take place (e.g. how does *U-ness* vary away from the divide?).

4.5. Semi-automated method of deriving mean valley profiles using ArcGIS

The method, based on the Phillips (2009) method, but solely using ArcGIS to derive mean valley profiles is semi-automated in nature, in that the ArcGIS inbuilt tools are used to find a mean valley profile for defined valley segments. To implement the method a series of steps have to be taken in a set order, from processing the initial DEM to producing average valley profiles for each valley segment. These are summarised in the flow diagram below (Figure 4.16). ArcGIS software is used throughout this stage of the method.

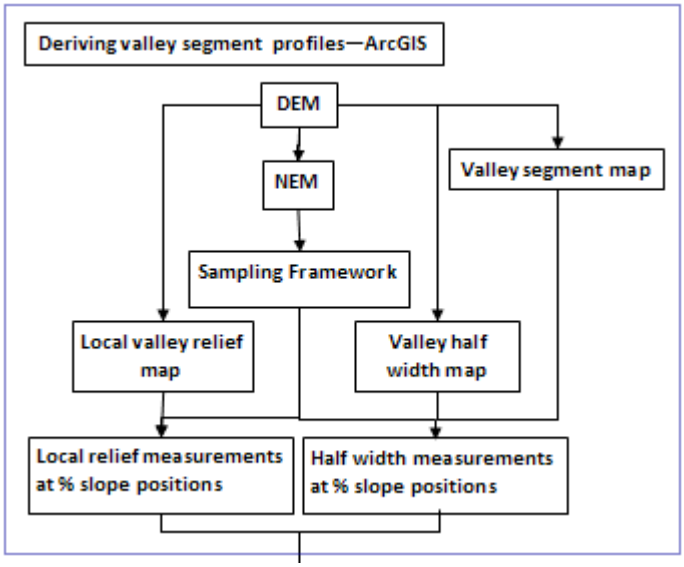

Figure 4.16 Flow diagram of GIS implementation of method.

4.5.1 Digital Elevation Model (DEM) pre-processing

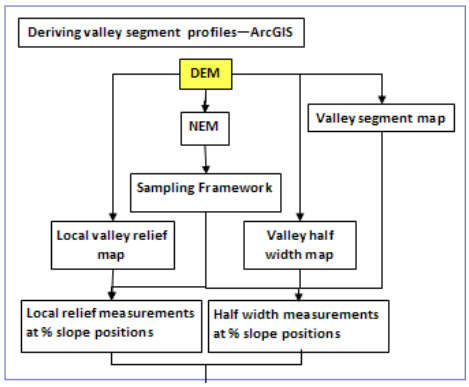

DEMs used in spatial and numerical analysis in ArcGIS must undergo several processes before analysis can take place. This pre-processing involves the selection of the sample area, projection of the selected area, followed by the correction of minor errors in order to create a hydrologically correct surface, therefore allowing unimpeded flow.

DEMs of suitable areas for investigation are selected (the strategy for selecting sample areas is covered in detail in Chapter 5). In ArcGIS this can be done using several methods one of which is using the clip tool. The sample area is then projected to the correct UTM map projection where the coordinates are in metres, using the inbuilt tool for raster projection in ArcGIS. Finally the DEM is processed so that the surface is hydrologically correct. This creates a surface where by depressions are filled so that subsequent flow surfaces and networks are not impeded by sinks which do not occur in the real landscape. The fill tool removes sinks, as well as spurious peaks, using a method where any depression is filled to the lowest level of its surrounding cells and peaks are levelled to a neighbouring cell's maximum value (Jenson & Domingue, 1988; Martz & Garbecht, 1992).

It can be argued that real glacial landscapes are fundamentally not hydrologically correct due to features such as overdeepenings but for the purposes of this research only hydrologically correct DEMs are used. This is justified by the fact that the DEMs used are not the scoured bedrock surface, they are the post-glacial surface which includes, sediment fill and the surfaces of lakes, which often conceal overdeepenings once ice recedes, and this is highlighted as a limitation in the summary conclusions of this thesis. Without a DEM being hydrologically corrected many of the GIS processing cannot take place as it relies on continuous flow from one cell to the next, and therefore this is a compromise which has to be made.

4.5.1.1 Using a DEM to create a surface which is normalised with respect to local relief

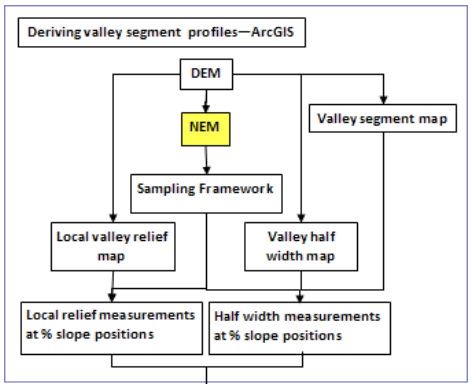

To extract mean cross-sectional values from valley segments a sampling framework is required. This framework allows for values to be taken from 0 to 100% valley slope position (at 10% intervals). To find where the 10% interval slope positions are for each valley the valley needs to be normalised with respect to local relief (i.e. de-trended). Once the DEM is normalised with respect to local relief, using the method detailed below, the result is a surface which is called a Normalised Elevation Model (NEM). In effect a NEM is created by giving all valley floors a value of zero elevation whilst peaks and ridges become a

value of 100. The valley slopes adopt the value proportional to their position between the minimum local valley relief (valley floor) and the maximum local valley relief (valley top which is the valley divide and could be a peak or ridge).

4.5.1.2 Finding the maximum and minimum slope positions for the NEM

To find the minimum and maximum local valley positions a drainage network is created. This is easy to do for the valley floors as a standard flow direction layer can be created using the filled DEM, a flow accumulation layer (created prior to the flow direction) and the flow direction tool can be used from the hydrology toolset. The standard flow direction tool uses the Deterministic 8 neighbourhood algorithm (Jenson & Domingue, 1988). A stream network can then be created by assigning a threshold of flow accumulation greater than 100 cells (Figure 4.17) (Jenson & Domingue, 1988; Tarboton *et al.*, 1991). However to find the peaks and ridges (i.e. the edges of the valleys), which constitute the maximum slope position, the DEM needs to be inverted so that the minimum elevation values are replaced by the DEM's maximum values. This is done by subtracting the maximum elevation found within the entire DEM from each DEM value. A ridge network is then produced from this inverted surface by creating a drainage network where the flow accumulation is, again, greater than 100 cells (Figure 4.18). Figure 4.19 shows both the delineated stream network and ridge network for Mt Kenya.

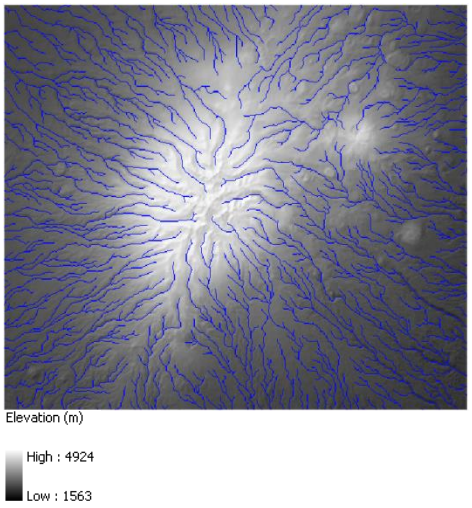

Figure 4.17 Original DEM with flow (stream) network. This stream network is used to define the minimum valley slope position.

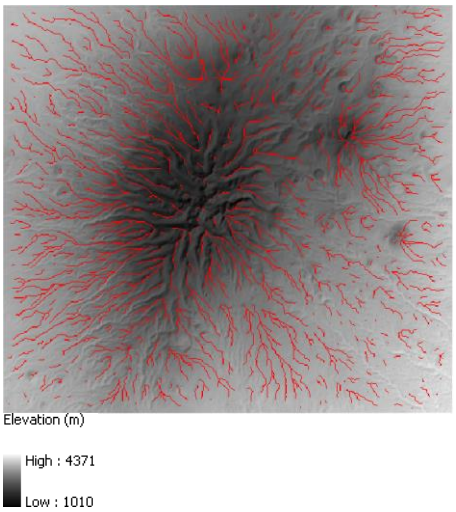

Figure 4.18 Inverted DEM with flow (ridge) network. This network is that which defines the maximum slope position. The network is not connected as the inverted DEM is not 'filled' as this would prevent the ridges and peaks from being indentified.

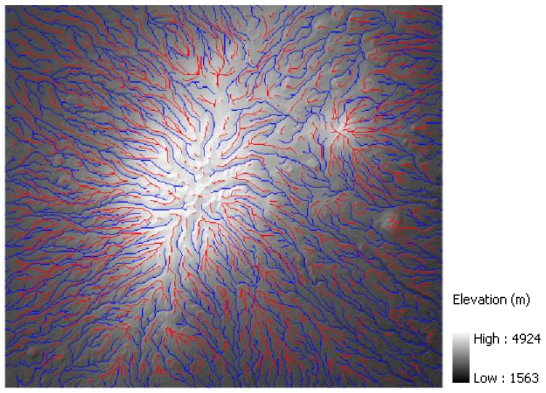

Figure 4.19 Shows both the stream network (minimum slope position, blue) and the ridge network (maximum slope position, red) which are used to define valley percentage slope positions where the stream network is the centre of the valley (i.e. 0% slope position and the ridge network is 100% slope position).

4.5.1.3 Justification of 100 cell threshold to create flow networks

The 100 cell threshold used from the flow accumulation layer to produce the stream and ridge network is the recommended threshold for ArcMap (Jenson & Domingue, 1988; Tarboton *et al.*, 1991) and appears to work well for the sample areas in the data library. The use of a single threshold to derive a drainage network from a DEM has been criticised in the literature and alternative methods suggested (e.g. Vogt *et al.*, 2003). Methods include 'burning in' a known, previously digitised, stream network (e.g. Beighley *et al.*, 2005) or a method based on landscape categorisation, like the criteria-based region growing method (CBRGM) by Colombo *et al.* (2007). In the CBRGM method it was found that in a European landscape the drainage network was mainly affected by relief and geology; the highest values for the categorisation being found in the Pyrenean and Alpine regions (Colombo *et al.*, 2007). As the areas which make up the data library were selected for their homogenous geology and mountainous relief it is therefore thought that a single threshold to derive flow networks is a suitable method. However a method demonstrated by Colombo *et al.* (2007) could be considered in the future for more complex landscapes.

4.5.1.4 Overcoming stream network delineation in flat areas

Although the standard ArcGIS tools provide a means of creating drainage networks some problems arise in very flat areas, such as the wide, relatively shallow valleys found in Patagonia-Antarctica type landscapes. Here stream networks creating by the standard ArcGIS toolset can often generate parallel streams in a network (Figure 4.20). This interferes with the creation of the NEM and therefore a more sophisticated tool is required which can tackle this problem.

The solution was to use the freely downloadable Terrain Analysis Using Digitial Elevation Models (TauDEM) tool (Tarboton, 1997) which is fully compatible with ArcGIS. This tool creates a flow direction layer which takes into account upslope and downslope areas therefore creating a drainage network without parallel flow paths. It also uses landscape curvature as well as contributing area to help to delineate a stream network Figure 4.21.

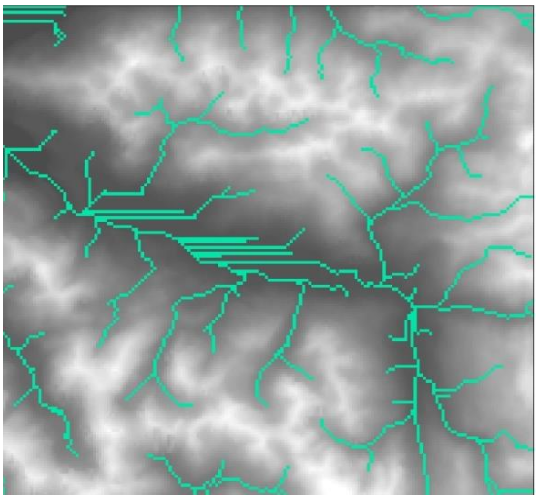

Figure 4.20 A stream network delineation using the standard ArcGIS. Note the many parallel streams.

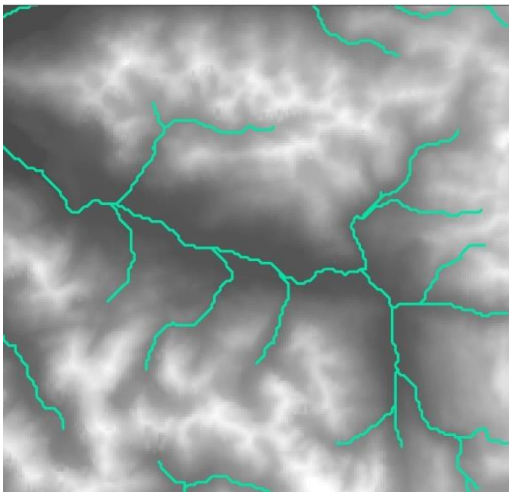

Figure 4.21 The same area as in Figure 4.20 where the TauDEM tool is used. It clearly shows the elimination of parallel streams in the flat valley floors and creates a more realistic stream network.

In nearly all cases a single stream in each valley can be achieved and is therefore a good framework for the minimum valley relief network. Where this does not occur, even using the TauDEM tool, the valley segments are eliminated from the dataset as it is thought that the valley floor is so infilled with glacial deposits or contains lakes that the valley would not be suitable for taking morphology measurements.

4.5.1.5 Using stream and ridge networks to create the NEM

To create the NEM a surface corresponding to the minimum elevations, identified from the stream network, and a surface representing the maximum elevations, identified from the ridge network, must be produced. These layers, as well as the filled DEM, can then be used in a calculation which produces the NEM, where all valley floors are a value of zero and ridges and peaks given a value of 100. The method utilises hydrologic analysis tools in ArcGIS to assign maximum and minimum values to the whole sample area.

The drainage networks created to represent the stream network (Figure 4.22) and ridge network (Figure 4.23) correspond to the local minimum and maximum elevation. As these networks are raster layers their individual cells can be populated with the value

from the DEM to which they spatially correspond. This creates a layer where each stream network cell has the elevation value from the DEM (Figure 4.24) and is repeated for the ridge network so that each ridge network cell now has the corresponding DEM value (Figure 4.25). To do this, as both the stream and ridge network cells have a value of one, the times tool is simply used with the DEM resulting in the DEM values being assigned to the networks. Where wide, flat valleys occur the ridge network occasionally extends down valley spurs into the flat area. This interferes with the next stage of the method and therefore the parts of the ridge network which extend to the valley bottoms are eliminated. This is done by deleting any of the ridge network cells which correspond to low slope values, found from a slope surface.

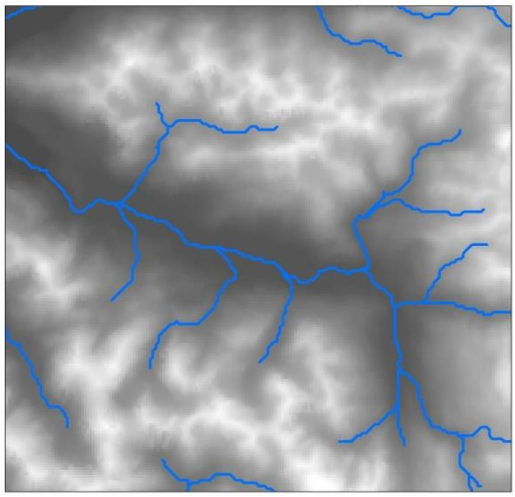

Figure 4.22 Stream network delineated using the TauDEM method to prevent parallel streams.

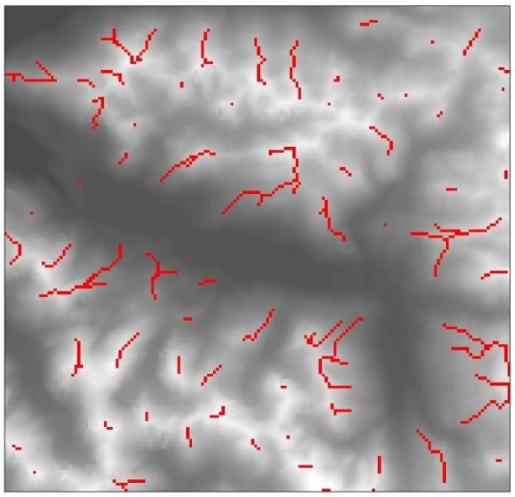

Figure 4.23 Ridge network of the same area as Figure 4.22.

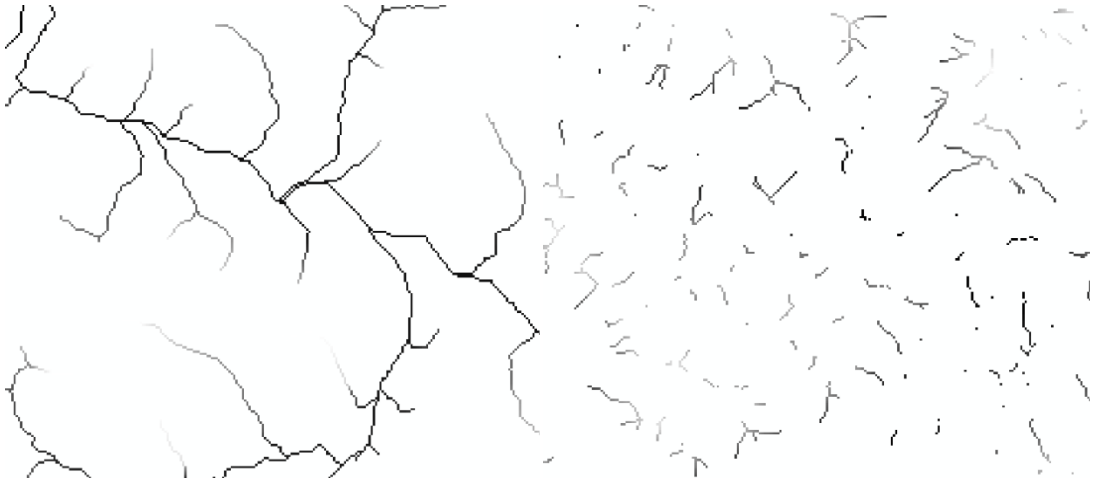

Figure 4.24 Stream network with DEM values. This creates a layer with all the local minimum local relief elevation values. Each pixel along the stream has a real elevation above sea level and is shaded in grey-scale accordingly above.

Figure 4.25 Ridge network, which has had values corresponding to low slope angles removed, populated with DEM values. Each pixel along the stream has a real elevation above sea level and is shaded in grey-scale accordingly above.

Following this, the entire sample area needs to be populated with the corresponding stream (minimum elevation) and ridge network (maximum elevation) values. To do this the watershed tool in ArcGIS is used. This populates the remaining cells with the minimum or maximum values by using the filled DEM and inverted DEM, respectively, to hydrologically delineated zones. Catchments are created for each individual network cell. These are areas which contribute flow to each of the network cells from which it originates (Figure 4.26). This is a simple step from the stream network stage as the flow direction produced from the filled DEM is used to create the catchments. However, for the ridge network, a flow direction raster of the inverted DEM needs to be produced in order to create these catchments (Figure 4.27). Some sections of the sample area are not populated with a value. This is especially true for the ridge network catchment surface due to the inverted DEM not being filled and therefore not being a hydrologically correct surface. To populate these data voids the maximum (or minimum, in the case of the stream network catchment surface) value in each data void is used to populate it. This procedure means that the ridge network catchment surface, as well as the stream network catchment surface, has a value for each cell in the sample area.

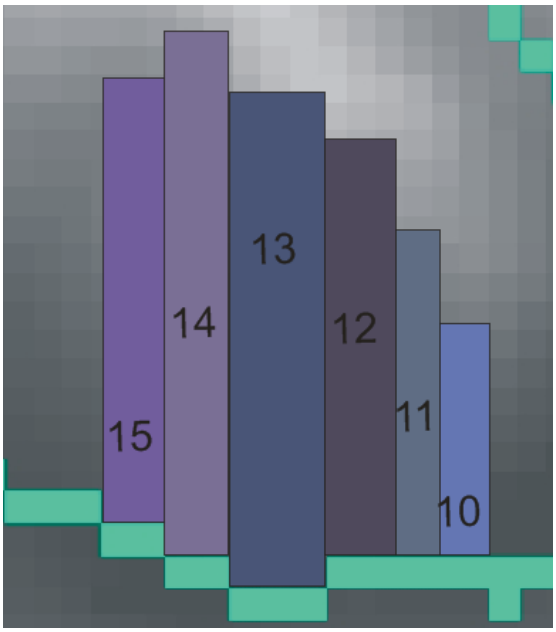

Figure 4.26 The sketch shows how the watershed tool is used to populated areas with the elevation for each stream network cell creating the valley floor watersheds.

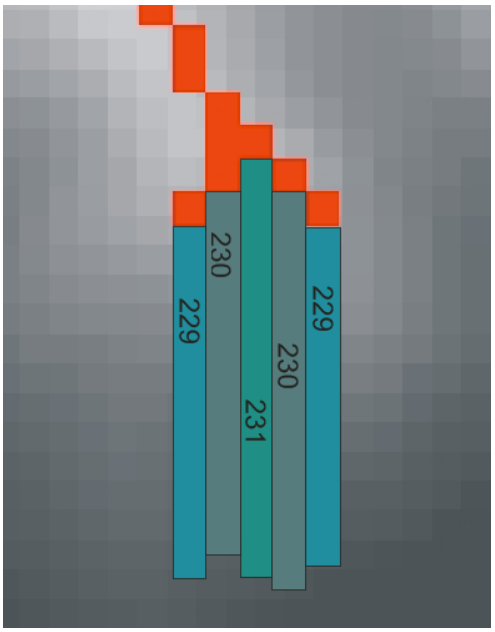

Figure 4.27 The sketch shows how the same method can be used to populate areas with the elevation value from the ridge network cells creating the ridge network watersheds.

Due to the longitudinal profile characteristics of fluvial and glacial valleys this method has slightly different response for different valley types. The method of dividing areas according to flow into a single network cell (stream or ridge network) appears to work well for U-shaped landscapes where the longitudinal valley profile is flatter than an upland fluvial landscape. This means that in a U-shaped valley the flow direction down the sides of the valley are perpendicular to the valley floor (Figure 4.28) rather than at an oblique angle which is the case for steep fluvial networks (Figure 4.29). Therefore, the steeper longitudinal profiles of fluvial networks mean that the valley floor watersheds (Figure 4.26) do not encompass the corresponding ridge cell perpendicular to the valley floor, they are instead slightly offset (Figure 4.29). However this is not such a problem with glacial landscapes and is therefore a valid method for use in glacial landscapes.

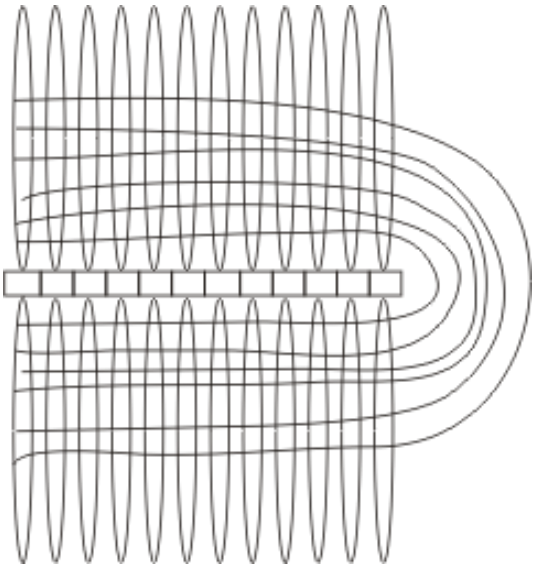

Figure 4.28 A sketch of a glacial valley with contours showing cell catchments running perpendicular to the valley floor cells.

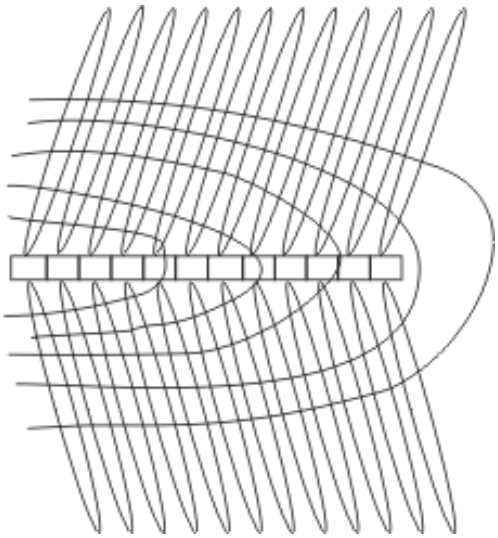

Figure 4.29 A sketch of a fluvial valley where cell catchments are oblique to the valley floors cells due to the steeper longitudinal profile shown through the contours.

To produce a surface which is normalised with respect to local elevation (the Normalised Elevation Model or NEM) the stream (minimum elevation) and ridge (maximum elevation) network catchment rasters, as well as the filled DEM can then be used to calculate the NEM using the ArcGIS raster calculator. The ArcGIS raster calculator calculates the value for each cell from the input surfaces. Equation 4.1 is used to calculate the NEM, where *min elevation* is the stream network catchment surface and *max elevation* is the ridge network catchment surface and *DEM* is the filled DEM:

$$NEM = (\,DEM - Min\ elevation) \times \left(\frac{1}{Max\ elevation - Min\ elevation}\right) \times 100 \qquad [4.1]$$

The first part of Equation 4.1 creates a relief map where local valley floors become zero and the valley sides adopt a value for their height above the local valley floor. The second part of Equation 4.1 normalises the local valley relief between zero and 1. This is then multiplied by 100 because ArcGIS copes better when dealing with integer numbers.

The final process involves the NEM undergoing a cleaning procedure. This is where any values which do not fall between 0 and 100 are deleted and become cells with no data assigned to them. The rasters produced are shown in Figure 4.30 – 4.33.

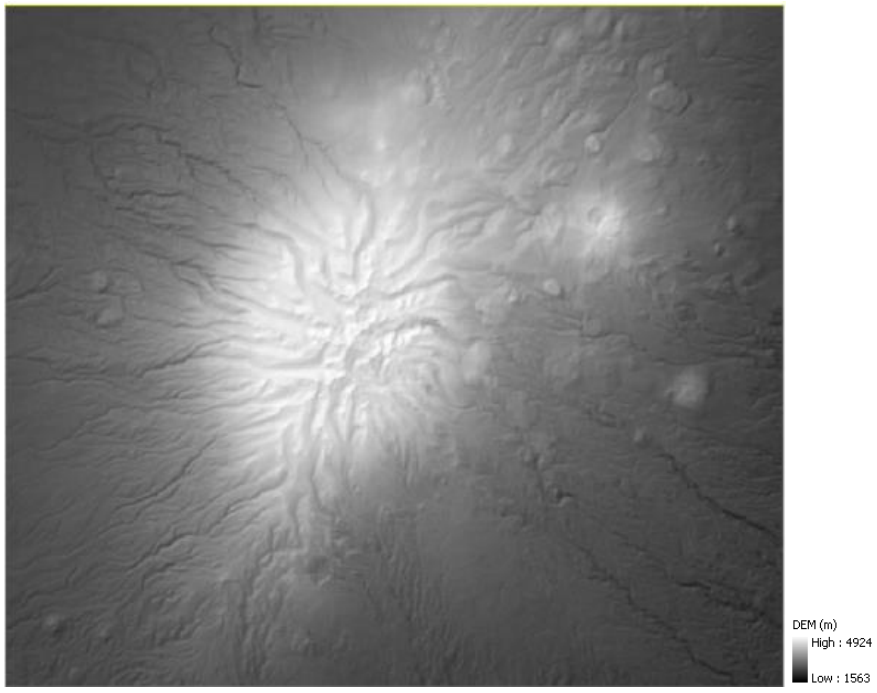

Figure 4.30 DEM with hillshade of Mt Kenya

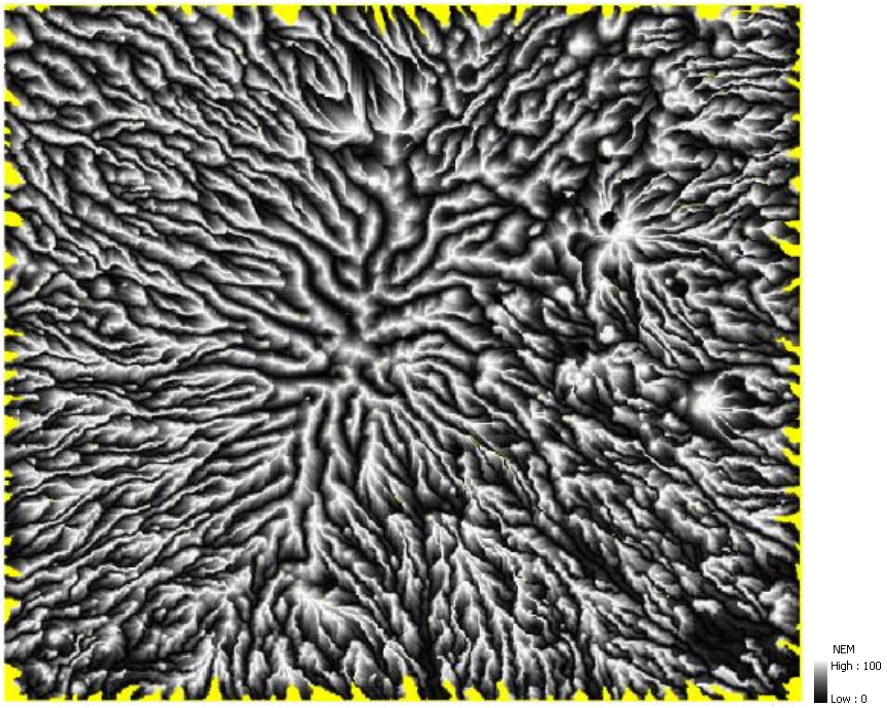

Figure 4.31 NEM of Mt Kenya clearly showing that all valley floors and ridges and peaks

have the same value. This is now a ‘de-trended’ Mount Kenya but retaining normalised valleys.

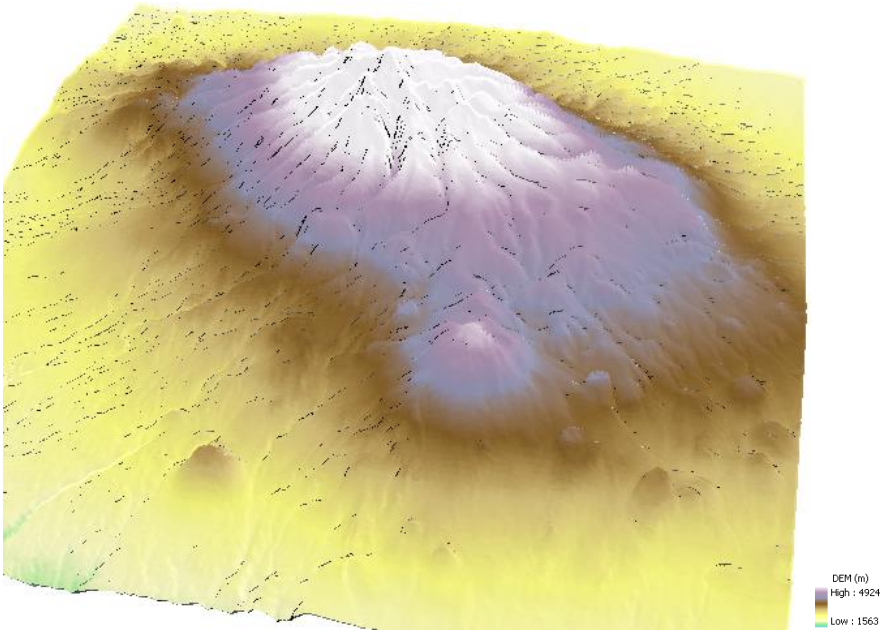

Figure 4.32 DEM of Mt Kenya visualised in 3D.

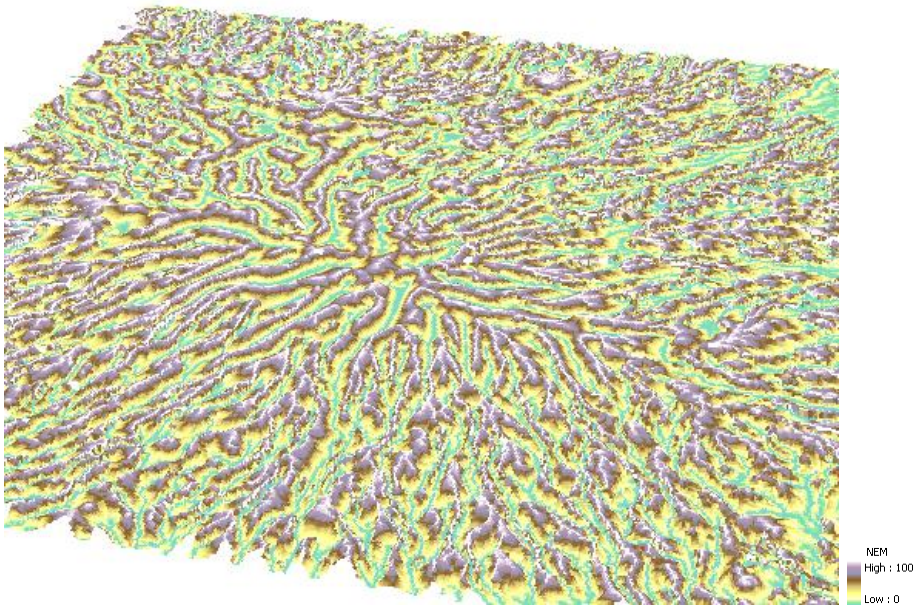

Figure 4.33 NEM of Mt Kenya in 3D showing a flattened peak where only the valleys show relief. The NEM here is displayed with a vertical exaggeration of 2.

4.5.2 Creating a sampling framework from the NEM

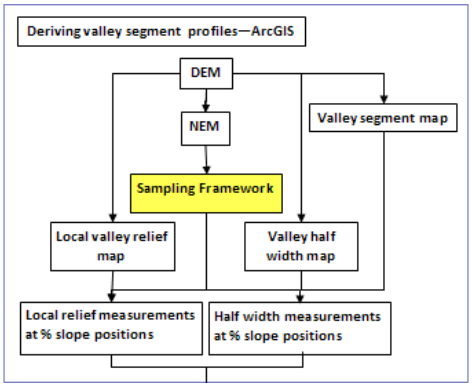

The purpose of creating an NEM is for the surface to be used as a sampling framework. This sampling framework is made up of 'contour' lines at set slope positions (i.e. 10%, 20%, 30% up valley sides). Having produced the NEM it is now a simple procedure in ArcGIS to generate the sampling framework.

Percentage slope positions at 10% increments are suggested for the sampling framework. This is achieved by using the contour tool in ArcGIS and applying it to the NEM. For further calculations, the 'contour' layer produced is divided into separate shape file layers corresponding to each contour value (10% to 90%) (Figure 4.34). The 0% 'contour' line is not needed as this is assumed to always have a value of zero and the 100% 'contour' line is not used as these are on the catchment divides and do not incorporate enough values to be meaningful, a conclusion found by Phillips (2009).

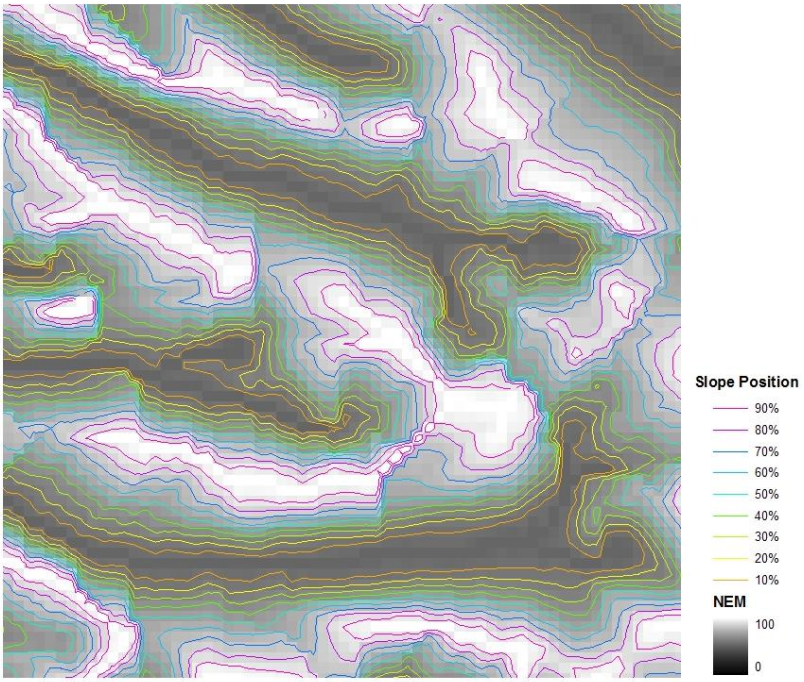

Figure 4.34 Shape file lines denoting NEM 10 – 90% slope position 'contours'.

4.5.3 Generating local relief and half width maps for mean valley segment profiles

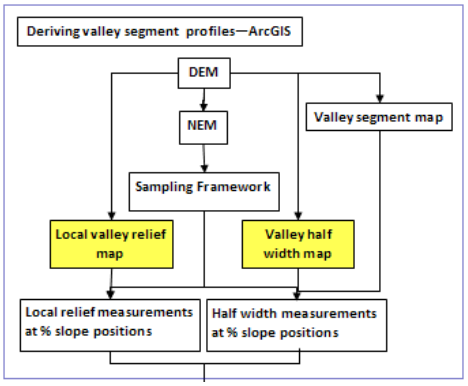

Once the sampling framework has been generated it can be used to produce the mean valley segment cross-sectional profile. The values needed to create the profile are the mean height above local valley floor (the local relief) as well as the corresponding mean distance from the centre of the valley, which is the half valley width, for each slope position in each valley segment. From these values a cross-sectional profile can be graphed and analysed. In order for this method to be automated it uses mean values from defined valley segments to give the mean valley segment profile. The method used to extract the local relief and half valley width values as well as the valley segmentation are explained and justified in the following Sections 4.5.4 and 4.5.5.

4.5.3.1 Local Relief Map

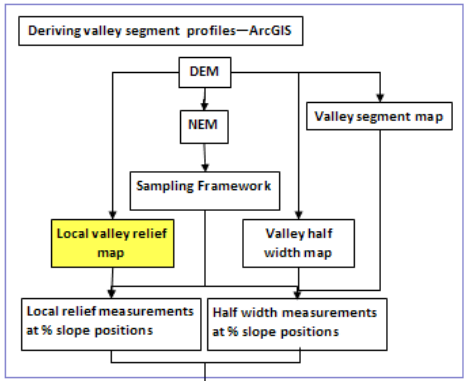

A local relief map is a surface created in ArcGIS which is the height at any location above the local valley floor. This surface is used together with the sampling framework to find the height above the local valley floor at each slope position. These values can then be averaged for each valley segment to find the mean height at each slope position with the valley segment in order to create a mean valley segment cross-sectional profile.

To create a local relief map in metres a raster layer of height above local valley floor is produced. This is calculated by subtracting the stream network catchment surface values (minimum local elevation) away from the original filled DEM (this is the first part of the NEM calculation found in Equation 4.1). Figure 4.35 shows an example of a local relief map produced by this method. It is a raster layer where each cell is the height in metres above local valley floor.

To gain the average local relief, for a valley segment, at any given slope position the slope percentage 'contours' are used in combination with the relief map (Figure 4.36). A tool is used whereby any line, in this case the slope position contour line, can be used to calculate an average value for the raster cell values which the line intersects (Figure 4.38). This is explained in more detail in Section 4.5.3.2.

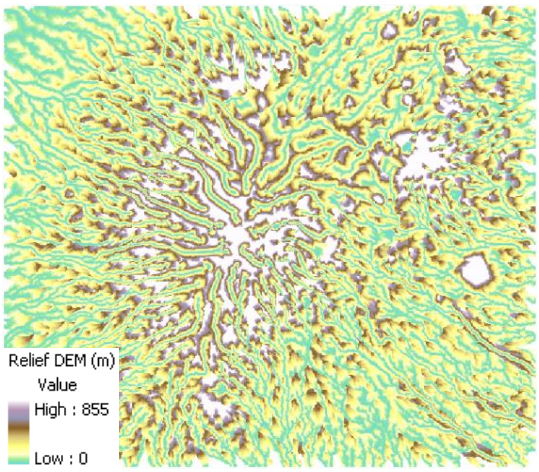

Figure 4.35 Local relief DEM showing valley floors as zero relief, remaining cells are given a value in metres above the local valley floor.

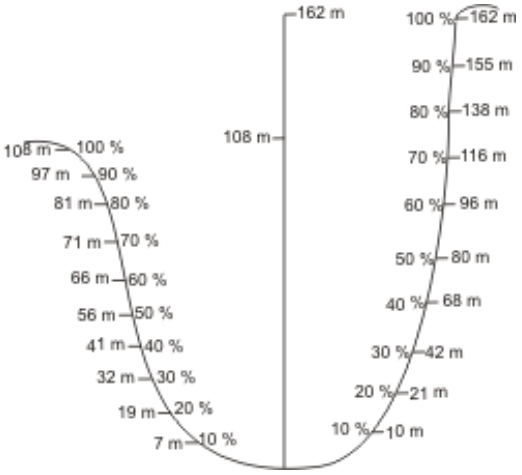

Figure 4.36 A sketch of a valley segment in cross profile showing how the percentage slope positions are used to gain average valley segment relief.

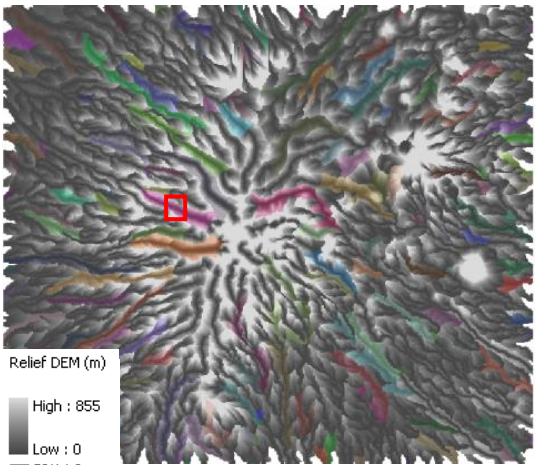

Figure 4.37 Local relief map of Mt Kenya. Coloured areas indicate the 2nd order catchment valley segments. Red box shows the area selected for Figure 4.38.

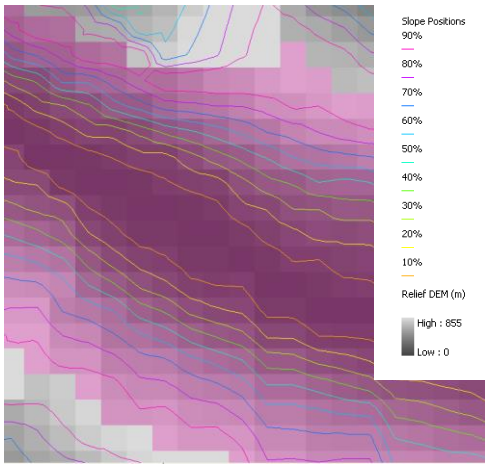

Figure 4.38 Shows how the percentage slope position lines pass across the raster cells of the relief map containing the height above local valley floor data. The length of the line in each cell is then used to calculate a mean for the slope position line within the valley segment (pink area).

4.5.3.2 Half Valley Width Map

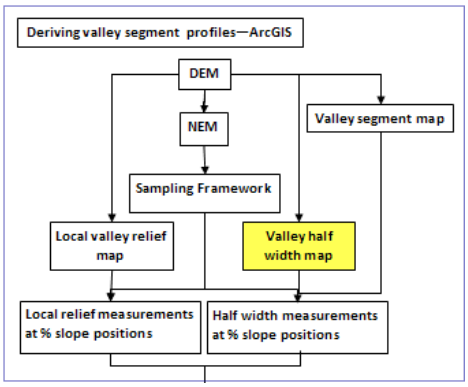

In conjunction with local relief values, described in the previous section, width values need to be computed in order to produce a cross-sectional valley profile. The valley width is the distance from the centre of the valley to each cell, and is calculated by producing a surface map with these values. A tool in ArcMap can be used to calculate this in any defined unit, in this case metres. The tool is called the path distance tool. This tool produces a surface where each cell value is the shortest distance from an allocated source. The source is the valley centre defined by the valley stream network. The tool gives a measurement for half the width of the valley, as it is the distance from the valley centre.

Tests showed that this tool could not simply be used on the whole stream network (the source), as tributaries interfered with the result. This was especially true with higher order streams which occupy wide, flat valley floors. Here smaller tributaries were closer to the source than the stream required for measurement, therefore, creating smaller valley widths than were observed. To combat this, the stream network was divided into separate layers, according to their stream order, and then the path distance tool was used for each layer (Figure 4.39 and 4.40). The path distance layer for each stream order is used to find the valley half width measurements by defining the area required with the valley segments for each stream order and disregarding the remainder (Figure 4.41).

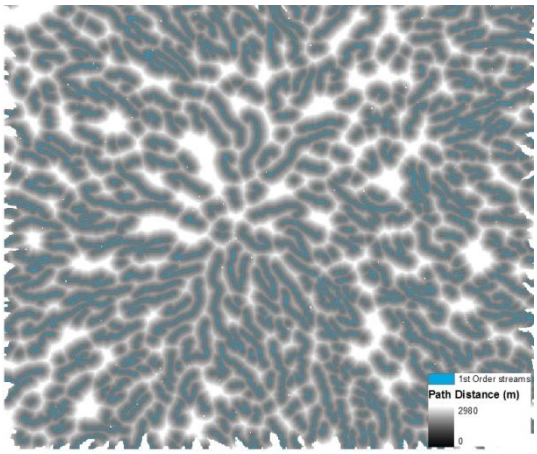

Figure 4.39 1st Order streams used as a source for the path distance tool and the path distance surface produced (lighter shades are greater distances).

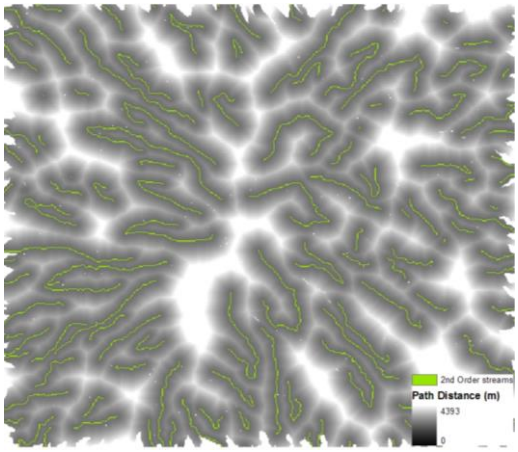

Figure 4.40 2nd Order streams used as a source for the path distance tool and the path distance surface produced.

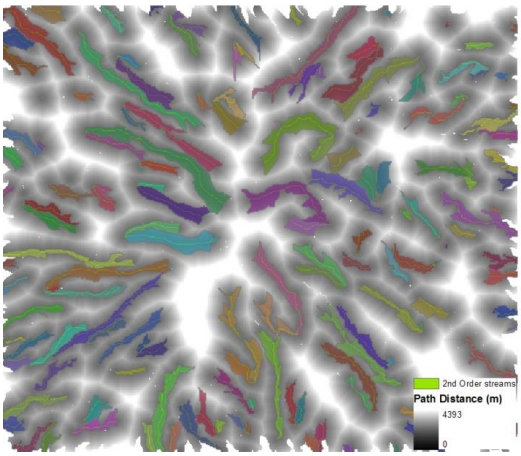

Figure 4.41 Coloured areas on the map show valley segments of 2nd order valley segments. Only values within these segments are used to derive average valley cross-sectional profiles.

To find the valley segment half width at each slope position the same tool is used as that to calculate local relief and is explained in more detail in Section 4.5.5 and 4.5.6. Figure 4.42 shows how a valley cross-sectional profile uses the valley slope position sampling framework to find the half valley width values.

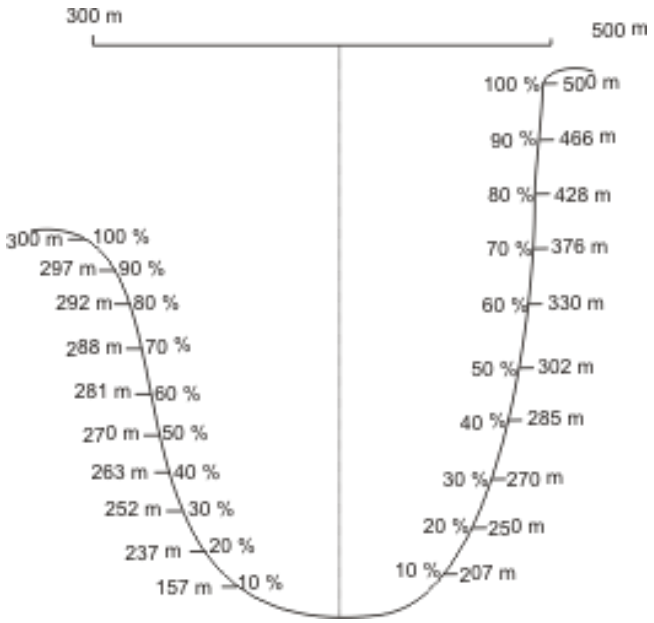

Figure 4.42 A sketch of a valley segment in cross-profile showing how the percentage slope positions are used to gain valley segment half width values.

4.5.4 Valley Segmentation

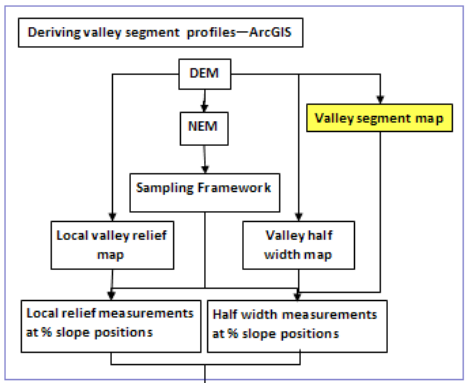

In order to analysis how a landscape's geomorphology changes spatially it must be divided into meaningful areas. As valley cross-sectional profiles are to be investigated a method for dividing the DEM into valleys and valley segments must be developed. Although there are many different methods of segmenting valleys in ArcGIS the main problem which has to be overcome is labelling each valley segment with an individual identification number.

Several methods were explored. The first method involved dividing valleys by stream order. This appeared to work well but created some very long valley segments. Very long valley segments potentially have a greatly different cross-sectional valley profile down valley. Therefore when an average of these long valleys is taken the resulting value would not be useful for understanding the spatial variability of valley cross-sectional profiles. Instead smaller valley segments were created by splitting segments at

set distances. This method satisfied the need for smaller segments but had the tendency to split segments at illogical points, for example just before or after tributaries. The final method experimented with, splits valley segments at tributaries. Although this does not give segments of equal length it provides a far more logical method as segments are divided between major flow inputs which have been attributed in the change of valley morphology below said tributary (MacGregor *et al.*, 2000).

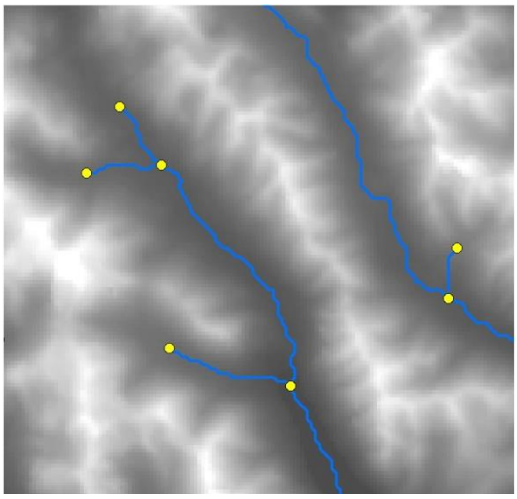

Figure 4.43 DEM with the stream network defined as a geo-network where the (blue) lines show the location of the stream network and stream junctions are shown as points (yellow). The points are used to split the line at their location. This enables each line segment to have an individual identification number.

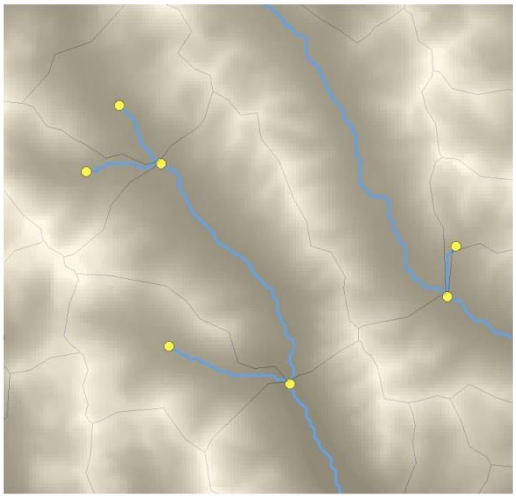

Figure 4.44 DEM divided into catchments by using the Hawth's Analysis Tools. The stream network and junctions are also displayed.

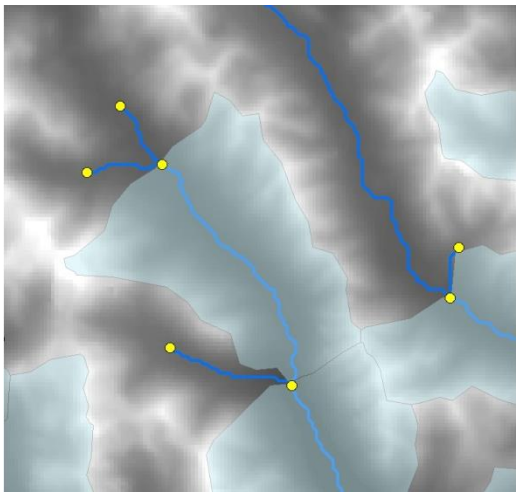

Figure 4.45 Catchments corresponding to the stream network are identified and merged. Gaps arise as first order catchments are not used in this analysis.

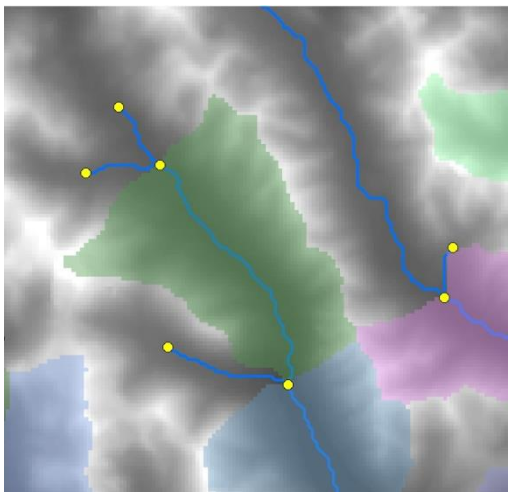

Figure 4.46 Catchments are given individual identification numbers which correspond to the geo-network line identification number.

To create valley segments by splitting areas at flow tributaries several steps have to be taken in ArcGIS, the first being to create a geo-network from the stream network. Unlike the stream network a geo network acknowledges where lines connect by creating a junction as a point feature (Figure 4.43). These point features can then be used to split the lines where they coincide. An inbuilt tool for this was not available in ArcMap but a 'linesplit' tool could be downloaded free and integrated into ArcMap, which made this step simple. Each split line had an individual identification number which is used to identify valley segments. The simplest method to create valley segments from the split lines was to use the catchments automatically created by Hawth's Analysis Tool Extensions (described in detail in Section 4.5.6) (Figure 4.44). Where the split lines intersect the catchments they are populated with the split line identification number (Figure 4.45 and 4.46).

4.5.4.1 Eliminating valley headwalls

The 1st order valley segments present a unique challenge. This is because they incorporate the headwalls of the valleys. Tests showed that although some valley headwalls did not interfere with the 1st order statistics many did due to their different morphology from valley sides. Therefore a method was developed to eliminate the

valley headwalls and only included valley sides in the average valley segment calculation.

This was achieved by isolating the source stream network cell at the head of the valley. To do this the flow accumulation layer was used with the zonal statistics tool to find the minimum value in each first order valley segment. Once these cells were isolated the watershed tool could yet again be used with the DEM flow direction layer to delineate a catchment above the source stream network cell (Figure 4.47). This area can then be converted into a polygon (Figure 4.48) and then by using the erase tool to delete the headwall area from the original 1st order valley segment polygons (Figure 4.49).

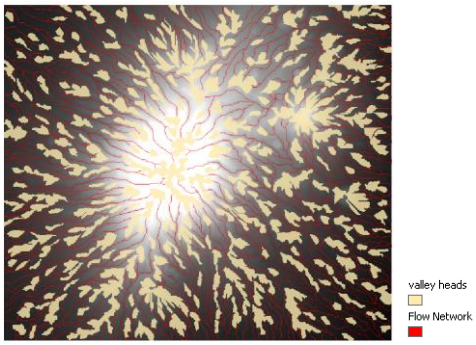

Figure 4.47 Coloured areas shown are valley headwall areas.

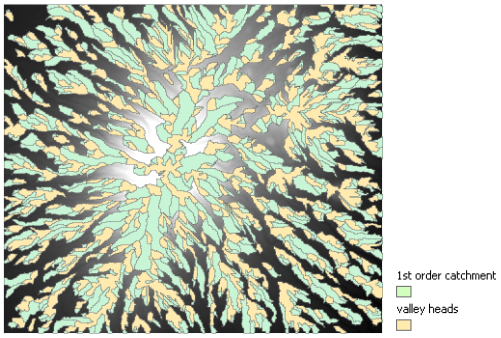

Figure 4.48 Polygons of valley heads and 1st order catchments.

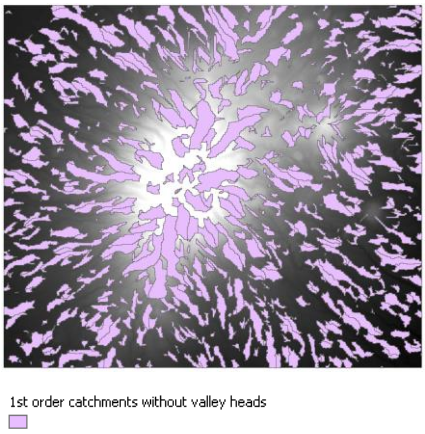

Figure 4.49 Polygons with valley heads eliminated.

Although this method was developed and therefore included in this chapter is was decided that first order valley segments would not be used in analysis as in some sample areas the landscapes still contained remnant glaciers which had retreated into cirque

glaciers. To avoid measuring this ice, 1st order catchments were not included in the dataset eliminating the requirement for this procedure. It was also thought that the limited flux in these valley segments would mean that they would not be as important as higher stream order valleys for investigating spatial variability of valley cross-sectional profiles.

4.5.5 Using the sampling framework with the valley segments to generate average valley profiles

Once valley segments are created (explained in the previous section, Section 4.5.4) the segments can be used to define areas in order to create average valley cross-sectional profiles. To gain meaningful results the slope position 'contour' lines, within each individual valley segment, need to be selected so that statistics for each valley segment can be found. In order for the valley slope position lines to be used for the average valley cross-profile analysis the valley segments, in conjunction with the intersect tool, are used to 'cut out' each valley slope position line for the original slope position layer (Figure 4.50 and 4.51). Finally, to make sure that the slope position lines are continuous within the valley segment and adopt the valley segment identification number the dissolve tool is used to allocate each line with the corresponding valley segment number.

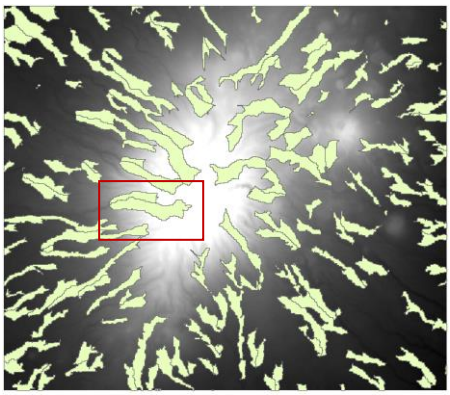

Figure 4.50 2nd order valley segments on Mt Kenya. Red box shows area in Figure 4.51.

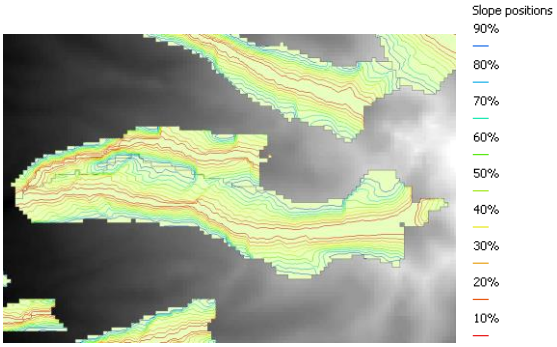

Figure 4.51 Percentage slope lines intersected by the valley segments.

4.5.6 Finding mean depth and width values to create mean valley cross-sectional profile

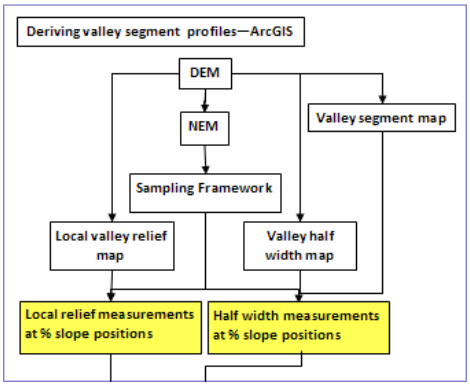

The adjusted sampling framework of slope position contours, explained in the previous section (Section 4.5.5), is used to find the mean local relief from the local relief map (Section 4.5.1.1) and width from the valley half width map (Section 4.5.3) for each valley segment. An ArcGIS extension, which can be downloaded and is fully integrated in the software, makes this task easier. The tool extension is part of Hawth's Analysis Tool Extensions, a collection of spatial analysis tools which can be used directly in ArcGIS (ArcMap) and are free to download. They provide simple spatial analysis functions that are not otherwise incorporated into the ArcGIS toolset.

The 'line raster intersection statistics' tool in Hawth's Analysis Tool Extensions produces data which represents a statistical summary of the cells of a raster layer which a line passes through, to be calculated based on the length of the line which intersects each cell. To derive the average cross-sectional profile of each valley segment the length weighted mean statistic is calculated for the local relief and half valley width layers within each valley segment (the use of the mean averaging statistic is justified in Section 4.5.6.1) The 'line raster intersection statistics' tool does this by multiplying the length of each line segment which crosses a raster cell value by that cell value, summing all these individual line segment values and then dividing that sum by the total length of the polyline, in this case the percentage slope position contour. This is shown in Equation 4.2 below,

$$\bar{x} = \sum_{1}^{i} (l_i v_i)/L \qquad [4.2]$$

where *l* is the length of the segment, *v* is the value of the raster cell for that segment, and *L* is the total line length.

This tool can not only find the mean value along a line for one raster layer but it is able to compute values over multiple raster layers concurrently. This reduces processing time as the valley local relief and half width mean values at each percentage slope position

can be calculated concurrently. The mean values at each slope position can be exported into Excel where mean valley cross-sectional profiles for each value segment can be visualised and statistics extracted. This is explained in detail in Section 4.6.

4.5.6.1 Averaging methods

Investigations were made into the most appropriate averaging statistic to use for the average cross-section profile of each valley segment. Hawth's 'line raster intersection statistics' tool gives the length weighted mean but an alternative method allowed the median, as well as, the mean to be calculated. This method converted the percentage slope position polyline shape files into raster layers of 5 m resolution. These 5 m raster cells could then be multiplied (using the times tool) with the half width and local relief maps to produce 5m cells containing the half width and relief values. It is then possible, using the zonal statistics tool, to find the statistics from these cells within each valley segment. The resultant mean valley cross-section profiles of these two methods were almost identical (Figure 4.52).

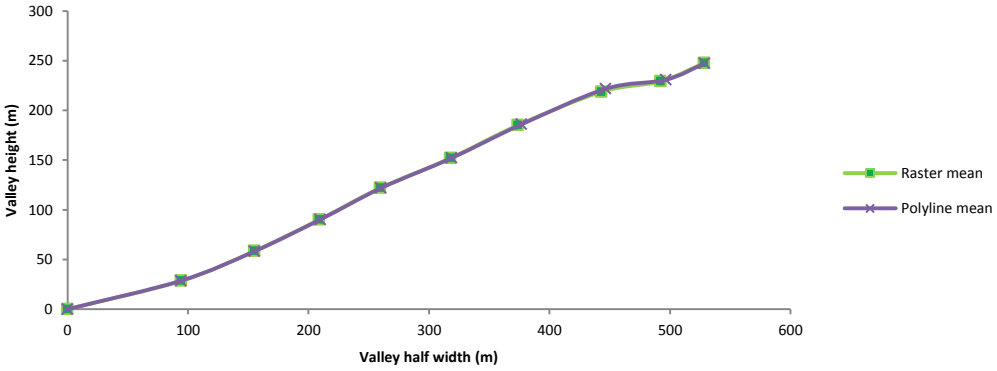

Figure 4.52 Graph showing the raster 5 m resolution and Hawth's 'line raster intersect statistics' polyline derived means for a half valley profile of a single valley segment on Mt Kenya. It shows identical results.

When exploring averaging statistics for valley cross-sections the mean and median values were compared. The resultant cross-sections are shown in the graphs below. The profiles show that the median results lack the smooth profile of the mean results (Figure

4.53 and 4.54). Although the results can be very similar, as in Figure 4.54, the mean profile has a smoothing ability that is preferable.

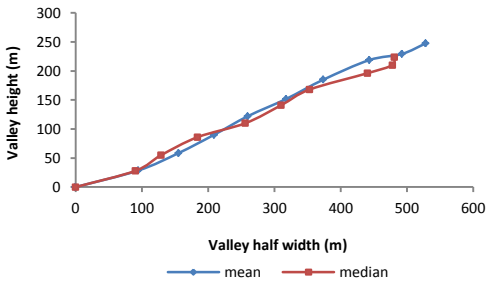

Figure 4.53 The half valley cross-section profile of a single 2nd order catchment on Mt Kenya.

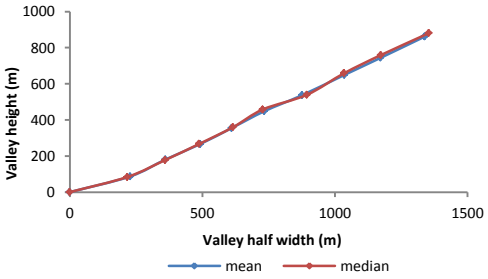

Figure 4.54 The half valley cross-section profile of a single 3rd order catchment in the Yoho area, USA.

For the mean to be an appropriate average statistic for use in producing mean cross-section profiles the data must have a normal distribution. The histogram in Figure 4.55 shows the distribution of half width values for 3rd order catchments at the 90% slope position. It shows that the data follows a normal distribution and therefore that the mean is an appropriate statistic to use.

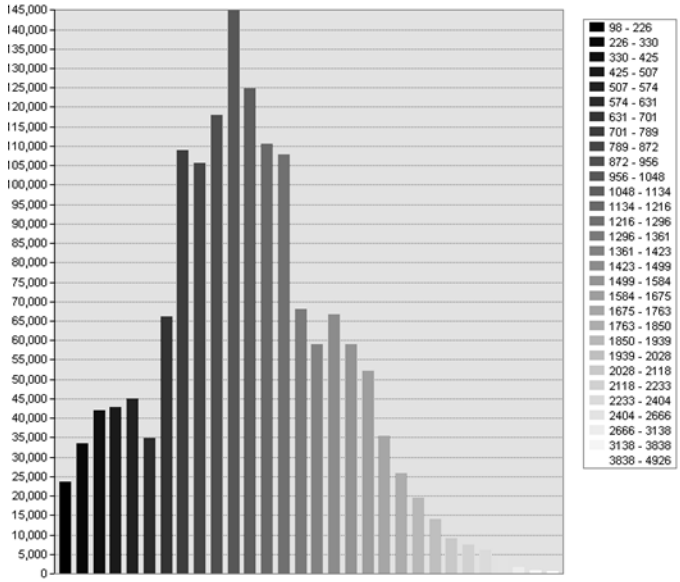

Figure 4.55 The distribution of half width values for 3rd order catchments in the Yoho area, USA, at the 90% slope position. The sample size is 905942 of 5 m raster cells.

Since the mean is an appropriate average measure to use Hawth's 'line raster intersection statistics' method is adopted. When using this method, as opposed to the raster 5m resolution method, the processing time for each sample area is reduced and, more significantly, this method requires less computational power and storage. This means that larger areas can be processed in more reasonable times and within normal computer storage capacities.

4.6 Creating Mean Valley Segment Cross-Sectional Profiles and Deriving Measures

The next stage in the method is to create mean valley cross-sectional profiles and derive measures which define the valley profile's degree of *U-ness*. To do this the mean values of local relief and valley half width for each valley segment, found in ArcGIS, are exported into Excel. Here the mean valley cross-sectional profile can be plotted from the mean local relief and half width values at each percentage slope position (10% through to 90% valley slope position). However for measures of *U-ness* to be found, calculations are either carried out in Excel, in the case of form ratio, or the data is exported into Matlab where values for cross-sectional area and *b*-value can be found. These values can then be returned to Excel where all the measures derived can be compiled in a spreadsheet. The flow chart in Figure 4.56 shows these stages of the method.

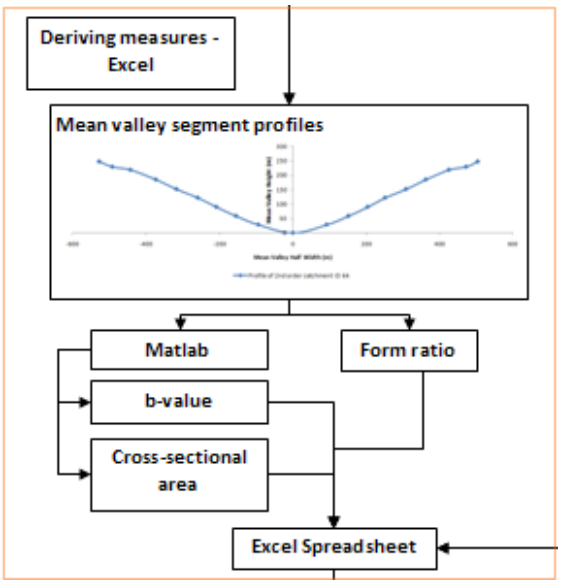

Figure 4.56 A flowchart showing the stages in the method where the mean relief and mean half width values are taken to make a mean cross-sectional profile and then used to derive *U-ness* measures.

4.6.1 Creating mean cross-sectional profiles

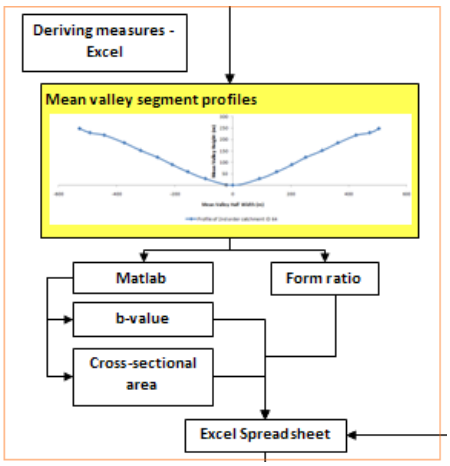

Values from ArcMap can be easily exported from attribute tables into Excel spreadsheets. Therefore the values for the mean relief and half width at each slope position can be collated in a spreadsheet. Here mean cross-sectional profiles can be visualised (Figure 4.57) and measures of valley glaciation calculated.

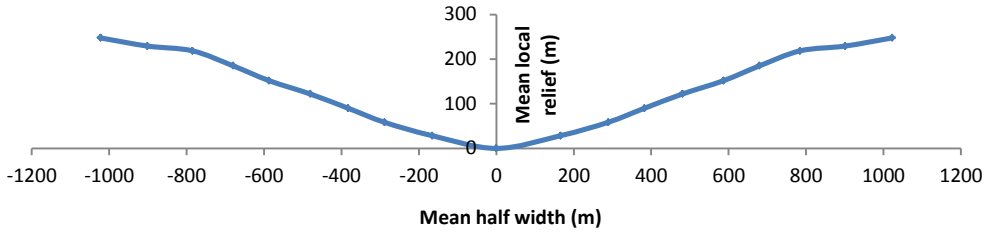

Figure 4.57 An example of a mean valley cross-sectional profile of a 2nd order valley segment on Mt Kenya. The average profile method uses both sides of the valley in the averaging method giving a mean half profile. Therefore the half profile is reflected across the y-axis to visualise a whole profile.

To make the process quicker in Excel, the data contained in ArcMap attribute tables, which comprises the mean statistics for the 9 percentage slope position lines (10% to 90% valley slope position) for each valley order segments (this is usually 5 or 6 but can be greater depending on the amount of stream orders a sample area contains), the data is combined into one attribute table before exporting into Excel. To incorporate the data into one attribute table for each valley order 9 percentage valley slope position tables, containing the mean values, are joined in ArcMap. This creates a single table for each valley order segment (usually 5 or 6 tables). This is done using the join function with the valley segment identification number as the common field for each slope position. These tables can then be exported into Excel and analysis can take place within Excel software (for example visualisation of profiles Figure 4.57).

Before any analysis can take place in Excel the data is filtered for any spurious results. Some filtering has already taken place in ArcMap during the joining of the tables process, where only valley segments containing all 9 percentage valley slope positions are input into the amalgamated table. In Excel, however, any valley segment with an area smaller than 1.62km² (this is 200 cells) are removed from the dataset. It is deemed that these valley segments are too small to gain meaningful results and may be influenced by edge effects.

4.6.2 Deriving U-ness measures

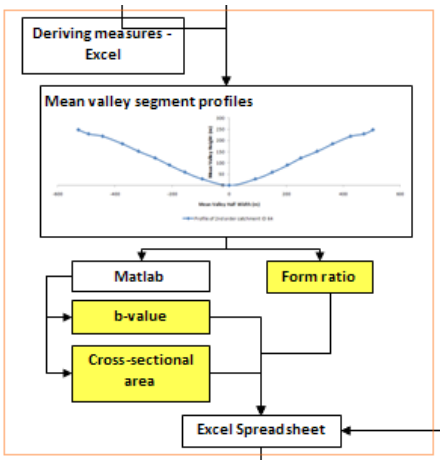

Now that a method for systematically generating mean valley cross-sections has been established the mean cross-sectional profiles can be quantitatively investigated. The *U-ness* measures identified from the literature can be calculated and comparisons made between valleys. At this stage of the method the data for each mean valley cross-section has been filtered and collated within an Excel spreadsheet. Form ratio for each valley segment can be calculated within the Excel spreadsheet whilst *b*-values and cross-sectional area require Matlab software for efficient calculation.

The average half width and average height values at the 10% to 90% slope positions compiled in an Excel spreadsheet for each stream order, therefore enabling calculations to be separated by stream order. The first calculation, form ratio, is carried out in Excel. Form ratio is a dimensionless ratio of a valley which uses the valley depth and width (Graf, 1970). In the case of the measures used this is the height from local valley floor at the 90% slope position (i.e. the maximum y value) and the valley width (i.e. the maximum x value doubled, as the x value represents the valley half width) (Figure 4.58 and 4.59). Equation 4.2 is used for the form ratio calculation,

$$Form\ Ratio = \frac{\max\ y}{(\max x)\ \times\ 2} \qquad [4.3]$$

where, *max y* is the mean local relief value at the 90% slope position and *max x* is the half width value at the 90% slope position.

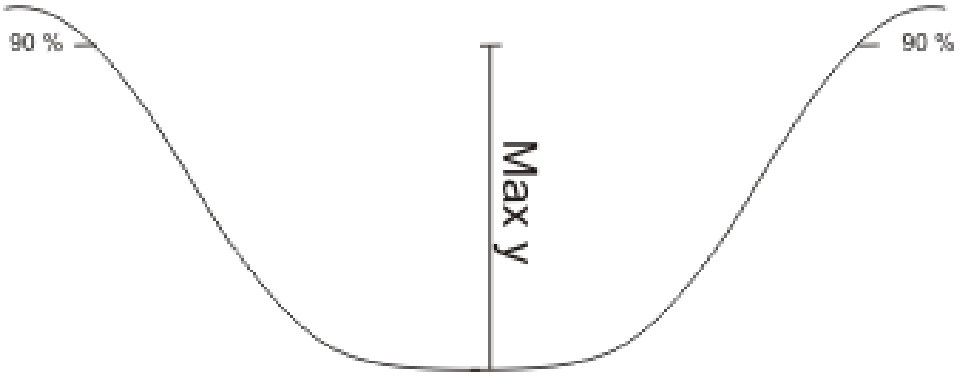

Figure 4.58 The depth measurement is taken from the 90% slope position.

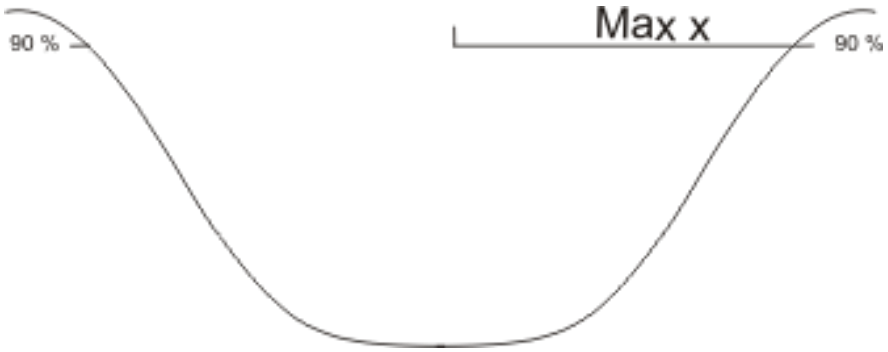

Figure 4.59 The width measurement is taken from the centre of the valley to the edge at the 90% slope position. For form ratios this value needs to be doubled.

Next the data is exported into Matlab where *b*-value and cross-sectional area can be calculated. For this calculation to be carried out efficiently a short Matlab script was written. This script takes the mean values for local relief and half valley width for the 10% through to 90% slope positions (the bottom of the valley, i.e. 0% slope position, is assumed to have a value of zero). The script fits a power-law curve to these values in order to obtain the *a* and *b* parameters of the power-law (Equation 4.4).

$$y = ax^b \qquad [4.4]$$

where *y* is the local valley relief and *x* is the half valley width at each slope position, whilst *a* coefficient and *b* exponent to be found. The *b*-value has been used extensively in valley cross-sectional form literature to describe the degree to which a glacial shape has been adopted (Svensson, 1959), a *b*-value of 2 representing a glacial U-shape, whilst a value of 1 a fluvial V-shape. The power-law curve in Equation 4.4 is fitted to the data to find the *a* and *b* parameters.

The final *U-ness* value calculated is the cross-sectional area of the valley profile. Integration of the power-law allows the area to be calculated using the *a* and *b* parameters. As the power-law is a continuous curve the location of the end of cross-section needs to be found. This is done by taking an average between the curve area which is at the 90% slope position of the x coordinate and the curve area which is at the 90% slope position of the y coordinate, thus preventing bias towards the x or y coordinate. Equation 4.5 is the result of the integration of the power-law that finds the cross-sectional area from inside the curve and therefore the valley cross-section area.

$$Area = 2\left[\frac{by\left(\frac{y}{a}\right)^{\frac{1}{b}}}{b+1}\right] \qquad [4.5]$$

For interest Figure 4.60 shows the power-law curve fitted to a mean cross-sectional profile. However, it is the *b*-value and cross-sectional area measures which are the critical data, and these *U-ness* measures associated with each valley segment are exported and compiled in an Excel spreadsheet.

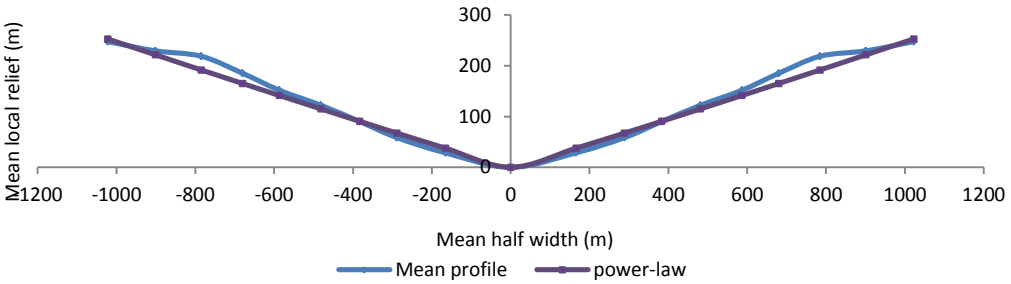

Figure 4.60 Mean profile of a 2nd order catchment valley segment (identification number 64) on Mount Kenya. The power-law computed the *a* and *b*-values to be 0.18033 and 1.0455 and this curve is shown.

4.6.3 Comparison of individually selected profiles with mean valley profile

In order to justify the use of mean valley cross-section profile as a valid method for producing valley profiles it was compared to the individually selected transect method. Six transects were drawn along selected valley segments and these were compared to the mean valley segment cross-section profile. Valley segments were selected from a 2nd order catchment on Mt Kenya and a 3rd order catchment in Yoho, USA (Figure 4.61 and 4.62).

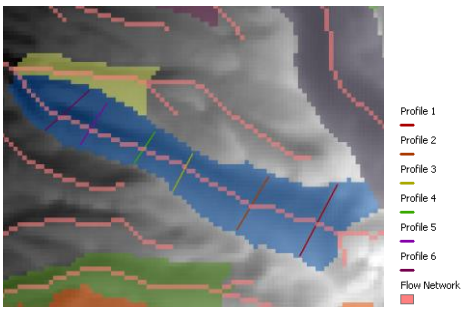

Figure 4.61 Map showing 6 individually selected profiles for a 2nd order valley segment on Mt Kenya.

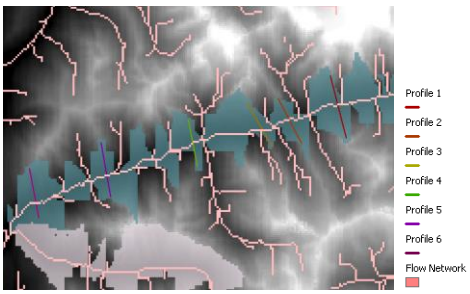

Figure 4.62 Map showing 6 individually selected profiles for a 3rd order valley segment in Yoho, USA.

The resultant graphs show that the mean valley segment profile for the selected valley segments lies within the individually selected transect limits (Figure 4.63 and 4.64). It is important to note that the six individually selected transects only represent a snapshot of the whole valley and are subject to the errors listed in Section 4.2. The mean valley

segment profile aims to capture the morphology of the entire valley. It is an average of the valley slope profile, which includes both sides of the valley and therefore the result gives a half valley profile. In the graphs in Figure 4.63 and 4.64 the mean profile has been mirrored over the y-axis to help visualise the cross valley profile.

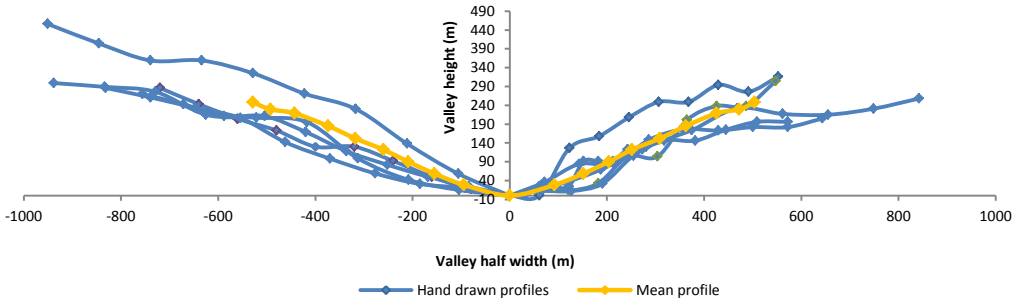

Figure 4.63 A graph showing six individually selected profiles of a 2nd order valley on Mt Kenya and the mean profile derived for the valley segment.

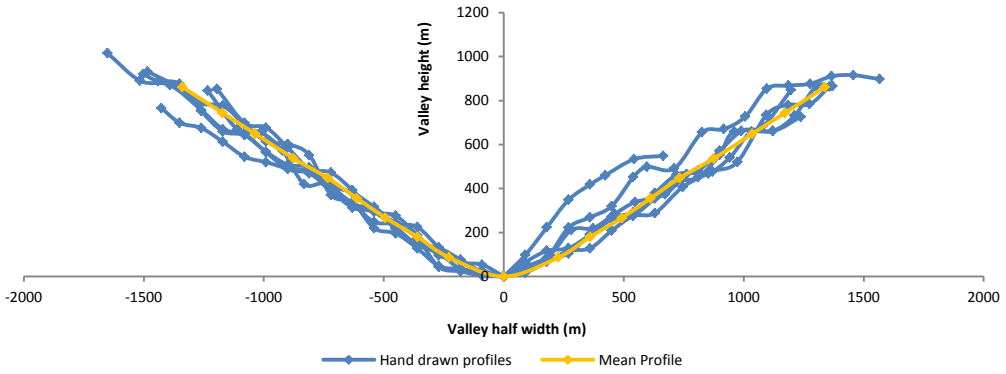

Figure 4.64 A graph showing six individually selected profiles of a 3rd order valley in Yoho, USA and the mean profile derived for the valley segment.

In order to estimate how many individually selected transects the mean valley profile method is equivalent to for each valley segment at the 90 m resolution the number of valley floor cells is found. In the case of the Mt Kenya the sample valley segment, shown in Figure 4.63, the mean cross-section profile is equivalent to drawing 103 individually selected profiles. Whilst for the Yoho sample valley segment (Figure 4.64) the mean profile cross-section represents an equivalent of 241 individually selected profiles.

During the Matlab analysis additional filtering of the data takes place. Any mean cross-section profiles which Matlab cannot fit to the power-law are removed from the dataset as well as any spurious results, for example negative *b*-values. Through all the cleaning processes which take place in ArcMap, Excel and, finally, Matlab approximately half to one thirds of the initial valley segments are removed from the dataset. This reduces with higher stream order valley segments. For example, Mt Kenya initially had 664 first order valley segments. Once the dataset was filtered for poor results 281 remained in the dataset which equates to 57.7% of valley segments removed from the dataset. This is compared to the second order valley segments where 158 were first identified and 97 were deemed adequate for the dataset; a total portion of 38.6% being removed from the dataset.

4.7 Deriving residence time and ice flux proxies

In order to assess the effects of glaciation on a landscape, to compare with valley development measures estimates for the scale of ice erosion are needed. Chapter 3 discussed suitable proxies and concluded that elevation was an appropriate proxy for ice residence time and catchment area for ice flux. The DEM, together with ArcGIS, can provide a means for calculating these proxies. Figure 4.65 shows the stage of the method to which the deriving of proxies fits.

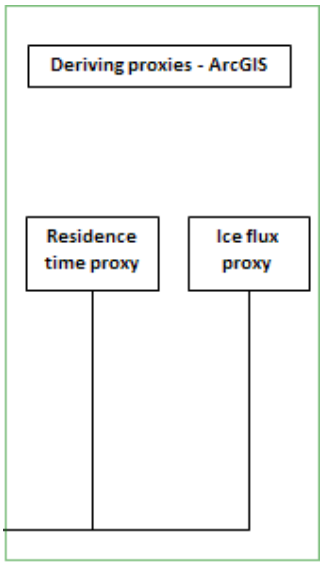

Figure 4.65 Method stage for deriving proxies

Elevation can be directly gained from the DEM. Elevation is used as a proxy for ice residence time because in general ice will be in existence for the longest period of time at the highest elevations. Correlations between mean valley segment profiles and mean valley elevation will give insight into valley development.

Meanwhile ice flux is the quantity of ice which passes through any valley segment and is thought to be proportional to the erosion rate. Although residence time accounts for the amount of time which a valley segment is subjected to glacial erosion it does not account for the quantity and erosive force of a glacier. As ice flux increases down glacier to a maximum at the equilibrium line, it is here where intense glacial erosion occurs. The ELA moves up and down valley (controlled by climate) as the glacier advances and retreats and therefore it is the point at the 'average ELA position', where the greatest flux has occurred over time. Valley connectivity dictates the amount of ice fed from other glaciers in an alpine glacial environment. This drainage pattern remains after deglaciation and can be utilised through a DEM of the landscape to obtain catchment areas. Relative to small catchments it is presumed that larger catchments will have received more snowfall and therefore will require a greater ice flux to transport it. Catchment area is thus a useful proxy for ice flux. In ArcMap catchment area can be easily calculated through flow measures of drainage pattern using inbuilt tools.

Once proxy values have been calculated relationships between proxies and *U-ness* measures can be investigated. Conclusions from both regression and spatial relationships could help to inform ideas on valley development.

4.7.1 Obtaining valley segment mean elevations

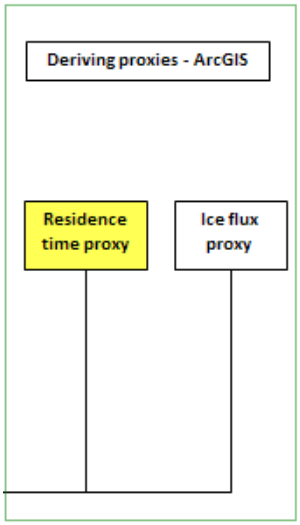

Mean elevation values will be used in analysis to indicate ice residence time for each valley segment. As valley segments have already been defined in ArcGIS in the previous stage of the method they are used in the same format to find the mean elevation in the segment. The process involves using the valley segment to define a zone in which the mean of all the elevation pixels, taken from the DEM, is calculated for each valley segment. This gives a single value for each valley segment, which can be both displayed visually in ArcGIS (Figure 4.66) and also exported into Excel.

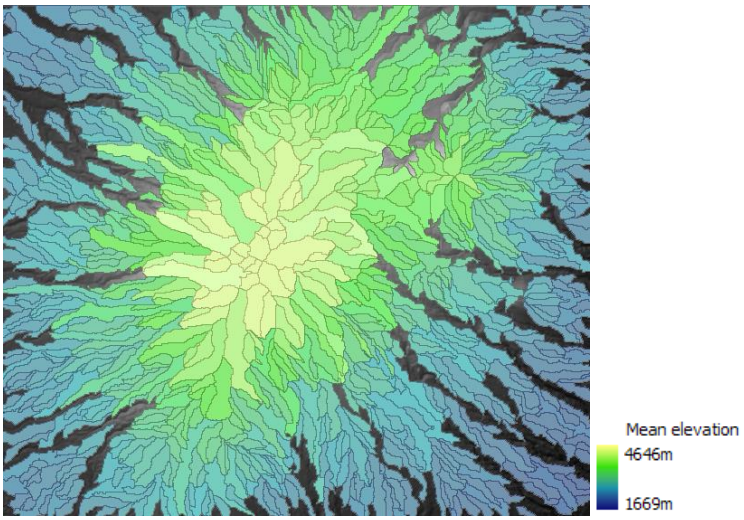

Figure 4.66 Sample area showing mean elevation for each valley segment.

4.7.2 Computing contributing catchment area values for each valley segment

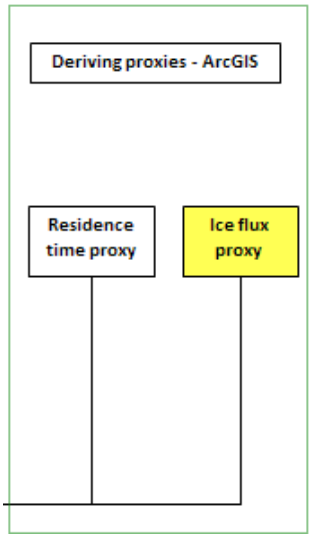

The catchment area of each valley segment which will be used in future analysis as a proxy for potential ice flux is found by a similar method as that used to find the mean elevation for each valley segment. The same valley segments as before are used to define zones in ArcGIS. Instead of simply using the DEM elevation values some processing needs to take place. Inbuilt ArcGIS tools for hydrological analysis are used to give a value for catchment area. This was achieved by using the flow accumulation tool to find out how many cells flow into each cell in the sample area. Using the valley segments to define zones the Zonal Statistics tool is used to select the maximum flow accumulation value in each valley segment. This results in each valley segment being assigned a value which represents the maximum flow value for that segment and therefore a measure of catchment area. The catchment area values for each valley segment can be exported into an Excel database, or display in ArcMap (Figure 4.67).

a.

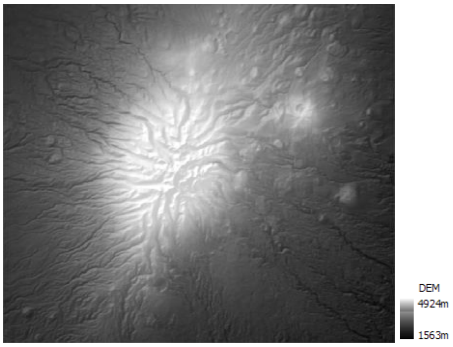

b.

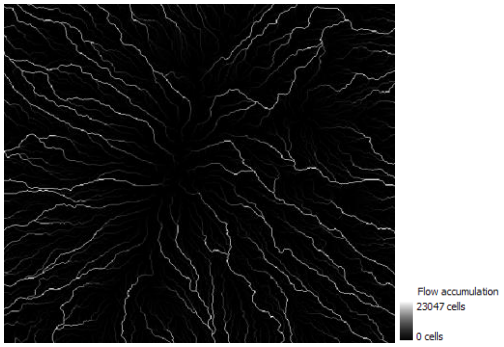

c.

d.

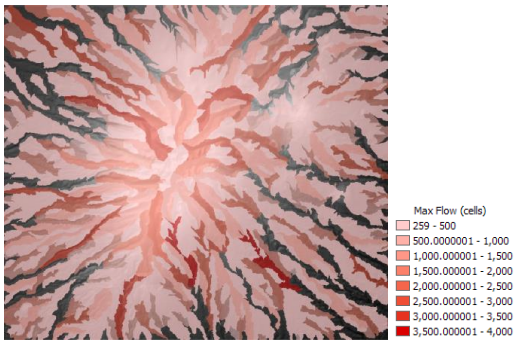

Figure 4.67 The stages in ArcGIS used to find a value for the ice proxy. a) is the original DEM of Mount Kenya, b) is the flow accumulation layer which is used with the valley segments (c) to produce a maximum flow accumulation value for each segment (d). The units here are the number of 90 m pixels which contribute flow to the particular valley segment, and of course, this increases down valley.

4.8 Relationships *between U-ness* measures and proxies

Once the *U-ness* measures and proxy values are collated in an Excel spreadsheet regression models between measures and proxies can take place. Figure 4.68 shows how the *U-ness* measures and proxies are brought together in the method. Understanding the relationship between *U-ness* measures and proxies can indicate the development of glacial valleys and inform process knowledge.

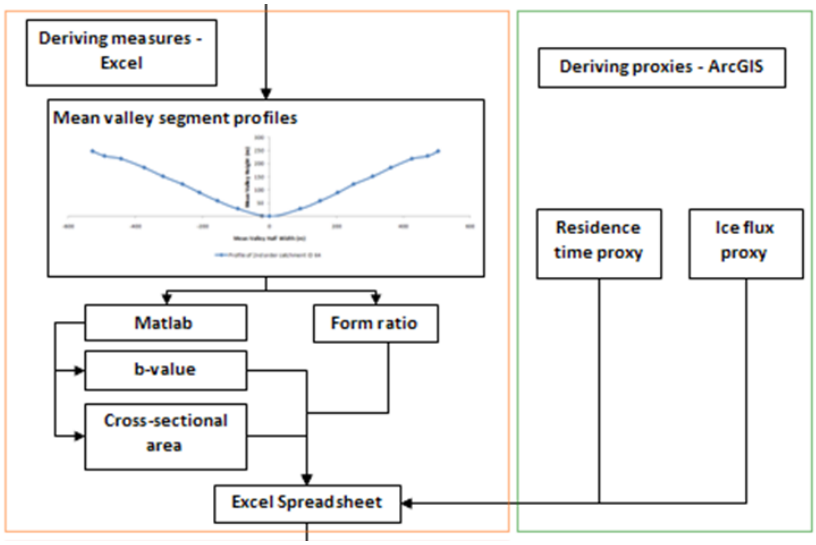

Figure 4.68 Diagrammatic representation of the method at the stage where *U-ness* measures and proxies are brought together to enable analysis of correlations.

Graphing *U-ness* and proxies values and analysing the degree of correlation can aid understanding of relationships and potentially valley development. Figure 4.69 shows an example, where the correlation between form ratio and mean elevation, which is a proxy for ice residence time, is graphed. This is discussed in more detail in Chapter 6 Section 6.5.2.

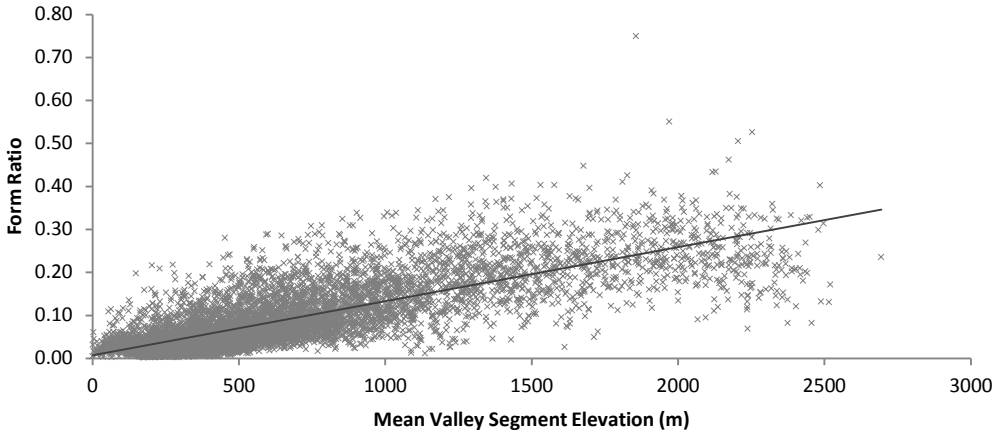

Figure 4.69 The relationship between form ratio and mean elevation (residence time) for all valley segments in the Pyrenees. The graph shows a line of best fit which has R-squared correlation of 0.618 for the 7573 valley segments which is significant above the 0.01% level and an estimated equivalent 294364 'individually selected' transects.

4.9 Spatial analysis of mean valley segment cross-sectional profiles

To understand the spatial variation of valley cross-sections, the mean valley segment cross-sectional profiles must be returned to ArcGIS where they can be analysed with reference to their locality (Figure 4.70). By conducting spatial analysis, spatial relationships could lead to the understanding of processes and temporal scales of valley development. Without referring to the spatial context of landforms significant results can be missed. ArcGIS is not only a useful tool for visualising data but complex analysis can take place using inbuilt spatial analysis tools which can be used to identify spatial relationships.

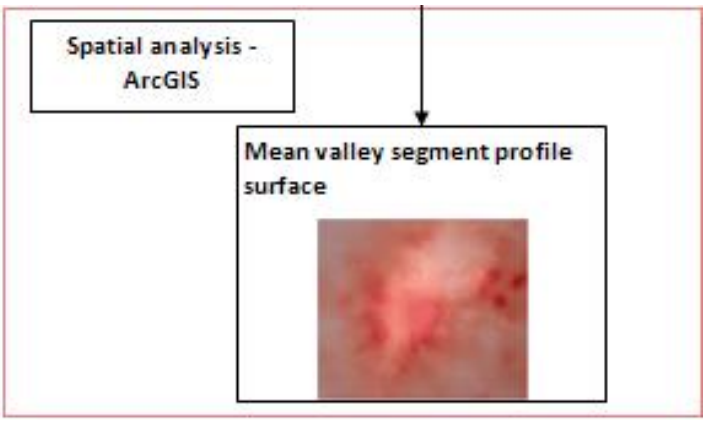

Figure 4.70 Final stage of the method which involves the spatial analysis of *U-ness* measures.

U-ness measures and proxy values have been found using the method described up to this point. These valleys have been compiled in a single Excel spreadsheet. To enable spatial analysis to take place in ArcMap this Excel spreadsheet must be imported into ArcMap and the identification number for each valley segment used to join the correct valley segment data to the corresponding mapped valley segment. The result is that each valley segment dataset is spatially referenced.

ArcGIS provides an array of spatial analysis tools. However, the simplest approach, which can be initially undertaken, is to display the derived measures of *U-ness* (form ratio *b*-value and cross-sectional area) of the sample area and observe spatial patterns (Figure 4.71). Any general trends can be noted.

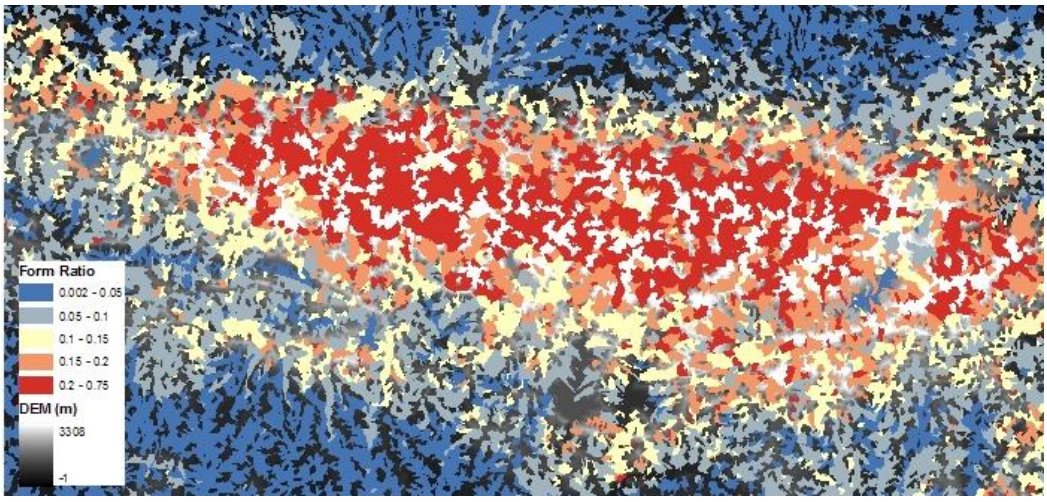

Figure 4.71 The spatial distribution of form ratio in valley segments across the mountain divide in the Pyrenees. The area displayed is 350 km by 150 km.

Following this simple display, standard ArcGIS analysis tools, such as interpolation tools, can be used to further understand the distribution of data. Interpolation tools can show visually areas of high and low values by smoothing out value extremes and filling in data gaps. It assumes that points closest together are more likely to be similar than those farther away. These tools require the valley segments to be converted into point features, this is a simple procedure, and the points assigned to represent the valley segments are centred on each segment. The interpolated surfaces produced from these points and their corresponding *U-ness* values cover the entire sample area. The surface provides a continuous layer which represents how each *U-ness* measure changes spatially (Figure 4.72). When compared to other data patterns can be observed.

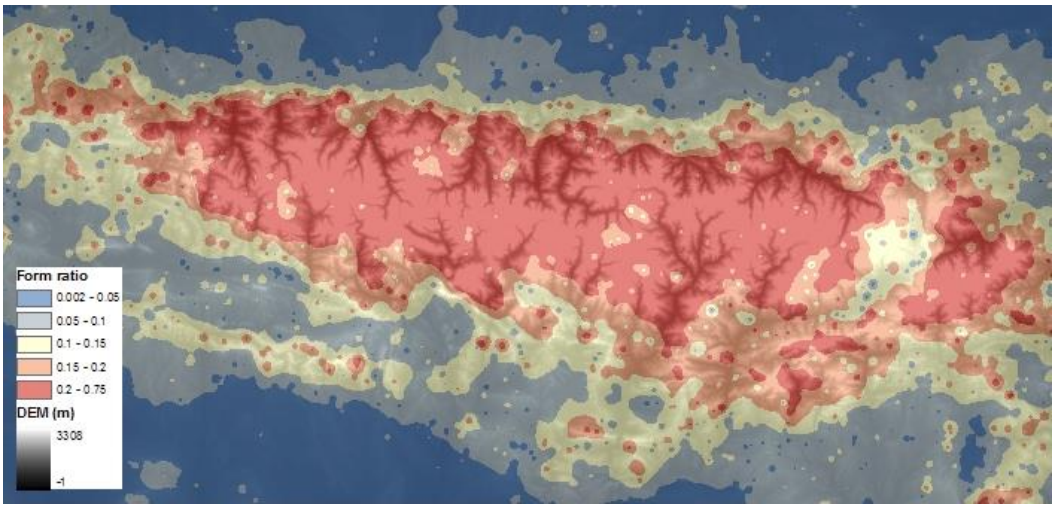

Figure 4.72 The same area and basic data as Figure 4.71 but using an Inverse Distance Weight (IDW) interpolation method to create a continuous surface of form ratio data using 30 neighbours.

The third and most sophisticated spatial analysis technique, and that which is predominately used in this thesis, is the Geographically Weighted Regression (GWR). GWR uses regression models between dependent and independent variables, in this thesis it is between *U-ness* measures and proxies respectively. GWR maps the relationships between *U-ness* measures and proxy values whilst acknowledging that the same regression model may not apply across the entire sample area. It, therefore, adapts the regression model according to the local relationships between variables (Brunsdon *et al.*, 1998) Figure 4.73. GWR will be described in more detail in Chapter 7 Section 7.2.

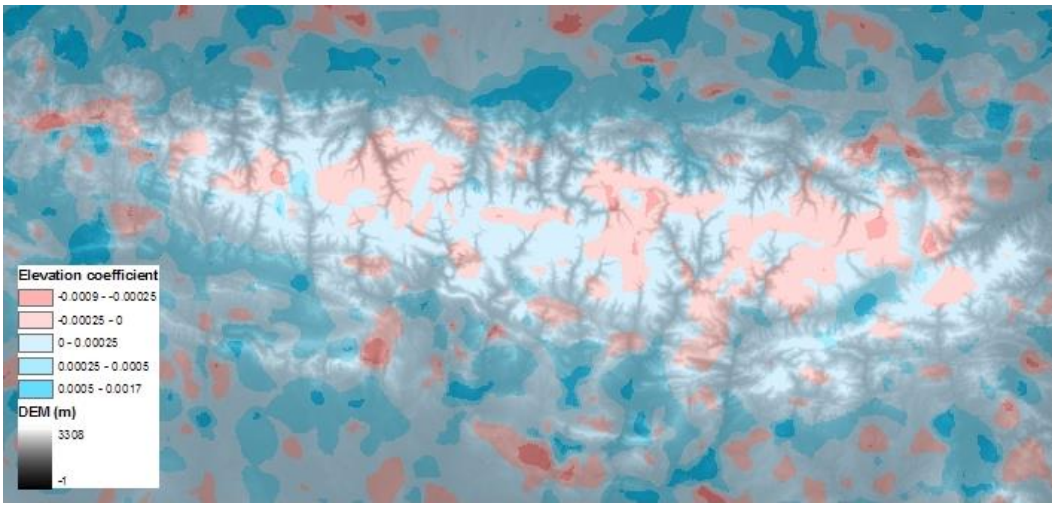

Figure 4.73 The same area as Figure 4.71 and Figure 4.72 but using the Geographical Weighted Regression (GWR) method to explore and display where in the mountain range that form ratio and elevation have a positive correlation (blue) and where a negative correlation is found (red).

4.10 Summary

The method presented in this chapter enables valley cross-sectional morphology of whole mountain ranges to be analysed. It negates the need to hand draw transects. This is useful because it provides an objective technique for analysing valley cross-sections and it overcomes many problems associated with the traditional transect method, such as sensitivity to choice of transect location.

Secondly, the average method permits large areas to be analysed on a semi-automated basis where whole valley cross-sectional shape is included in profile outputs. This is an improvement over the transect method which is both subjective and only gives a snapshot of a valley's shape. Problems such as profile orientation and tributaries, are eliminated. Although the problem of defining the valley top is not totally removed (and is tackled in more detail in Chapter 6 Section 6.2.), it does at least provide a constant sampling method by always taking the 90% slope position to be the valley top.

The mean cross-section profile method is conceptually based on a method first proposed by Phillips (2009). It further improves on the Phillips (2009) method by integrating the method fully into one piece of software (ArcGIS). This enables each step to the scrutinised. The method in this chapter also improves computational efficiency, improving both processing speed and reducing the size of data for storage, which

therefore allows larger areas (whole mountain ranges or sample areas spanning mountain divides) to be analysed at once. Another major achievement with this method is that it allows valley segments to be analysed, rather than in the Phillips (2009) method where only sample areas or stream orders within sample areas could be analysed. Therefore spatial analysis of valley segment cross-sectional profile can be investigated. These improvements advance the Phillips method from a technique which could analyse several catchments at any one time to a technique which can output valley cross-sectional morphology statistics and their spatial distribution for whole mountain ranges.

As can be seen from the examples provided of equivalent number of individually selected transects which the mean valley cross-section profile method represents, this method is an extremely powerful tool in analysing valley cross-sectional morphology. It can perform a cross-sectional analysis for whole valley segments, giving the complete picture of a valley's cross-sectional morphology. The technique has performed well in small to medium mountain ranges, such as Pyrenees, France/Spain and across mountain divides, such as the Patagonian Andes, which amounts to 10,000s of valley segments. In conclusion this method could transform the way researchers analyse valley cross-sectional morphology, their spatial variability and inform landscape evolution and glacial process studies.

5. Thesis sampling strategy; which landscapes to choose?

5.1. Introduction

This chapter considers which mountain regions should be selected for investigation of *U-ness* measures and assessment of their spatial variability. Four key influences on glacial processes, and consequently the geometry of landforms created, have been identified as:

1. Lithology - High resistance bedrock compared to weak bedrock.
2. Tectonic settings - Rapid uplift during glaciations in comparison to tectonically stable regions.
3. Climate - Encompassing a range of average annual temperatures and precipitation, as well as local climate factors such as slope aspect. More intense erosion is expected in areas with greater mass balance flux such as areas with high levels of precipitation.
4. Degree of glaciation - Areas which have been lightly glaciated to those which have undergone intense or prolonged glacial periods.

The four key influences above are likely to affect glacial landform characteristics, such as U-shaped valleys, and are discussed in turn in this chapter. They will form the basis of the sampling strategy in order to inform which areas are selected. Following this, details regarding the source data, in the form of Satellite Radar Topography Mission (SRTM) DEMs, are discussed in relation to their use in this thesis. The final selection of sample areas chosen is then justified in relation to the sampling strategy and source data, and environmental data is outlined to inform discussions later on in this thesis.

5.2. Defining glacial erosion and landscape characteristics

Quantitative assessment of the four key influences on landscape characteristics, identified in the previous section, is required to be able to assess their impact on *U-ness* measures. Where it is difficult to quantitatively assess characteristics it must be gauged as to where the sample area lies, relatively, in relation to other sample areas. For example, has the sample area undergone more intense glaciations than an area such as the Pyrenees? Independent assessment of characteristics is required in this study as the landscape cannot be used to infer characteristics, for example the degree of glaciation. Use of such characteristics has often been used in studies of large areas, such as where wide, flat valleys were thought to have undergone ice sheet type glaciation whilst deep narrow valleys have undergone alpine type glaciation (Hirano & Aniya, 1988). Using landforms to infer characteristics of glaciation would not be a satisfactory method in this thesis as it is a circular approach and therefore would not give meaningful results.

There is, however, difficulty in classifying sample areas according to the four characteristics identified and this is highlighted in subsequent sections. The literature is used to inform classification. Quantitative measures are attempted but in some cases it is more realistic to simply gain an appreciation of the relative degree to which a landscape characteristic lies within the range observed throughout the sample areas selected.

5.2.1. Lithology

Lithology encompasses all aspects of the physical structure and composition of rocks and rock formations. The lithology of a landscape is an important factor in its resistance to erosion and slope stability. This contributes to the form a landscape adopts and the rate in which it is created and thus, is an important consideration in selecting the sample areas.

An example of lithology influencing geomorphology in a glaciological context is given by Augustinus (1992a) who examined the influence of lithology on U-shaped valleys in New Zealand. He found that the lithology, together with the age of a landscape, was an important control on the U-shape of a valley. Where the landscape was set in areas of high Rock Mass Strength (RMS), such as the plutonic rocks of Fjordland, valleys were deep and narrow. This was compared to the less resistant greywackes of the Mount

Cook region. Here the wide relatively shallow valleys were concluded to be a result of less resistant lithology due to the close jointing and foliated schists and greywacke and their orientation, which controlled the valley cross-sectional shape and allowed rapid modification (Augustinus, 1992a). Brook *et al*. (2004) concurred with these results with a study of Scottish and Icelandic valley cross-profiles. Beyond just glacial contexts, RMS and slope gradient have been linked by a 'strength-equilibrium' relationship (Selby, 1980). Relating this relationship to glaciated valleys it was found that glacially oversteepened valleys, once deglaciated, would adjust to their slope angle according to the valley lithology RMS (Augustinus, 1995b; Brook & Tippett, 2002). Valleys with high RMS values were found to maintain steep slopes whilst those with low RMS were subjected to greater modification post-glaciation (Augustinus, 1995b).

The examples detailed above demonstrate that lithology has an important influence on landform shape, but interactions are complex which can mean classification by landform alone is difficult. Therefore classifications, such as RMS, are used to identify the degree of resistance and stability. Classifications not only identify the intact strength of a rock type, but also the jointing and its nature, as well as any rock type combinations. There have been several studies which classify rock masses according to strength. Three examples demonstrate the difficulty of classification, these are Rock Mass Rating (RMR) (Bieniawski, 1984), Geological Strength Index (GSI) (Hoek, 1994; Hoek & Brown, 1997) and Rock Mass Strength (RMS) (Selby, 1980).

The RMR is based on six parameters, measures of which are taken in the field. The parameters measured are: uniaxial compressive strength of rock material, rock quality designation, joint spacing, joint condition, groundwater conditions and joint orientation.

The GSI method uses a chart approach to assess the structure of a rock type from measurements taken in the field. The measurements taken are block volume and a joint condition factor which includes spacing and roughness. These measurements are then used in the Hoek-Brown Strength Criterion equation (Hoek, 1983) to rate the strength of a rock mass. It is in this equation where several constants, m_i, for intact rock, and m_b and s for a jointed rock mass, as well as, σ_{ci}, the uniaxial compressive strength of intact rock elements are included. These four constants are derived from the rock type.

Selby (1980) developed the RMS classification specifically for geomorphologists. It took into account the following eight characteristics which could be measured in the field:

1. Strength of intact rock
2. State of weathering of the rock
3. The spacing of joints, bedding planes, faults, foliations and other partings within the rock mass
4. Orientation of the partings with respect to a cut slope
5. Width of the joints, bedding planes and other partings
6. Lateral or vertical continuity of the partings
7. Gouge or infill material in the partings
8. Movement of water within or out of the rock mass

This classification was used by Augustinus (1992a), combined with a modification chart by Moon (1984), to ascertain a RMS value for rock type in the Southern Alps, New Zealand. RMS has also been used in other glacial geomorphology studies, for example valley cross-sectional shape in Scotland and Iceland (Brook *et al.*, 2004b), bedrock channels (Wohl & Legleiter, 2003) and the post glacial evolution of valley slopes (Augustinus, 1995b; Brook & Tippett, 2002).

The main problem with the rock classifications listed above is that they require measurements taken in the field. For this thesis, which uses large sample areas from around the globe, taking field samples is not a realistic approach to classifying rock types. Due to the complexity of lithology, and the many permutations, there is no classification method which encompasses all these factors without field measurements. The small exception to this is the defining of constants related to intact rock strength according to rock type by Hoek (2001), for classification of rock types where laboratory tests are not practical. Hoek (2001) provides tables for the uniaxial compressive strength of the intact rock in a rock mass (σ_{ci}) and the intact rock strength constant (m_i),Table 5.1 and 5.2 respectively.

Table 5.1: Field estimates of uniaxial compressive strength of the intact rock in a rock mass (σ_{ci}) (Hoek, 2001).

Grade*	**Term**	**Uniaxial Comp. Strength (MPa)**	**Point Load Index (MPa)**	**Field estimate of strength**	**Examples**
R6	Extremely Strong	> 250	>10	Specimen can only be chipped with a geological hammer	Fresh basalt, chert, diabase, gneiss, granite, quartzite
R5	Very strong	100 - 250	4 - 10	Specimen requires many blows of a geological hammer to fracture it	Amphibolite, sandstone, basalt, gabbro, gneiss, granodiorite, peridotite , rhyolite, tuff
R4	Strong	50 - 100	2 - 4	Specimen requires more than one blow of a geological hammer to fracture it	Limestone, marble, sandstone, schist
R3	Medium strong	25 - 50	1 - 2	Cannot be scraped or peeled with a pocket knife, specimen can be fractured with a single blow from a geological hammer	Concrete, phyllite, schist, siltstone
R2	Weak	5 - 25	**	Can be peeled with a pocket knife with difficulty, shallow indentation made by firm blow with point of a geological hammer	Chalk, claystone, potash, marl, siltstone, shale, rocksalt,
R1	Very weak	1 - 5	**	Crumbles under firm blows with point of a geological hammer, can be peeled by a pocket knife	Highly weathered or altered rock, shale
R0	Extremely weak	0.25 - 1	**	Indented by thumbnail	Stiff fault gouge

* Grade according to (Brown, 1981).

** Point load tests on rocks with a uniaxial compressive strength below 25 MPa are likely to yield highly ambiguous results.

Table 5.2: Estimated values of constant m_i used in the Hoek-Brown Strength Criterion equation to define intact rock strength (Hoek, 2001).

Rock Type	Class	Group	Texture			
			Coarse	**Medium**	**Fine**	**Very Fine**
Sedimentary	**Clastic**		Conglomerates 21±3 Breccia 19±5	Sandstone 17±4	Siltstone 7±2 Greywacke 18±3	Claystones 4±2 Shales 6±2 Marls 7±2
	Non-Clastic	**Carbonates**	Crystalline limestone 12±3	Sparitic limestones 10±2	Micritic limestones 9±2	Dolomites 9±3
		Evaporites		Gypsum 8±2	Anhydrite 12±2	
		Organic				Chalk 7±2
Metamorphic	**Non-Foliated**		Marble 9±3	Hornfels 19±4 Meta-sandstone 19±3	Quartzites 20±3	
	Slightly Foliated		Migmatite 29±3	Amphibolites 26±6		
	Foliated*		Gneiss 28±5	Schists 12±3	Phyllites 7±3	Slates 7±4
Igneous	**Plutonic**	**Light**	Granite 32±3 Granodiorite 29±3	Diorite 25±5		
		Dark	Gabbro 27±3 Norite 20±5	Dolerite 16±5		
	Hypabyssal		Porphyries 20±5		Diabase 15±5	Peridotite 25±5
	Volcanic	**Lava**		Rhyolite 25±5 Andesite 25±5	Dacite 25±3 Basalt 25±5	Obsidian 19±3
		Pyroclastic	Agglomerate 19±3	Breccia 19±5	Tuff 13±5	

* The values for foliated metamorphic rock are for intact rock specimens tested normal to the foliation. The value will be significantly less if stress is applied along a weakness plane.

Details presented in Table 5.1 and 5.2 show that rocks, such as gabbro and granite, are extremely strong in their intact form, whilst shales, siltstones and dolomites, are much weaker. Intact rock strength, however, is one of many parameters which contribute to the erodibility of a rock mass. Jointing, the other major factor, can be exploited by erosional forces and therefore considerably increases erosion rates. Due to the great

variety of jointing, even within the same rock type, a numerical generalisation for this as well as the other categories of erodability, have not been attempted. The problem with only using intact rock strength was discussed by Augustinus (1992a), however other research found that resistance to abrasion was strongly influenced by intact rock strength (Brook *et al.*, 2004b).

Two approaches emerge from this discussion and can be summarised as; firstly, using RMS field measurements, which is extremely time consuming and would only result in a handful of valleys sampled, or secondly, simplifying the lithology, whilst taking many valley cross-section measurements over large areas, in order to compare results. The second approach is taken in this thesis. To be effective, sample areas must incorporate a range of lithologies to enable comparisions to be made. To do this, without the need to take field measurements, the intact rock strength tables together with the literature is used to estimate the rock resistance of a complete rock specimen, as well as the jointing which generally occurs within the specific rock type. From this there is a basis for categorising how resistant a sample area is to glacial erosion.

5.2.2. Tectonic settings

The topographic evolution of a mountain range is a complex interaction between tectonic forces, climatically-driven erosion (Molnar & England, 1990), lithology strength (Hack, 1960) and isostatic rebound. Tectonic uplift, made up of tectonic forcing and isostatic rebound, is one of the major mountain building processes. For the purposes of this discussion the term uplift is meant in the tectonic sense rather than isostasy (the rebound of the Earth's crust due to unloading, either from erosion or reduction in ice mass). Tectonic uplift is greatest at active collisional plate boundaries, such as the Himalayas where the Indo-Australian Plate and the Eurasian Plate collide. In the context of this research, uplift has to occur during glaciation and as such when glacial erosion takes place. Therefore sample areas with active uplift during the Quaternary have been selected.

It has been shown that uplift has an impact on erosion; whether indirectly through climate (Molnar & England, 1990) or by directly by enlarging accumulation areas, in a glacial context (Brozović *et al.*, 1997) and by adjusting in base-level and increasing hillslope processes readily supplying material, in a fluvial context (Burbank *et al.*, 1996; Small & Anderson, 1998). High erosion rates are linked to high uplift rates (Schlunegger

& Hinderer, 2001), although there is evidence that a time lag exists (e.g. Kooi & Beaumont, 1996; Tucker & Slingerland, 1996) and modification of fluvial drainage patterns in relation to uplift rates have been investigated through modelling (Tucker & Slingerland, 1996; Tomkin & Braun, 1999). In conjunction with erosion intensity, the interaction between erosion and tectonics on relief production has been investigated resulting in several different conclusions. Molnar and England (1990) proposed that erosion increased relief due to isostatic uplift, whilst a glacial 'buzzsaw' approach suggests (Brozović *et al.*, 1997) that erosion limits relief, which has since been supported by modelling experiments (Egholm *et al.*, 2009). MacGregor *et al.* (2000) concluded that erosion reduced relief, again supported by modelling experiments (Tomkin & Braun, 2002).

Despite clear links between uplift and erosion rates, few field observations and little modelling work has been carried out to investigate differences in glacial geomorphology where landscapes exhibit differing tectonic settings. Due to areas of high uplift being subjected to greater erosional forces it is suspected that geomorphological forms, such as U-shaped valleys, become larger and more defined during rapid uplift rather than tectonically stable settings.

Therefore, in order to inform the relationship between valley cross-sectional shape and uplift, this thesis must use sample areas which reflect the range of tectonic uplift rates observed around the globe. Rapidly uplifting landscapes must be compared with tectonically inactive mountains. Where literature is available, the uplift rate in mm per year is used to categorise the sample areas into areas of high, moderate and low uplift. Where the values of uplift are not available, the literature is used to establish the evolution of the landscape and therefore the likely tectonic setting.

5.2.3. Climate

Climate impacts the morphology of the landscape by controlling temperature and precipitation and can be linked to tectonic uplift through feedback mechanisms (Molnar & England, 1990). In order for glaciation to occur, precipitation in an accumulation zone must be in the form of snow and the temperatures must be cool enough for it to persist from year to year. Sufficiently cold temperatures may occur as a result of high altitude or latitude, or a combination of the two.

There are many different climate regimes across the globe. Regimes can largely be divided into continental and maritime climates. Continental climates can be characterised by well-defined seasons, with hot summers and very cold winters, as well as low precipitation rates. Whilst maritime climates do not have such temperature extremes, they have high precipitation. One exception is a monsoon regime where a strong seasonal precipitation cycle dominates. For the purposes of ice accumulation, total annual precipitation is the primary factor for ice flux and not whether it falls continuously throughout the year or within a couple of months. Consequently the most important influence on the erosive power of glaciers is the cumulative precipitation, rather than whether it is monsoonal or not and therefore monsoonal regimes are not specifically included in the sample.

Erosion occurs when ice slides over the land surface. The more ice that slides over the surface the more a glacier erodes. This ice flux is primarily controlled by input from precipitation. For sliding to occur, the basal ice temperature must be at pressure melting point to enable the production of water as a lubricant. The greater the volume of ice, and the faster it moves, the more excavation can take place. Climate has a key role in controlling this sliding by controlling precipitation quantity and whether it falls as snow. However, if temperatures become too cold, glaciers can become frozen to their beds so that sliding, and therefore erosion, does not occur. These are known as cold-based glaciers. If warming occurs, basal conditions can become warm-based (i.e. pressure melting occurs and therefore so does sliding and erosion), but there is a fine balance, as if warming continues the ELA rises and as a consequence ice thinning and retreat occurs due to melting. This results in both a reduction in a glacier's erosional power as well as the landscape area experiencing glacial processes. As a consequence the amount of ice in valleys is reduced, reducing ice residence times and flux which may impact on the cross-sectional profile of U-shaped valleys. Less precipitation or temperatures moving away from the optimum for basal sliding and accumulation could result in less well-developed U-shaped valleys, i.e. smaller form ratios, *b*-values and cross-sectional areas.

Although temperature and precipitation are the dominant climate factors which control a glacier's mass balance and by definition ice flux and residence time, Derbyshire and Evans (1976) listed seven local climate conditions and landscape factors which can influence glacier mass balance in relation to cirque development.

1. High latitudes. Low temperatures and low solar radiation found in these regions encourage snow to persist.
2. High altitudes. Here low temperatures and increased snowfall can occur, although at extreme altitudes air moisture reduces the chance of precipitation.
3. A more maritime climate. There is increased precipitation, and cloudiness reduces ablation.
4. Poleward aspects. This reduces ablation by having locally lower temperatures and solar radiation.
5. Leeward aspects which, in some cases, aids snow accumulation and inhibits ablation from heat transfer from the air.
6. Eastward aspects as ablation is less effective in the morning.
7. In topographic concavities which provide shelter and shade.

Although these concepts concerned climate impacts on cirque development, they could be directly related to the evolution of U-shaped valleys. Graf (1970) noted that the location and orientation of valley cirques had a great effect on valley cross-sectional geometry, with favourable cirques creating valleys with greater *b*-values and form ratios. However, little other research has related U-shape valley development to these local climate effects. An exception is a conclusion that valley floor shading could have been one contributing factor to better developed cross-sectional and longitudinal profiles in the Sierra Nevada and Sangre de Cristo Range, USA (Brocklehurst & Whipple, 2006), as it created more favourable conditions for accumulation, which increases ice flux and residence time.

It is assumed, for the purposes of selecting sample areas, that today's climate is a proxy for past climate regimes during the Quaternary, a period when the majority of glacial erosion took place on the landscape morphology seen today. Different climates are considered for sampling so that continental to maritime regimes are represented. Sample sites across the latitudes, from the equator to high latitudes in both the North and South hemispheres, are selected to allow comparisons to be made. Also taken into consideration are areas of different altitudes, from regions glaciated down to sea level, to areas where glaciation has only taken place at the high mountain peaks. Different mountain range orientations, for example the North-South orientation of the Patagonian Andes and the East-West orientation of the Pyrenees, should also be included. Climate gradients *within* sample areas may help identify interesting spatial

relationships with *U-ness* measures informing glacial understanding and therefore should be included in some of the sample areas.

5.2.4. Degree of glaciation

The degree of glaciation is arguably the most difficult of the characteristics to evaluate quantitatively. It can be summarised as the cumulative basal sliding which a point on the landscape has been subjected during the Quaternary. It takes into account the length of time an area underwent glacial processes, the force with which these processes eroded the landscape and the amount of glaciation which occurred. In reality there is no data that quantifies cumulative basal sliding over the timescales of interest. Past studies have used the landscape's geomorphology to indicate the degree to which it has been glaciated (Svensson, 1959; Graf, 1970). As this is a circular argument, it is therefore best to select sample sites according to the degree of glaciation by using the literature to establish any evidence of glacial activity and number of glaciations, note the current extent of ice, if any, and incorporating knowledge of the influence of altitude, latitude and climate on glaciations. From this an understanding of whether the region was a 'core' glacial area or on the periphery of glaciation and therefore only lightly glaciated.

5.3. DEM data

The data used in this thesis is from the Shuttle Radar Topography Mission (SRTM). SRTM was a National Aeronautics and Space Administration (NASA) mission to use the space shuttle to gain the topography of most of the globe. The data produced provides consistent, near-global, high quality DEMs. DEMs were produced from Synthetic Aperture Radar (SAR) interferometric images where the phase-difference of two images is used to measure topography (Farr *et al.*, 2007). The data was sampled over a grid of 1 arc-second by 1 arc-second (approximately 30 m by 30 m) which had a linear vertical absolute error of less than 16 m, a linear vertical height error of less than 10 m, a circular absolute geolocation error of less than 20 m and a circular relative geolocation error of less than 15 m (Farr *et al.*, 2007). The relative height error of the X-band SRTM data is less than 6 m and all quoted errors are at 90% confidence level (Farr *et al.*, 2007). The result of this mission is publicly available data with 30 m resolution for the United States of America land mass whilst the remainder is available in a 3 arc-second

resolution at approximately 90 m (Farr *et al.*, 2007). The data covers 80% of the world's surface, between the 60° North and 56° South latitude (Farr *et al.*, 2007).

5.4. Sample areas

The sample areas chosen for investigation take into account the 4 key influences on glacial processes and landscape characteristics discussed in previous sections. By selecting areas with different characteristics thought to influence the glacial form of valleys, and their spatial relationships, patterns can be investigated. Areas with spatial gradients in characteristics (i.e. the Pyrenees where a climate gradient exists and precipitation decreases from north to south) are chosen so that spatial variability of *U-ness* characteristics can be examined. However, areas with a combination of many characteristic gradients, as well as complex geological and tectonic settings, are avoided as this complexity may make extracting fundamental relationships difficult.

Sample areas are selected where the majority of valleys are free of ice. This enables the valley shape to be investigated, unhindered by an ice surface. An additional consideration is that the method for extracting average valley cross-sections is constrained by a processing limit which restricts the size of the area which can be handled. This area is approximately 10.5 million 90 m x 90 m cells which is equivalent to small mountain ranges such as the Pyrenees.

A final consideration in the sample area selection is the latitude restrictions of the SRTM data. SRTM data is available between 60° North and 56° South latitude, therefore polar regions cannot be included in the sample. This means that areas such as Alaska, northern Canada, Greenland, northern Scandinavia, northern Siberia and Antarctica are all excluded. Research, therefore, concentrates on large expanses of alpine glaciated regions. In fact, alpine regions are of far more use in this research, due to deglaciation exposing the geomorphology to be measured. Final considerations are that areas which still contain ice cannot be analysed and, for ease of projecting the data, the sample areas are kept within discrete UTM zones so that they do not cross UTM boundaries.

5.4.1. Pyrenees

Located at 42° to 43° N the Pyrenees is a relatively small mountain range, 491 km long and with an average width of 200 km, which delineates the French – Spanish border and encompasses Andorra (Figure 5.1). Its area is at the maximum size for processing, when using the average cross-sectional profile method (Chapter 4).

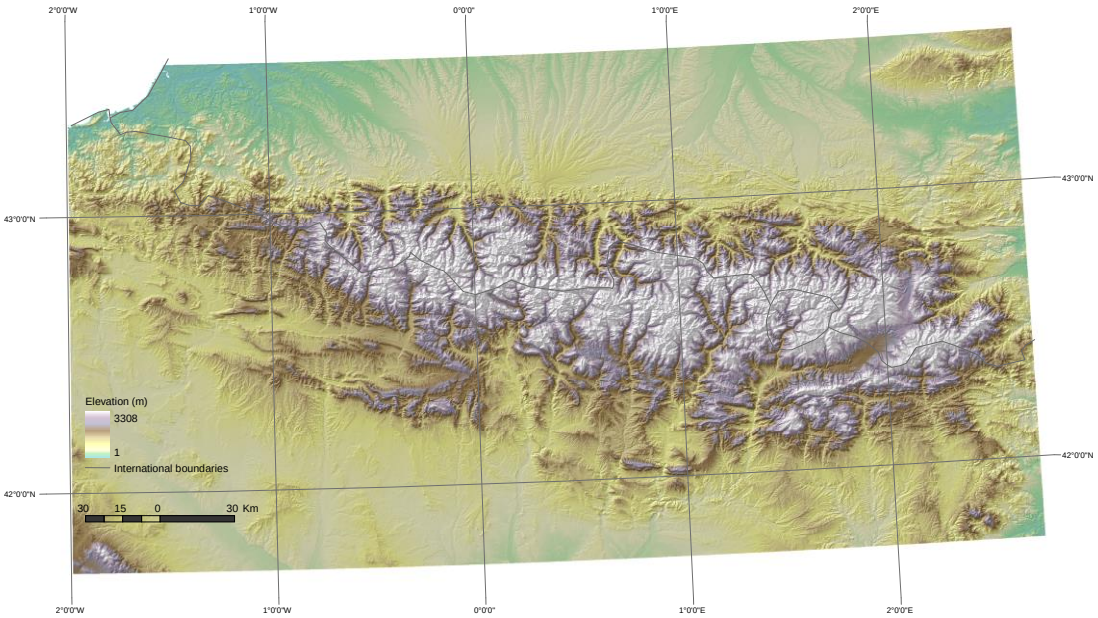

Figure 5.1 The Pyrenees sample area showing the French (in the north), Spanish (in the south) and Andorran (a small, landlocked country in the high eastern Pyrenees) borders. The mountain range has an East-West orientation. The mountain orientation creates a North-South split in the range which divides the area into distinct climatic zones. South of the divide is in a rain shadow and is particularly arid, whilst the north receives much more precipitation. The highest mountain is Aneto at 3404 m, to the West is the Atlantic Ocean and to the East the Mediterranean.

5.4.1.1 Lithology and Tectonics

The lithology in the Pyrenees is relatively homogenous. It was formed when there was convergence between the Iberian and European plates during the Cretaceous and culminating in the Eocene (Choukroune, 1992). Then the Iberian Plate subducted beneath the European Plate. The Pyrenees can be divided into five structural zones. In the north the Aquitaine foreland basin comprises deformed cretaceous sediments of the European Plate. The north Pyrenean thrust zone incorporates the thrust faults of the crystalline basement together with the Mesozoic sediments. The main bulk of the mountains lies in the Axial zone (Figure 5.2) made up of granite and gneissose

(metamorphic) rocks. At the western extent of the range there are also some limestones. It is one of the few modern mountain chains where no remnants of the oceanic crust are observed (Choukroune, 1992). The nature of the rock type, out of the limestone area, means that the lithology is considered hard and therefore resistant to erosion. The south Pyrenean thrust zone comprises deformed early Eocene to Miocene sediments whilst the Ebro foreland basin is filled with relatively undisturbed sediments. As a result of the faulting the Pyrenees is asymmetric in shape across the mountain divide, with steep slopes to the south compared to the north.

Mountain building in the Pyrenees occurred during the Cretaceous period with little uplift since. During the Quaternary, when major glacial cycles occurred, the region has been stable so that no "glacial buzzsaw" (Brozović *et al.*, 1997) feedbacks have taken place. Therefore the Pyrenees can be categorised as a mountain area with low tectonic uplift for the purposes of this thesis.

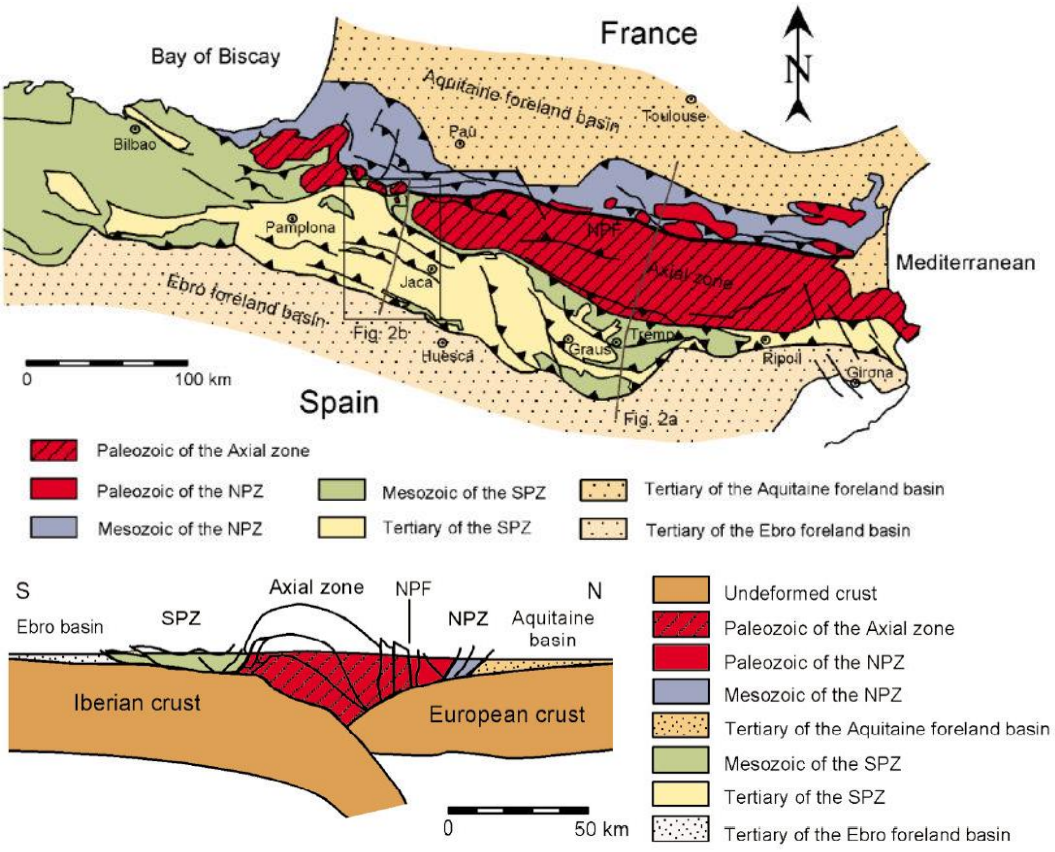

Figure 5.2 The faults and thrusts of the Pyrenean region caused when the Iberian Plate subducted beneath the European Plate and the major geological structures (Schellart, 2002).

5.4.1.2 Climate and Degree of Glaciation

The mountain range acts as a barrier to the north and north-westerly winds from the Atlantic which provide the primary source of humidity (Pallàs *et al.*, 2010). Orographic rainfall means that a north-south precipitation gradient exists with the majority of rain falling to the north (Figure 5.3). A lesser west-east gradient also exists as there is an eastward transition from Atlantic to Mediterranean conditions (Lòpez-Morneo & Beniston, 2009). From the north-westerly winds, a Foehn wind is regularly generated on the southern slopes. This enhances temperatures, increasing the temperature gradient between north and south of the mountain divide (Lòpez-Morneo & Beniston, 2009). In the Central Ebro Depression average annual precipitation is 300 mm and average annual temperatures are 13-15°C (Lòpez-Morneo & Beniston, 2009) whilst in the mountains precipitation exceeds 600 mm, reaching 2,000 mm at the mountain crests (Lòpez-Morneo & Beniston, 2009). Precipitation is seasonal with most falling in the winter (December to March) in the Atlantic areas and during spring (April to June) and autumn (September to November) in the Mediterranean regions (Lòpez-Morneo & Beniston, 2009).

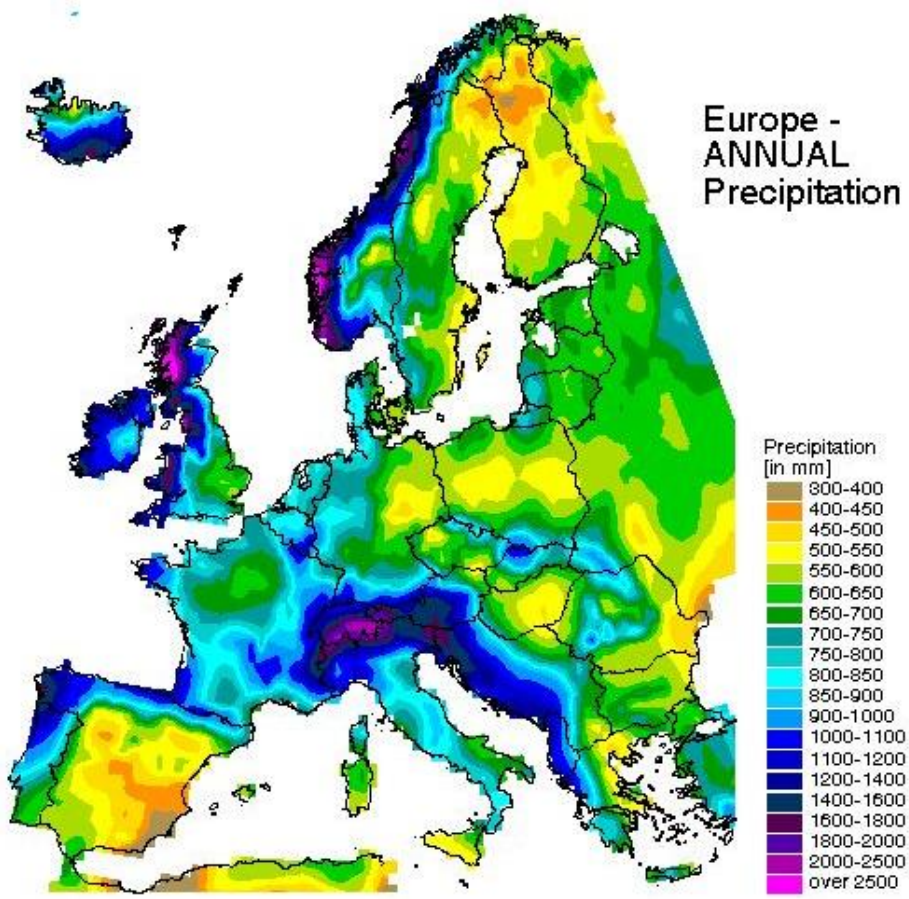

Figure 5.3 A precipitation map of Europe. Focusing on the France and Spain border where the Pyrenees lies, there is higher precipitation north of the divide and to the west of the mountain range. There is a steep precipitation gradient from the divide south into Spain (European Environment Agency, Climate change, impacts and vulnerability in Europe 2012).

Not only does the northern part of the Pyrenees receive more rainfall, and a greater proportion of this in winter, but the east-west orientation of the mountains creates more favourable conditions for glaciation in the north as this part of the Pyrenees receives less solar radiation, both from greater shadier and cloudier conditions (Calvet, 2004). This is reflected in observations of snow accumulation. North of the divide snow exists for longer (169.2 days per year) whilst south of the divide it is present for much less of the year (81.7 days per year) (Lopez-Morneo, 2009). This is partly due to greater accumulation and snow depths, 559.6 mm accumulated snow-water equivalent compared to 152.3 mm (Lopez-Morneo, 2009) but also due to the enhanced conditions for snow persistence created by a northerly aspect in the north compared to the south.

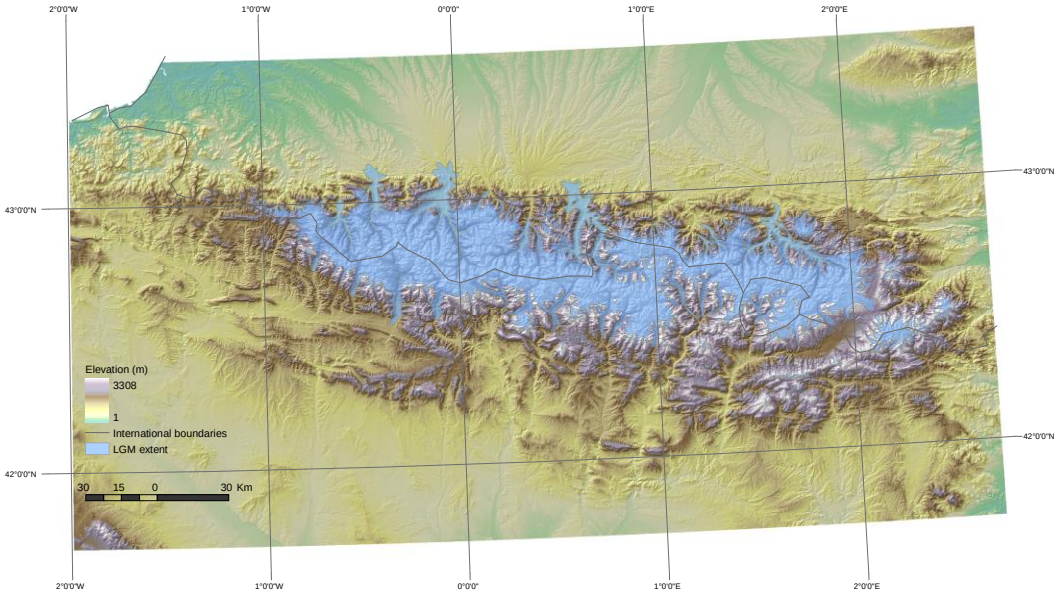

Figure 5.4 LGM limits (Calvet, 2004) depicted for the Pyrenees. Note the ice extent for major tributaries which, at certain locations, extends beyond the mountain range.

The Pyrenees has undergone alpine glaciation and evidence has been found for 6 to 7 glaciations (Calvet, 2004) centred on the mountain divide and some cirque glaciers still remain here (Figure 5.5). Geomorphic evidence indicates that at the LGM glaciers in the north of the Pyrenees reached thicknesses of 900 m and maximum lengths of 65 km descending to 400 m above sea level (Taillefer, 1969). South of the divide glaciers only reached thicknesses of 600 m and lengths of 30 km (Garcìa-Ruiz & Martì-Bono, 1994) This difference is attributed to the more favourable conditions for glaciation north of the divide. Recent evidence points towards glaciers in the Pyrenees having reached a maximum before the global LGM (Pallàs *et al.*, 2010).

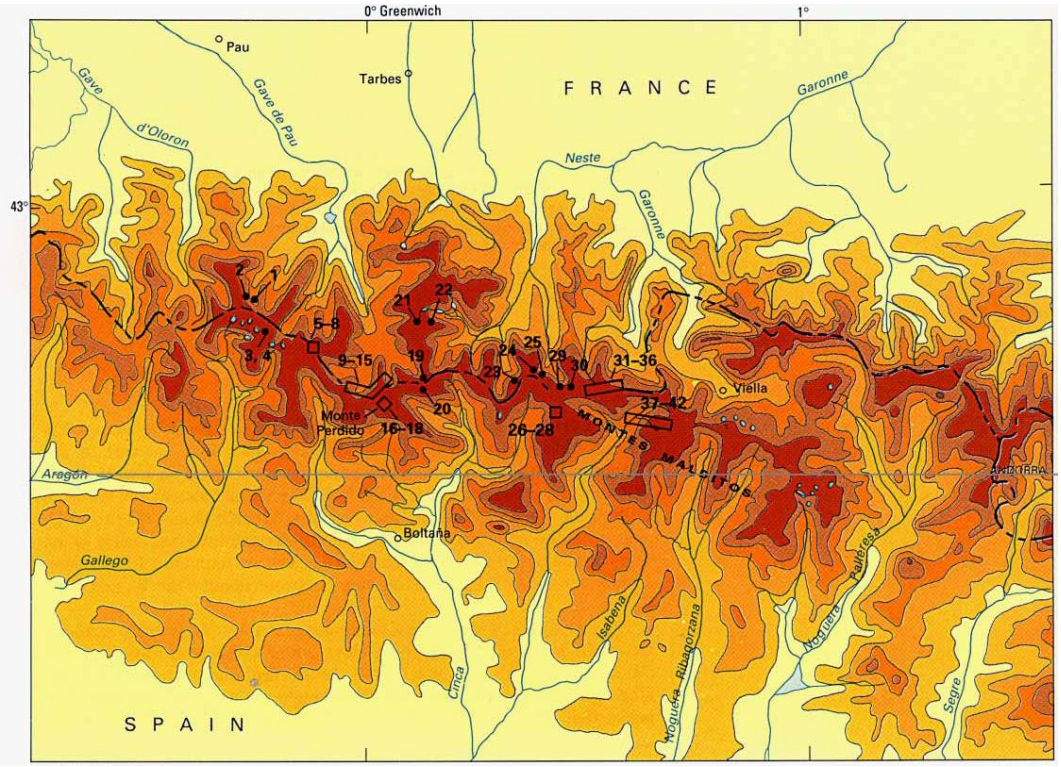

Figure 5.5 Location of present day glaciers in the Pyrenees. Only some cirque glaciers remain, all located in the central Pyrenees (Serrat & Ventura, 1993).

Today only small cirque glaciers at the highest elevations remain (Figure 5.5). Present-day glaciers are confided to northeast-facing cirques (Figure 5.6) with maximum areas not exceeding 1 km² (Serrat & Ventura, 1993; Chueca & Julián, 1996). Current ELAs are at approximately 3,000 m in the central Pyrenees (Copons & Bordonau, 1994; Chueca & Julián, 1996).

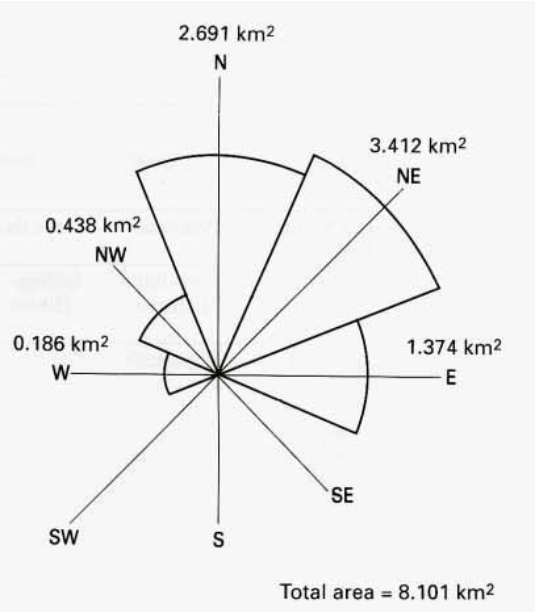

Figure 5.6 The orientation of glaciers in the Pyrenees. The distribution is weighted by area in square kilometres (Serrat & Ventura, 1993).

5.4.1.3 The Pyrenees as a sample area

The Pyrenees also provides an interesting test area for investigating the influence of climate on *U-ness*. There are strong climate contrasts across the mountain divide in the Pyrenees, especially as the snow accumulation north of the divide is also enhanced by its northerly aspect, making it considerably more favourable for glacier occupation and therefore it is anticipated that valleys will display stronger *U-ness* measures. Another test which could be undertaken here is that of the distance from the divide. As the nature of the glaciation has radiated out from the divide, quantifying *U-ness* according to distance from the divide may be an interesting test.

5.4.2. Southern Alps, New Zealand

The Southern Alps in New Zealand is a mountain range (Figure 5.7) which not only experiences some of the greatest uplift rates in the world, but has also recorded some of the highest annual precipitation. The sample area encompasses the Greywacke region of Mount Cook, as well as the chorite and biotite schists on the west coast (Augustinus, 1995a). The climate is strongly maritime in New Zealand, dominated by westerly winds supplying a humid air mass to fuel orographic rainfall. Glacial activity has been predominantly alpine in nature and some valley glaciers still remain today.

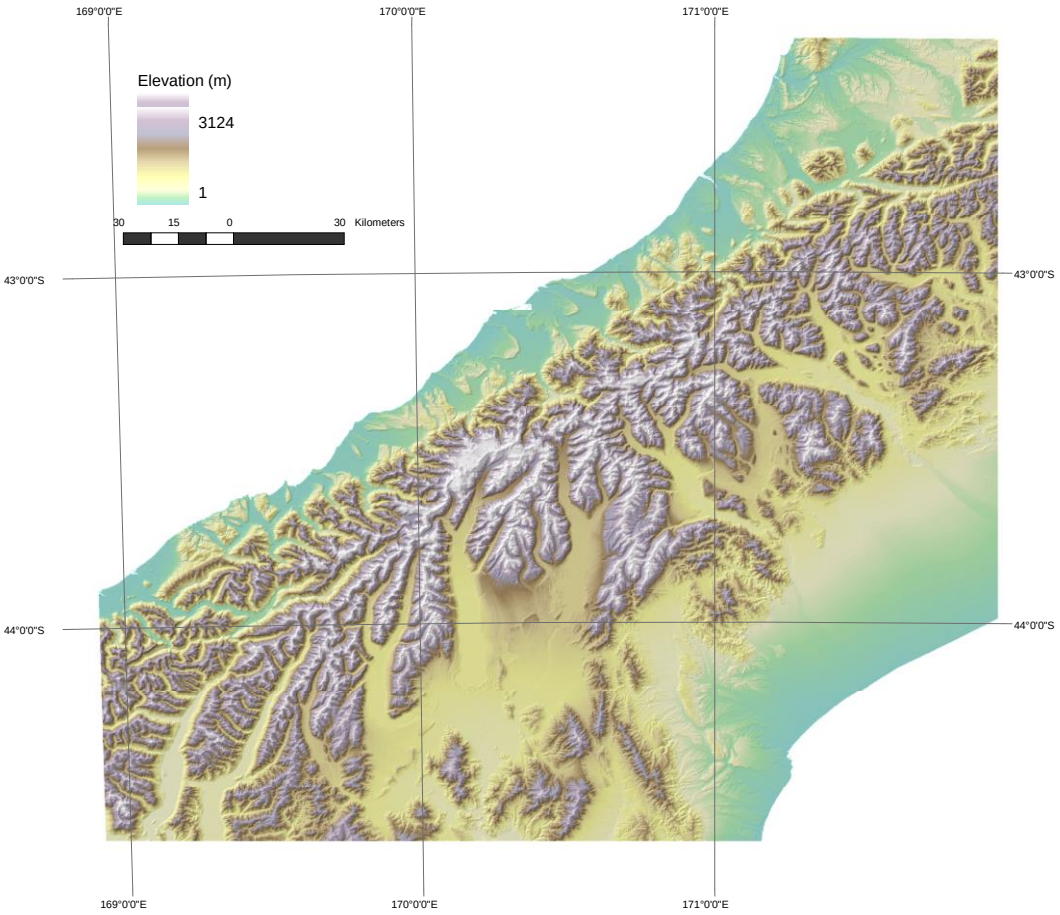

Figure 5.7 Southern Alps sample area is on the South Island, New Zealand. It has not only one of the highest uplift rates in the world but also extremely high precipitation. The sample area includes some particularly weak lithology to the east of the mountain divide, whilst the region at the divide and to the west comprises slightly more resistant bedrock. It is wetter on the west coast with precipitation decreasing to the east of the divide from a rain shadow effect. The sample area encompasses the highest mountain in New Zealand, Mount Cook, at 3754 m.

5.4.2.1 Lithology and tectonics

New Zealand's South Island is dominated by a fault system which runs the length of the island and demarcates the Pacific and Australian Plate boundary. The Southern Alps is a result of the convergence of these plates, Figure 5.8, which during the late Cenozoic Period onwards created uplift of the Pacific Plate (Tippett & Hovius, 2000). From the point of plate convergence a 100-200 km wide zone of deformation is evident in the South Island whilst several subduction zones exist; the Puysegur Trench to the

southwest near New Zealand's Fjordland and where the Australian Plate subducts beneath the Pacific Plate, whilst at the Hikurangi Trench to the northeast, which extends to North Island, the Pacific Plate subducts beneath the Australian Plate. In the northeast of South Island the main alpine fault splits into a number of strike-slip faults in the Marlborough region which extend out to the Hikurangi Trench.

The compression along the plate boundary is dated between 11-12 ma ago (Sutherland, 1995; 1996) to 9.8 Ma ago (Stock & Molnar, 1982) and was caused as a result of a change in migration direction. It is thought that although there have been periods of acceleration the plate motion has not changed significantly over the last 5 Ma (Sutherland, 1995). The current rate of plate displacement in the central segment of the Alpine fault is 071 ± 3°, with an average rate of 38.5 ± 3 mm a^{-1} (De Mets *et al.*, 1990). This motion is oblique to the plate boundary and has a normal rate to the average fault strike (055°) of 11 ± 2 mm a^{-1} and a fault parallel rate of 37 ± 2 mm a^{-1} (De Mets *et al.*, 1990).

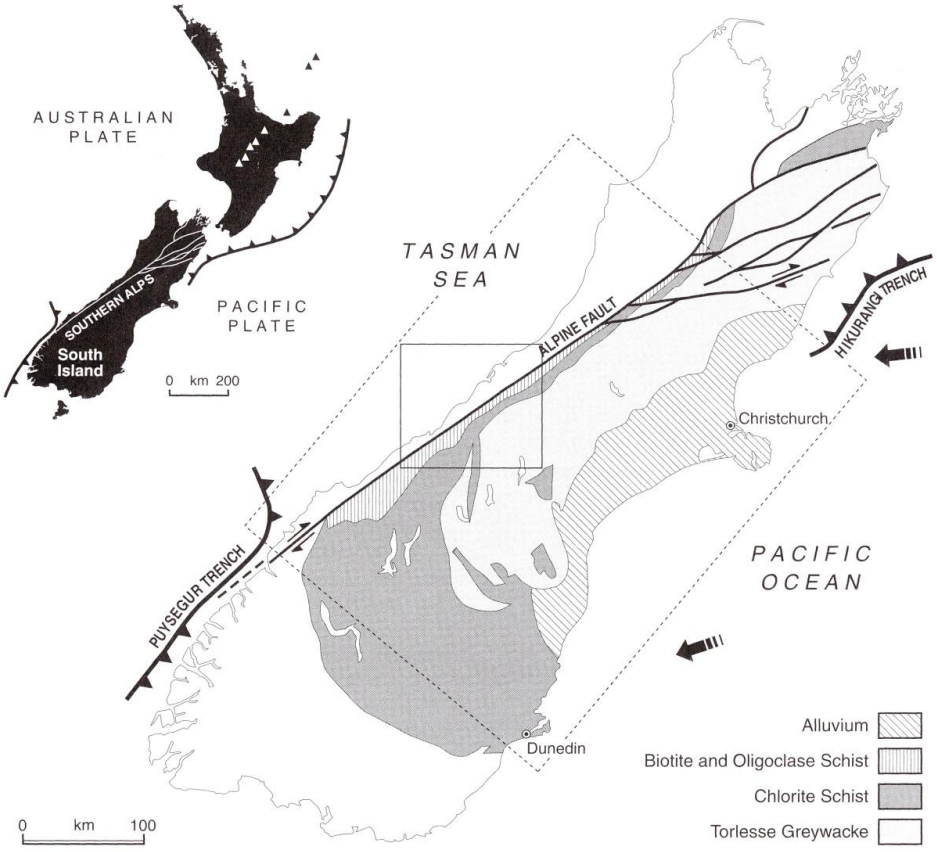

Figure 5.8 The tectonic setting and lithology of the Southern Alps. The arrows show the direction of plate motion towards the Australian Plate is fixed. The dashed box shows the area in Figures Figure 5.9, Figure 5.16 and Figure 5.17 whilst the solid box shows the area in Figure 5.13 (Tippett & Hovius, 2000).

The Southern Alps is a relatively small mountain range of 350 km in length, when measured from the Huruni River to the Arawata River (Figure 5.9) (Tippett & Hovius, 2000). Interaction and feedbacks between uplift and denudation characterise the mountains of the Southern Alps. A particular characteristic is the range's asymmetry, which rises steeply in the west, close to the Alpine fault, and drops away more gently to the east. Mountains range between 2,000 – 4,000 m, with the highest peak being Mt Cook at 3,754 m.

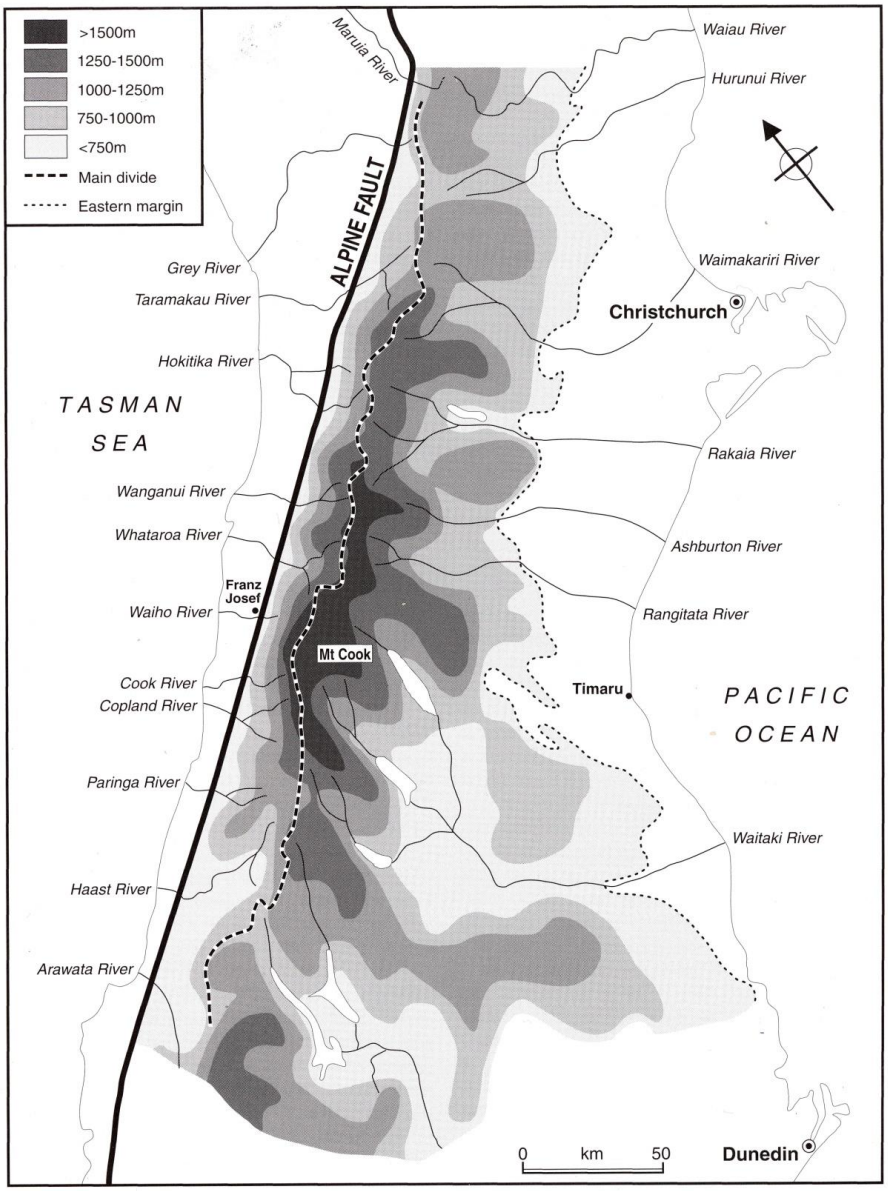

Figure 5.9 The topography of the Southern Alps showing mean surface elevation (metres), the major rivers and valleys, the location of the divide and Alpine fault and the eastern margin of the basin outcrop (Tippett & Hovius, 2000).

During glacial cycles there has been intense tectonic uplift from tectonic collision. Horizontal movements of plates are much easier to estimate than vertical movements partly because vertical movements are generally smaller and partly because they are harder to measure (Beavan *et al.*, 2010), therefore literature on uplift rates in the Southern Alps is sparser. A still regularly cited estimate is that by Wellman (1979) who mapped the uplift rates across the Southern Alps (Figure 5.10). Wellman (1979) estimated areas close to the mountain divide in the Central Southern Alps to have vertical rates of up to 10 mm per year. Subsequently uplift rates have been estimated to be at 7-10 mm/yr (Tippett & Kamp, 1993). More recent research using GPS data sites and modelling found that present-day uplift rates were closer to 5 mm per year near the crest of the mountains (Figure 5.11 and Figure 5.12) (Beavan *et al.*, 2010).

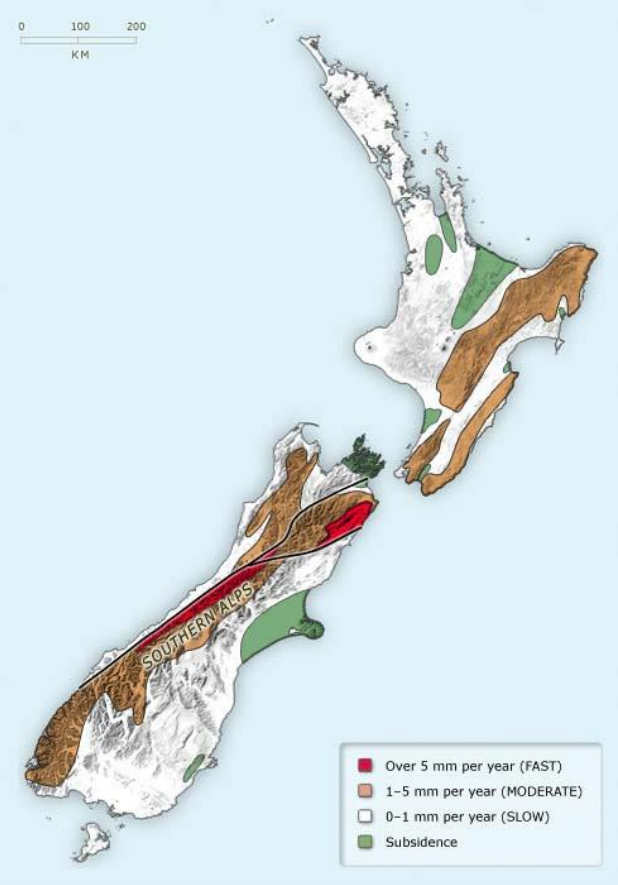

Figure 5.10 Surface uplift map from Wellman (1979) for South Island and Pillans (1986) for North Island, with some generalisation by Carolyn Hume, GNS Science.

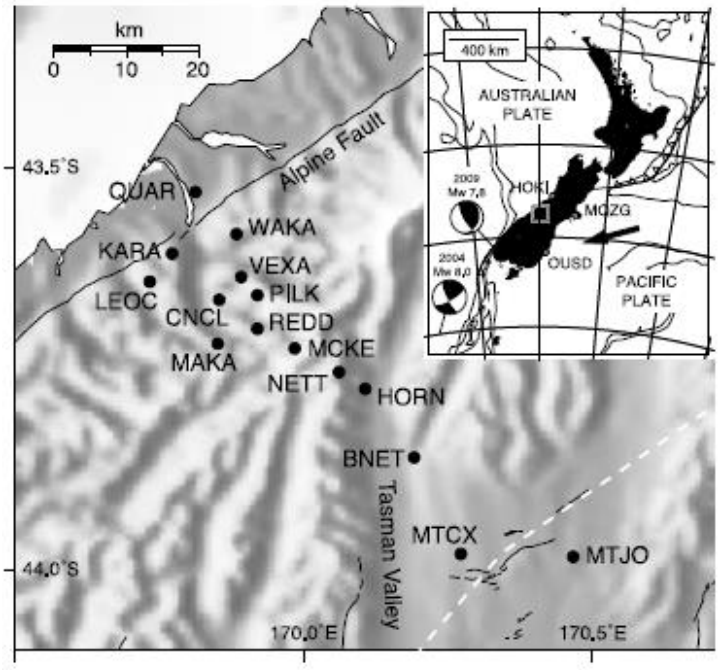

Figure 5.11 GPS sites used to monitor surface uplift and their location within the Southern Alps and in relation to the alpine fault (Beavan *et al.*, 2010).

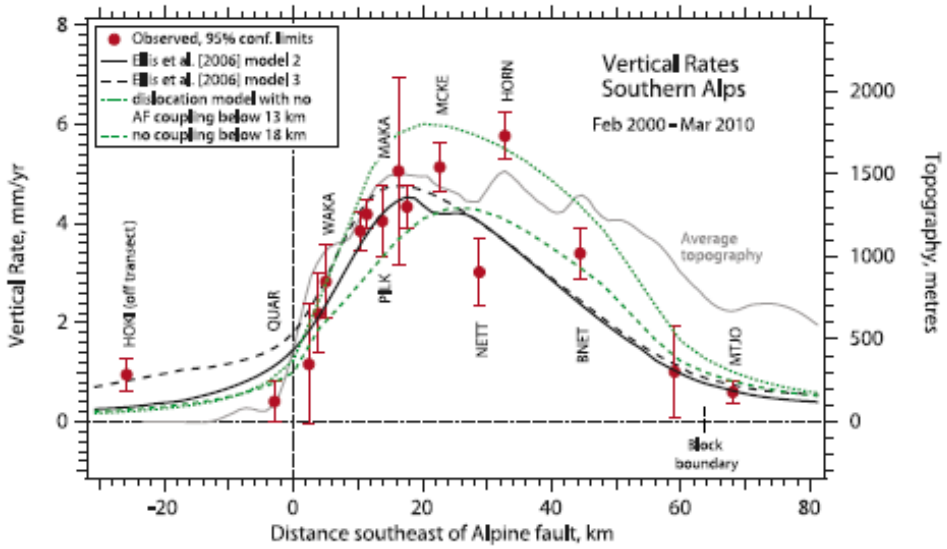

Figure 5.12 Relative vertical uplift rate across the mountain divide in the Southern Alps uplift. Showing observed GPS data and errors, as well as model predictions (Beavan *et al.*, 2010).

The lithology in the central Southern Alps is dominated by schists and greywacke (Figure 5.13), with the mountain divide being close to the rock type divide. Greywacke is a rock type which comprises a series of alternating sandstone and mudstone (argillite) layers, together they are known as greywacke. Additional rock types such as limestone, chert,

conglomerate and spilite can also be found faulted into this rock type. Although greywacke has a high Intact Rock Mass Strength (IRMS) it has a low Design Rock Mass Strength (DRMS) due to the interbedding of the sandstone and mudstone which cause weakness from the large amount of foliations in the lithology. Overall the greywacke region has a low RMS value of 79.1±5.3 (Augustinus, 1992a). Greywacke is found predominantly to the east of the mountain divide whilst schists dominate the west. Here the lithology comprises closely jointed and foliated metamorphosed chlorite and biotite schists. Due to the close jointing, overall, the schists have a slightly higher RMS of 83.1±7.4 than the greywacke (Augustinus, 1992a).

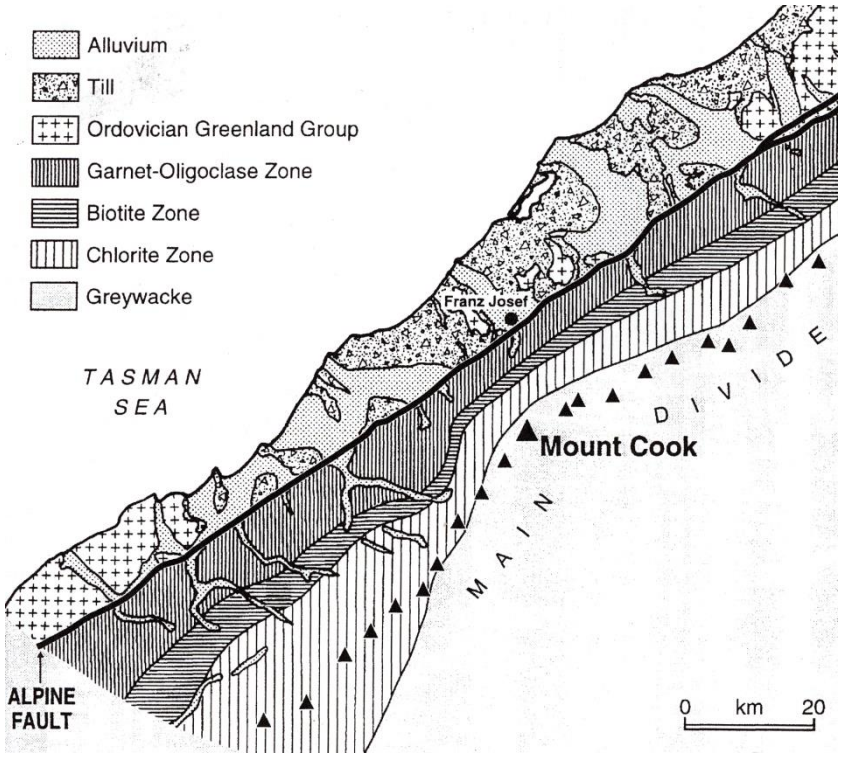

Figure 5.13 A simplified geology map of the Southern Alps showing all major lithologies (Tippett & Hovius, 2000).

5.4.2.2 Climate and Degree of Glaciation

Present-day climate in New Zealand is strongly maritime. The weather is dominated by humid westerly winds from the Tasman Sea causing orographic rainfall once this air mass is forced to rise over the Southern Alps. Rainfall is also a product of anticyclones and troughs of low pressure and a strong foehn effect often occurs (Chinn & Whitehouse, 1978). Due to the westerly winds a rain shadow effect occurs on the eastern mountain slopes. Precipitation distribution is also a function of elevation and horizontal distance from the divide (Griffiths & McSaveney, 1983). As much as 10,000

mm of annual precipitation can occur on the western slopes of the Southern Alps (Hicks *et al.*, 1990) but decreases to 5,000 mm at the divide and reduces to 1,000 mm further east (Hicks *et al.*, 1990) (Figure 5.14 and Figure 5.15). There are not strong seasonal influences and precipitation tends to be evenly distributed throughout the year (Chinn & Whitehouse, 1978).

Research based around modelling has been used to establish climate in the Southern Alps during the LGM. It found that not only were temperatures cooler but, to create ice extents indicated by empirical data, the climate also had to be much drier. Estimates of a 25% drier than the present day climate are proposed (Golledge *et al.*, 2012).

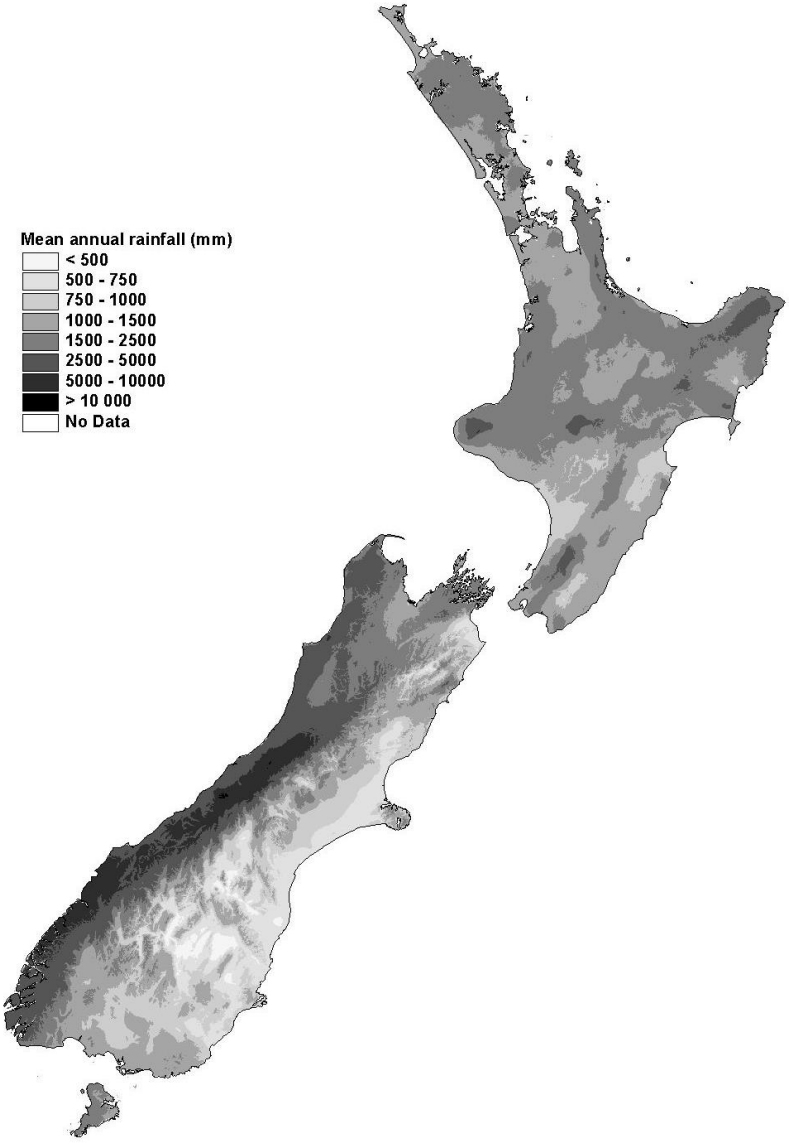

Figure 5.14 Precipitation map of New Zealand depicting the extremely high precipitation on the west coast of South Island (Leathwick *et al.*, 2002).

Snow makes up part of the precipitation in the Southern Alps and is dependent on the altitude (Figure 5.15 and Figure 5.16). For example Ivory Glacier at an altitude of 1,400 - 1,800 m receives approximately 25% of its precipitation as snow (Anderton & Chinn, 1978). Mt Cook on the crest of the mountain divide has a glacier snowline at 1,800-2,000 m at the end of the summer (Tippett & Hovius, 2000) (Figure 5.16). Although westerly winds prevail, and as noted earlier are key for the delivery of precipitation to the region, southerly winds are important sources of snow (Chinn & Whitehouse, 1978). Winter precipitation contributes to accumulation of present-day glaciers (Figure 5.17).

The precipitation gradient impacts the altitude of current glacier extent. Glaciers on the west coast, where precipitation is greatest, reach altitudes as low as 1,700 m, whilst the altitude increases with distance east (Figure 5.17), creating ELA gradients across the divide (Figure 5.18).

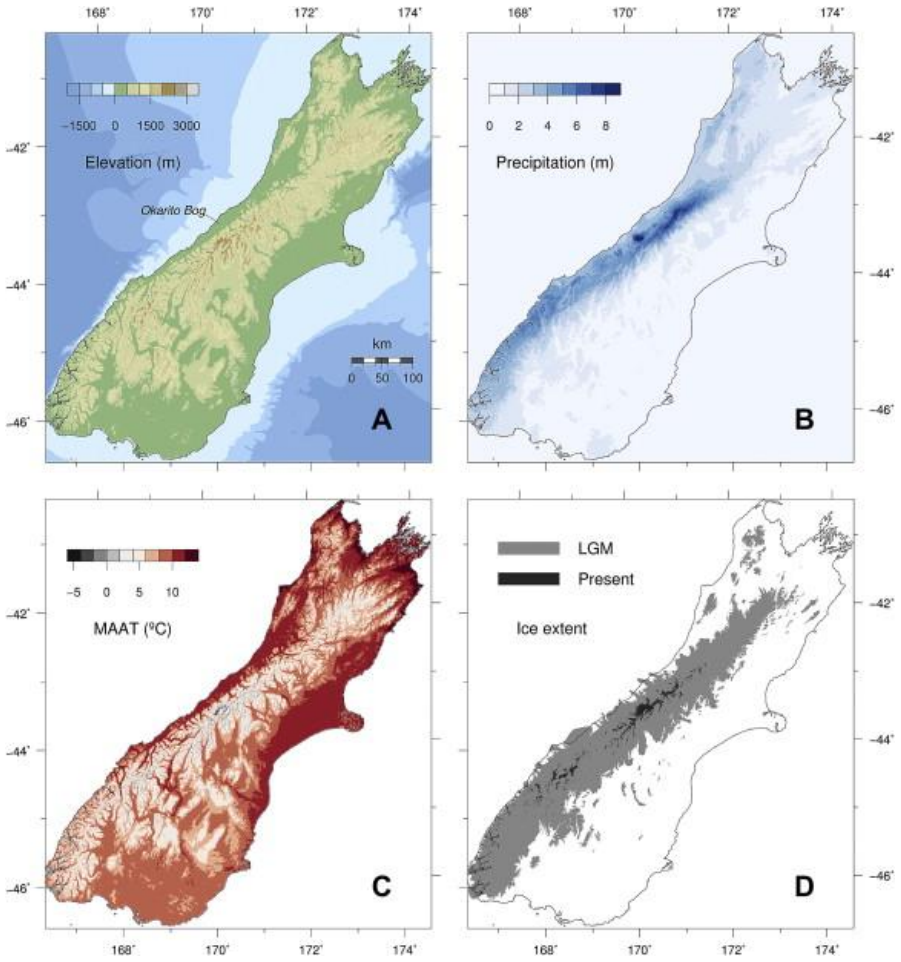

Figure 5.15 Climate characteristics of the Southern Alps showing (a) the topography, (b) the mean annual precipitation, (c) mean annual air temperature and (d) the LGM and present day ice extent (Golledge *et al.*, 2012).

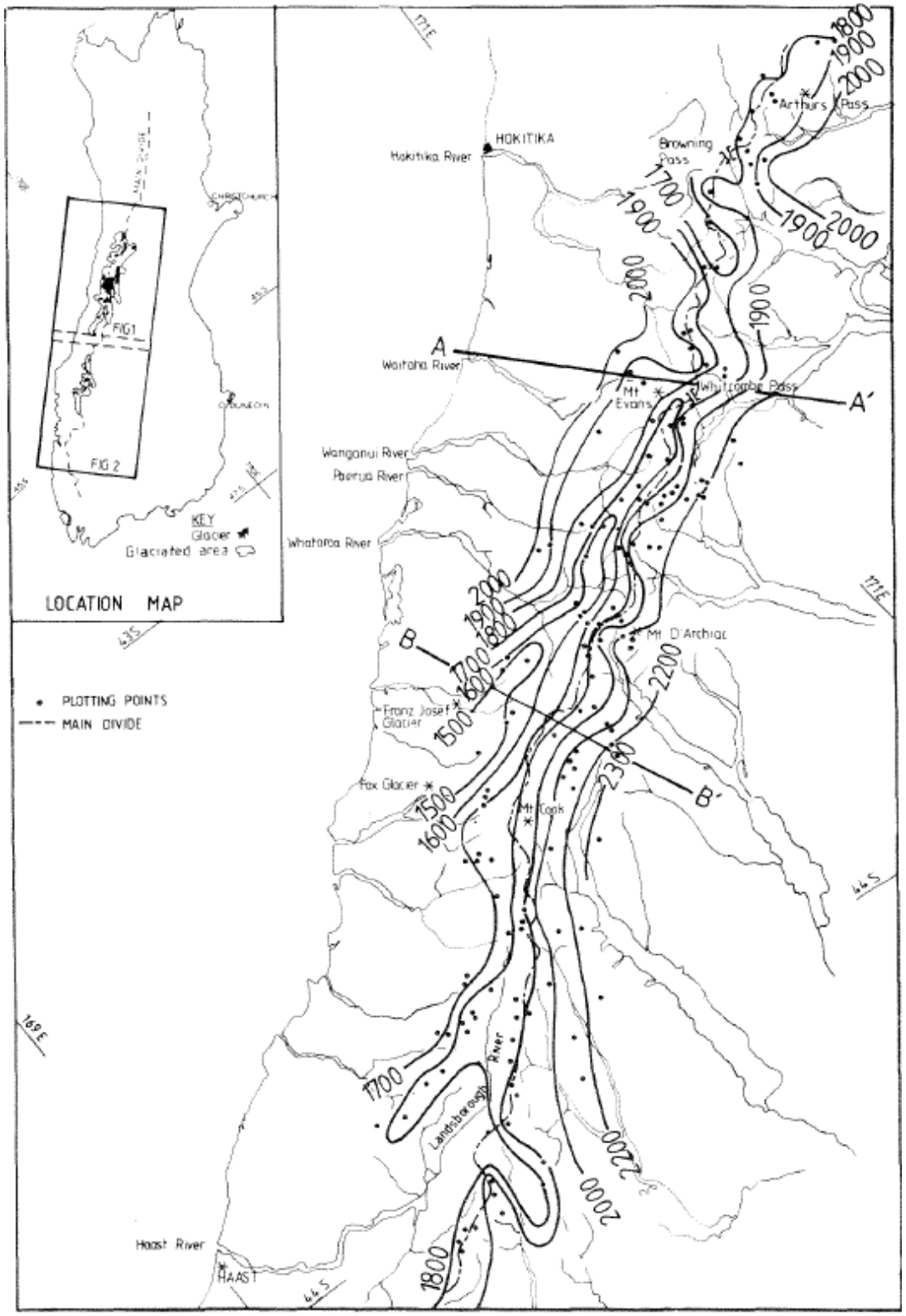

Figure 5.16 1978 glacier snow line elevation contours for the northern section of the glaciated Southern Alps (Chinn & Whitehouse, 1978).

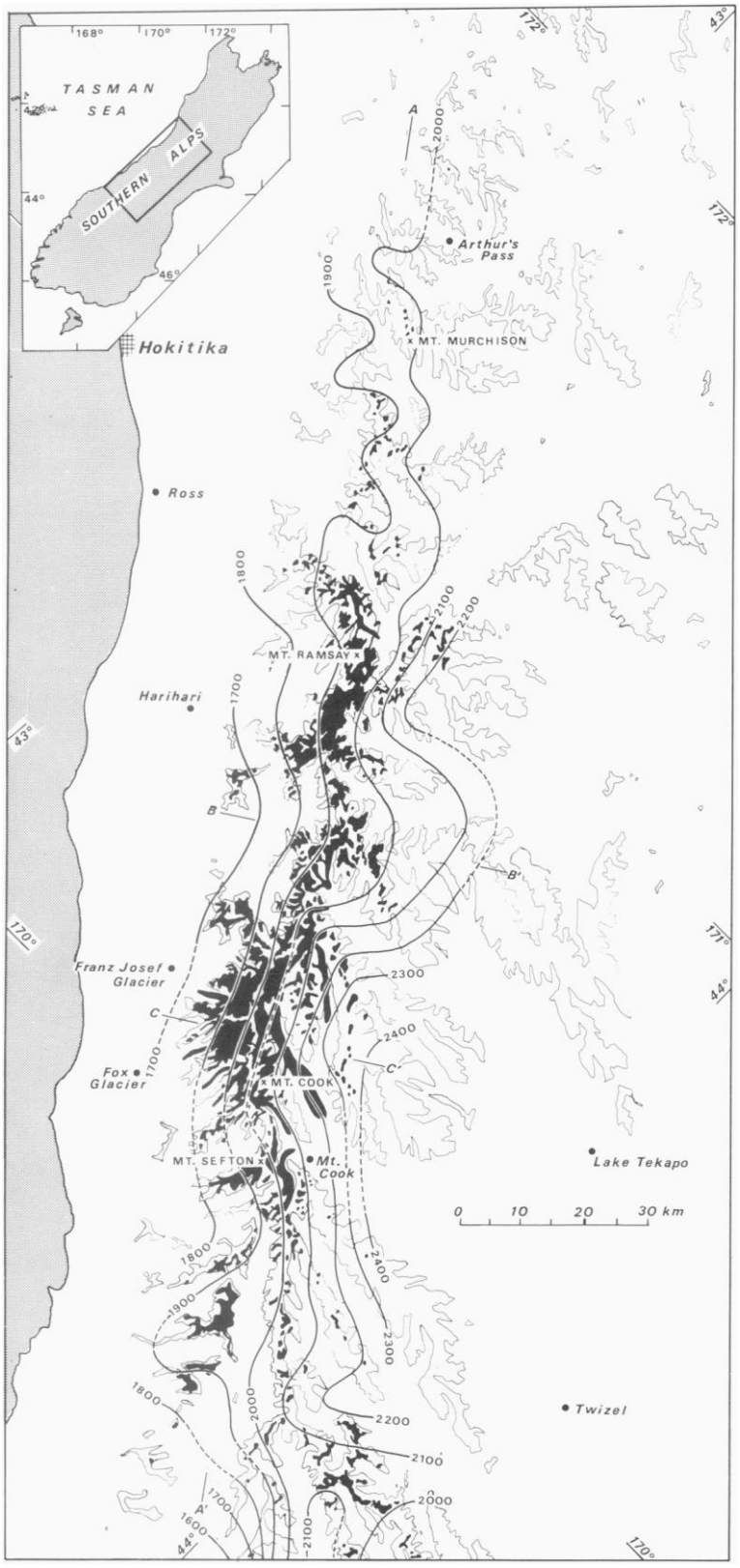

Figure 5.17 Map of the Southern Alps showing isoglacihypses (m), lines showing the elevation of current glacial extent. The range is between 1,600 and 2,400 m and generally rises southeastward away from the west coast (Porter, 1975).

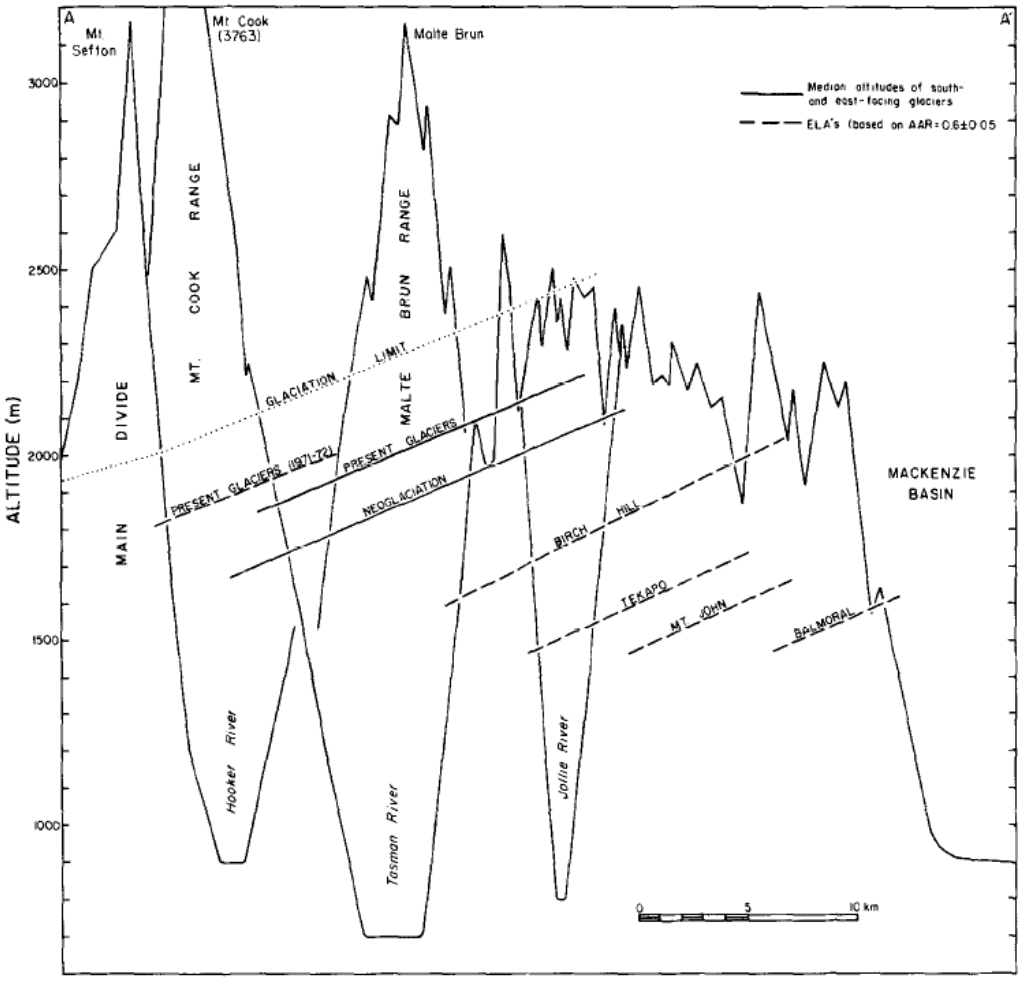

Figure 5.18 A cross-section which bisects the main divide along the Tasman River-Lake Pukaki drainage basin showing reconstructed ELA gradients for Pleistocene ice advances, gradients of median altitude of east and south-facing glaciers at present and during Neoglacial advance and glaciations limit (dotted line) (Porter, 1975).

More local effects at the valley-scale also influence snow accumulation in the Southern Alps including avalanching, wind affects and aspect. Polar facing (south) aspects tend to have lower snowlines at the mountain and individual glacier scale (Figure 5.19) (Chinn & Whitehouse, 1978). Although, similar to ELAs, snowline altitudes mimic the precipitation gradient across the divide and are exaggerations of the glaciation limit (Porter 1875), being up to four times as steep (Chinn & Whitehouse, 1978) and 10-20 times as steep as those measured for the arctic and sub-arctic regions (Andrews & Miller, 1972) (Figure 5.20). Chinn and Whitehouse (1978) did find that this was not always true (Figure 5.21) as in some regions a strong precipitation gradient existed but no snowline altitude gradient and this was attributed to local effects mentioned previously (Figure 5.19).

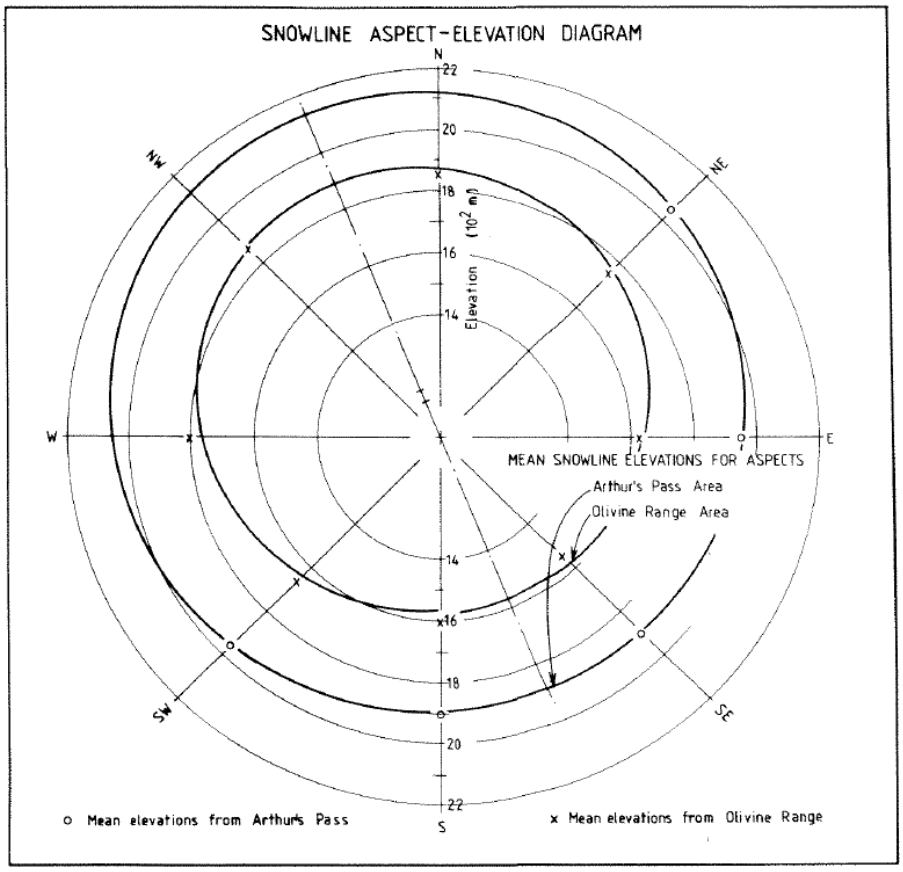

Figure 5.19 Plot of snowline elevation and aspect showing the variation of mean glacial snowline elevation with aspect. Note the decrease in snowline altitude towards the south and southeast.

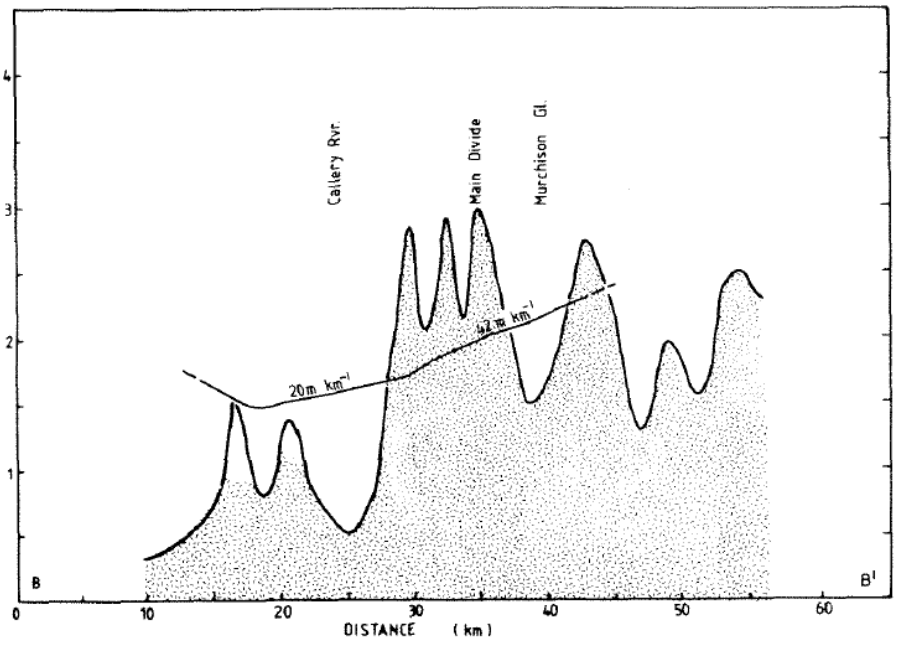

Figure 5.20 Topographic profile across the Southern Alps, north of Mt Cook, showing the glacier snowline gradient as snowlines increase to the east (Chinn & Whitehouse, 1978).

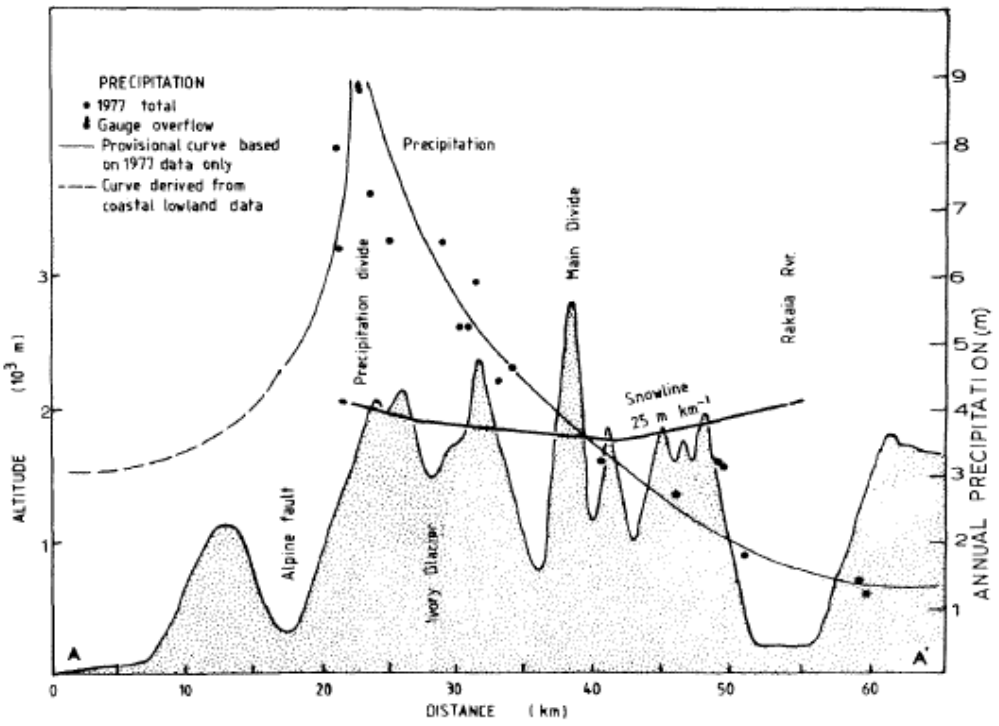

Figure 5.21 Annual precipitation gradient and snow line gradient across the Southern Alps Main Divide including the topographic profile near Whitecombe Pass. Showing a strong precipitation gradient but a steady snowline altitude (Chinn & Whitehouse, 1978). Here snowline gradient appears to have an inverse relationship with precipitation gradient.

Glacial activity has been predominantly alpine in nature. At the LGM the glaciers extended to the edges of the mountain range in the east and the coast in the west (Figure 5.22) and some valley glaciers still remain today. It is estimated that up to 12 glaciations occurred in the region, for which there is evidence for 8 (Suggate, 2004). A combination of extremely high uplift rates and high precipitation has intensified erosion. Research has suggested rock exhumation rates of up to 10mm per year (Batt & Braun, 1999) Figure 5.23 shows an estimate of late Cenozoic erosion in the Southern Alps. Estimates near the Alpine divide give a total of 18 km of erosion. Therefore the Southern Alps can be classified as having a high degree of glaciation.

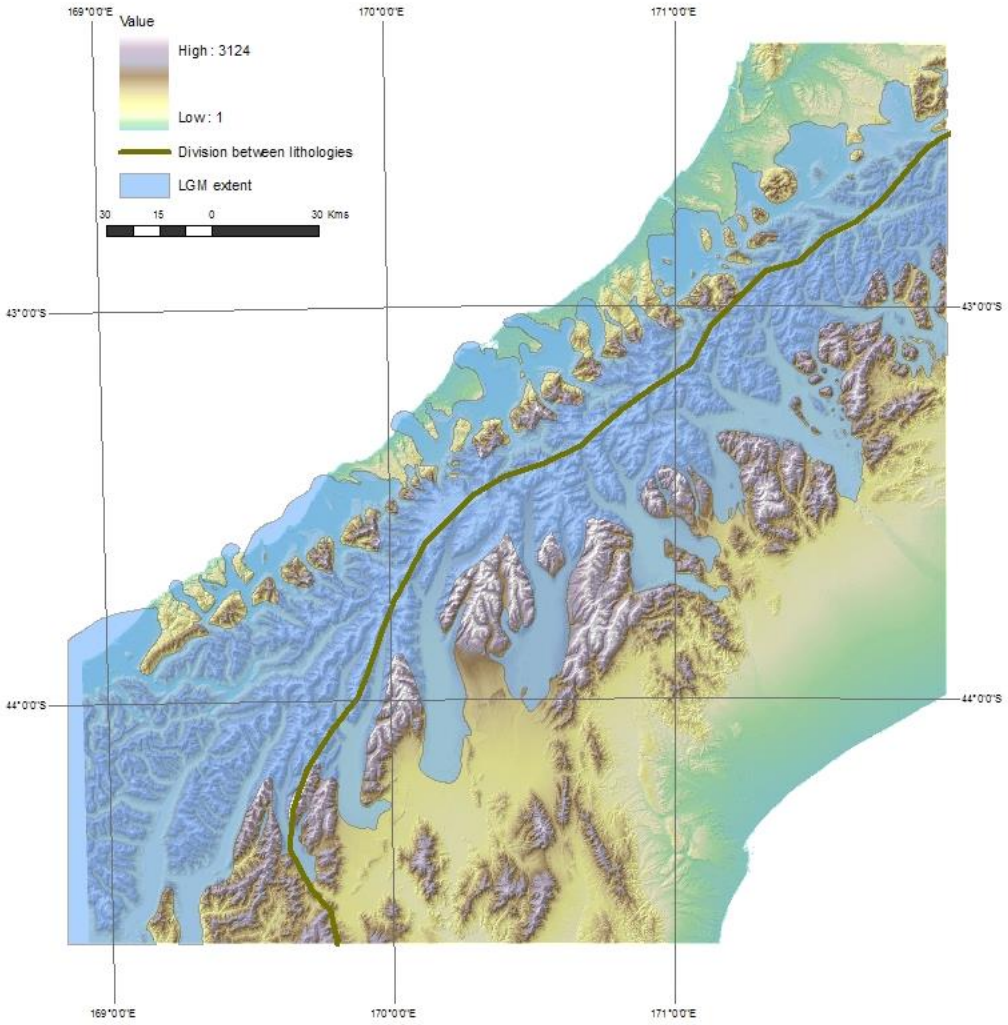

Figure 5.22 The LGM ice extent of the Southern Alps (Calvet, 2004). Ice extends to the coast west of the divide and large tongues of ice extend east. The division between lithologies is shown.

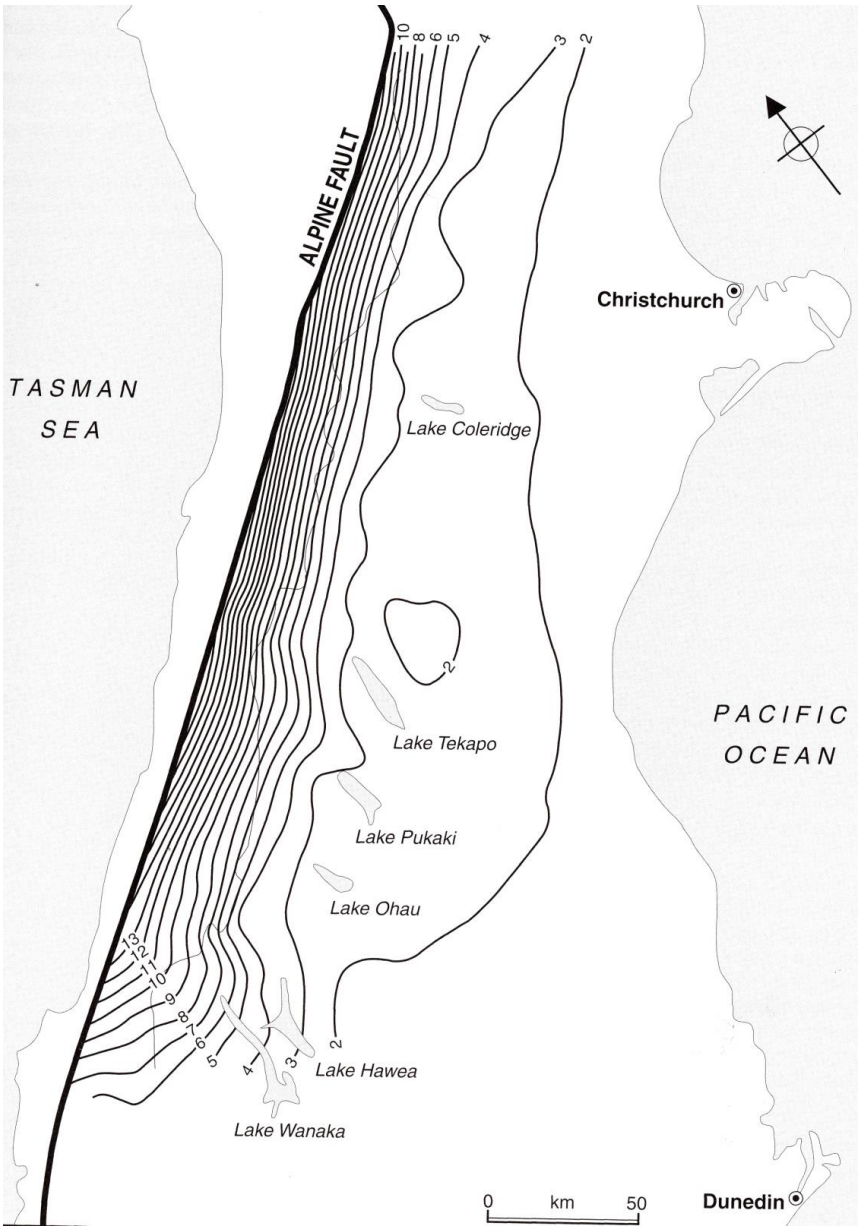

Figure 5.23 Contour map showing the amount of late Cenozoic erosion (in Kilometres) of the Southern Alps (Kamp & Tippett, 1993). The Alpine Fault (thick black line) and position of the main divide (line grey line) are shown.

5.4.2.3 The Southern Alps, New Zealand as a sample area

Due to the Southern Alps having some of the greatest precipitation and uplift in the world, it is an obvious choice to compare *U-ness* measures to *U-ness* measures of sample areas which do not have such high precipitation and have not been so tectonically active during the Quaternary. The precipitation gradient within the mountain range itself also provides a test without needing to compare different sample areas. Different lithologies as well as mountain asymmetry may provide an area for testing hypotheses, but further investigations will have to be made as to whether the

complexities of these characteristics are too great and/or differences are not significant enough for clear conclusions to be drawn.

5.4.3. Southern Andes

The Andes is a mountain range which stretches 7,000 km; the full length of South America. Although far too large to be evaluated in its entirety, several sites can be sampled at different locations along this greater range to provide an interesting experiment for examining how *U-ness* measures change over different latitudes (Figure 5.24). The Andes southern range creates the border between Chile and Argentina at approximately the mountain divide. At its southern extreme the region of Patagonia has undergone ice sheet erosion.

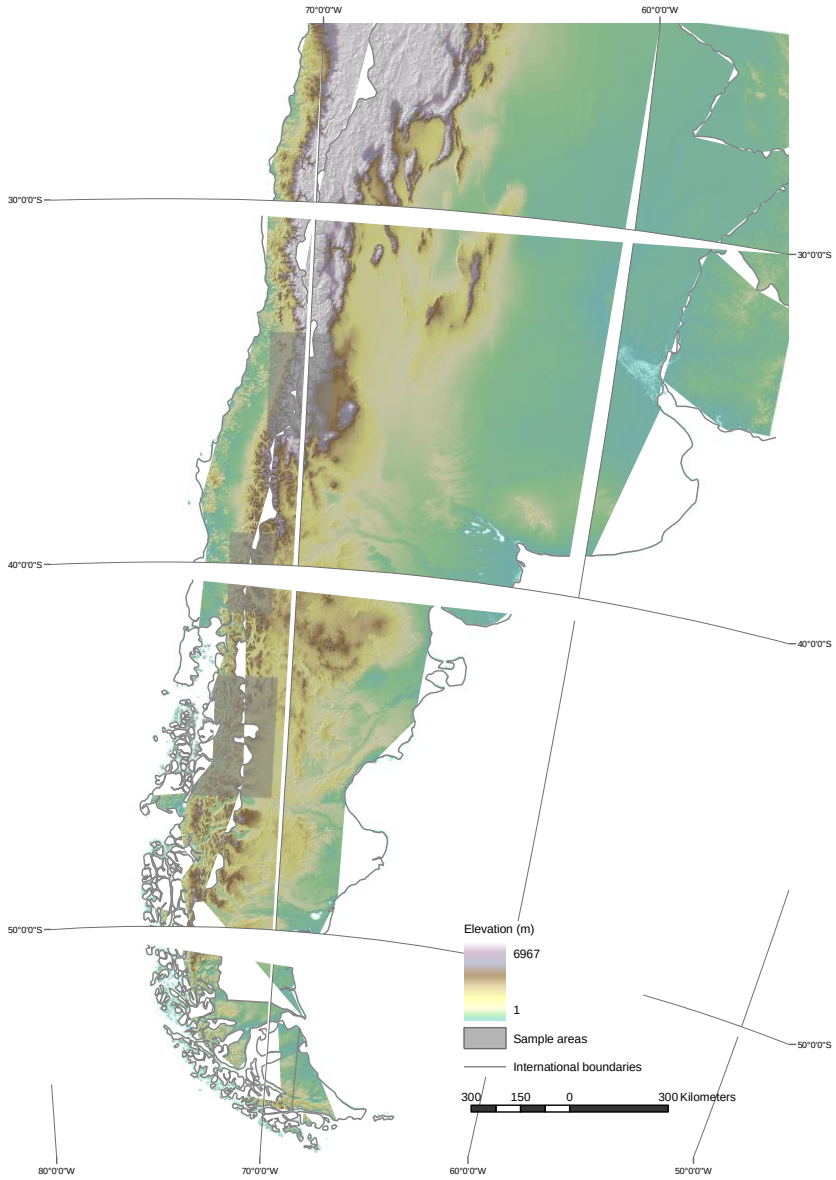

Figure 5.24 The three southern Andes sample areas (shown as greyed out regions), which bisect the Chilean / Argentine border, shown in relation to the South American continent. In contrast to the Pyrenees the Andes has a North-South orientation with more precipitation found on the western slopes and to the south. Created by an active subduction zone, uplift is moderate and the degree of glaciation increases southward due to being located in the southern hemisphere. Therefore these sample areas provide an opportunity to investigate how changing intensity of glaciations (latitude) influences valley cross-sections.

5.4.3.1 Lithology and tectonics

The present-day mountain belt developed mainly during the Mesozoic to recent times, as the Nazca and Antarctic Plate subducts beneath the South American Plate (Figure 5.25), creating an active volcanic arc with a fold-thrust belt in the foreland. As a consequence, the lithology is characterised by igneous intrusions and silicic volcanics (Moores & Twiss, 1995).

Again, as noted for the Southern Alps, literature on slip and subduction rates are more widely reported than uplift in the region. From geological indicators uplift and deformation can be dated from Cenozic times and dating clearly shows that deformation moved from south to north (Kennan, 2000). Although initial denudation rates were high, a drop was evident by ~60 Ma BP (Nelson, 1982). The youngest deformation is in the extreme south and is from the Eocene period (Winslow, 1981). Northwards the deformation is younger, ~15 Ma to the late Miocene (Ramos, 1989; Flint *et al.*, 1994). In conclusion, there has been negligible crustal surface uplift during the Quaternary. Today, mountains in the region are at altitudes of up to ~3,700 m and greatly influence the climate in the region, which is discussed in the following section. Recently, very high crustal vertical uplift rates, 39 mm yr^{-1}, have been recorded (data for the period 2003-2006) (Dietrich, 2010) (Dietrich *et al.*, 2010). This has been attributed to isostatic rebound due to ice loss. For this research it is more relevant to look at the rate over the Quaternary period when glaciations have taken place, so the recent unusually high uplift rate can be discarded. Therefore it can be concluded that the region can be categorized as having moderate to low uplift across the Quaternary period.

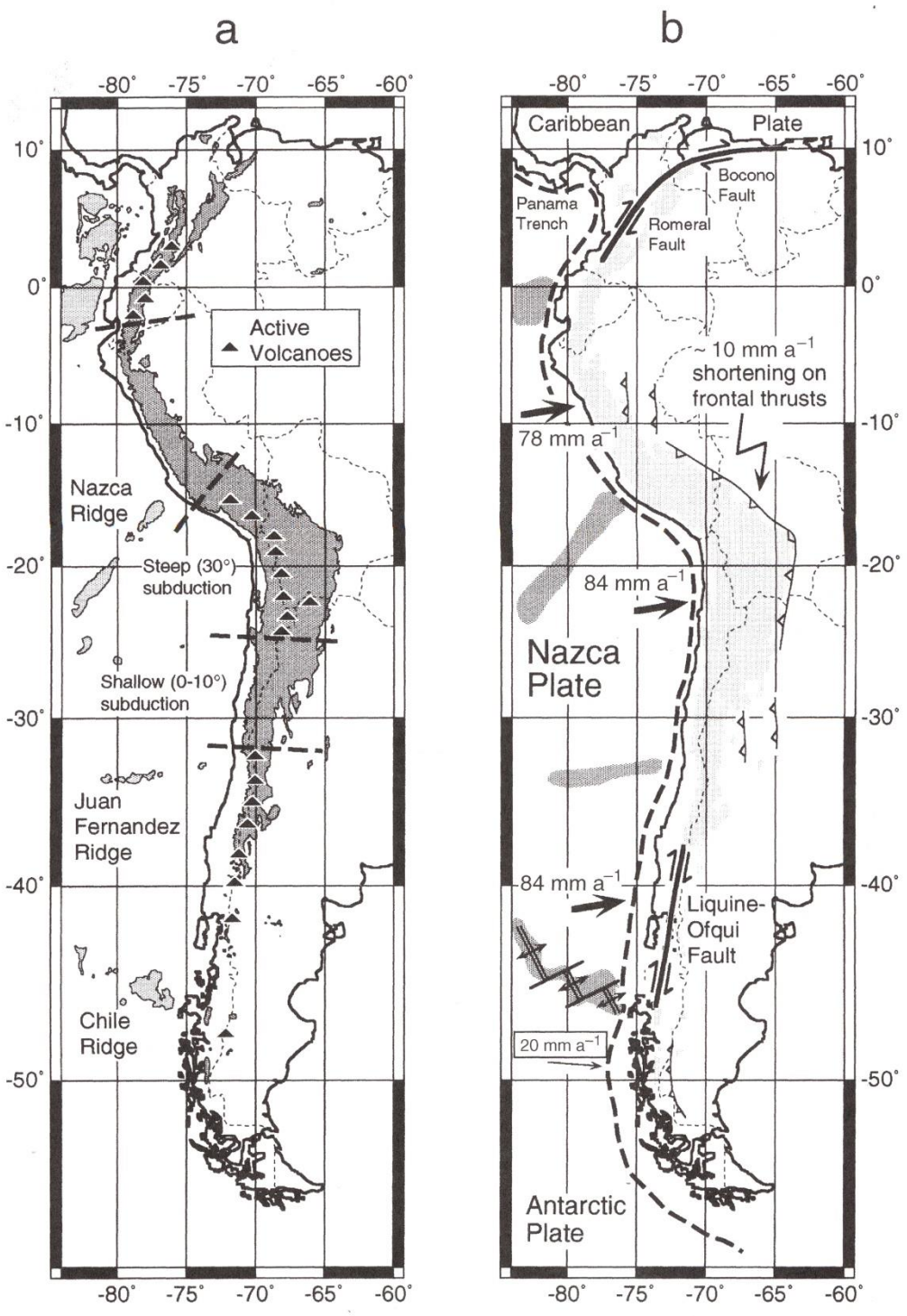

Figure 5.25 Tectonic structure of South America showing (a) active volcanoes, sea floor ridges and areas over 1500 m above and 3000 m below sea-level. Note that recent volcanoes are located in zones of moderate to steep subduction (~30°) (b) shows the major plate kinematic features with approximate rates of movement. Note that approximately 10% of the Nazca Plate slip is due to shortening at the continental margin whilst 90% is due to subduction zone slip. Active continental deformation is concentrated in the eastern Andes (Kennan, 2000)

A significant geological feature of the Andes is the presence of basalt intrusions from volcanism (Figure 5.26 and Figure 5.27). Extensive intrusions have created the Patagonia Batholith, a series of igneous plutons made of granite, granodiorite and tonalite (Figure 5.28). The batholith intruded through Paleozoic to early Mesozoic metamorphic complexes such as the Taitao Ophiolite and the Sarmiento Complex which is also volcanic in origin (Kaeding *et al.*, 1990; Rapalini *et al.*, 2008) and some sedimentary rock (Figure 5.29). The geological setting of Patagonia results in the lithology being highly resistant in nature with high RMS values.

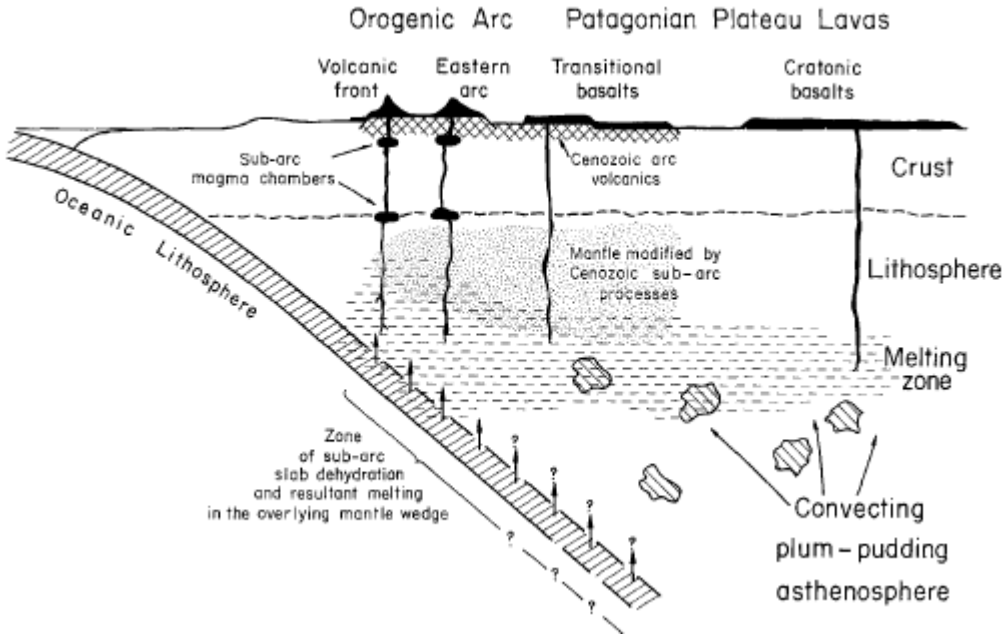

Figure 5.26 Schematic cross-section of the southern South American western continental margin (south of 39 ~ S) modified after Stern *et al.* (1986), Hickley *et al.* (1986) and Hickey-Vargas *et al.* (1989). Below the Andean orogenic arc relatively large amounts of volatile-rich melts or fluids derived from the subducted oceanic lithosphere cause relatively large degrees of melting of the plum-pudding. Below the "cratonic" lavas to the east, smaller degrees of melting of the asthenosphere are associated with convection in response to slab subduction and asthenosphere derived melts metasomatize the lower lithosphere prior to melting of this so-modified mantle (Stern *et al.*, 1990).

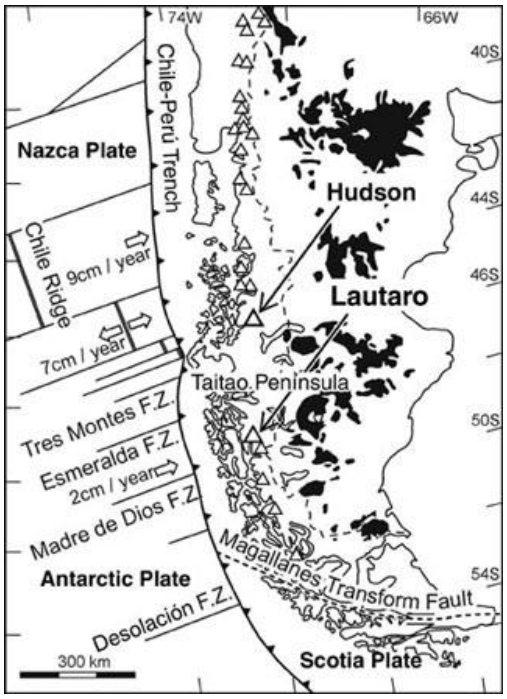

Figure 5.27 Simplified tectonic map of southern Patagonia with location of the volcanic centres and the distribution of the Cenozoic Patagonian plateau Basalts (in black) (Stern *et al.*, 1990; Stern & Kilian, 1996)

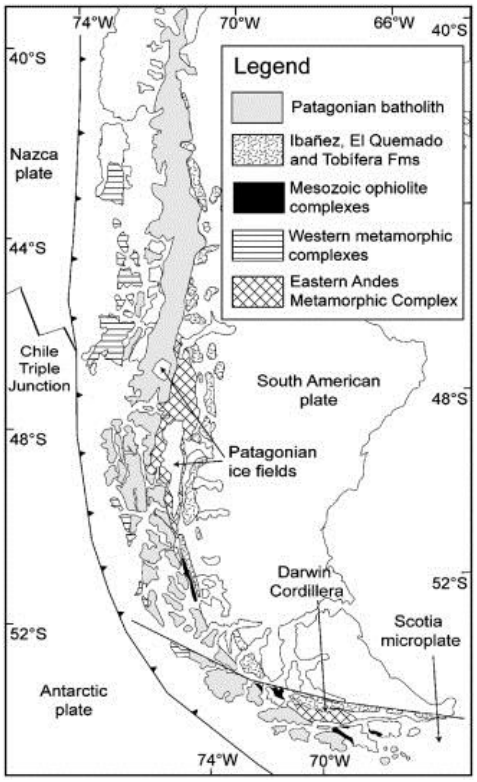

Figure 5.28 Location map of the South Patagonian batholith (SPB) in the Patagonian Andes. Also indicated are the late Paleozoic to early Mesozoic metamorphic complexes into which the SPB is intruded, the Mesozoic ophiolitic complexes which formed in the Rocas Verdes basin including the northernmost Sarmiento complex, and the mainly silicic volcanic Late Jurassic Tobífera Formation (Hervé *et al.*, 2007).

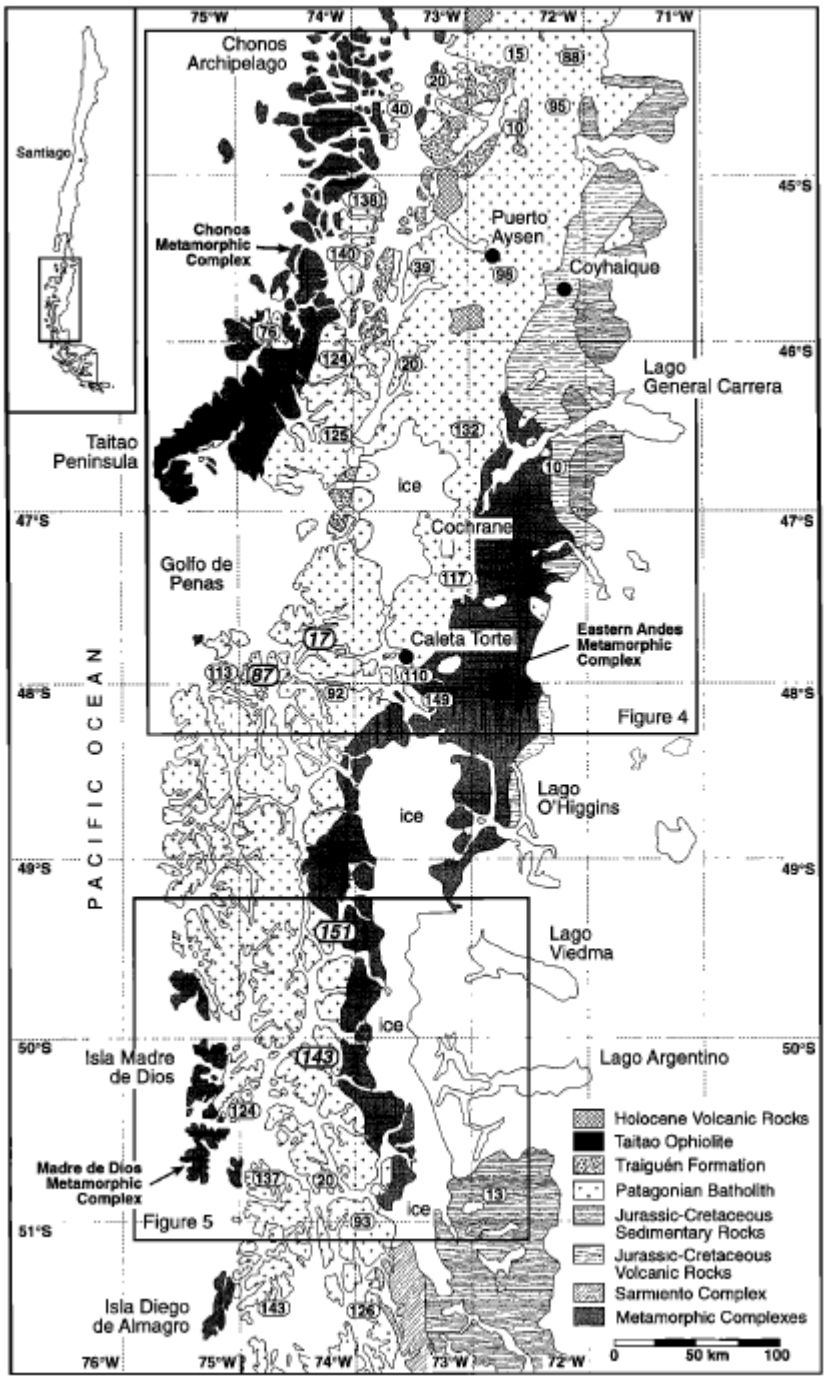

Figure 5.29 More detailed geological map of the Patagonia Andes where numbers represent rock intrusion ages in Ma yrs. (Thomson *et al.*, 2001).

5.4.3.2 Climate and degree of glaciation

The climate of the region is maritime in nature (Ariztegui *et al.*, 2007). The mountains form a significant topographic barrier to atmospheric circulation in the southern hemisphere westerlies and cause one of the most dramatic orographic rain shadow effects on earth (Blisniuk *et al.*, 2005). In the humid western foreland precipitation is

high, reaching 5,000 mm/yr at sea-level (Hulton *et al.*, 1994) and decreases eastwards to ~300 mm/yr (Figure 5.30 and Figure 5.31) (Ginot *et al.*, 2002; Blisniuk *et al.*, 2005). There is also a north-south gradient for precipitation, with decreasing precipitation northwards (Legates & Willmott, 1990). The cool temperature belt which is a feature of the Patagonian climate extends south of 42°S (Miller, 1976) and westerlies and precipitation have a maximum at around 50°S (Hulton *et al.*, 1994). Precipitation decreases sharply northward of 40°S, where annual amounts are around 2,000 mm compared to <150 mm at 30°S, due to the frequency of fronts crossing the coast and the influence of the Pacific subtropical anticyclone (Hulton *et al.*, 1994). In the far south mean annual temperatures are 5.5°C, rising to 11°C at 42°S and 14°C at 33°S.

It is important to note that the location of the westerlies and the temperate belt which now exists at 42°S southward has not been static throughout time. During the last glaciation there was a migration of 5° northward of this belt bringing more precipitation north of 42°S (Hulton *et al.*, 1994).

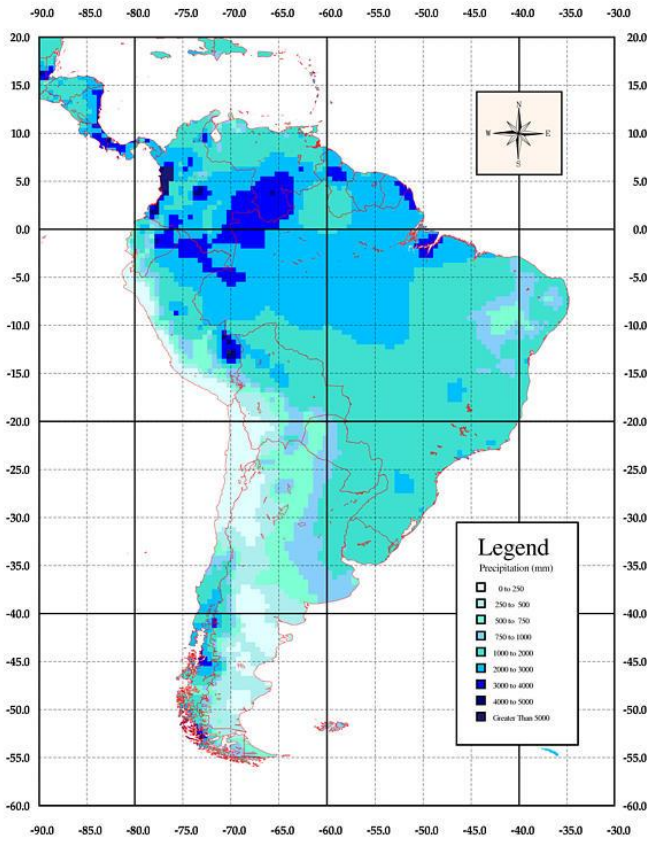

Figure 5.30 South America precipitation map showing the high amount of annual precipitation on the west coast of Patagonia (Legates & Willmott, 1990).

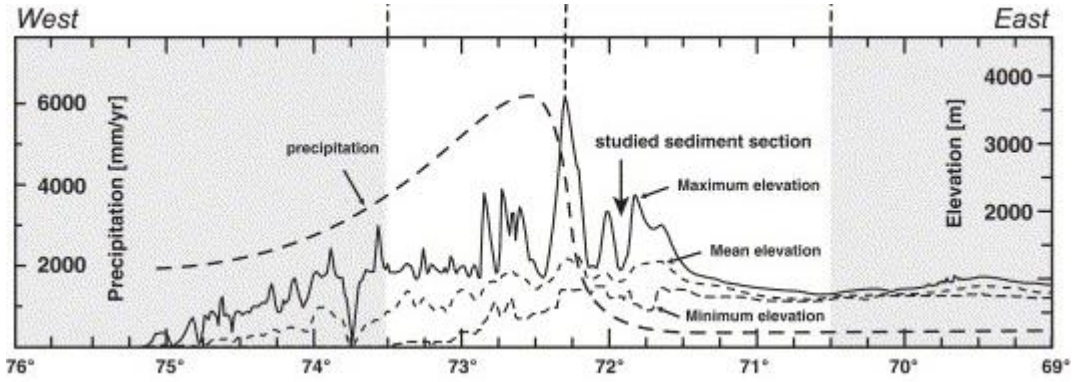

Figure 5.31 Rain shadow effect across the southern Andes; high precipitation is found to the west of the mountain divide (Blisniuk *et al.*, 2005).

A major climatic episode in Patagonia has been an increase in aridity to the east. Increased aridity is attributed to surface uplift during the Miocene (Blisniuk *et al.*, 2005) and an increase in the rain shadow effect on the region. Even during the Quaternary glaciations where temperatures were lower, precipitation was higher to the east of the divide than it is today (Figure 5.32) (Kaplan *et al.*, 2007).

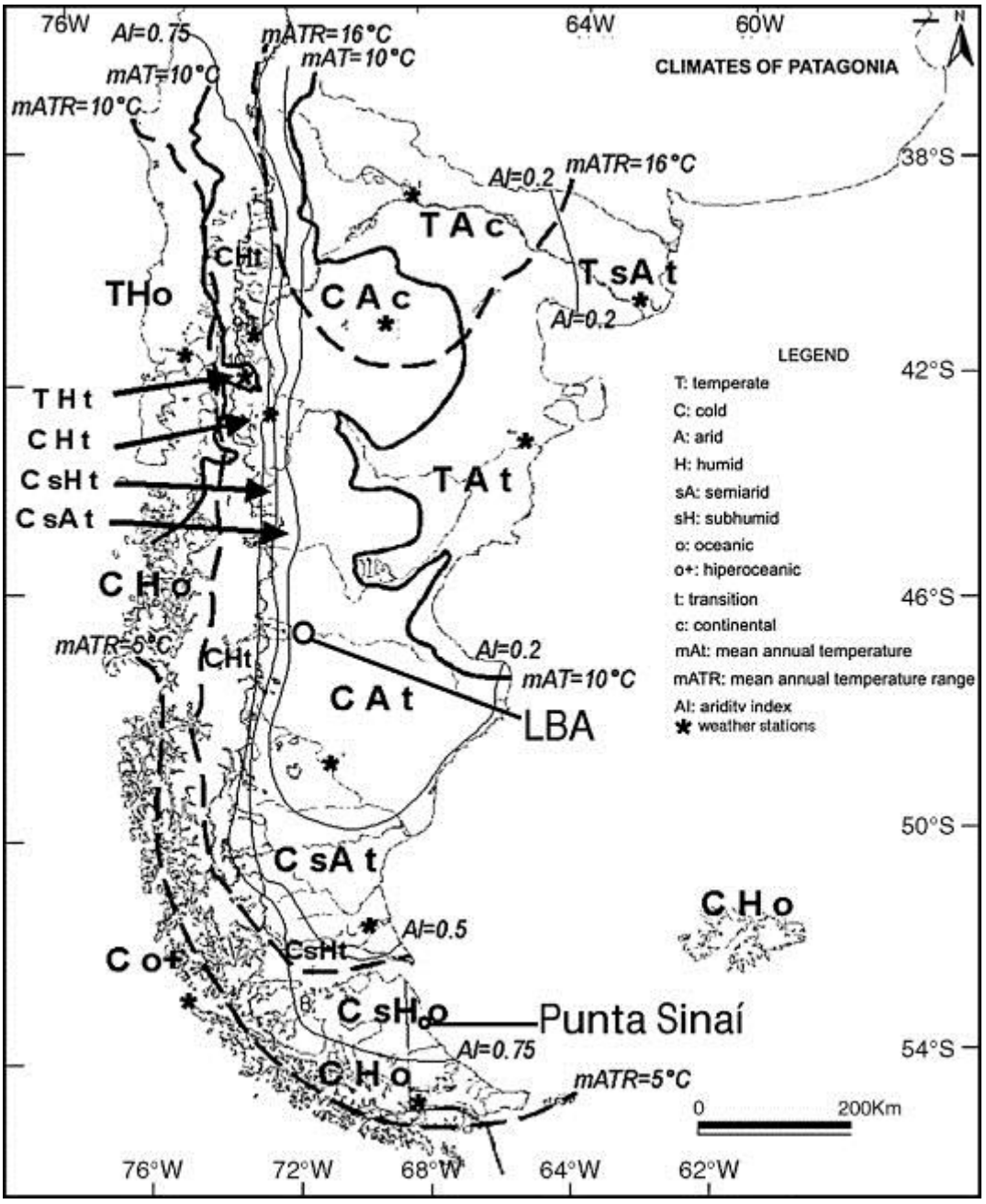

Figure 5.32 Temperature data and climate 'zones' indicating aridity index (AI) showing increased aridity to the east being defined as arid (0.2) in the far east progressively moving to semi-arid (0.2<AI<0.5), sub-humid (0.5<AI<0.75) (Coronato *et al.*, 2008).

Research using multi-centennial to present-day precipitation data shows that a difference in summer and winter precipitation distributions exists in Patagonia (Figure 5.33) (Neukom *et al.*, 2010). The data over the last century shows that during the summer the western region of Patagonia has lower precipitation than during the winter when there is not only a greater amount of precipitation but also a larger region is influenced. The rain shadow is effect enhanced in the winter producing greater precipitation gradients. Enhanced winter precipitation is important for the accumulation

of snow on glaciers and will increase the influence of precipitation on glacial erosion. Multi-centennial scale data shows that winters in Patagonia have become drier whilst the summers have become wetter indicating a changing climate (Neukom *et al.*, 2010).

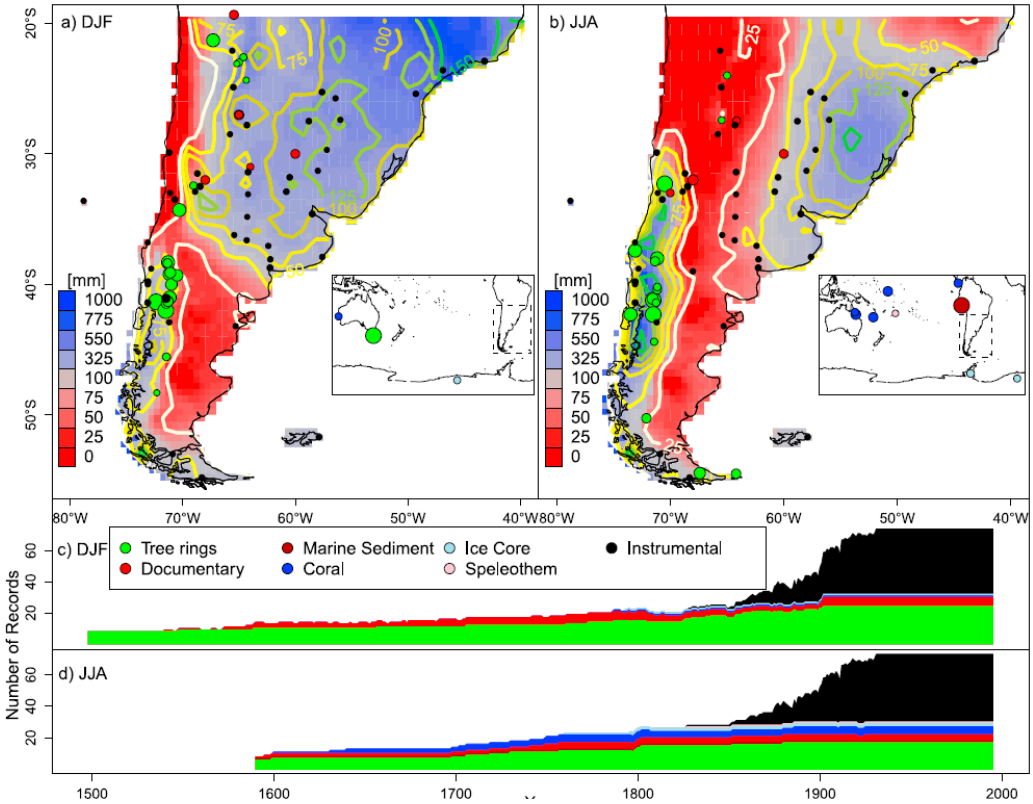

Figure 5.33 Summer (a) and winter (b) precipitation for the period of 1931-1995. Dots indicate the type and location of climate predictors used in analysis on precipitation change at a multi-centennial scale (Neukom *et al.*, 2010).

ELAs reflect the precipitation gradient to an extent by being up to 500 m lower to the west (Hulton *et al.*, 1994). However data shows that the further south the less exaggerated this gradient is (Figure 5.34) (Hulton *et al.*, 1994).

During the LGM the ELA was much lower, being at 560 m at 40°S, 160 m at 50°S and 360 m at 56°S (Hulton *et al.*, 1994). This is explained by an overall fall in temperature of about 3°C and the northwards migration of precipitation belts by ~5° latitude. Annual precipitation change is also a cause with a decrease of ~0.7m at 50°S and an increase of ~0.7 m at latitude 40°S.

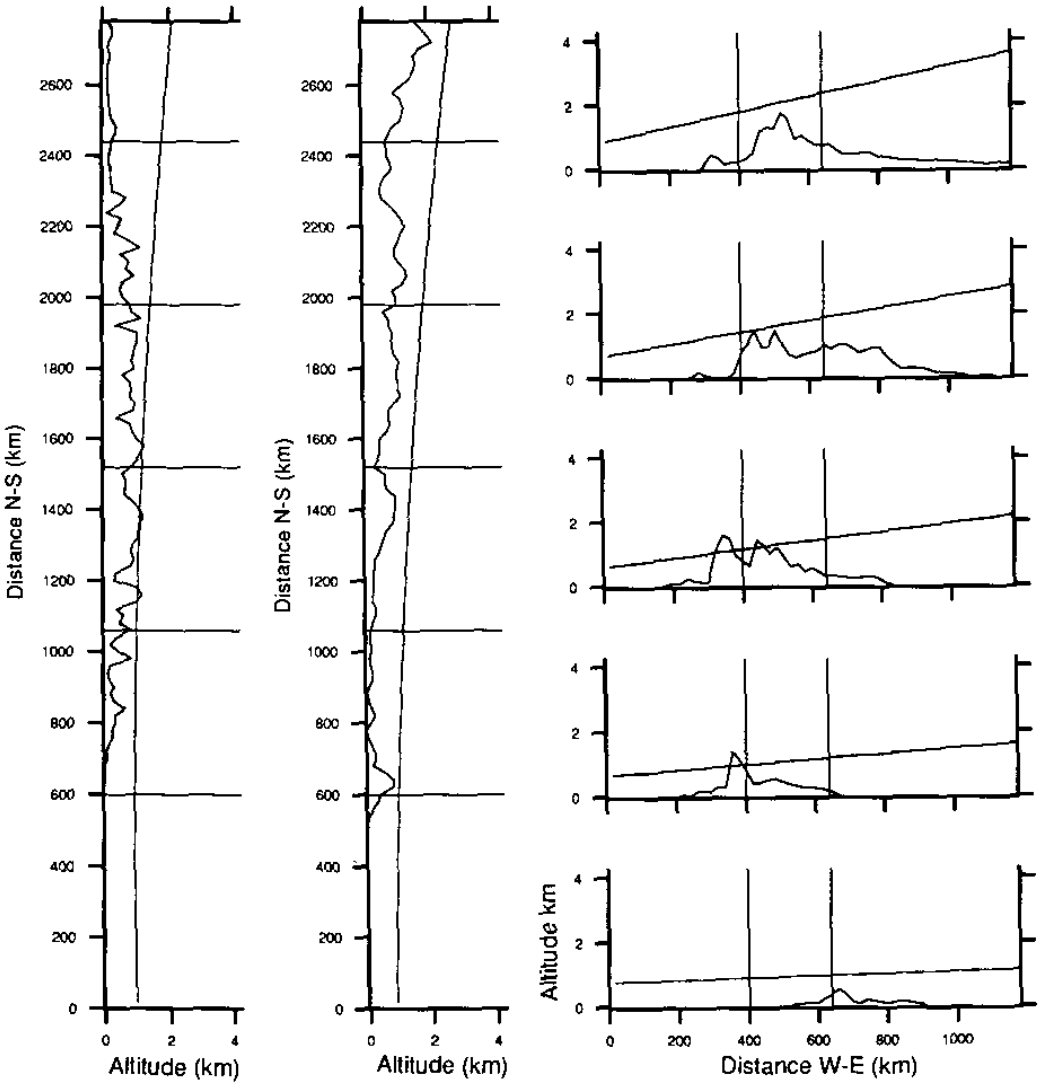

Figure 5.34 Trend surfaces produced from present-day glacier ELAs. (a) and (b) are two north/south transects, (a) being on windward slopes and (b) being on leeward slopes, showing the increase in ELA with decreased latitude. Note that the leeward transect (c) has a steeper gradient. (c) shows the east/west transects showing ELA gradients across the divide (Hulton *et al.*, 1994).

A total of 13-14 glaciations have been identified in Patagonia, the earliest evidence being from the Late Miocene (*c.* 5-7 Ma), spanning until the Late Glacial (*c.* 16-10 ka B.P.) (Coronato *et al.*, 2004). In the far south ice-sheet glaciation dominated and as the range becomes more northerly, and closer to the equator, it is increasingly dominated by alpine type glaciations with a decrease in glacial erosion intensity and extent (Figure 5.35). Ice still remains today in the form of isolated alpine glaciers and two prominent ice fields (Figure 5.36); the Southern Patagonian icefield (~13,000 km² (Aniya et al., 1996)) and the Northern Patagonian icefield (~4,200 km² (Riveria *et al.*, 2007)).

Unlike other regions of the world the ice in Patagonia did not reach a maximum at the same time. The global LGM is between 23 – 19 ka (Mix *et al.*, 2001) whilst the Patagonian maximum known as the Great Patagonian Glaciation (GPG) occurred earlier, from 25 to 18 ka, with a peak of 25-24 ka (Kaplan *et al.*, 2008). GPG ice covered 542,000 to 558,000 km² whilst the LGM ice extent covered an area of ~442, 000 km² (Kaplan *et al.*, 2009) (Figure 5.36).

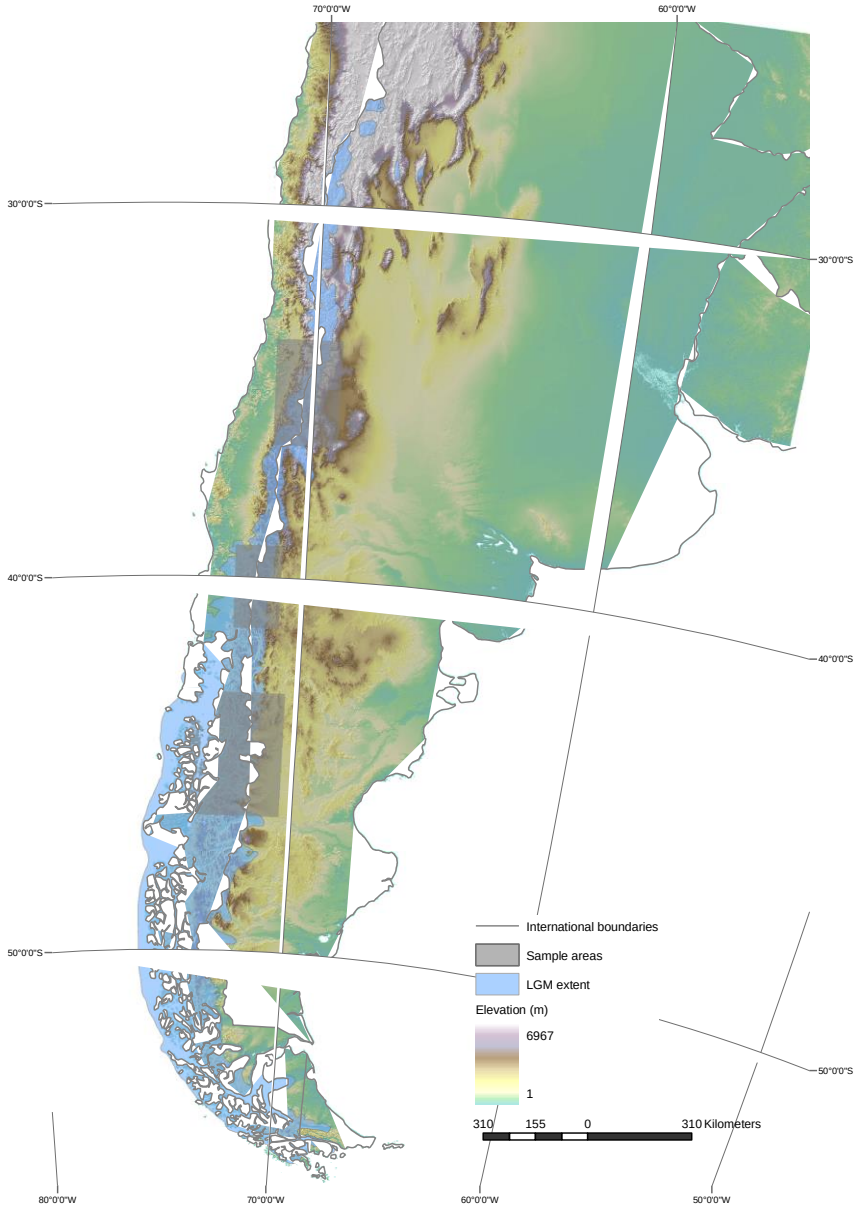

Figure 5.35 The Southern South America region showing the maximum ice extent (Calvet, 2004) and the 3 sample areas which are located at different latitudes along the Andes range.

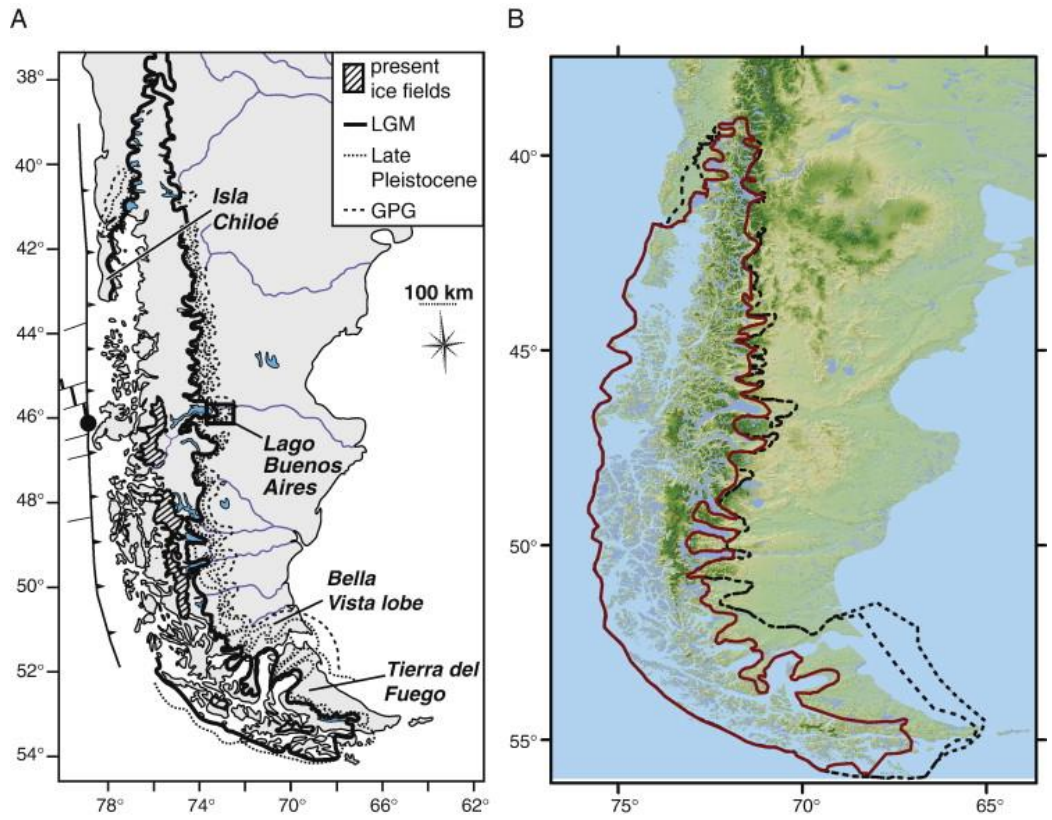

Figure 5.36 A map of Patagonia showing present day glaciers and ice fields, the LGM ice extent (red line in B), Late Pleistocene extent and the Great Patagonian Glaciation (GPG) extent (black dash line in B. The two different lines denote two different possibilities of extent) (Kaplan *et al.*, 2009).

5.4.3.3 Patagonia as a sample area

Three sample areas, which span the mountain divide, whilst being located at different latitudes, are used to understand the spatial variability of *U-ness* in the context of a greater range. The gradient regarding the degree of glaciation is the main point of interest with these sample areas and it is anticipated that this is the first order influence on *U-ness*. However, there are also gradients concerning precipitation which could also be considered and may be second or third order factors in valley development. By comparing this sample area with the Pyrenees and the Southern Alps it may also provide insight into the degree of glaciation of a heavily glaciated mountain range.

5.5. Summary

In this chapter four key influences on glacial processes and landform development, which could affect *U-ness,* have been identified. These consist of lithology, tectonic

settings, climate and degree of glaciation. Methods of quantifying them have been discussed in order to provide a basis for selecting suitable sample areas. During this discussion the difficulty in characterising sample areas was highlighted. The topographic data to be used, in the form of SRTM DEM, is outlined.

In order to investigate these characteristics, five sample areas in the three regions chosen have been selected to investigate *U-ness* under several hypotheses, to enable experiments and comparisons, regarding valley cross-section development and spatial variability, to be carried out. This is not an easy task. No real world mountain range has set parameters regarding each of these characteristics and therefore we cannot find the perfect control experiment. There are problems with both changing characteristics in time and space and it cannot be assumed that today's conditions are representative of the past. For example, in Patagonia the temperate belt was 5° further north during the last glaciation; today these mountains are a lot more arid. In the Southern Alps of New Zealand in the past precipitation was 25% less (Golledge *et al.*, 2012). Ultimately only modelling can provide truly controlled experiments. One of the aims of this thesis is to provide real world examples for modellers and therefore the inconvenience of the complexity of real world environments must be tackled. One way of doing this is to map in minute detail all the characteristics for each sample. This would result in a small amount of high quality data. The approach that this thesis will take, however, is to produce large volumes of data, across whole mountain ranges, in order to look for large-scale patterns in valley cross-sectional shape. It is accepted that individual valley patterns may not be understood but hoped that larger, regional-scale patterns may be revealed.

6. Investigating relationships between measured *U-ness* parameters and ice activity proxies

6.1. Introduction

This chapter explores the extent to which any single factor dominates the glacial landscape. If a single factor, for example climate, is the overriding control on the cross-sectional shape and size of glacial valleys, then strong correlations should be consistently seen across all sample areas. If only weak correlations exist, no correlations at all, unexpected relationships, or correlations in only certain areas or valley systems then it would be concluded that the idealised glacial valley form only occurs under a set combination or several combinations of conditions. It is important to highlight that this chapter is an investigation into whether simple relationships exist between *U-ness* parameters and individual ice activity proxies which can then be used to inform subsequent research. Multiple-regression is tackled in Chapter 7 to address combinations of conditions.

In this Chapter the mean valley cross-section method (Chapter 4) is applied to valley segments within the sample areas selected in Chapter 5. However, before the method is applied to entire sample areas, some thought into the details of the exact valley profile thresholds used must be carried out to tackle some of the problems which were highlighted in the literature review chapter (Chapter 2). One such problem was the extent to which the cross-sectional profile should span a valley. Different approaches with the individually selected transect method included valley-top to valley-top transects (Montgomery, 2002) as well as transects between trimlines (Graf, 1970; Pattyn & Decleir, 1995; Li *et al.*, 2001b) and, when using the mean valley method, the 90% contour was used (Phillips, 2009). A second consideration is the sensitivity of *b*-values, especially with regard to measurements close to the valley floor (Pattyn & Van Huele, 1998). Both of these issues are tackled in the first section of this chapter.

Once thresholds are satisfactorily understood and constrained within the context of the mean-method, then the method can be used to gain insight into the relationships between *U-ness* measures (form ratio, *b*-value and cross-sectional area) and ice activity

proxy variables (elevation used as a proxy for ice residence time, and contributing catchment area as a proxy for ice flux). It is anticipated that *U-ness* will increase with greater residence time (elevation) and ice flux (catchment area), whilst also increasing in areas of more favourable climatic conditions, less resistant lithologies and greater tectonic uplift.

This thesis is not aimed at exploring geomorphology of particular regions but the controls on georphology in general. Sample areas are simply tools to aid this research. As such this chapter is structured so that variables can be investigated in accord with *U-ness* measures.

6.2. Defining cross profile extent

In Chapter 4.2 it was recognised that the orientation of individually selected transects impacts *U-ness* measures, such as *b*-value and cross-sectional area, although previous research rarely acknowledged this limitation of the transect method. The mean valley cross-sectional profile method circumvents this problem by finding a mean shape of the valley. However, a secondary problem still remains, which is to what extent the profile should span the valley. In individually selected transects different extents have been used. Investigations into valley shape have used transects which span the valley, from valley-top to valley-top (Montgomery, 2002), whilst other research has used the location of the trimline to denote the limits of the profile (Graf, 1970; Li *et al.*, 2001b). When applying the mean valley cross-section method, Phillips (2009) used the 90% slope position line of a valley simply because the 100% slope position (i.e. valley-top) was discontinuous in nature and therefore not well defined. The mean method was unable to assign a continuous line to the ridge, peak or valley-top, instead any 100% slope position line was broken and therefore there was not enough information to create a valley profile from valley-top to valley-top.

In alpine glaciation it is conceivable that only the lower part of a valley may have been affected by glacial erosion whilst valley sides above where the ice was located are likely to be dominated by processes such as freeze/thaw. The trimline is a landscape feature which signifies a change in weathering between hillslope and/or periglacial processes with glacial processes (Goudie, 2004). This weathering boundary can appear as a break in slope on valley walls but is sometimes not visible at all (Goudie, 2004). When the

trimline is visible it denotes the upper limit of glacial ice abrasion (Goudie, 2004). It therefore follows that making measurements above the trimline would not give a fair representation of the valley shape created by glacial erosion, although glacial over-steepening will of course affect the hillslope processes above. The amount to which valley sides have been exposed to glacial erosion is complicated by the fact that, as with the ELA, ice moves up and down the valley sides as mass balance changes, varying the degree to which glacial erosion has occurred within a valley cross-section.

When individually selected transects are extracted, the trimline can sometimes be identified and used to delineate the transect extent. However this is a rare occurrence and due to the wide range of areas investigated here this is not feasible because most of the time trimlines are imperceptible. Instead a sensible threshold, compatible with the mean valley cross-section method, must be developed to overcome this.

From the example mean-profile used in Section 4.6.2 in the Mount Kenya area (Figure 6.1), it can be seen that there is a break in slope from the 70% slope position. This has resulted in the power-law curve not fitting the lower half of the valley particularly well, which is the section of the valley which has undergone the greatest glacial erosion.

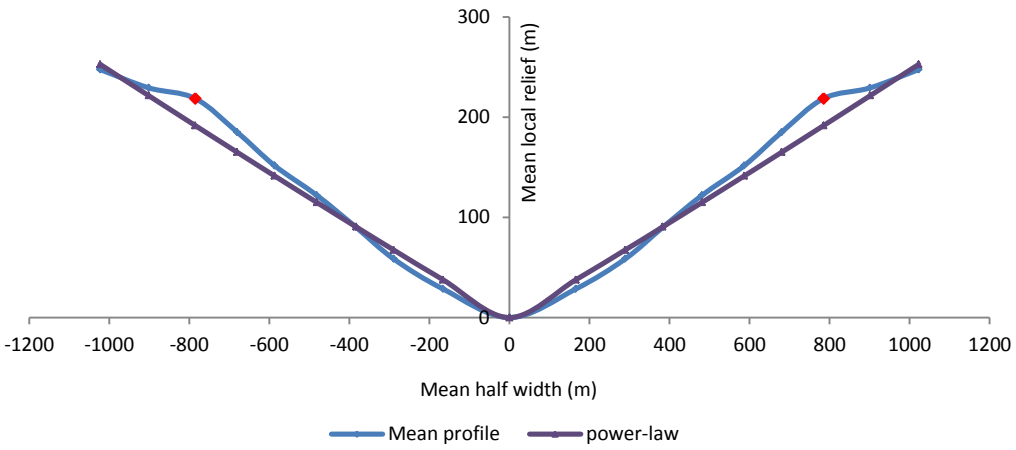

Figure 6.1 Mean profile of a 2nd order catchment valley segment (identification number 64) on Mount Kenya. The power-law computed the *a* and *b*-values to be 0.18033 and 1.0455 and this curve is shown. A clear break in slope occurs at the 70% slope position (marked in red).

To understand how the amount of the valley slope used in the power-law equation influences the resultant *b*-value, an investigation into different valley slope position thresholds is carried out. This involves using x and y-values which represent the mean valley positions at the 30% through to 90% slope positions (i.e. for 30% measurements 0%, 10%, 20% and 30% x and y-values are used). A power-law curve is fitted for each set of values and the *U-ness* results compared. Results in Figure 6.2 and 6.3 show that the power-law which uses the slope measurements up to 90% and 80% slope positions do not fit the lower section of the valley, close to the valley floor well, as the power-law attempts to fit the curve past the break in slope. As the resultant power curve is not particularly concave the lower half of the valley is poorly represented, the *b*-values are low at 1.04 and 1.14 respectively. When the mean valley slope position measurements of up to 70%, where there is a break in slope, are used, the curve produced by the power-law closely follows the mean cross-section profile. The 70 - 50% *b*-values are between the values of 1.27 to 1.3, with the lower value attributed to the values up to and including the 70% slope position, and the larger *b*-value includes slope positions up to 50%. A change in the power-law curve for the values up to 40% and 30% slope positions is illustrated by a just visible change in the mean valley profile at the 40% slope position, which causes higher *b*-values of 1.39 and 1.41 respectively.

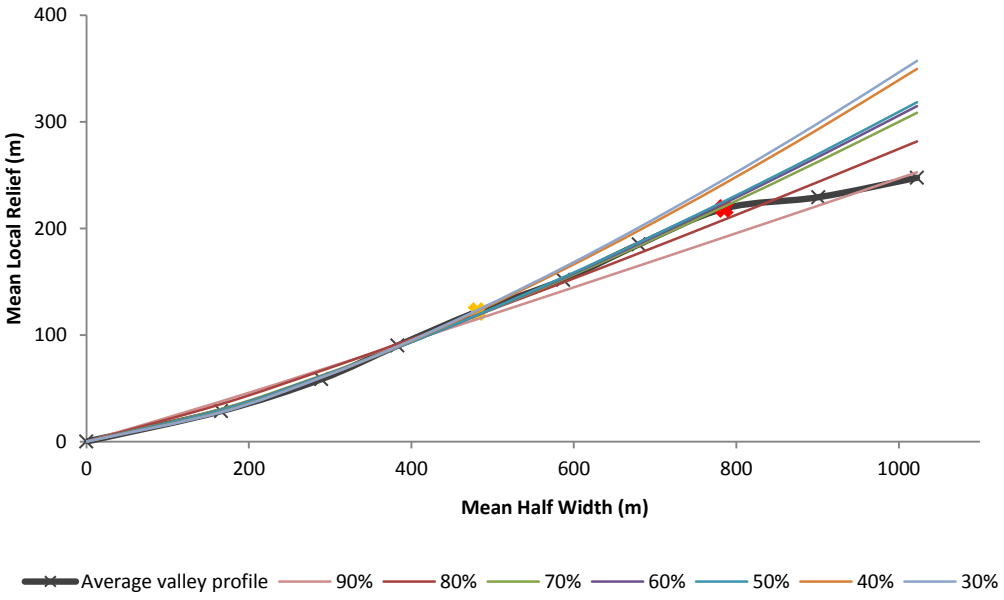

Figure 6.2 Mean valley profile from Figure 6.1 with power-law curves using the 90% slope measurements through to the 30% slope measurements. The graph shows that where there is a break in slope, at the 70% (red) and 40% (orange) slope positions, the power-law curve is influenced by creating more concave curves with higher *b*-values.

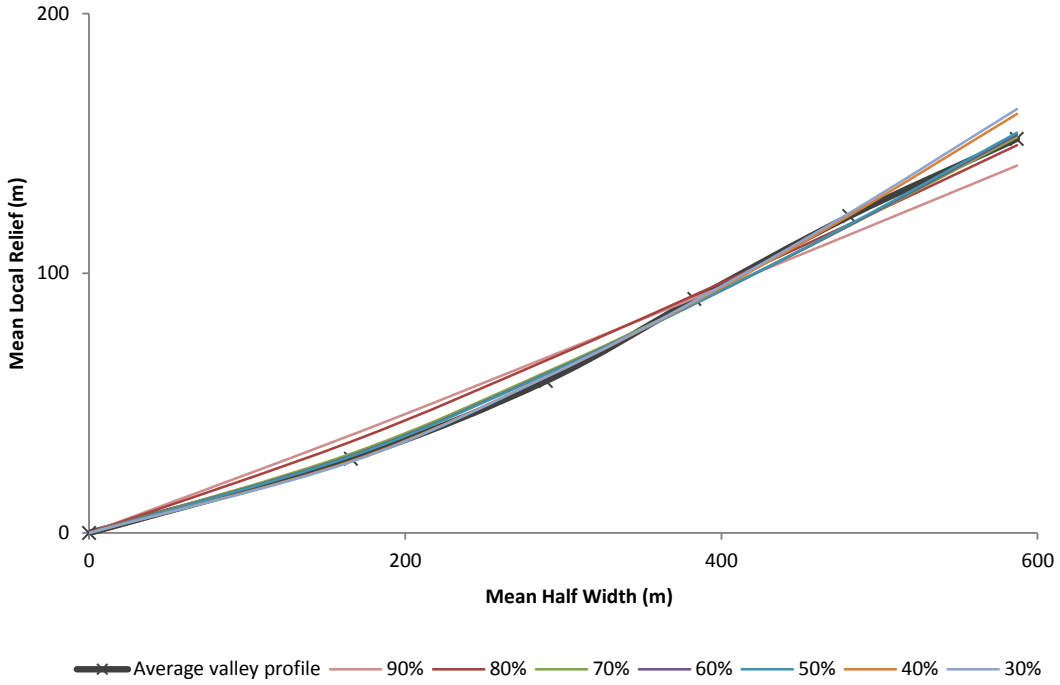

Figure 6.3 A close up of the lower half of the profile and power-law curves shown in Figure 6.2. It highlights the desirability of fitting of the power-law curves to the lower half of the mean valley profile where the most glacial erosion would have taken place.

Ideally each profile would be analysed to identify breaks in slope and then a suitable threshold chosen. However when analysing 10,000s of valleys using the semi-automated method developed in Chapter 4, this is not practical and detracts from the method rationale. Therefore a suitable threshold suggested is the 50% slope position. This allows for the lower half of the valley, which is most likely to have been exposed to glacial erosion, to be investigated. It prevents upper slopes of a valley, which in an alpine glaciation scenario have mainly undergone periglacial and slope processes, distorting the power-law equation, whilst still encompasses enough of the valley sides to investigate valley size and shape.

6.3. Power-law considerations

Several limitations in using the power-law to define the shape of a glacial trough were identified in the literature review and were summarised in Sections 2.2.2 to 2.2.4. Many of these limitations are overcome by using the mean valley cross-section method and are discussed in this section. In addition, the General Power Law (GPL) (Pattyn & Van Huele, 1998), a proposed solution to some of the restrictions imposed by the power-law (Svensson, 1959), is applied to mean cross-sectional profiles in order to explore its potential.

The mean valley cross-section method circumvents several limitations of the power-law discussed in the literature due to the nature of the method. One concern was that the power-law is fitted to each side of the valley individually (Wheeler, 1984; Harbor, 1992), therefore not considering the valley cross-section as a whole. The mean valley cross-section method not only considers the whole valley lengths, it also takes a mean of both sides of the valley segment, therefore creating a symmetrical mean valley profile incorporating the shape of both sides of the valley along the length of the valley segment. As the mean profile encompasses both sides of the valley, it negates a concern that the power curve only fits to one side of the valley.

Harbor and Wheeler (1992) also raised concerns that the logarithm transformation created a bias which favoured points closest to the origin (valley floor). The valley floor is likely to have been modified the most by either depositional fill or fluvial erosion. Again the mean valley cross-section method avoids this problem, by the use of percentage valley slope positions. Percentage valley slope positions enable measurements to be taken at consistent positions up valley sides, therefore avoiding taking of measurements along flat valley bottoms, which is the case when measurements are taken at set distances from the valley centre. This allows the power-law curve to be fitted to the valley sides rather than for valley floor measurements, with the exception of the origin (the point at the valley floor in the centre of the valley cross-section), denoted as the 0% slope position which is always given a value of x = 0 and y = 0. When a valley with a broad, flat floor (often as a result of post-glacial deposition) is measured, the first measurement at the 10% slope position is taken at a proportionally greater distance away from the valley centre (i.e. along the x-axis) compared to the distance between the x-axis distance of the 10% and 20% slope positions, therefore countering the logarithmic transformation bias of measurements closest to the origin.

Also, by only including slope positions up to 50% and therefore simply investigating the lower half of any mean valley cross-profile, upper measurements which may have been influenced by periglacial processes are not considered in the power-law equation.

An additional concern regarding the power-law equation is that it forces the curve through the origin (present day valley floor), which may be influenced by fill and therefore not reflect the valley cross-sectional form created purely by glacial processes. An infilled valley bottom would mean the present day valley floor would be higher than it had been under glacial processes, distorting the cross-sectional profile. When the power-law is applied to such a valley, the resultant curve has greater curvature (a higher *b*-value) and a broader valley bottom (a smaller *a* coefficient). This gave rise to Wheeler (1984) suggesting the quadratic equation as an alternative. However this solution comes with its own limitations which are detailed in Section 2.2.3. Another adaptation suggested for the power-law is the GPL (Pattyn & Van Huele, 1998), which allows negative y-values, something the power-law does not and therefore it is able to use the valley sides to extrapolate below the fill to produce an estimation of the glacial trough under entirely glacial processes.

The GPL is an adaptation of the power-law and is defined as

$$y - y_0 = a|x - x_0|^b \qquad [6.1]$$

where x_0, y_0 are the coordinates of the origin of the cross-section (Pattyn & Van Huele, 1998).

To do this, the GPL is investigated to see whether it has merit for use in thesis and especially with the mean profile method which has been developed. The power-law and GPL equation (Equation 6.1) are both applied to mean valley segment profiles and the results are compared. This is done for the Southern Alps (New Zealand), where the interbedding of the greywacke rock in the Mount Cook region creates weakness in the lithology. Here the landscape has been significantly modified by valley slope failure and floor fill (Augustinus, 1992a; , 1995a) predominately because of the weak lithology. Due to the large amounts of valley floor fill, it is a useful area for testing the GPL equation compared with the power-law equation for mean valley profiles. Figure 6.4 and 6.5 show the power curves produced using the power-law and GPL equations for mean valley profiles. As expected, the GPL results for *b*-values are smaller than those produced by the power-law. This is because in both cases the GPL lowered the origin of

the power curve to below the present day valley floor origin. However, despite evidence that these valleys may be considerably modified post-glaciation, the differences between power-law and GPL curves and values are quite small. This could be due to several reasons. Firstly, the GPL may not adjust the power-law curve as much as it suggests in the literature. Secondly, the mean valley profile method may lessen the influence of areas with significant valley modification on the overall profile. Finally, because the mean valley profile method uses valley slope positions rather than data at set positions from the centre of the valley, the values for the power-law calculation are taken from the valley sides rather than the valley floor, no matter how broad it is. This may be the reason why there are only small differences between the power-law and GPL results, despite the evidence for valley modification.

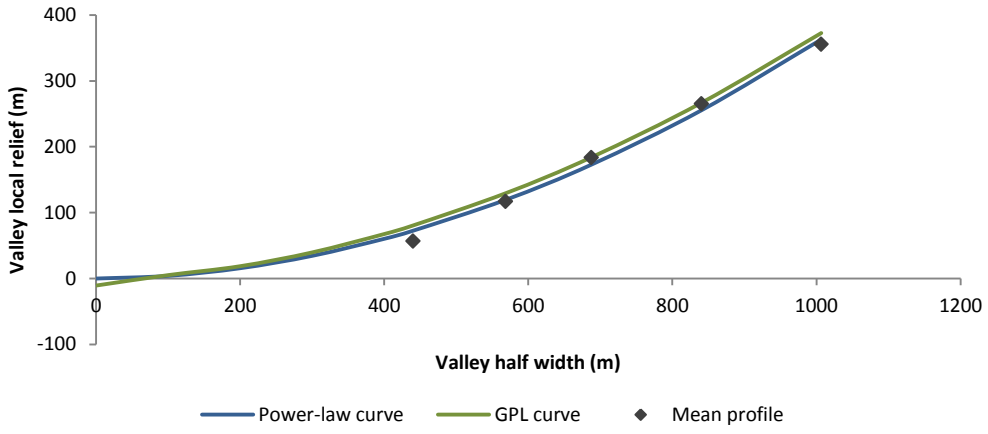

Figure 6.4 A profile affected by valley fill (individual profiles would illustrate this with flat valley bottoms). The mean valley profile depicted by the grey diamonds shows the broadness of the valley but the fill is not immediately visually obvious. When valley slope positions at the 10% through to 50% locations are graphed with the power-law and GPL solutions there is only a marginal difference in profiles. The power-law has an *a* coefficient of 0.000527 whilst the *b*-value is 1.944. The GPL *a* coefficient is 0.001001 whilst the *b*-value is smaller than the power-law value at 1.850. The GPL has found the profile origin to be -10.62 on the y-axis suggesting that there is 10.62 m of fill from this profile. Even though the potential of 10.62 m of fill is a large amount in an absolute sense, in the context of the whole valley cross-section it is small.

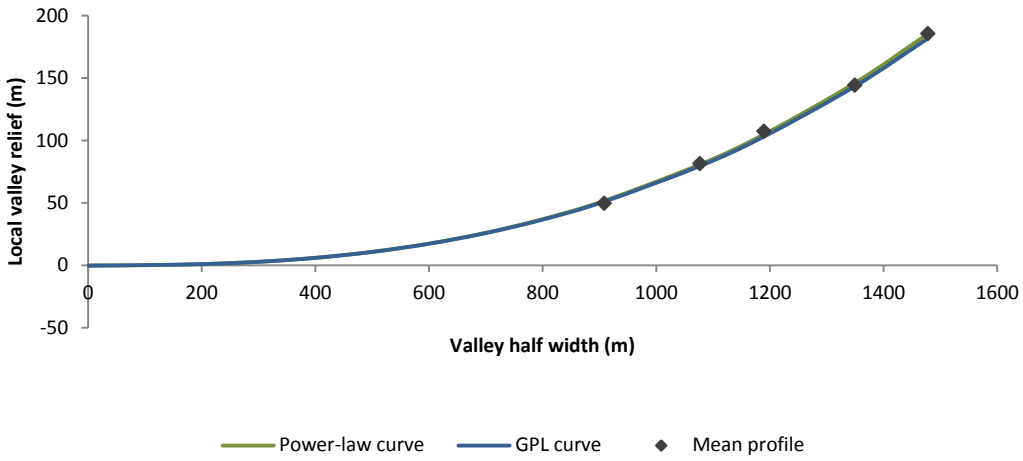

Figure 6.5 A profile of a different valley to Figure 6.4. In this graph the power-law *a* coefficient is 0.00000089 whilst the *b*-value is 2.624. The GPL *a* coefficient is 0.00000097 whilst the *b*-value is again smaller than in the power-law solution at 2.61. The GPL has found the profile origin to be -0.62 on the y-axis.

In conclusion, the mean valley profile method overcomes several limitations when using the power-law equation. Other suggestions for power-law improvements include the GPL (Pattyn & Van Huele, 1998). When the GPL was compared to power-law results for the mean valley profiles there was little difference in the values. For this investigation it is proposed that the power-law, rather than the quadratic or GPL solutions, is used in this thesis, firstly because the mean valley profile method in itself overcomes many of the limitations of the power-law and secondly because this is the technique almost exclusively used in previous literature and therefore will enable better comparisons to be made.

6.4. Overall results

The mean valley profile method (Chapter 4) was applied to the five sample areas chosen in Chapter 5. A summary of all the results are presented in this section. Table 6.1 shows the total number of valley segments analysed and an estimate of the equivalent number of profiles if individually selected transects were carried out (method for estimating equivalent number of individually selected transects is detailed in Section 4.6.3). The number of valley segments which lie within LGM limits (Sugden *et al.*, 1992; Calvet, 2004; Suggate, 2004) were also summarised giving an estimate for the number of glacial valleys observed, including an estimate of the equivalent number of profiles. The equivalent number of individual profiles is 857,781, of which 334,068 are defined as glacial. This amounts to over 1,000 times more profiles than have been produced in the last 100 years of research, which totalled have 696 profiles (Section 2.4).

Table 6.1 A summary of the number of mean valley profiles collected in each sample area, including the number within LGM limits. An estimate for the equivalent number of individually selected transects is also included. Over the last 100 years the number of individually selected transects amounts to 696 profiles, therefore this research contributes over a 1000 times more equivalent profiles to valley cross-section research.

Sample area	Total number of mean valley profiles	Estimate of equivalent number of individually selected transects	Number of mean valley profiles which lie within LGM limits	Estimate of equivalent number of individually selected transects within LGM limits
Pyrenees	7573	294,364	674	27,337
Southern Alps (NZ)	2410	106,599	1114	51,984
North Patagonia	5734	220,361	1745	66,063
Central Patagonia	3453	136,520	2606	105,977
South Patagonia	2242	99,937	1866	82,707
Total	**21,412**	**857,781**	**8005**	**334,068**

The *U-ness* measures for the complete dataset of the 8,005 valley segments found within LGM limits (Table 6.2 and Figure 6.6), and including all sample areas, show the

variability of glacial valleys. Some points to note here are that *b*-values are generally smaller than expected and this is encountered throughout this study. Svensson (1959) suggested that a parabola approaching 2 would be the idealised glacial valley form for mature glacial valleys. However, the mean *b*-value for glaciated valleys was 1.38 and the mode only 1.13; this is attributed to the fact that the method takes into account the entire valley, including all its irregularities, therefore not producing a perfect parabolic shape. It is also rare to find a valley which has solely undergone glacial processes and therefore all deglaciated valleys could potentially show signatures of fluvial and hillslope processes. This has always been a problem for glacial geomorphologists and therefore not unique to this method. High variability with other values is probably due to all valley segments being included in the dataset, not just the valleys which present the best cross-profile form. It is suspected, for example, that when taking individually selected transects that these are often deliberately or inadvertently positioned at prominent U-shaped cross-sections. Although this approach is a valuable contribution within glacial erosion research, a different approach, such as that being taken in this thesis, provides an alternative perspective in this area of research and is equally valid. Histograms of the *U-ness* data (Figure 6.7 – 6.9) show a tendency towards a positively skewed distribution, and this is expected as it reflects that there are more tributary valleys than trunk valleys, which are smaller in size and may be less mature, in a valley system.

Table 6.2 A summary of the *U-ness* statistics for valley segments within LGM limits, a total of 8005 valley segments are included which results in 334,068 equivalent individually selected transects.

	Minimum	**Mean**	**Median**	**Mode**	**Maximum**
***b*-value**	0.003	1.38	1.24	1.13	3.56
Form ratio	0.0009	0.20	0.19	0.20	1.74
Cross-sectional area (m^2)	301	206,058	171,460	102,550	1,736,100

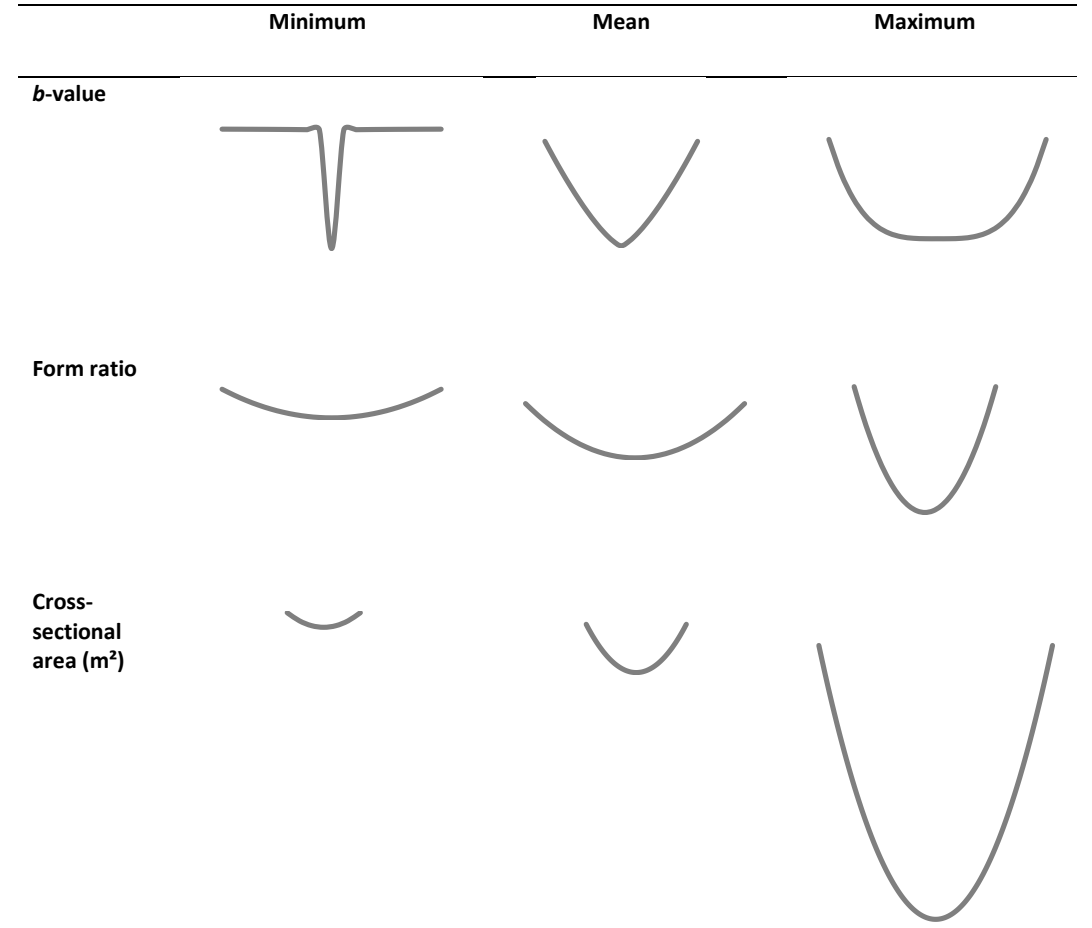

Figure 6.6 The minimum, mean and maximum *U-ness* statistics taken from mean valley profiles, shown in Table 6.2, for the entire dataset of glacial valleys represented schematically. These are analytical profiles drawn in Excel from the mean valley profiles based on the results in Table 6.2.

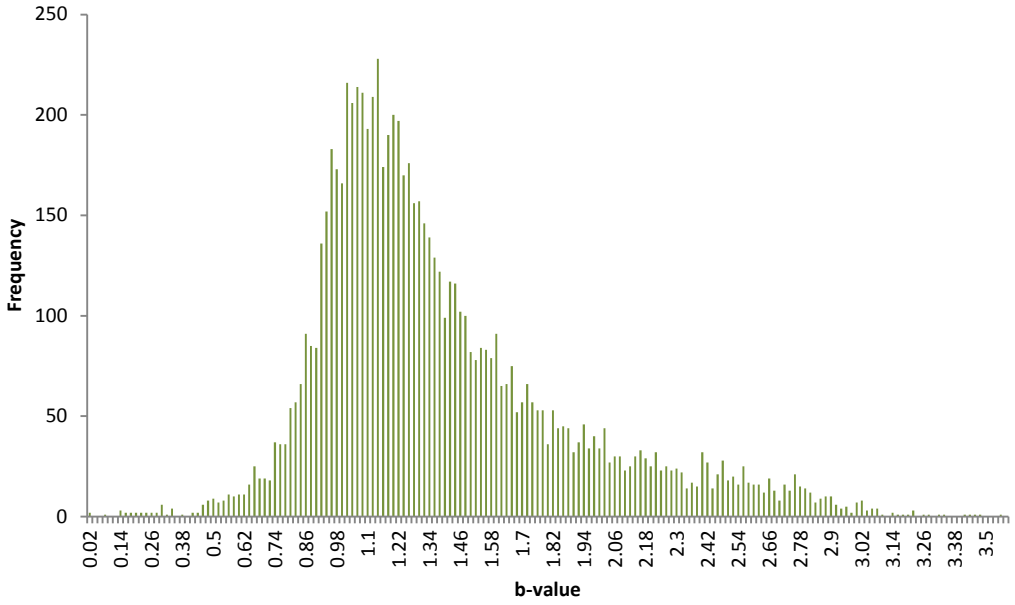

Figure 6.7 A summary histogram of the *b*-values for all glacial valleys analysed. The histogram shows that the data has a near normal distribution with a prominent positively skewed-tail.

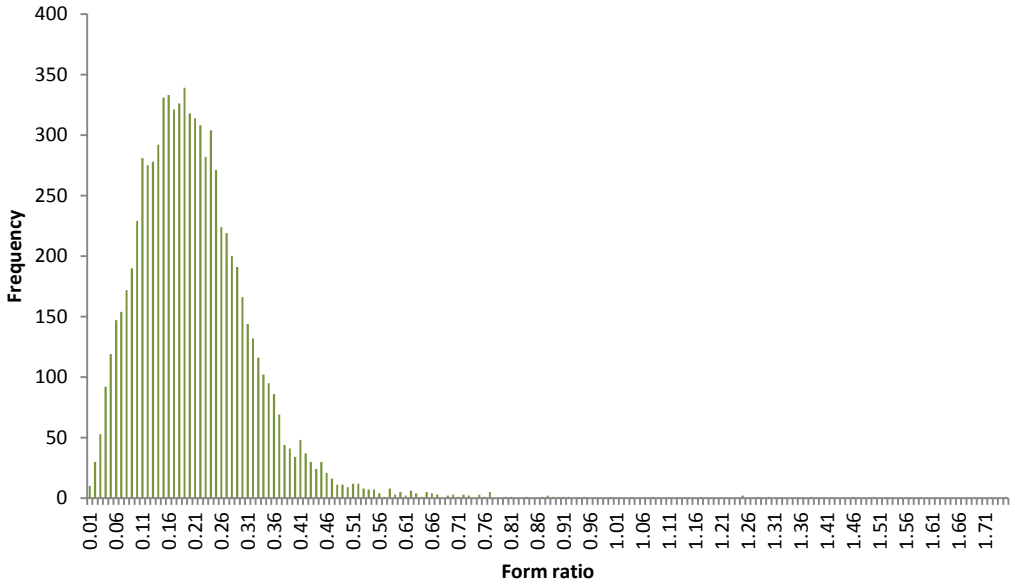

Figure 6.8 The histogram for form ratio shows a slightly positive skewed distribution for glacial valleys.

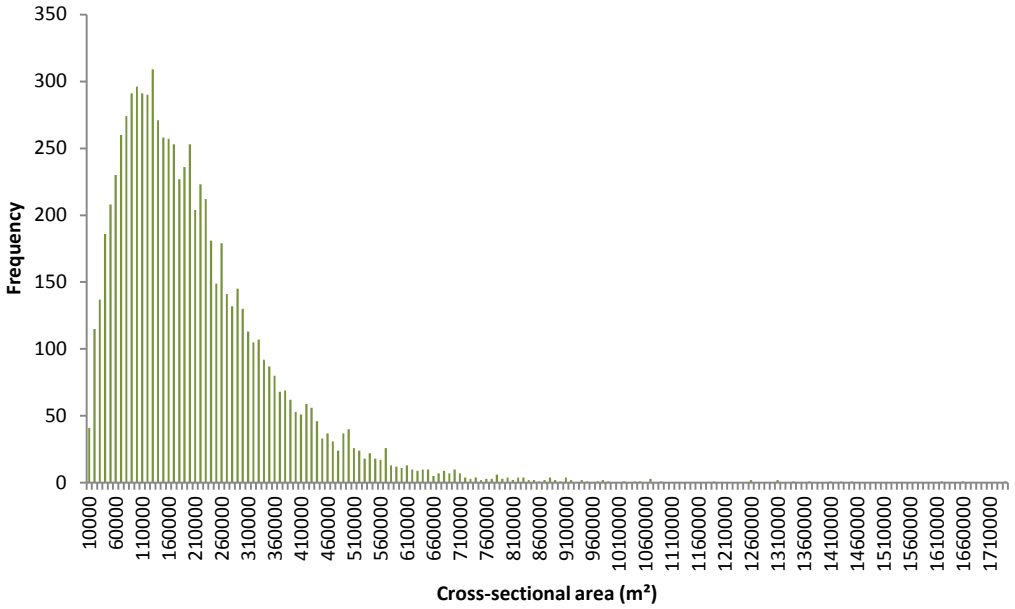

Figure 6.9 The histogram for cross-sectional area shows a strong positively skewed distribution for glacial valleys. This is a reflection of the fact that there are more tributary valleys, which are smaller in size, when compared to main trunk valleys.

6.5. Whole sample area analysis of *U-ness* measures

In this section sample areas are used to highlight interesting results found when *U-ness* measures are related to proxies for ice residence time and flux, as well as for differing physical settings. The sample areas selected in Chapter 5 provide the opportunity to compare results, both within the sample area, as well as between sample areas to explore how different conditions could influence the development of glacial valleys.

6.5.1. Examining changes in U-ness with intensity of glaciation

The three sample areas in the Southern Andes provide an opportunity to examine how *U-ness* measures change with latitude. It is a fair assumption that the further towards the equator, in this case in a northerly direction, the less the influence of glacial erosion and therefore the degree of glaciation on a landscape. This is because both ice flux and residence time, which in combination contribute to the intensity of glacial erosion, have had less influence. Consequently, *U-ness* measures should be lowest for the most northerly sample area compared to the most southerly.

This may appear to be a very simplistic view for testing such a control on glaciation by simply using latitude to test glacial intensity when there could be dozens of other factors that impact the valley shape. Due to site selection some of these factors have been reduced compared to other sample areas. The uplift during the Quaternary, for example, has been minimal across the region (as detailed in Section 5.4.3.1) and therefore has not had a great influence on the large-scale glacial geomorphology in the area. Although a precipitation gradient does exist from north to south (as well as east to west) being drier in the north (and east), there is evidence that during the LGM increased precipitation extended north. This, combined with the fact that the precipitation gradient between the north and south is less exaggerated in the winter months (Section 5.4.3.2) when the majority of snow is accumulated on glaciers, means the impact of precipation gradients on glacial erosion is reduced. The approach is to look for first order controls which override any subordinate controls. In Patagonia it is hypothesised that the temperature gradient through latitudinal change is the first order control on glaciation and that precipitation variations (e.g. east-west) is subordinate to this. To test this hypothesis a large sample size is used to search for a consistent trend.

Initial results tentatively support the hypothesis.

Table 6.3, 6.4 and 6.5 show that on the whole the *U-ness* measures of form ratio, *b*-value and cross-sectional area, increase towards the south. There are some exceptions, for example form ratio has the same value of 0.17 in central and southern Patagonia (Table 6.3). The data is explored further by separating it into first and second order valley segment catchments (Table 6.4 and 6.5).

Table 6.3 A summary of the *U-ness* statistics for all valley segments in the three Patagonia sample areas. The table shows there is an increase in *U-ness* values increasing with latitude, with the exception of form ratio for central and southern Patagonia which has the same value.

	Number of valley segments	**Mean form ratio**	**Mean *b*-value**	**Mean cross-sectional area (m^2)**
Northern Patagonia (35°S)	5734	0.15	1.30	123,307
Central Patagonia (40°S)	3453	0.17	1.39	164,248
Southern Patagonia (44°S)	2242	0.17	1.45	220,324

The *U-ness* statistics for second order and greater valley segment catchments are dealt with separately from the first order catchments valley segments, in Table 6.4 and 6.5 respectively. This is done because a far greater number of first order valley segments exist, and these catchments are unique in the sense that they do not have any contributing flow from tributaries and it might be that such catchments overly bias the data. In both tables (6.4 and 6.5) however, similar patterns prevail with the exception of form ratio which decreases in first order valley segments (Table 6.4) between the central and southern sample areas.

Table 6.4 Summary of mean *U-ness* statistics for all first order catchments, showing an increase in *b*-value and cross-sectional area with latitude but a decrease in form ratio between the central and southern sample areas.

	Number of valley segments	**Mean form ratio**	**Mean *b*-value**	**Mean cross-sectional area (m^2)**
Northern Patagonia (35°S)	3841	0.17	1.24	109,602
Central Patagonia (40°S)	1941	0.29	1.29	145,137
Southern Patagonia (44°S)	1281	0.19	1.33	180,690

Table 6.5 A summary of mean *U-ness* statistics for second order and greater valley segments, showing an increase in all mean *U-ness* values as latitude increases.

	Number of valley segments	**Mean form ratio**	**Mean *b*-value**	**Mean cross-sectional area (m^2)**
Northern Patagonia (35°S)	1893	0.128	1.41	151,000
Central Patagonia (40°S)	1512	0.139	1.52	188,782
Southern Patagonia (44°S)	961	0.140	1.62	273,156

The results above (Table 6.3, 6.4 and 6.5) are for valley segments which are both within and outside of estimates of the Last Glacial Maximum (LGM) extent. This means that the sample areas cover both fluvial and glacial valley segments, particularly in the northern sample area which had much less ice extent during the LGM. To investigate whether only valley segments that have been influenced by glacial processes during the LGM a second test was undertaken, in which glacial valleys were separated from those that did not fall within LGM limits (fluvial valleys), and the results compared. The LGM limits (Sugden *et al.*, 1992) were defined in ArcGIS and valley segments within these limits identified (Figure 6.10).

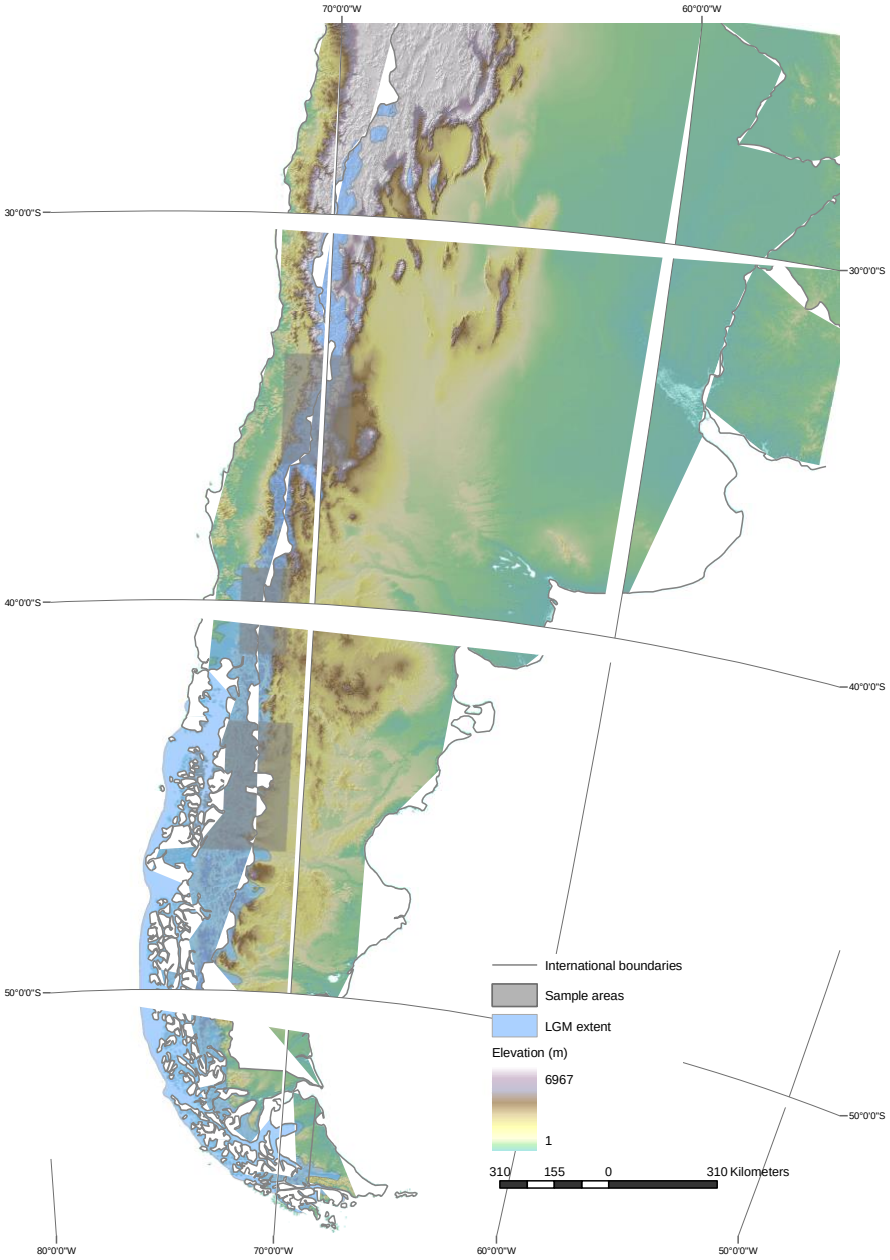

Figure 6.10 LGM extent in the Southern Andes (from Sugden *et al.*, 1992) together with the location of the three sample areas. Note that the area covered by LGM ice decreases the more northerly the latitude, despite the higher elevations.

When dividing *U-ness* data into glacial and fluvial valley segments for each sample area in Patagonia three key observations from the data can be made (Tables 6.6 and 6.7). Firstly, the trends for glacial valley segments are compared between each sample area. Here results for *b*-values are similar to those found for the combined fluvial and glacial valley segments, in that they increase with southerly latitude, as expected. Form ratio,

on the other hand, decreases with southerly latitude, especially for second order and greater valley segments (Table 6.7). Initially this seems surprising, however if a 'Patagonia-Antarctica' type valley evolution exists, as suggested by Hirano and Aniya (1988), this would follow, as valleys become broader and relatively shallower as their *b*-value increases. Therefore the results from the sample areas in Patagonia support this theory. For first order glacial valley segments cross-sectional area increases with latitude (Table 6.6), but with second order and greater catchments this is only true for the northern sample area compared to the central sample area (Table 6.7). When the central sample area is compared to the southern sample area cross-sectional area decreases (Table 6.7). This is again surprising when considered in isolation, however it could be explained by the fact that the cross-sectional area is a combination of the *U-ness* values which describe valley shape, form ratio and *b*-value. More alpine regions have higher relief and therefore valleys have greater local relief, as well as form ratio, which is the case in the northern Patagonia sample area. As local relief increases it may also contribute to greater cross-sectional area, by valleys being deeper. Where local relief decreases, which has been found in areas strongly influenced by glacial erosion both by limiting relief (Brozović *et al.*, 1997) or even lowering relief (MacGregor *et al.*, 2000), and where the Patagonia-Antarctica model persists, the valley form ratio will decrease unless valleys widen at proportionally the same rate as the valley-tops lower. Therefore to increase the cross-sectional area, valleys need to widen and/or deepen and if valleys become shallower (it is not possible for them to become narrower in absolute terms), then the cross-sectional area of a valley will decrease (this is discussed in detail with a diagram in Section 8.4.3.). It is proposed that absolute cross-sectional area reduces in the central Patagonia sample area, as here the relief is less, so lower form ratios are observed but valley widening has not yet compensated for this, leading to a reduction in cross-sectional areas. In the southern Patagonia sample area widening of valleys has been significant, as well as some deepening, as the form ratio is marginally lower but the cross-sectional area is much larger.

Another observation which can be made from this data is a comparison between *U-ness* measures for glacial and fluvial valley segments. Here the *U-ness* results for glacial valleys are almost exclusively greater than for fluvial valleys. One exception stands out and that is the result for the mean *b*-value in the northern sample area, for both first order (Table 6.6) and second order and greater (Table 6.7) valley segments. Here a lower value is found for glacial valleys compared to fluvial valleys. This may be due to the *b*-

values not being the best descriptor for *U-ness,* either due to a parabolic form not being as prevalent as first thought across the entire population of glaciated valleys and/or other conditions apart from glacial ones producing parabolic forms (this is discussed in Section 8.4.2), a conclusion made by Phillips (2009) in his study investigating the best measures to discriminate between fluvial and glacial valleys. However, as anticipated, the cross-sectional area and form ratios of glacial valley segments are greater than those for fluvial valley segments in each sample area.

Table 6.6 A summary of *U-ness* mean statistics for first order valley segments found within LGM limits (glacial) and outside LGM limits (fluvial). It shows greater *U-ness* values for glacial valleys compared to fluvial valleys, with the exception of the mean *b*-value in the northern Patagonia sample area.

		Number of valley segments	**Mean form ratio**	**Mean *b*-value**	**Mean cross-sectional area (m^2)**
Northern Patagonia	Glacial	1171	0.22	1.16	157,197
	Fluvial	2670	0.14	1.27	88,690
Central Patagonia	Glacial	1479	0.21	1.35	163,221
	Fluvial	462	0.15	1.12	87,246
Southern Patagonia	Glacial	1061	0.21	1.35	195,419
	Fluvial	220	0.11	1.25	109,656

Table 6.7 A summary of mean *U-ness* values for second order valley segments within LGM limits (glacial) and outside LGM limits (fluvial). The results are similar to those for first order valley segments (Table 6.6). When compared to first order catchments, glacial valleys here have lower form ratios but larger *b*-values and cross-sectional areas (with the exception of northern and central Patagonia).

		Number of valley segments	Mean form ratio	Mean *b*-value	Mean cross-sectional area (m^2)
Northern Patagonia	Glacial	574	0.179	1.37	240,073
	Fluvial	1319	0.105	1.43	112,481
Central Patagonia	Glacial	1127	0.152	1.59	216,887
	Fluvial	385	0.104	1.32	106,512
Southern Patagonia	Glacial	805	0.150	1.62	296,043
	Fluvial	156	0.075	1.40	155,058

A final observation is a comparison between first order (Table 6.6) and second order and greater (Table 6.7) valley segments. It is expected that as second order and greater valley segments have greater ice flux then mean *U-ness* values should be greater. This is true in Patagonia for mean *b*-values and mean cross-sectional areas but not for form ratio. Mean form ratios are smaller for second order valley segments when compared to first order valley segments in all three sample areas. This may be due to widening rather than deepening or that second order and greater valleys being further away from the mountain divide and therefore have less potential relief to erode vertically.

The results from the sample areas in the Southern Andes strongly support the hypothesis that *U-ness* increases with increased intensity of glaciation. However there are some deviations from this trend. A decrease in glacial valley form ratio as latitude increases can be explained by a transition from a Rocky Mountain model to a Patagonia-Antarctica model (Hirano & Aniya, 1988). Hirano and Aniya (1988) identified two types of glacial valleys broad; relatively shallow valleys, found in regions such as Patagonia and Antarctica, and deep, relatively narrow valleys found in Alpine regions (Rocky mountain model). Patagonia-Antarctica valleys have low form ratios for mature valleys (those with high *b*-values) whilst Rocky mountain valleys have high form ratios for mature valleys.

The literature related to this research is reviewed in Section 2.3.8. Anomalies with cross-sectional area can also be explained by a non-linear relationship between widening and deepening. Comparisons between glacial and fluvial valleys show that form ratio and cross-sectional area can discriminate between the two valley types and support Phillips (2009) view that *b*-value is not such a useful measure for this purpose. Comparing first order against second order and greater valley segments (for both glacial and fluvial valleys), show that mean *b*-values and mean cross-sectional areas are larger in the larger stream orders in all sample areas, but the mean form ratio is smaller. This may indicate that greater ice flux creates widening rather than deepening or that form ratio is limited by available relief.

The initial results in this section demonstrate that the method is capable of tackling large areas and analysing measures of cross-sectional valley shape and size. Observations of valley cross-sections in the southern Andes indicate that measures of size and shape increase with the degree of glaciation. A transition from a more Alpine regime to a more Patagonia-Antarctica regime is also observed.

6.5.2. Influence of ice residence time on U-ness

To investigate the influence of residence time on *U-ness,* elevation is used as a proxy. It is assumed that where elevation is greatest so is ice residence time, whilst a decrease will occur with decreasing elevation as conditions become less favourable for ice to persist. The elevation range of the Pyrenees enables *U-ness* measures, with respect to changes in elevation, to be investigated. The Pyrenees sample area encompasses the Atlantic coast to the West and Mediterranean coast to the East whilst including the Pyrenees' highest peak, Peak Aneto (3404m). The west-east disposition of the mountain chain means that there is minimal north-south gradient in glaciation intensity due to latitude change like that found along the Andes. However, reviewed in Section 5.4.1.2, a difference in precipitation amount exists between the north and south of the mountain divide. It is hypothesised that precipitation is subordinate to ice residence time due to elevation, however it is possible that correlations may separate into two clearly identifiable valley segment clusters north and south of the divide as a result of this.

Two statistics for elevation were initially investigated for use as a proxy for ice residence time. The first being the mean elevation above sea level found within defined valley segments; this statistic includes all elevation values making up the valley which comprise

the valley floor, valley wall sides and wall tops. The second statistic investigated was the mean elevation of the valley floor above sea level.

Regression analysis of elevation and form ratio was carried out on the 7573 valley segments (both fluvial and glacial) from the Pyrenees sample area, which include valleys from first to sixth order. It found a strong positive linear relationship between the two variables (Figure 6.11 and 6.12). The correlation between form ratio and the complete valley segment mean elevations was slightly better than that for mean elevations where only valley floor elevations were used. This is possibly due to the fact that deep valley segments are likely to have greater form ratios as well as higher elevations when valley side elevations are included in the mean elevation calculation. Therefore, it is suggested that to prevent any bias, the valley floor mean elevations are used for the valley segment elevation value throughout this thesis.

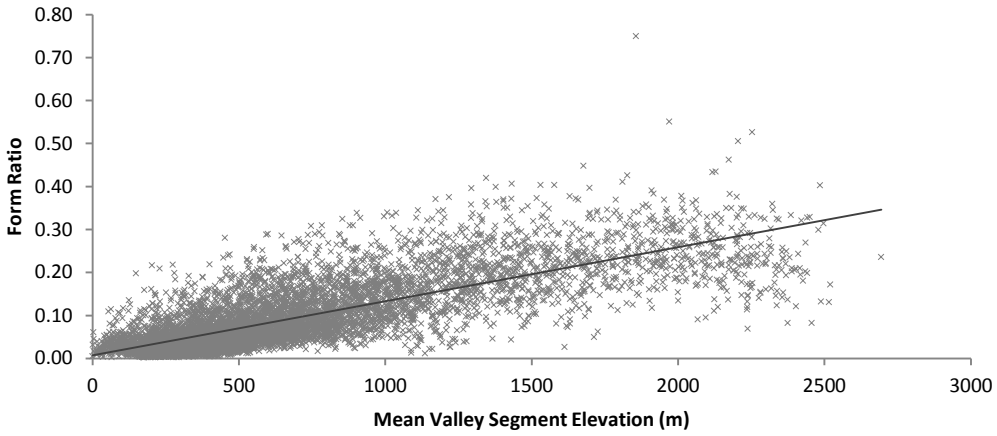

Figure 6.11 A clear positive (and highly significant above the 99.99% level) linear relationship between the mean valley segment elevation (a mean elevation defined by valley segment boundaries) and valley segment form ratio with a strong correlation of R-squared = 0.618 for the 7573 valley segments. With such high sample sizes it is not surprising that the correlation is highly significant, as such significance levels will only be reported when much smaller samples are used.

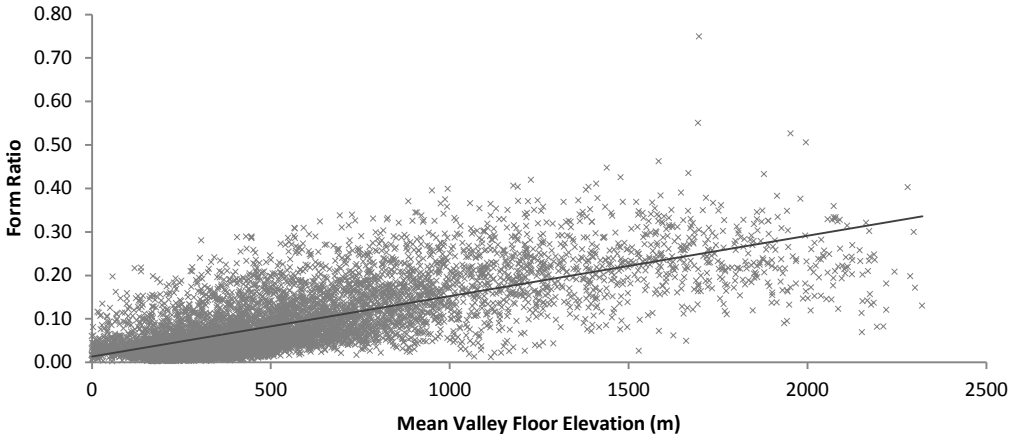

Figure 6.12 A similar plot to Figure 6.11 but using mean valley floor elevation in each valley segment. This prevents a bias, whereby higher form ratios have higher mean elevations. The R-squared value of 0.5257 shows a strong correlation for a linear regression of the 7573 valley segments.

The positive relationship between form ratio and elevation shown in Figure 6.11 and 6.12 supports the hypothesis that fluvial values (valleys at the lowest elevations) have lower form ratios than glacial valleys (those at the highest elevations), as well as the hypothesis that form ratio increases with greater ice residence time. Here erosion is concentrated downwards without widening, increasing local relief, creating deeper valleys and therefore giving greater form ratio values.

In order to expand understanding of the *U-ness* measure's response to elevation, data from valley segments in the Pyrenees were separated into those that fell within the LGM limits defined by Calvet (2004) and those that fell outside these limits (Figure 6.13). It can be seen in Figure 6.13 that large tongues of ice from large valleys, connected to extensive catchment areas, extend to low elevations. This is reflected in the data where there is a large spread in mean elevations for valley segments.

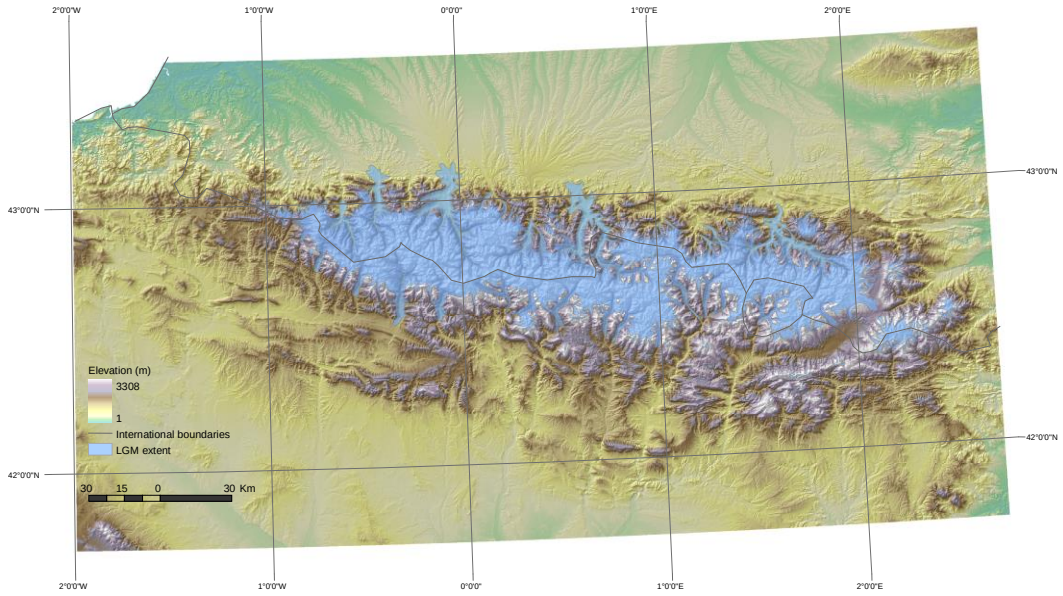

Figure 6.13 LGM limits (Calvet, 2004) depicted for the Pyrenees. Note the ice extent for major tributaries which, at certain locations, extends beyond the mountain range.

The data for form ratio against elevation (Figure 6.14) shows that the fluvial valley segments exhibit a correlation with elevation (R-squared is 0.4243) whilst glacial valley segments have a very weak correlation (R-squared is 0.0979) with elevation, although it is still significant. This is interesting. It may reflect the fact that at higher elevations slopes are steeper, so fluvial erosion is more intense, as rivers and streams erode to their base levels (Burbank *et al.*, 1996) and produce gorge forms rather than more open valleys. Glacial erosion is not controlled by base levels, instead increased erosion (and therefore form ratios) is attributed to greater accumulation areas at higher elevations (Brozović *et al.*, 1997). The lower correlation in the glacial valley segments may be due to glacier accumulation areas being more susceptible to local climate effects, like valley floor shading (Brocklehurst & Whipple, 2006), and therefore correlation with elevation is not good (this point is returned to in the discussion chapter (Chapter 8)).

The data also shows (Figure 6.14) that, for glacial valleys, the relationship between form ratio and elevation does not follow the same rate as fluvial valleys. Form ratio for glacial valleys does not increase as rapidly with elevation as it does with fluvial valleys. This may indicate that erosion is not solely downward and, especially in this more lightly glaciated sample area, erosion is focused on the valley sides, supporting Harbor's (1992) theory of valley evolution. Or it may be a result of peak erosion limiting relief and thus form ratio,

a theory presented by Brozović *et al.* (1997) and supported by various modelling experiments (Tomkin & Braun, 2002; Egholm *et al.*, 2009), or a combination of the two.

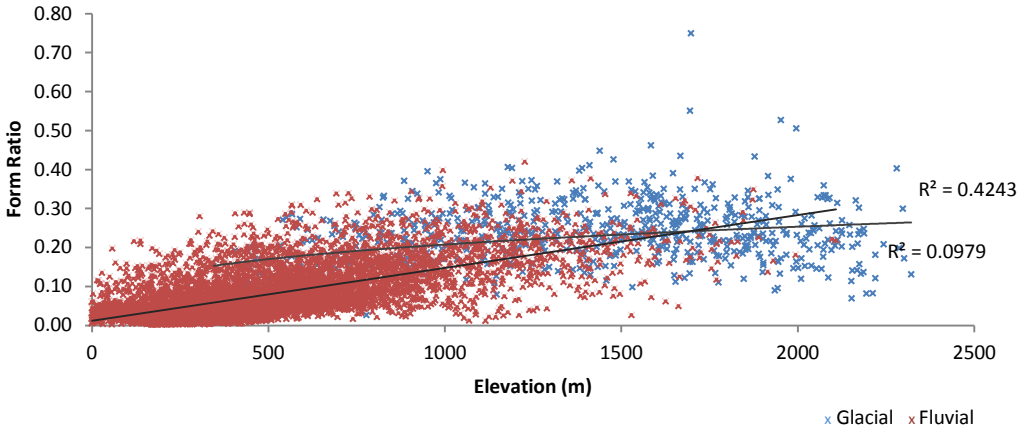

Figure 6.14 Form ratio against elevation with fluvial valley segments showing a medium positive linear correlation (R-squared = 0.4243) for the 6899 valley segments, whilst glacial valley segments show no correlation between the variables (R-squared = 0.0979).

When the relationship between *b*-value and elevation (Figure 6.15) is investigated for glacial and fluvial valley segments no relationship or significant correlation emerges but the glacial valley segments occupy a narrower range of *b*-values and conform more closely to a parabola between the values of 1 to 2, whilst fluvial valleys show a high variability of *b*-values. This pattern is not unique to the Pyrenees but occurs across all the sample areas investigated. It may demonstrate that the power-law is not good at defining fluvial valleys or that there is a larger variation in fluvial valley shape. However, the power-law is much better at representing glacial valley shape giving consistent results mostly between 1 and 2 for the *b*-value. The fact that glacial valleys are more likely to produce a consistent form is important in its own right, leading to the idea that glacial valleys have a steady state morphology. The considerable overlap between fluvial and glacial *b*-values was no doubt the reason why Phillips (2009) concluded that *b*-value was not a good discriminator between glacial and fluvial valleys. Standard deviations of glacial and fluvial valley segments do not show a distinct difference (standard deviation for glacial valleys is 0.32 and fluvial valleys 0.39) and will need further investigation. If the standard deviation of all valleys above 1250m is found it is 0.206, whilst the standard deviation of valleys below 1250m is 0.394, showing a lesser degree of *b*-value spread at the highest (potentially more glacial) valley segments.

An additional result which is noticed from this data is that within the glacial valleys, the *b*-values do not increase significantly with elevation; remaining constant. This may be due to local climate effects, as suggested for form ratio, or the influence of ice flux which can cause a confounding problem, anticipated in Section 3.3.2.1, whereby greater ice flux causes an increase in erosion down glacier and consequently at lower elevations.

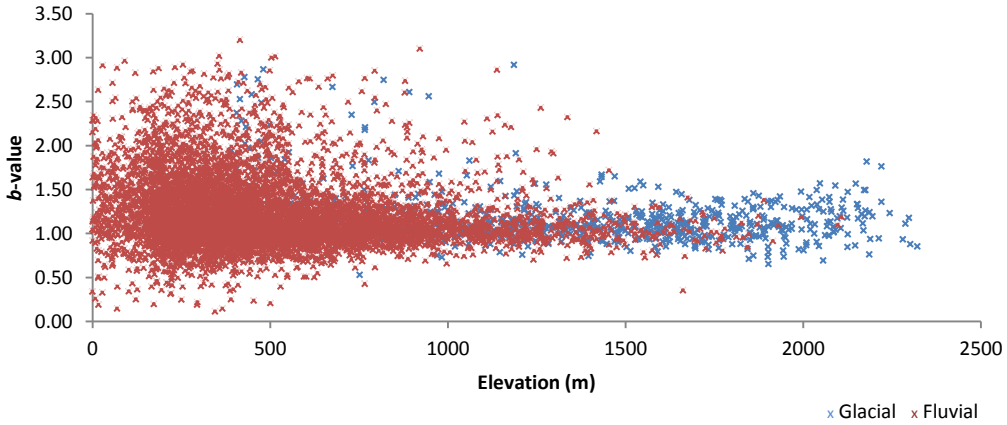

Figure 6.15 The elevation/*b*-value plot showing a lower spread of *b*-values at the highest elevations, where glacial valley segments dominate.

Correlations between elevation and valley segment cross-sectional area (Figure 6.16) show that, again, the glacial valley segments have no correlation (R-squared = -0.02) compared to fluvial valleys which have a weak correlation (R-squared = 0.18). Also the glacial valley data has a negative correlation, suggesting that for glacial valleys cross-sectional area decreases with elevation. This could, as with *b*-values, be explained by the confounding problem, whereby residence time increases with elevation whilst ice flux decreases with elevation. Here greater ice fluxes at lower elevations could have created larger valleys. Conversely, the fluvial valleys have greater erosive power at higher elevations as they strive to reach their base level and therefore create greater cross-sectional areas, as well as form ratios, with increased relief.

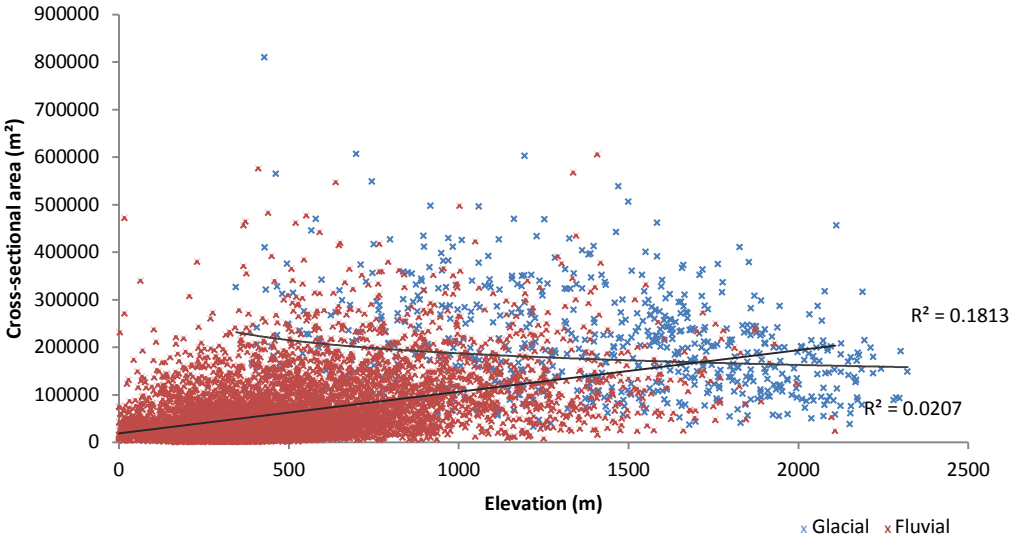

Figure 6.16 The relationship between cross-sectional area and elevation is plotted here for glacial (674 valley segments) and fluvial (6899 valley segments). The fluvial valleys have a weak positive linear correlation (R-squared = 0.18) whilst the glacial valleys have a negative linear relationship which has little correlation (R-squared = -0.02). The even relationship in glacial valleys is attributed to the confounding problem.

By investigating the relationship between *U-ness* measures and elevation it is clear that glacial valleys do not conform to the hypothesis that *U-ness* increases with ice residence time, or at least the proxy for it used here. Initially, when all the valley segments in the Pyrenees were analysed this hypothesis looked probable, as form ratio and cross-section area showed strong positive relationships. However, once glacial and fluvial valleys were analysed separately, the glacial valleys showed both poorer correlations and less distinct relationships to elevation. It is concluded that the proxy for ice residence time, elevation, may not be the first order control on *U-ness*. To understand which conditions, or combination of conditions, are required to give well-developed glacial valleys requires further investigation. It is hypothesised that for glacial valleys in the Pyrenees local climate effects may be significant and the confounding problem with ice flux may complicate results, whilst fluvial valleys' erosive power, and therefore relief production, is governed by a more universal control; the base level. *B*-values appear to show that fluvial valleys have a high variability in shape whilst glacial valleys conform to a parabolic form with a *b*-value between 1 and 2.

6.5.3. Correlations between ice flux and U-ness

Here I investigate whether ice flux is a first order control on *U-ness* by using contributing catchment area as a proxy for ice flux. It is thought that other factors such as climate are subordinate to ice flux in controlling U-form in large samples which cover whole mountain ranges. It is expected that as ice flux increases so will *U-ness* measures. In order to investigate *U-ness* measures and catchment area the data from the Pyrenees was divided into glacial and fluvial valley segments and observations made.

When examining the relationship between catchment area and the *U-ness* measure form ratio (Figure 6.17) there is a difference in the position between the two lines of best fit for glacial and fluvial valley segments. For catchment areas of the same size a glacial valley form ratio is greater than a fluvial valley segment. This may reflect that glaciers erode deeper valleys, but may also be a reflection of the fact that glacial valley segments are in the mountains and, therefore, have more potential to increase local relief by erosion as there is more relief available, or even that fluvial valleys are close to their base levels. The negative correlation for glacial valleys may also be a consequence of relief as valleys with the largest catchment areas are more likely to be on the mountain periphery and therefore have both a short ice residence time and less available relief to erode.

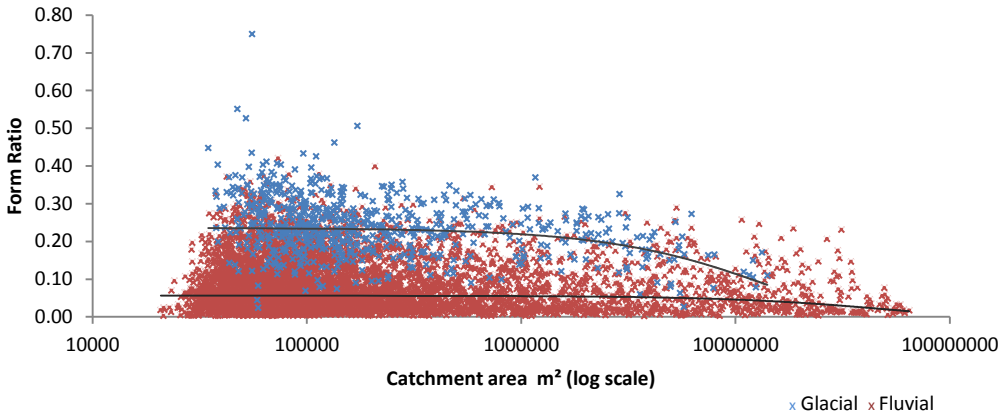

Figure 6.17 Form ratio is investigated with respect to catchment area in the Pyrenees. Glacial valleys (674 valley segments) and fluvial valleys (6899 valley segments) with R-squared values of -0.105 (small correlation) and 0.0135 (no correlation) respectively. Both datasets show an exponential relationship with a slight decrease in form ratio with larger catchment areas, which is more pronounced in glacial valleys (note the log scale on the x-axis).

Plotting *b*-values against catchment area (Figure 6.18) shows a large spread of results for both glacial and fluvial valley segments. Correlations show that glacial valleys have a small correlation (R-squared is 0.25), whilst fluvial valleys have no correlation (R-squared is 0.039). As the glacial valley correlation is positive it indicates that glacial valleys may create more glacially defined valley shapes with increased flux. When compared to the results in Section 6.5.2, where there was no correlation with elevation and *b*-values, these results suggest that ice flux is more important in creating a parabolic valley form than residence time.

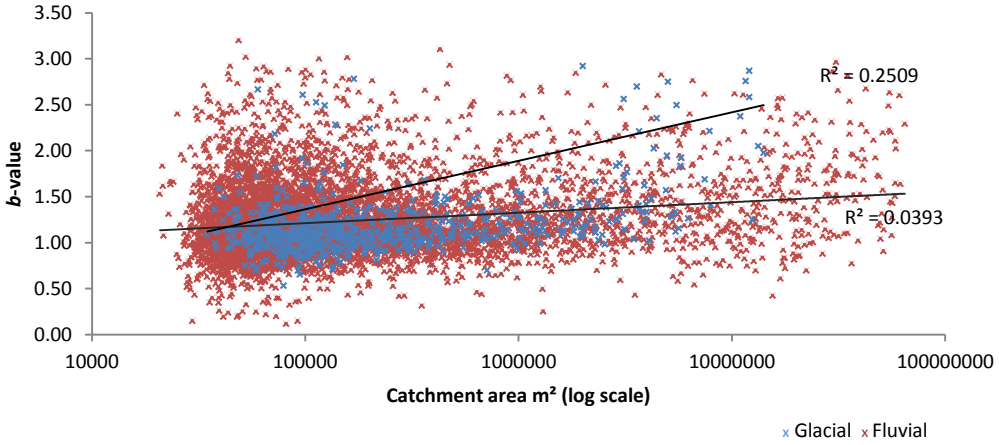

Figure 6.18 Results for the Pyrenees glacial and fluvial valley segments show a positive relationship. Glacial valleys have a small correlation (R-squared = 0.25 for 674 valley segments) whilst fluvial valleys show no correlation (R-squared = 0.039 for 6889 valley segments) between catchment area and *b*-values. Note the log scale on the x-axis which means the glacial line of best fit at first appears improbable.

Investigation into the relationship between catchment area and cross-sectional area (Figure 6.19) show that, as with form ratio, cross-sectional areas in glacial valley segments tend to be higher when compared to fluvial valley segments with similar catchment sizes. However, in combination with this, glacial valley segments also have a positive correlation between catchment area and cross-sectional area, similar to *b*-values. This indicates that valley segment cross-sectional area is influenced by contributing catchment area and, potentially, ice flux for glacial valleys. The correlation is less clear for fluvial valleys and needs further investigation. It is interesting that the form ratio (Figure 6.17) does not increase with catchment area, yet cross-sectional area does (Figure 6.19). This suggests that in the Pyrenees glacial valleys have similar

proportions irrespective of size. If ice flux does have a strong control on valley size, it may explain why in Section 6.5.2 a negative relationship was found between cross-sectional area and elevation. This may be due to a confounding effect whereby the smallest catchment areas are found at the highest elevation but the greatest catchment areas are found at lower elevations. As catchment area appears to have a stronger correlation with cross-sectional area than elevation in the Pyrenees, together with the fact that there is only a positive relationship found between catchment area and cross-sectional area, it is suggested that ice flux has a stronger influence on valley size than ice residence time. This result means that more erosion occurs during the shorter periods of large flux than in valleys which have lower flux but prolonged residence times.

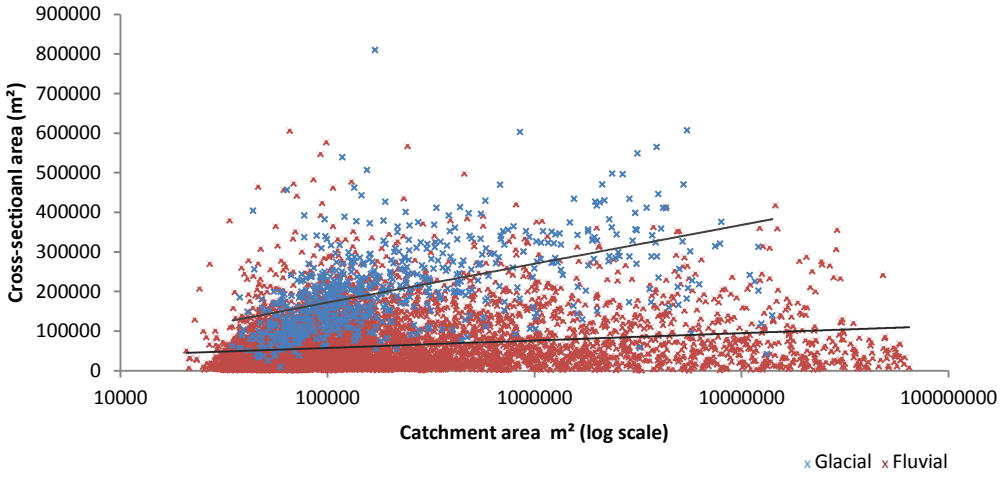

Figure 6.19 Data for glacial and fluvial valleys investigating the relationship between catchment area and cross-sectional area. A positive small correlation (R-squared =0.278) exists for the glacial valleys (674 valley segments) whilst fluvial valleys do not increase cross-sectional area with catchment area (showing no correlation as R-squared = 0.037 for 6889 valley segments). Again note the log scale used on the x-axis.

6.5.4. Influence of aspect and precipitation on U-ness measures

The contrast of climate north and south of the mountain divide in the Pyrenees, particularly with respect to aspect and precipitation, creates an opportunity to investigate the influence of climate on *U-ness* measures (Figure 6.20). The specific details of the climate in the Pyrenees are detailed in Section 5.4.1.2. It is expected that a region with higher precipitation and lower solar radiation will accumulate more ice which will persist for longer, therefore having greater ice flux and residence times. These conditions prevail north of the divide in the Pyrenees and as such should result in

greater *U-ness* measures. It is hypothesised that the differences in aspect and precipitation in the Pyrenees will be the first order controls on *U-ness* and other factors will be subordinate to this.

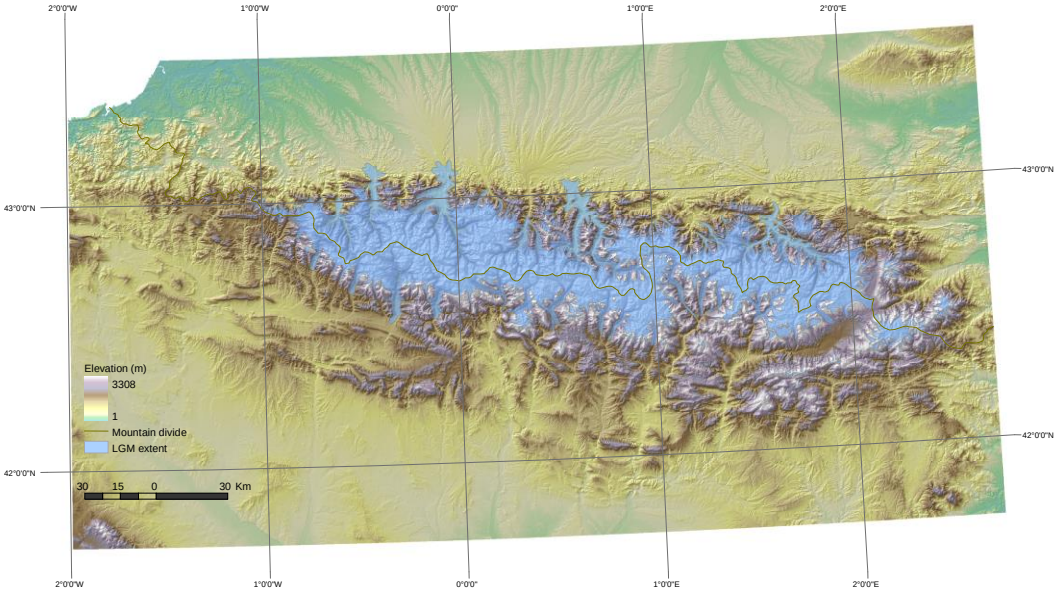

Figure 6.20 Map depicting the mountain divide in the Pyrenees. North of the divide experiences high precipitation rates whilst experiencing lower solar radiation. South of the divide is in a rain shadow therefore experiencing much lower precipitation as well as more hours of direct sunlight increasing potential melt.

Initial results (Table 6.8) for all glacial valley segments show a marginal difference with higher *U-ness* measures in the north compared to valleys south of the divide. When second order and greater valley segments are investigated (Table 6.9) there is little difference between the mean form ratio north and south of the divide, but a marginally greater mean *b*-value and cross-sectional area value.

Table 6.8 A summary of mean *U-ness* results for all valley segments within LGM limits. Higher values are found in the north in all cases. This is as expected in the hypothesis as the northern region of the Pyrenees not only has more precipitation, but faces north so has less exposure to solar radiation.

	Number of valley segments	**Mean form ratio**	**Mean *b*-value**	**Mean cross-sectional area (m²)**
North	417	0.243	1.200	205,202
South	256	0.229	1.156	201,863

Table 6.9 A summary of second order and greater valley segments within the LGM limits of the Pyrenees. Here form ratios are marginally smaller in the northern region although *b*-values and cross-sectional areas are still larger.

	Number of valley segments	**Mean form ratio**	**Mean *b*-value**	**Mean cross-sectional area (m²)**
North	135	0.215	1.327	271,369
South	84	0.217	1.292	257,580

Regression analysis for *U-ness* measures and proxies with respect to climate was carried out on the dataset for second order and greater valley segments in the Pyrenees. When the different climates across the mountain divide were compared, higher form ratios were found in the north compared to valley segment form ratio values at the same elevation in the south (Figure 6.21). This supports the hypothesis of greater *U-ness* values where there is a more favourable climate, although differences are small (but statistically significant due to large sample sizes). More investigation is therefore needed to make conclusions.

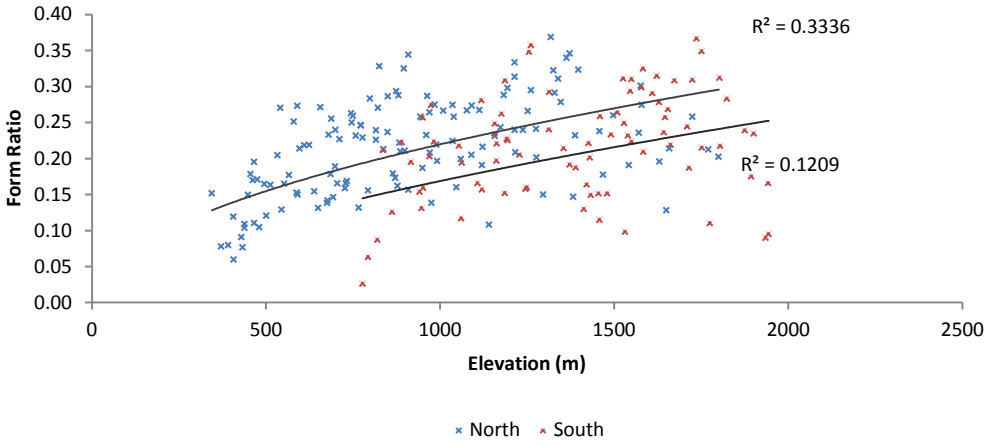

Figure 6.21 The relationship between form ratio and elevation show that northern second order and greater glacial valleys segments (135) in the Pyrenees have higher *b*-values at the same elevation compared to southern valleys (84). They both have a positive power correlation northern valleys having a medium correlation (R-squared = 0.3336) with a high level of significance (above the 99% level) and southern valleys having a weak correlation (R-squared = 0.1209) and significance above the 99% level.

When the influence of climate on the relationship between *b*-values and elevation is considered, both the pattern and correlation is reversed when compared to the form ratio/elevation relationship. Higher *b*-values for the same elevation are found in the southern section of the Pyrenees, although only marginally (Figure 6.22) and a significant difference cannot be seen. This needs further investigation.

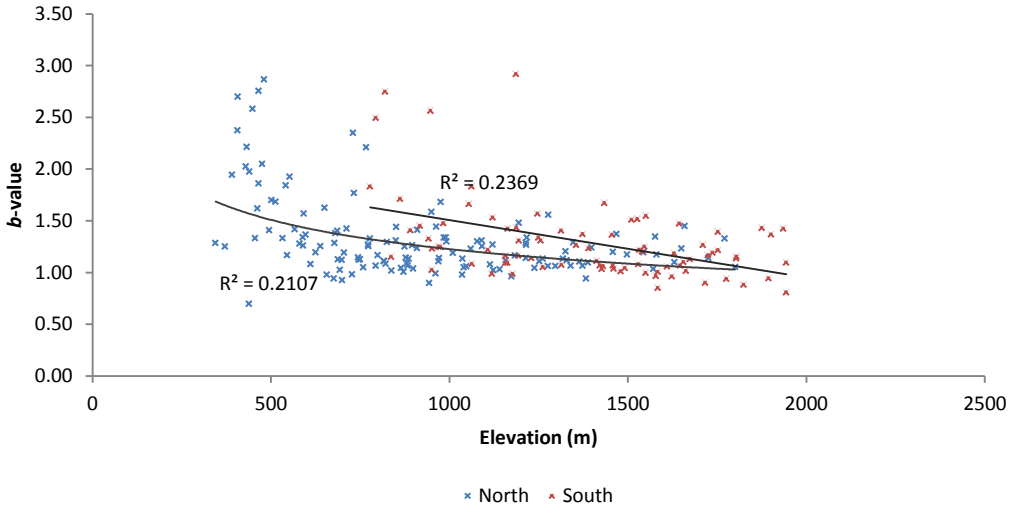

Figure 6.22 Although the summary of *b*-values (Table 6.9) showed that second order and greater glacial valleys in the north had a higher mean *b*-value, the results from the *b*-value elevation plot show that for the same elevation southern valleys have a higher *b*-value but without a statistically significant difference between datasets. Both are significant at the 99.9% level with northern valleys having a negative medium power correlation at R-squared = 0.2107 for 135 valleys and a linear negative medium correlation at R-squared = 0.2369 for valleys south of the divide.

Interestingly, regression analysis with cross-sectional area and elevation showed no clear relationship for the two sides of the divide, suggesting that there was not a clear distinction between this *U-ness* variable's responses to elevation between the two climatic regimes. Similarly, there is no difference each side of the divide for each of the *U-ness* measure's relationships to catchment area (for example Figure 6.23). These results could suggest that climate and valley orientation are not of significant importance in the development of *U-ness* measures. From this initial investigation it does not appear that aspect and precipitation difference between the north and south of the Pyrenees is the first order control on *U-ness*. Climatic effects operating at a more local level may be of more importance (e.g. individual valley segment orientation) for example, and this needs further investigation. The initial summary of mean results (Table 6.8 and Table 6.9) may have been due to the northern LGM limits having greater extent and therefore encompassing higher order valleys with larger catchment areas resulting in larger *b*-values and cross-sectional areas. The Pyrenees is also slightly asymmetrical, having steeper slopes north of the divide. This asymmetry may have

resulted in the first order valley segments having greater form ratios. However, further spatial analysis is needed. At this stage of analysis it is clear that the expected north-south difference, arising from climate, is lacking.

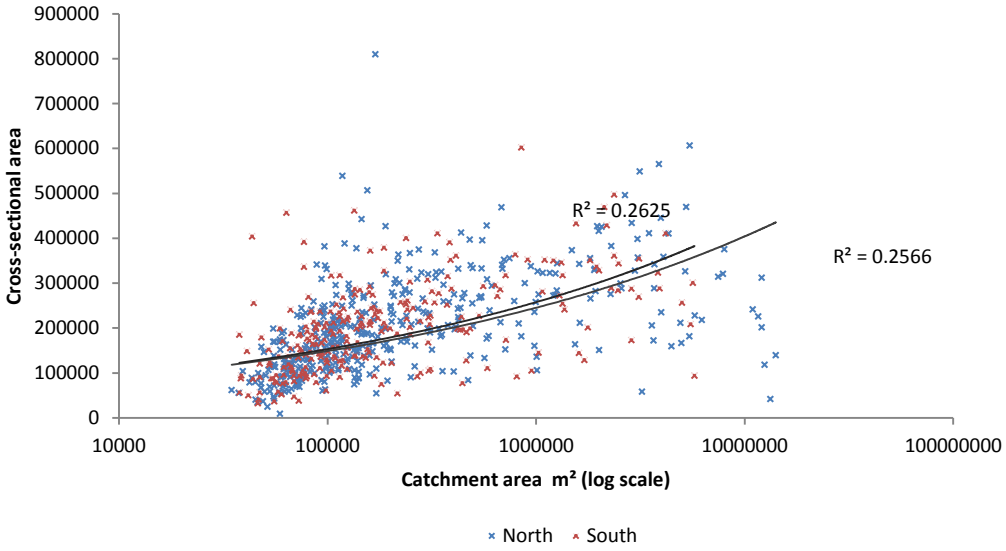

Figure 6.23 A plot showing the almost identical relationship north and south of the Pyrenees for cross-sectional area and catchment area, where there is a positive power correlation significant to the 99.9% level for the northern region (R-squared = 0.2566 for 417 valley segments) and southern region (R-squared = 0.2625 for 256 valley segments).

6.5.5. Influence of tectonic settings on U-ness

The Southern Alps has some of the highest uplift rates (7-10 mm/yr (Tippett & Kamp, 1993)) found globally, so it is an interesting sample area against which to compare *U-ness* measures to those found in more stable tectonic settings. It has been suggested that erosion is greater when intense uplift is occurring (Brozović *et al.*, 1997), and this was discussed in Section 5.2.2. In this section the hypothesis is explored to see whether there is any difference in the geomorphology of glacial valley cross-sections located in different tectonic settings. Two sample areas were chosen to compare to the Southern Alps, firstly, the Pyrenees, which underwent uplift before Quaternary glaciation (Choukroune, 1992). The Pyrenees has been much more lightly glaciated than the Southern Alps, this has been deduced partly by the extent of existing ice today; in the Pyrenees only cirque glaciers remain (Section 5.4.1.2), whilst in the Southern Alps valley glaciers still persist (Section 5.4.2.2), partly due to the glacial history detailed in Section

5.4.1.2 and 5.4.2.2. Comparing sample areas is difficult due to factors such as climate and lithology not being constant and therefore results must be treated with caution. The Northern Patagonia sample area was included in the sample as another area to compare to the Southern Alps. Northern Patagonia has undergone moderate glaciation (Section 5.4.3.2) and is a region dominated by pre-Quaternary uplift (Section 5.4.3.1) and is therefore considered a stable tectonic region, like the Pyrenees. Initial investigations in Table 6.10 and Table 6.11 show that in all cases, apart for form ratio in the second order and greater glacial valleys in the Pyrenees, mean *U-ness* measures were greater for the Southern Alps, supporting the hypothesis.

Table 6.10 Summary of mean *U-ness* measures for all valley segments within LGM limits for each sample area. The Southern Alps has had intense uplift during glaciation whilst the Pyrenees and north Patagonia has not. Mean *U-ness* measures are greater for the Southern Alps than the Pyrenees and north Patagonia supporting the hypothesis that *U-ness* will be greater in uplifting mountain ranges due to more intense erosion.

	Number of valley segments	**Mean Form ratio**	**Mean *b*-value**	**Mean cross-sectional area (m²)**
Southern Alps (high uplift)	1115	0.25	1.37	259,687
Pyrenees (stable)	673	0.24	1.18	203,932
North Patagonia (stable)	1745	0.21	1.23	184,458

Table 6.11 Summary of mean *U-ness* results for second order and greater valleys segments within LGM limits. Results are similar to Table 6.10 with the exception of form ratio which is the same for the Southern Alps and North Patagonia. Note the mean form ratio in the Pyrenees highlighted in bold. This value is the only mean *U-ness* measure not to be greater in the Southern Alps (actively uplifting region).

	Number of valley segments	**Mean Form ratio**	**Mean *b*-value**	**Mean cross-sectional area (m^2)**
Southern Alps (active uplift)	343	0.18	1.58	331,778
Pyrenees (stable)	219	**0.22**	1.31	266,080
North Patagonia (stable)	574	0.18	1.37	240,073

The relationships between *U-ness* measures and proxies were considered in a tectonic uplift context where values for the Southern Alps (active uplift) were compared to a more tectonically stable region, in this case North Patagonia. Differences were identified between cross-sectional area and catchment area (Figure 6.24). The relationship shows that both areas have a positive relationship, but for the similarly sized catchment areas in the Southern Alps, valley segments have larger cross-sections than in Northern Patagonia. For this finding it is inferred that for similar ice fluxes more erosion occurs in the Southern Alps, an actively uplifting region, than in a stable tectonic region (North Patagonia).

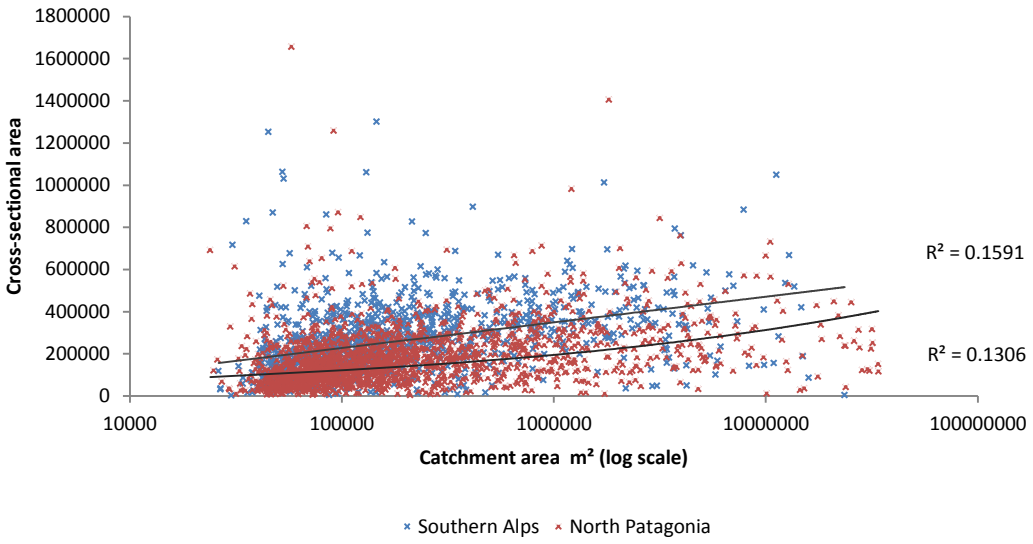

Figure 6.24 The relationship between cross-sectional and catchment area is considered for the two tectonic settings. It shows that the Southern Alps have larger cross-sectional areas for similar sized catchment areas. Both datasets show a positive relationship with a weak correlation. The Southern Alps has a R-squared = 0.1591 for 1115 valleys whilst North Patagonia has a R-squared = 0.1306 for 1745 valleys.

6.6. Summary

The initial investigations presented in this chapter show that the mean valley profile method has the potential to aid the understanding of valley cross-section evolution. The chapter argues that for the average valley profile method only the bottom half of the valley should be analysed. It also investigates the general power law (Pattyn & Van Huele, 1998) and concludes that it does not greatly adjust valley profiles and as such is not used in this research. The results also show the ability of the mean valley profile method to handle large volumes of data. Investigations in this chapter concentrated on looking for first order controls on glacial valley cross-sectional form by using large sample sizes in a variety of areas.

The initial results can be summarised as:

1. In the Andes *U-ness* was shown to increase with the intensity of glaciation, as indicated by an increase with southerly latitude.
2. Form ratio increased with elevation (proxy for ice residence time) but, surprisingly, to a lesser degree in glacial valleys when compared to fluvial valleys.

3. Glacial valleys displayed a smaller degree of *b*-value variation (between 1 and 2) than fluvial valleys, which exhibit both very high and low values. From this finding it is inferred that fluvial valleys have a wide variety of cross-sectional shapes and that the V-shaped valleys (*b*-value = 1) is a misnomer. Glacial valleys on the other hand do appear to develop towards a steady state form.
4. Cross-sectional area increased with catchment area (proxy for ice flow), whilst for glacial valleys this relationship does not occur between cross-sectional area and elevation. This suggests that ice flux is more significant in eroding valleys than prolonged ice residence is.
5. Mean *U-ness* values for climates more favourable to glaciation (i.e. high precipitation and more poleward orientations) were shown to be greater. From this it is inferred that glacial erosion is more intense in regions more favourable to ice accumulation, consistent with expectations.
6. For different tectonic settings, the largest mean *U-ness* values were found in the sample area with highest uplift (New Zealand).

Initial results suggest that, when using the mean valley profile technique, valley cross-sectional area is the best *U-ness* measure for discriminating between fluvial and glacial valleys. From investigations in this chapter it is evident that no clear first order control exists for valley form. It is thus expected that complex conditions and feedbacks create glacial geomorphology. One complicating factor that can be identified from these results is that ice residence time and ice flux are spatial in opposition; in that ice flux increases with catchment size and thus down valley, whilst ice residence time increases with elevation and thus up valley. This creates a confounding problem whereby ice flux and residence time conflict. The confounding problem complicates the interpretation of results for *U-ness*. Anomalies in results throughout this chapter may be due to this confounding problem. In addition to the confounding problem, another question arising for the research in this chapter is a suspicion that local factors, such as climate, orientation and geology structure, may also play a part in valley cross-sectional shape and size. To investigate localised effects within sample areas spatial analysis techniques must be used.

In the following chapter (Chapter 7) both the confounding problem, as well as the influence of local effects, are investigated. Analysis is more advanced, involving multiple regression, which will enable both ice residence time and ice flux proxies to be taken

into consideration together, whilst mapping correlations spatially may reveal any changes in correlations across the mountain range sample areas.

7. Examining variation of glacial valley form within mountain ranges

7.1. Introduction

The analysis of datasets for whole sample areas has shown some interesting results (Chapter 6). However, some results were not as expected, whilst others showed poor correlations and a simple first order control on *U-ness* was not found. A major problem of regressing variables over whole datasets, for spatial data, is that it assumes that the relationship between variables is constant over space. In the complex environments found in the real world this is unlikely to be true over large areas. Some sub-regions may show a positive correlation between variables whilst other sub-regions, within the same dataset and between the same variables, may be less well correlated or even negatively correlated. When grouped over large areas correlations at a local level can thus be masked. It was suspected in the previous chapter (Chapter 6) that this might have occurred due to local conditions, such as local climate conditions and rock structure, causing different responses to glacial processes and therefore impacting the valley cross-sectional profile shape and size. If differing responses to the majority constituted a large enough area within that being sampled, and with a response which is greatly different to the rest of the dataset, correlations may not show clear results for the dataset as a whole. In addition, the influence of a confounding problem between ice residence time and flux where they are in opposition when forming glacial valleys, and identified in Chapter 6, needs further investigation.

In this chapter spatial analysis is undertaken in order to investigate relationships at a more local scale and taking account of multiple factors in combination. This is done within ArcGIS using the relatively newly available spatial statistical modelling method known as Geographical Weighted Regression (GWR). It is hoped that by using this technique further insight will be gained into valley cross-sectional shape and size. This chapter explains the GWR technique and defines and justifies suitable parameter sizes, before presenting the results of the spatial analysis.

7.2. Geographically Weighted Regression

GWR is a statistical technique which allows use of location when computing linear regressions. The result is that it can produce a surface showing how regressions change spatially across the dataset. Each location is also assigned values related to the goodness of fit of the regression model. A specific GWR tool is now integrated in ArcGIS 9.3 allowing for easy application of this technique.

A GWR model is effectively a linear regression model applied to each location, in this case point data that represents the centre of each valley segment. The linear regression calculation for each location uses a defined number of neighbours, or points, closest to the location under investigation, and weighted according to their proximity to the original data point. Therefore each location uses different sets of data to compute the regression. The result is that each point has a unique regression equation and corresponding error statistics.

The global linear regression equation is shown in equation 7.1. To allow for local rather than global parameters it is rewritten to become equation 7.3.

A global linear regression model can be defined as:

$$y_i = a_0 + \Sigma_k a_k x_{ik} + \varepsilon_i \quad [7.1]$$

One parameter is used to estimate the relationship between each independent variable (x) and the dependent variable (y) and this relationship is assumed to be constant across the study area. Whilst ε is an error term and i represents a point in space at which observations on the ys and xs are recorded (Fortheringham *et al.*, 2002). The estimator for the parameters (a) in this model is:

$$a = (X^t X)^{-1} X^t y \quad [7.2]$$

where *a* represents the vector of global parameters to be estimated, *X* is a matrix of independent variables with the elements of the first column set to 1, and *y* represents a vector of observations on the dependent variable. The GWR allows for local, rather than global, parameters to be estimated, therefore rewriting the equation as:

$$y_i = a_0 (u_i, v_i) + \Sigma_k a_k (u_i, v_i) x_{ik} + \varepsilon_i \quad [7.3]$$

where (u_i, v_i) denotes the coordinates of the *ith* point in space and $a_k (u_i, v_i)$ is a realisation of the continuous function $a_k (u, v)$ at point *i* (Fortheringham & Zhan, 1996; Brunsdon *et al.*, 1998). Values for each point denote spatial variability and a continuous

surface of parameter values are created as well. For the estimation of the $a_k\ (u_i, v_i)$'s it is assumed that the observed data near the point *i* to have a greater influence than data of point further away. Therefore measuring the relationship around each point *i* similar to that of the weighted least squares method. By weighting an observation according to its proximity to point *i* the result varies with *i.* Observations close to *i* have a greater weight than those farther away.

The GWR estimator which results is as follows:

$$a(u_i, v_i) = (X^t W(u_i, v_i) X)^{-1} X^t W(u_i, v_i) y \qquad [7.4]$$

Where $W(u_i, v_i)$ is a *n* by *n* matrix whose off-diagonal elements are zero and whose diagonal elements denote the geographical weighting of observed data for point *i*. That is,

$$W(u_i, v_i) = \begin{matrix} w_{i1} & 0 & 0 & \dots & 0 \\ 0 & w_{i2} & 0 & \dots & 0 \\ 0 & 0 & w_{i3} & \dots & 0 \\ . & . & \dots & \dots & . \\ 0 & 0 & 0 & . & w_{in} \end{matrix} \qquad [7.5]$$

where w_{in} denotes the weight of the data at point *n* on the calibration of the model around point *i*. The weights vary with *i* which differentiates the GWR method from the weighted least squares method where the weighting matrix remains constant.

Not only does the GWR method produce localised parameter estimates but it is also able to calculate goodness of fit statistics for these localised parameters, for example R-squared values.

7.2.1. Spatially Adaptive Kernels

In GWR, kernels can be defined by distance or number of neighbours. A kernel defined by number of neighbours is spatially adaptive in order to accommodate the defined number of neighbours. The spatially adaptive kernel method is used so that where areas are densely populated with data points the kernel bandwidth is smaller than in areas where data points are sparser. The following provides an equation for spatially adaptive kernels:

$$w_{ij} = \begin{matrix} [1 - (d_{ij}/\, h_i)^2]^{\,2} & \text{if } d_{ij} < h_i \\ 0 & \text{otherwise} \end{matrix} \qquad [7.6]$$

where *i* is a calibration point, and varies around the study area, and *j* is a data point. The weighted function w_{ij} is specified as a continuous function of d_{ij}, the distance between *i* and *j*. The bandwidth is determined by *h* and therefore h_i is the *Nth* nearest neighbour distance from *i*. Essentially, this means that for each data point *i*, those observations closer to *i* have a greater influence in the estimation of the parameters than those data points farther away.

7.2.2. Kernel size sensitivity test

Techniques for choosing kernel size have been developed. For example, the cross-validated sum of squared errors method finds an optimum kernel value (Brunsdon *et al.*, 1998) and is used in Brunsdon *et al.* (2001). However, Silverman (1986) suggests a degree of subjective choice is necessary to which Brunsdon *et al.* (1998) agree and despite using the cross-validated sum of squared errors method, Brunsdon *et al.* (2001) ignore the results and simply double its suggested value. A sensitivity test was applied to the dataset in order to test for stability and to find an optimum kernel size. If the kernel size was too large the linear regression model will be close to the global model and obscure local trends. If the kernel size was too small the parameter estimates will be highly dependent on data points in close proximity to *i* and could show high variance, again obscuring any meaningful pattern. In the sensitivity test the stability of patterns across the sample area were observed at different kernel sizes. A judgement on the best kernel size to display patterns was made by a compromise between the level of detail and the broad patterns shown.

To investigate kernel size sensitivity within the sample areas, form ratio was used as a dependent variable and valley segment mean valley floor elevation as the explanatory variable for the Southern Alps sample area. The valley segments used in this sample area are those found within the LGM limits as only glacial valleys are required for investigation. By investigating sensitivity to kernel size for goodness of fit (R-squared values), the regression intercept, as well as the coefficient values (steepness of slope) it not only allows an informed choice of kernel size but also allows an introduction to the results and type of analysis produced by GWR in ArcMap.

7.2.2.1. Kernel size sensitivity investigated with goodness of fit values

The goodness of fit statistic of R-squared is one of the GWR outputs. It indicates how well the linear regression model fits the data in the defined local area or within the set number of nearest neighbours. The R-squared value is useful in understanding whether the data has a significant relationship. The GWR analysis in ArcMap gives an R-squared value for each valley segment, which is displayed as point data, but does not produce a surface. To enable easier comparison between the results of different kernel sizes of the R-squared data an Inverse Distance Weighted (IDW) surface is produced. By comparing the goodness of fit using the R-squared values a comparison between highly and poorly significant areas of data points can be made. In Figure 7.1 to 7.5 the R-squared data is displayed in points as well as an IDW surface produced from the point data. As expected, large kernel sizes show less well correlated data than smaller kernel sizes, confirming the idea earlier expressed that grouping of large areas might mask correlations.

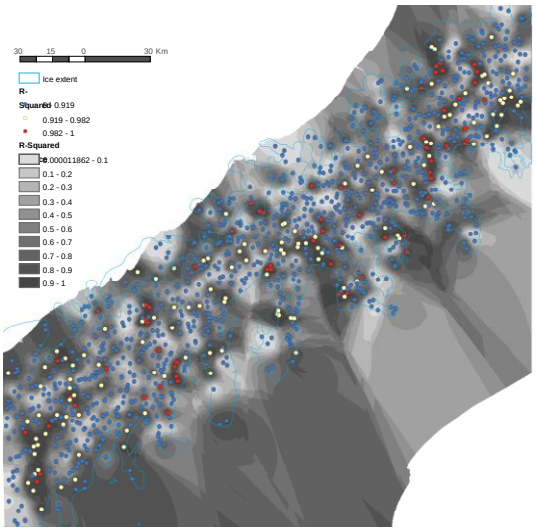

Figure 7.1 R-squared results with the IDW surface (in greys and black) for the GWR of valley elevation and form ratio, showing that when using only 5 neighbours there is a lot of variability. Red points indicate valley segments with 99.9% and better significance, yellow points show valleys with 99.9% to 99% significance and blue points 99% and less significance. This means there is a large spread of data with a minimum value of 0 and a maximum of 0.9996, a standard deviation of 0.3361 and a mean of 0.5495. Out of the 1114 valley segments within the LGM limits, 199 had a significance level of 99% or better.

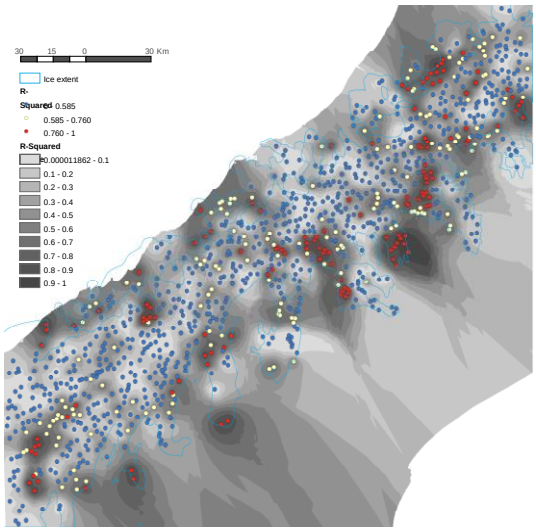

Figure 7.2 The same as Figure 7.1 but using 10 neighbours. This figure still shows high variability with a minimum value of 0 and a maximum of 0.9759. The data has a standard deviation of 0.2883 and a mean of 0.3668. There are 299 valley segments with a significance level of 99% or better.

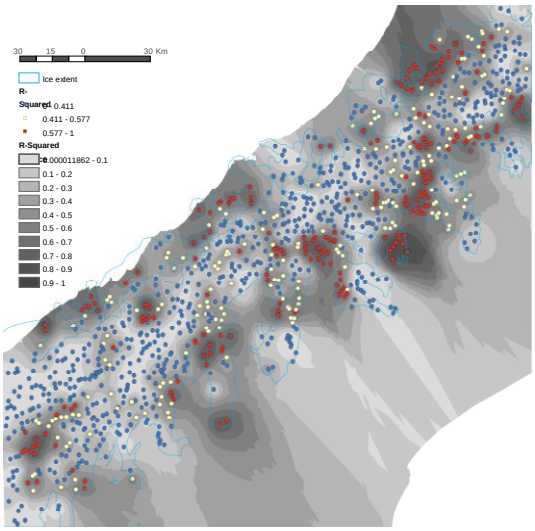

Figure 7.3 Similar to Figure 7.1 but using 15 neighbours. The spread of data is reduced when compared to fig 1 and 2 with a minimum of 0.000003 and a maximum of 0.9318 (standard deviation 0.2592) The mean is 0.3212 and the number of valley segments which have a significance level of 99% or better is 420.

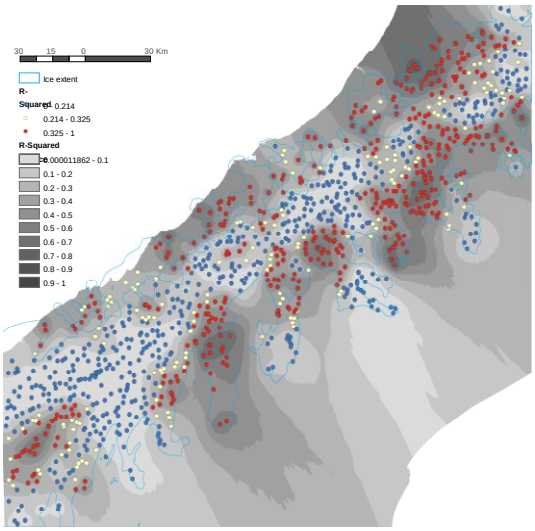

Figure 7.4 Data displayed as for Figure 7.1 to 7.3 but using 30 neighbours in the GWR analysis. The spread of R-squared values is again lower with a minimum of 0.000008 and a maximum of 0.7813 (standard deviation is 0.2084). The mean is 0.2628 and there are 598 valley segments with a significance level of 99% or better.

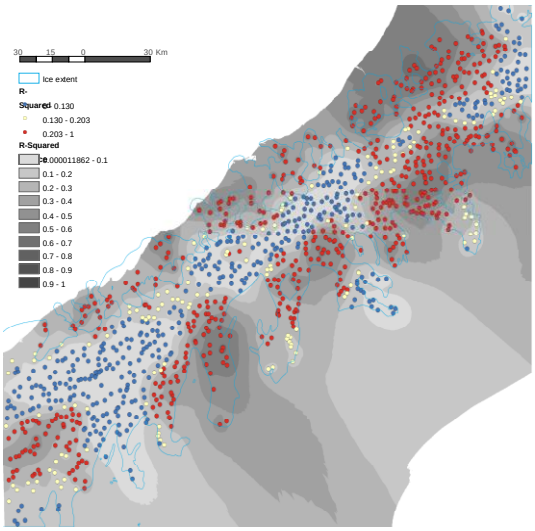

Figure 7.5 Finally this figure shows the results for the GWR using 50 neighbours. It shows a very smoothed surface which is reflected in the reduced spread of data (minimum R-squared value is 0 but the maximum is only 0.6984 and the standard deviation the lowest yet at 0.1871) The mean is 0.2365 and the greatest number of valley segments are within the 99% significance level (711).

Visual comparisons can be made between different kernel size solutions but in addition the minimum and maximum R-squared values, as well as the mean and standard deviation of R-squared values can be found and compared in order to inform a decision on kernel size. The ideal GWR results would show local variation on a valley system scale rather than on a smaller or larger scale.

Results for each valley segment GWR model show R squares which have a fairly similar mean but the standard deviation of the data increases as the amount of neighbours used is decreased, which represents the variability of the data. There is less of a difference between the means and standard deviations when using larger numbers of neighbours, i.e. 15 and 30 neighbours (Figure 7.3 and 7.4) compared to 5 and 10 neighbours (Figure 7.1 and 7.2).

7.2.2.2. Observations of the intercept (a coefficient) surface sensitivity to kernel size

The intercept surface produced by the GWR is useful as it indicates the value for the dependent variable, in this case form ratio, when the explanatory value (elevation) is zero, according to the linear regression produced. When using the GWR tool in ArcMap a surface for the intercept is automatically created, as well as the intercept value for each valley segment. When a comparison is made between different surfaces produced with varying kernel size the impact of kernel size can be observed (Figure 7.6 to 7.10). The figures below are also displayed with the R-squared values. The R-squared values enable an understanding of where linear regressions were able to fit the data well. Results, including intercept values, for valley segments with low R-squared values cannot be relied upon as much as valley segments with high R-squared values. As expected small kernel sizes showed high variance in the surface and larger kernel sizes a smoothing effect. However the surfaces appear stable, in that variance develops around the same points. Particular stability is observed between 15 to 30 neighbour kernels, and valley system level variability at 30 neighbours.

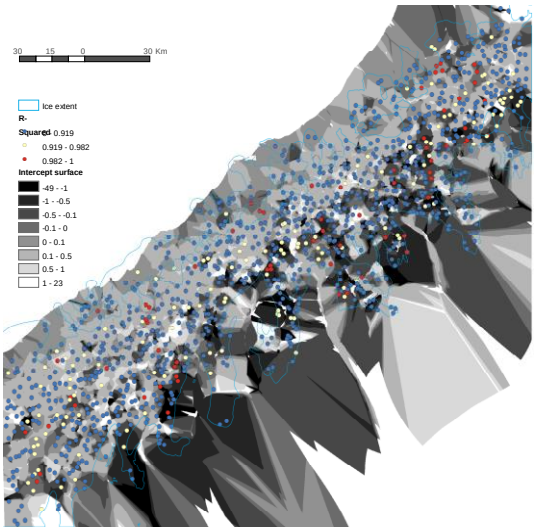

Figure 7.6 The intercept surface produced by the GWR for analysis between form ratio and elevation. The surface shows the intercept results using 5 neighbours. The R-squared values are also shown for comparison. The intercept surface shows not only a high variability of data within small areas but also a large spread of values (minimum value is -6.69 and maximum is 3.59, the standard deviation is 0.7031). The mean value is 0.0307.

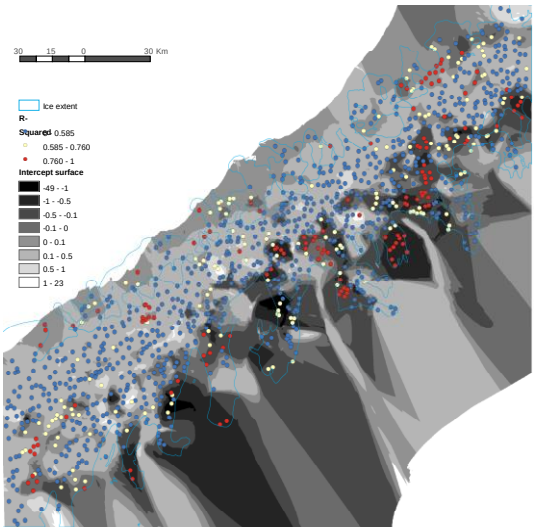

Figure 7.7 The same surface displayed in Fig 9 but using 10 neighbours in the GWR analysis. The variability of intercept values is smaller with the larger number of neighbours used in the GWR (Minimum value of -1.86, a maximum value of 1.47 and a standard deviation of 0.3170) The mean intercept value is 0.0499.

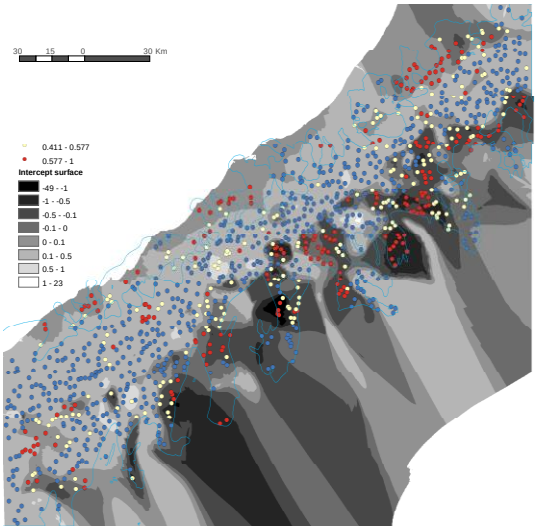

Figure 7.8 Data displayed as for Figure 7.6 but using 15 neighbours in GWR. The minimum intercept value is -1.65, with a maximum of 1.05 and a standard deviation of 0.2656. The mean is 0.0737. There is still high variability east of the divide.

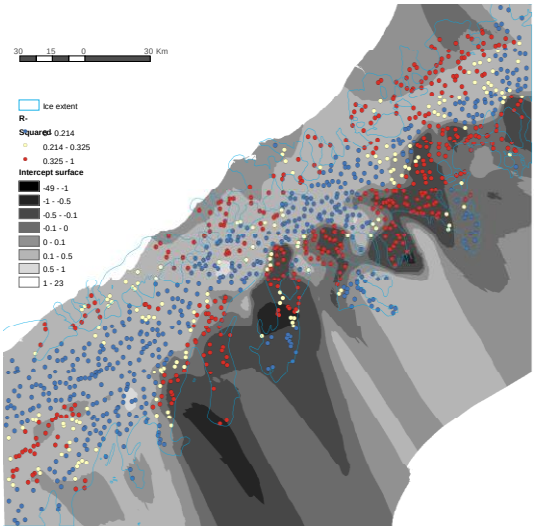

Figure 7.9 Intercept surface and R-squared data, as in Figure 7.6 but using 30 neighbours. The variability of the data is reduced to between trunk valley systems. The minimum intercept value is -0.79, the maximum is 0.64 and the standard deviation is 0.1999. The mean is 0.103.

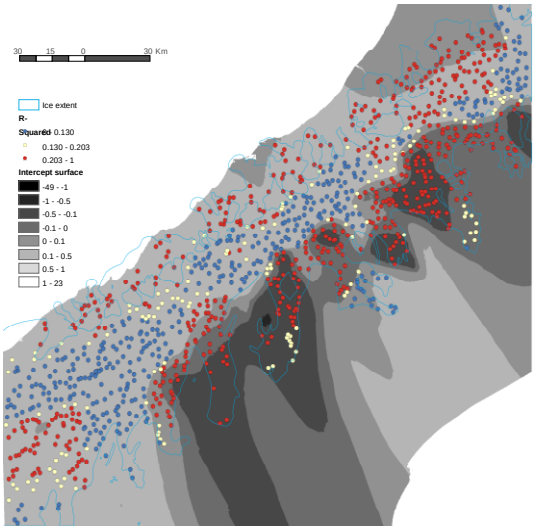

Figure 7.10 This figure displays the same data as in Figure 7.6 but using 50 neighbours in the GWR. Variability is greatly reduced (minimum intercept value of -0.39, a maximum of 0.47, a standard deviation of 0.1615 and a mean of 0.1192) especially at the divide and to the west whether much detail is lost.

7.2.2.3. Regression line slope coefficient sensitivity to kernel size

The second surface automatically produced by the GWR tool in ArcMap is the b coefficient surface, in this case the regression line slope coefficient for elevation. This surface indicates the slope of the regression line and is useful in identifying whether the relationship between variables is positive or negative and to what degree. Figure 7.11 to 7.15 show the elevation coefficient surfaces observed from form ratio and elevation relationship in the Southern Alps sample area using different kernel sizes. Comparisons between kernel size, again, show stability between 15 to 30 neighbours, with variability contained to the valley system level at 30 neighbours.

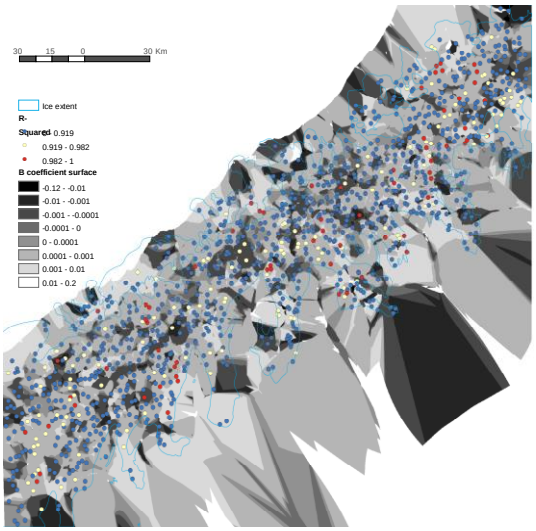

Figure 7.11 The elevation coefficient surface produced when mean elevation and form ratio are analysed in GWR. This figure shows the coefficient surface created when 5 neighbours are used. As in previous surfaces produced with only 5 neighbours high variability is evident (minimum value of -0.01, maximum of 0.01, standard deviation 0.0014 and a mean of 0.0005) which obscures any local trends.

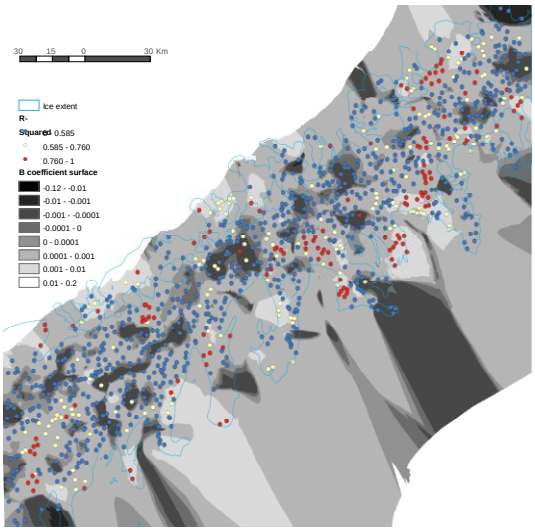

Figure 7.12 Displayed as for Figure 7.11 but using 10 neighbours in the GWR analysis. High variability is still evident (minimum value of -0.0029, maximum value of 0.0036, standard deviation of 0.000484 and a mean of 0.00036) and valley system level trends are still difficult to identify.

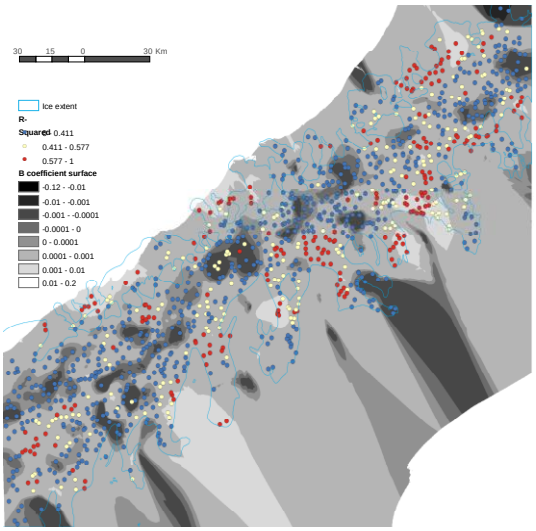

Figure 7.13 GWR results as for Figure 7.11 but using 15 neighbours in the analysis. Variability has reduced when compared to Figure 7.11 and 7.12 with a minimum value of -0.0012, a maximum of 0.0023, standard deviation of 0.000375 and a mean of 0.00032. There is, however, still sub valley system variability.

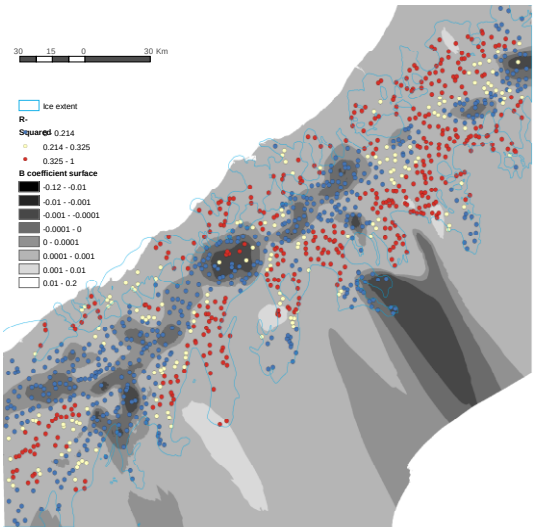

Figure 7.14 Intercept surface displayed as for Figure 7.11 but using 30 neighbours in GWR analysis. Variability at the divide is clear where there is a minimum of -0.000275, a maximum of 0.001296, a standard deviation of 0.000234 and a mean of 0.00025.

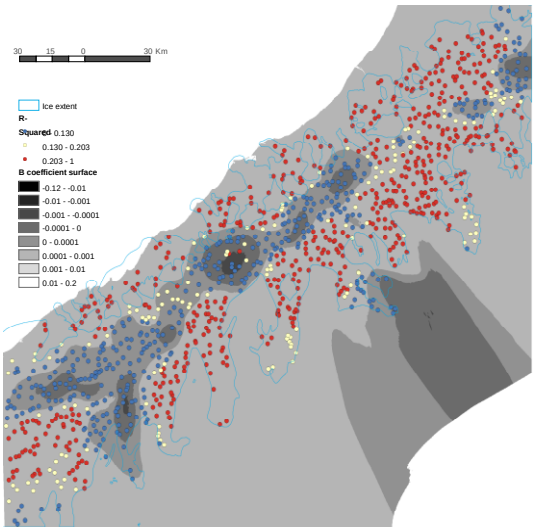

Figure 7.15 The same map as for Figure 7.11 but using 50 neighbours in the GWR analysis. Variability is greatly reduced (it has a minimum value of -0.00011, a maximum of 0.000912, a standard deviation of 0.000173 and a mean of 0.000216) and valley system detail is lost.

7.2.2.4 Conclusions of kernel size sensitivity tests

Results from the sensitivity analysis show that surfaces are relatively stable when different kernel sizes are applied, particularly between 15 and 30 neighbours, for the Southern Alps sample area. A larger kernel size gives more of a smoothing effect and it is suggested that a kernel size of 30 neighbours is able to show meaningful local variations whilst limiting noisy, high variance results, and allow analysis at the valley system level. Although the kernel size analysis was only carried out on the Southern Alps sample area it is, however, reasonable to expect that the same kernel size can be used on the other sample areas if valley segments have a similar density.

7.3. GWR application

Geographically Weighted Regression (GWR) has been widely used as a statistical technique in human geography applications (e.g. Brunsdon *et al.*, 1998) but less so in physical geography despite spatial variation in data being just as apparent. A notable exception is Brunsdon *et al*.'s (2001) paper on the spatial variations in the average rainfall-altitude relationship in Great Britain. Using GWR Brunsdon *et al*. (2001) found a clear non-stationary relationship between average annual rainfall and altitude in Great Britain which was hidden when the data was analysed as a simple global linear regression.

In this chapter GWR will be used in a similar way to the above but to reveal any spatial variation in the valley shape data. Whole mountain range regression models (Chapter 6) have shown some interesting results but in some cases relationships between variables could not be established, in spite of reasonable expectations that they should. GWR enables the mapping of local trends between variables which could help to understand the lack of global relationships by looking at the spatial variability of correlations. An additional feature of GWR is that the tool is able to compute multiple regressions where many explanatory variables (proxies) can be attributed to each dependent variable (*U-ness* measures). This is useful as in the whole mountain range analysis it was identified that a confounding problem of ice residence time and flux existed. The confounding problem has made it difficult to untangle the influence of each contributing factor (ice residence time and flux). In addition, several specific questions also arose from analysis in Chapter 6. These questions mainly related to local variability and therefore GWR should be a useful tool in tackling them. Results from GWR could further the understanding of the relationship between glaciology, landscape evolution, and the geomorphological finger-print left on landscapes in the present day.

Sample areas shown in the spatial analysis represent the patterns which occur in all sample areas unless otherwise stated. It is important to state that GWR is used here to answer questions which arose in whole mountain range analysis (Chapter 6) rather than explain the reason for each variability between each individual valley segment, which is beyond the aim of this thesis.

7.4. Spatial analysis of *U-ness* within mountain ranges

7.4.1. Does GWR analysis shed light on the ice flux-residence time confounding problem?

In Chapter 6 it was suspected that a confounding problem existed whereby ice residence time (which increases with elevation and decreases away from the divide) and flux (which increases with distance from the divide and at lower elevations) worked in opposition where valley shape and size is concerned. As GWR can compute multiple regressions a comparison can be made between results of single regression models and multiple regression models where both elevation and catchment area (proxies for ice residence time and flux) are used. If correlations are better when both proxies are considered in the regression model then it can be concluded that a confounding problem exists as the model has been improved.

Table 7.1 clearly shows that when multiple regression is undertaken using GWR many more valley segments are significant. This is compared to when regression analysis is carried out using elevation and catchment as explanatory variables separately. The conclusion drawn from this analysis is that a confounding problem does indeed occur and affects all *U-ness* measures. However, catchment area and elevation do not account for all the variability found in *U-ness* measures suggesting there are other factors that contribute to valley cross-sectional form variability.

It is also interesting to note that when comparing cross-sectional area and *b*-value correlations in single regression models (with the exception of *b*-value GWR results in the Southern Alps) there are more significantly-correlated valley segments with catchment area than for elevation (Table 7.1). Whilst for form ratio the opposite is true (with the exception of the South Patagonia), better correlation is achieved for form ratio and elevation. This may indicate that catchment area has more control on cross-sectional area and *b*-values but elevation has more control on form ratio.

Table 7.1 Analysis of the correlation of *U-ness* measures (cross-sectional area, form ratio and *b*-value) with proxies (elevation and catchment area) in regression models. Each *U-ness* measure is examined using single regression (elevation only and catchment area only) before multiple regression (both) is tackled, and the results compared. The table shows that, without exception, all sample areas improved correlation between *U-ness* measures and proxies when multiple regression is conducted using both elevation and catchment area as explanatory coefficients rather than separately.

Sample area	***Total number of glacial valley segments***	***Explanatory coefficients used in regression model***	***Number of valley segments with a significance level of 99% or better***		
			Cross-sectional area	***Form Ratio***	***b-value***
Pyrenees	*674*	*Elevation only*	*305*	*154*	*167*
		Catchment area only	*360*	*125*	*201*
		Both	*446*	*304*	*300*
North Patagonia	*1745*	*Elevation only*	*446*	*344*	*309*
		Catchment area only	*716*	*238*	*415*
		Both	*973*	*815*	*742*
Central Patagonia	*2606*	*Elevation only*	*500*	*469*	*468*
		Catchment area only	*750*	*269*	*659*
		Both	*1169*	*886*	*1069*
South Patagonia	*1866*	*Elevation only*	*819*	*639*	*805*
		Catchment area only	*975*	*782*	*1048*
		Both	*1619*	*1363*	*1592*
Southern Alps, New Zealand	*1114*	*Elevation only*	*162*	*598*	*432*
		Catchment area only	*445*	*469*	*378*
		Both	*603*	*898*	*676*

7.4.2. Investigating b-value variability

It was noted in Section 6.5.2 that *b*-values showed high variability, as well as evidence of little correlation with proxies when whole sample areas were analysed. Variability of *b*-values reduced when only glacial valley segments were taken into account, however no clear pattern emerged. It was hypothesised that *b*-values should be greatest at the highest elevations (where residence time is greatest) and for valley segments with the largest catchment areas (where ice flux is greatest). In this section it is investigated whether correlations between *b*-values and proxies occur on a local level using GWR.

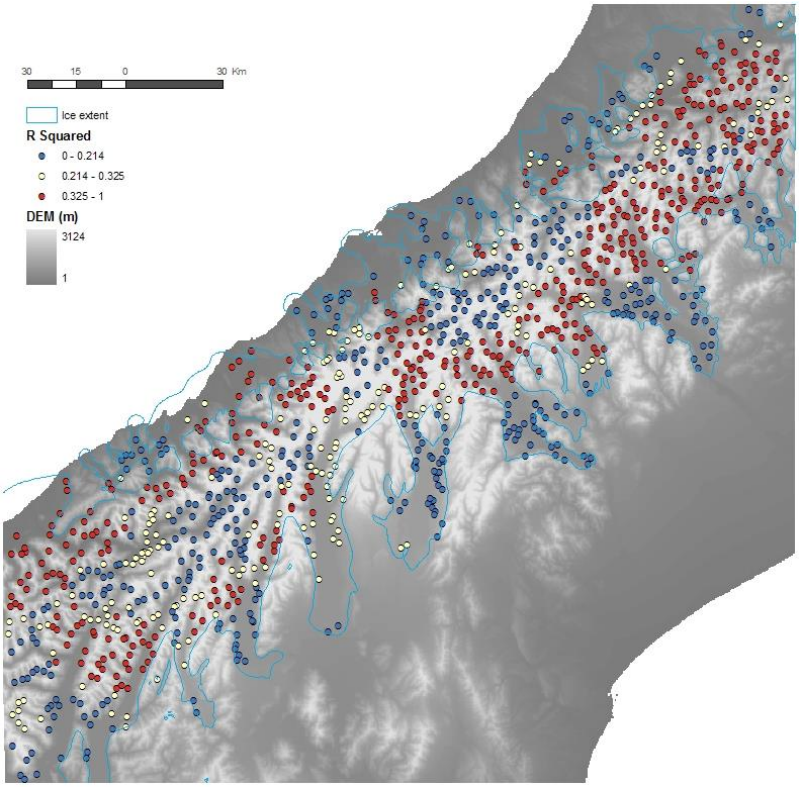

Figure 7.16 R-squared results for GWR multiple regression of *b*-values and proxies (elevation and catchment area) in the Southern Alps, New Zealand, using 30 valley segments in local regression analysis. Points signify the centre of each valley segment, red points are those valley segments which have a 99.9% significance level or better with the 30 closest valley segments. Yellow points are those valley segments with a significance level of between 99.9% and 99%, whilst blue points have a low local significance between (worse than 99%) *b*-values and proxies on a local basis (30 neighbours). It can be seen that the highest correlations (high R^2 values) are mid-way between the mountain divide and the LGM ice extent, whilst the worst are at the divide and near the limits of the LGM ice extent.

GWR analysis shows several interesting results. Firstly, it shows that that there are regions within the Southern Alps sample area where *b*-values are highly correlated with proxies, at a significance level of 99%, whilst other areas have poor correlations (Figure 7.16). Correlations appear to occur within valley systems, rather than between them, and poor correlations are found at the divide, where regression models would have used valley segment data from either side of the divide i.e. from different valley systems. This suggests that within valley systems correlation between *b*-values and proxies occurs but the regression model is not the same between valley systems.

Secondly, it can be seen in Figure 7.16 that the valley segments with the best correlations are found mid-way between the divide and the LGM ice limits, both in major trunk valleys as well as their tributary valleys. The lack of correlation at the divide has already been noted. The lack of local correlation near the LGM ice limit could have several explanations including the influence of variable sediment fill in the valley floor, an increased likelihood of fluvial modification and the fact that the defined ice limits (Suggate, 2004) could be incorrect in this region, in particular by excluding tributary valleys. The LGM limits, by their very nature, are likely to have had the least glacial modification. It has already been observed in Section 6.5.2 (Figure 6.15) that glacial valleys trend towards a distinct form whilst fluvial valleys have a greater spread of form and this could be reflected here by poor correlations.

When the correlations for *b*-values and individual proxies are investigated it is found that in areas where valley segments are significant (to the level of 99% or better) the relationship between elevation and *b*-value is negative whilst the correlation between catchment area and *b*-value is positive. It was hypothesised that *b*-values would become greater with ice residence time (increased elevation), as well as ice flux (increased contributing catchment area), even though these are conflicting. That a negative correlation is found for elevation whilst a positive correlation is found for catchment area suggests that ice flux is more important than ice residence time for forming valleys with large *b*-values in the Southern Alps sample area.

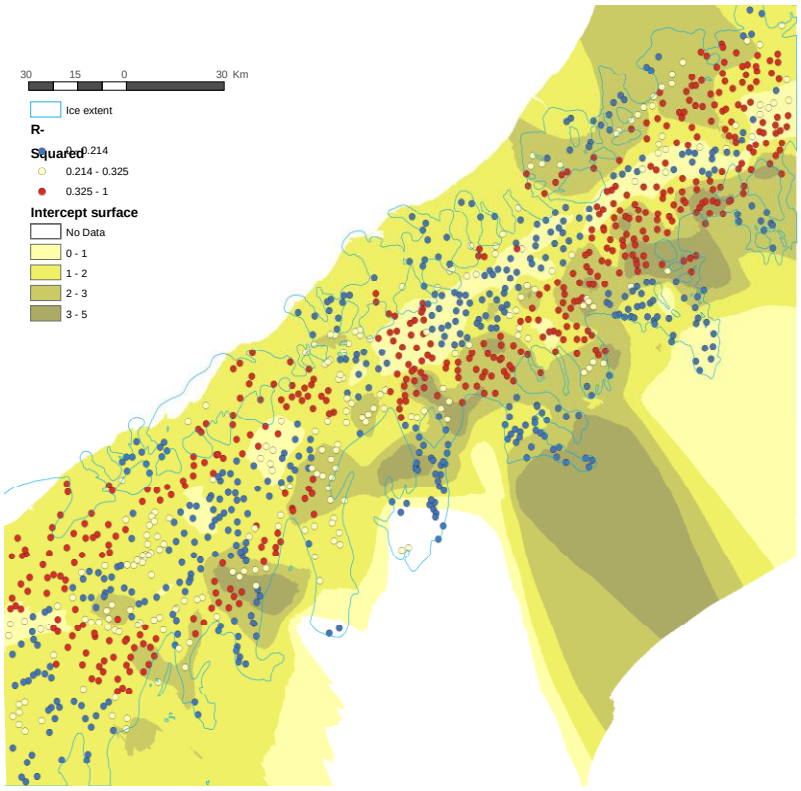

Figure 7.17 The intercept surface for local multiple regressions shows that the highest *b*-values are found mid-way between the divide and LGM ice extent particularly east of the divide. Low *b*-values are found at the divide and at some of the ice extent extremities. However, at the edges of the ice extent the correlation is poor (low R-squared values) and therefore these results cannot be relied upon.

The intercept surface (Figure 7.17) reveals that when catchment area and elevation are excluded (i.e. zero value), by using the local multiple regression models for each valley segment, high *b*-values are found either side of the divide, and low values at the divide itself, the highest *b*-values, however, are found to the east of the divide. This could be due to several factors including different lithology to the east, the gentler slopes, increased shading effects, as well as a different climate regime.

Predicted model (Figure 7.18) results show that high *b*-values are anticipated by the local multiple regression models, to be further away from the divide, towards the edges of the LGM limits, again indicating that ice flux is the more important factor in creating valleys with large *b*-values, rather than ice residence time. Low *b*-values are found at the divide and the highest *b*-values can be followed along the major trunk valleys where there would have been the greatest ice flux. The majority of valley segments are predicted to have *b*-values between 1 and 1.5.

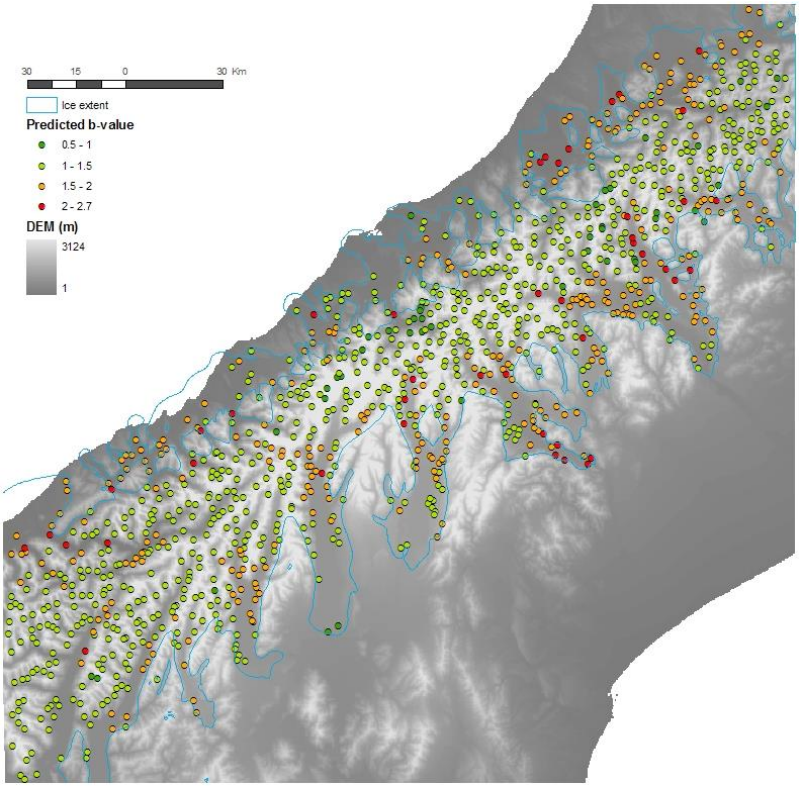

Figure 7.18 Using the GWR multiple regression models to predict where the highest *b*-values should be found when catchment area and elevation are taken into consideration, shows that the highest *b*-values predicted are in the main trunk valleys part way between the divide and the LGM ice extent, this could be where the average ELA lies. Small tributary valleys are predicted to have smaller *b*-values.

In conclusion, GWR shows that *b*-value variability exists between valley systems, but strong correlations can exist within valley systems, suggesting that where valleys are linked *b*-values and proxies have a relationship and thus explaining why an entire sample area analysis (Section 6.5.2.) did not show a relationship. Correlations were best mid-way between the divide and LGM ice extent. Here, especially in the east, the highest intercept values were found and when predicted *b*-values were investigated they were also found to be greatest in valley segments located in the major trunk valleys.

7.4.3. Is form ratio simply a consequence of available relief?

In whole sample area analysis it was found that form ratio had a strong relationship with elevation and it was suspected that this may have been due to the amount of available relief for erosion rather than anything glaciological. By comparing the GWR results for elevation and form ratio to those which included both elevation and catchment area it

can be seen whether catchment area also contributes to form ratio. If correlations are better for elevation and form ratio, than for both proxies and form ratio, then the conclusion can be drawn that high form ratios are merely a consequence of available relief. However, if correlations are better if ice flux (catchment area) is considered as well, then it can be concluded that it is also a factor in determining the form ratio.

Coefficient surfaces showed that, as for the whole sample area analysis, there is a positive correlation between elevation and form ratio (Figure 7.19), with the notable exception of valley segments at the divide. Catchment area, on the other hand, had a negative relationship with form ratio (Figure 7.20), indicating valley widening over deepening with increased catchment area. Whilst valleys with small catchment areas (mainly found at higher elevations close to the divide) have deep, relatively narrow valleys. Therefore, this indicates that high residence time valleys found at high elevations, generally with small catchment areas, have high form ratios (deep, narrow valleys) whilst valleys at lower elevations are more likely to have large contributing catchment areas (ice flux) and have wide, relatively shallow valleys.

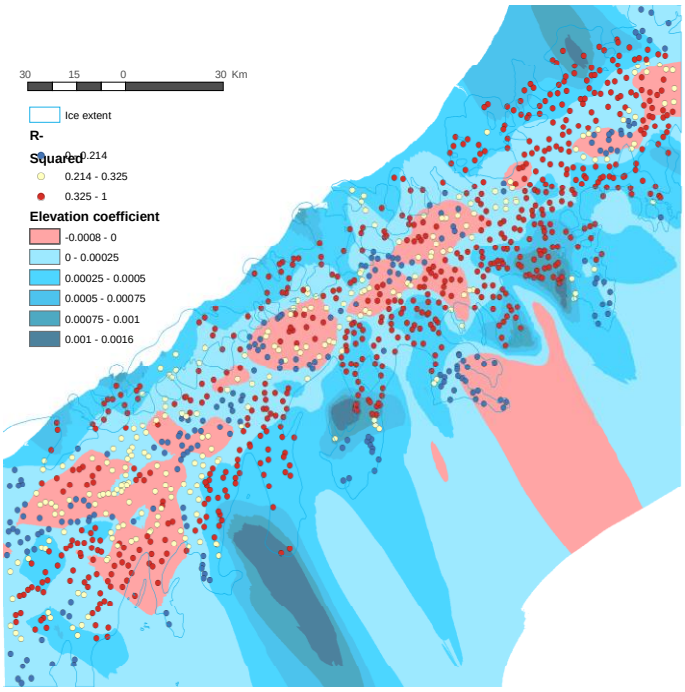

Figure 7.19 Regression line slope coefficient surface for the local (GWR) multiple regression correlation between form ratio and proxies. It shows that form ratio and elevation generally have a positive relationship which is strongest near the LGM ice extent limit, especially to the east of the divide but also in the northwest. Weak negative correlations are found at the divide. A small area of negative correlation is found at the ice extent east of the divide but this is not reliable as the R-squared values in this area have poor significance. Reds are negative and blues are positive correlation.

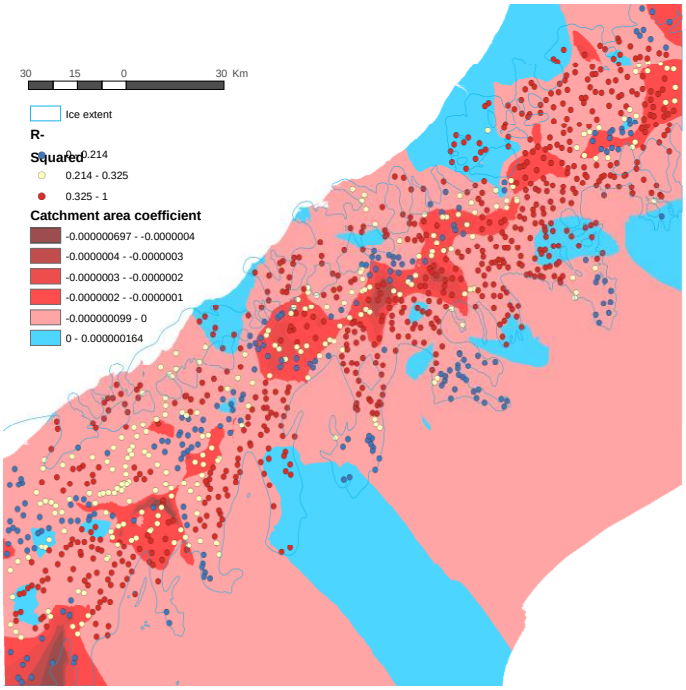

Figure 7.20 Local correlation between form ratio and catchment area are, on the other hand, the opposite of that of elevation (Figure 7.19) in that they are mainly negative (red) with the strongest negative correlations being at the divide.

Local correlations showed that 598 out of the 1114 glacial valley segments had a significance level of 99% or better when GWR results were computed for elevation and form ratio (Figure 7.21). However, when catchment area was also used in the GWR analysis the amount of valley segments which showed a 99% or better significance rose to 898 (Figure 7.22). This suggests that elevation, and in particular available relief, is not the sole control on form ratio, catchment area also influences the form ratio of a valley. This also supports the conclusions drawn from the elevation and catchment area coefficient surfaces discussed previously, whereby valleys with larger catchment areas (which are found at lower elevations) have wider and relatively shallower valleys which result in lower form ratios.

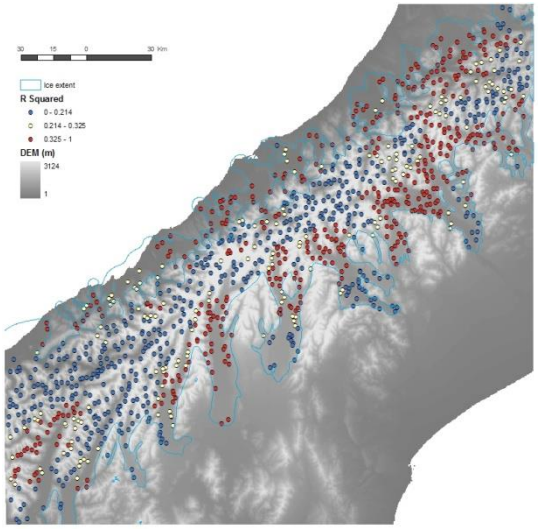

Figure 7.21 There are 598 valley segments out of a total of 1114 which have an R-squared value of 99% or better when GWR is undertaken for form ratio and elevation only.

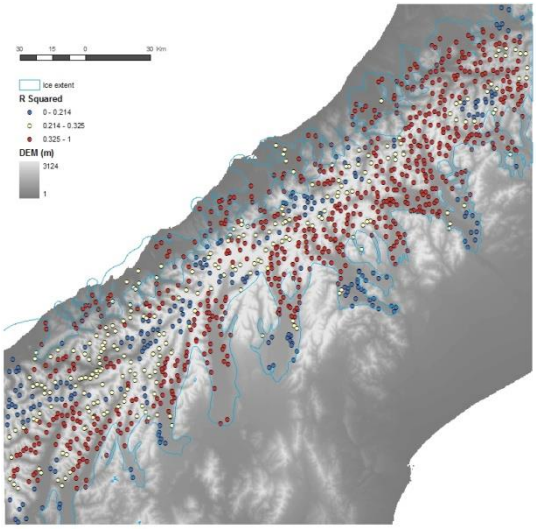

Figure 7.22 When GWR multiple regression is undertaken for form ratio and both proxies (elevation and catchment area) many more valley segments have a significant (at 99% and better) for local regression. Over three quarters of all valleys (898 out of 1114) become significant.

The intercept surface for elevation and catchment area (Figure 7.23) shows model-predicted form ratios to be high near the divide, and to the west, and lower to the east. As the intercept surface disregards the influence of catchment area, the greater LGM ice extent to the east and therefore the greater potential for valleys to have larger

contributing catchment areas cannot be attributed to the larger form ratios. Instead, other factors must influence this difference east and west of the divide.

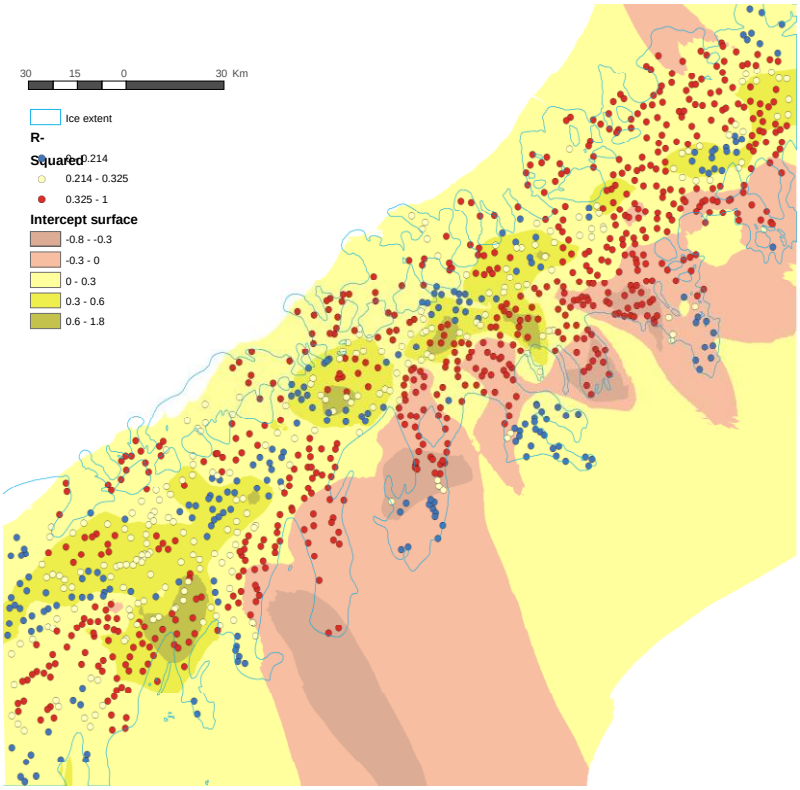

Figure 7.23 The intercept surface for the GWR multiple regression analysis for form ratio and both ice proxies showing high form ratio values close to the divide which decrease with distance away from the divide. Negative values are found towards the LGM ice extent in the east. Negative values occur as it is unrealistic to have zero catchment area and therefore regression model produces negative values in the areas with the highest contributing catchment areas. It is, however, still a valid and useful result demonstrating that here form ratios become very low as widening occurs over deepening.

The relationship between catchment area and form ratio was explored further. As the measure of form ratio is the relationship between width and depth these measures were explored separately. In the Southern Alps no clear relationship could be seen for whole sample area analysis so analysis was undertaken for the valley segments which showed significant local regression relationships. When this was carried out for valley segments with small catchment areas a positive relationship emerged between width and catchment area (Figure 7.24) although the relationship for depth is not clear. However, when valley segments from larger catchments are analysed a positive relationship is evident for width and catchment area (Figure 7.25) but a negative relationship emerges between depth and catchment area (Figure 7.26).

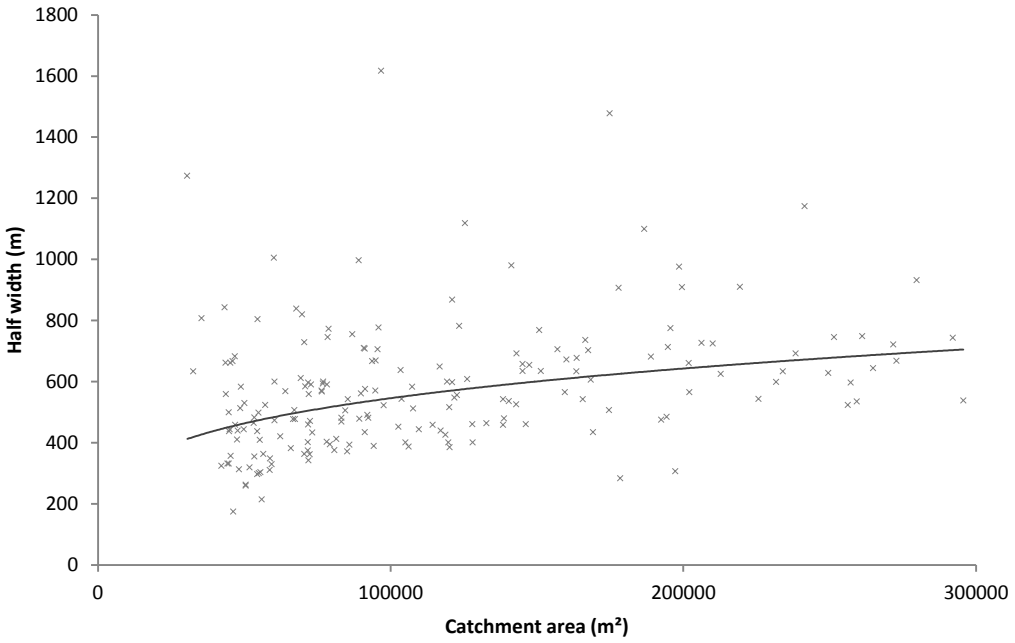

Figure 7.24 Small catchment areas (less than 300,000) in the Southern Alps, New Zealand which have a significant local relationship between form ratio and catchment in GWR analysis (to the 99.9% level or better). Graph shows that half width has a positive correlation with catchment and a power line of best fit with an R-squared of 0.1431, which for the 189 valley segments has a high significance.

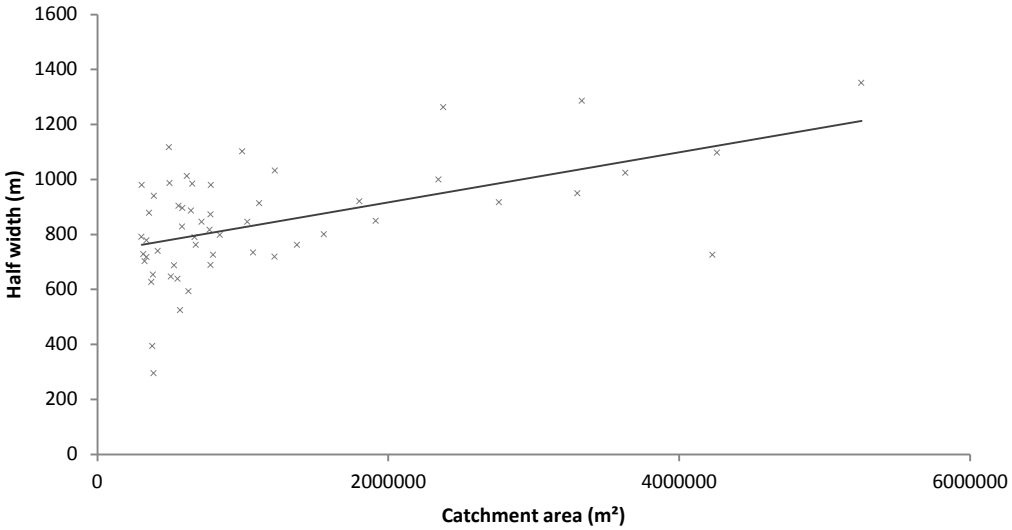

Figure 7.25 Taking the significant (at the 99.9% level and better) valley segments in the Southern Alps sample area for GWR analysis of form ratio and catchment area with large catchment areas (greater than 300,000) width is seen to increase with catchment area (R-squared is 0.2855).

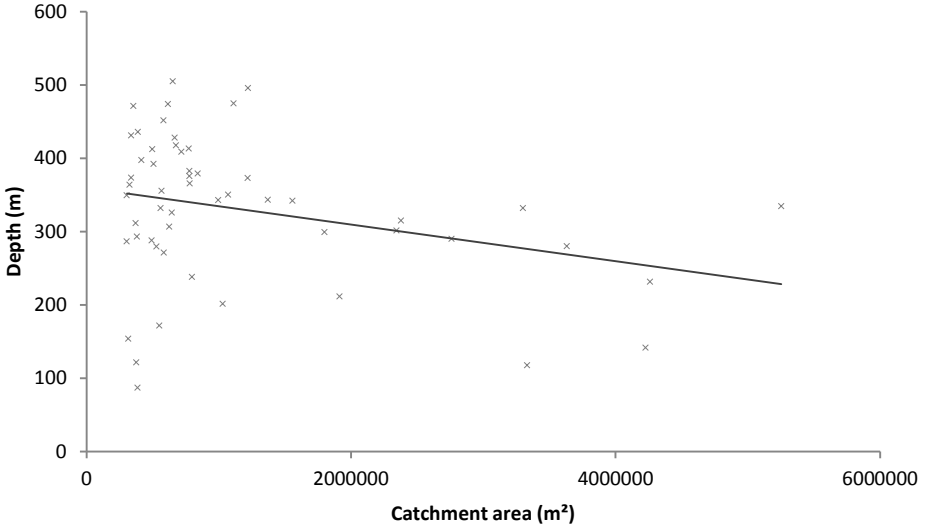

Figure 7.26 With the same valley segments as for Figure 7.25 it is seen that depth decreases with catchment area. The R-squared value for the line of best fit is lower than for the width correlation with catchment area at 0.0864.

Width and depth relationship to catchment area was analysed for the entire Pyrenees dataset within LGM limits. Here, despite local variation, the same pattern emerged as with the significant Southern Alps valley segments. For the Pyrenees analysis the dataset

was divided into first order valleys (small catchment areas) and second order and greater valleys (larger catchment areas). Here the first order valleys show a strongly positive relationship between both width and depth, and catchment area (Figure 7.27 and 7.28), whilst the second order and greater valleys show positive relationship between width and catchment area (Figure 7.27) but a negative relationship between valley depth and catchment area (Figure 7.28).

(a)

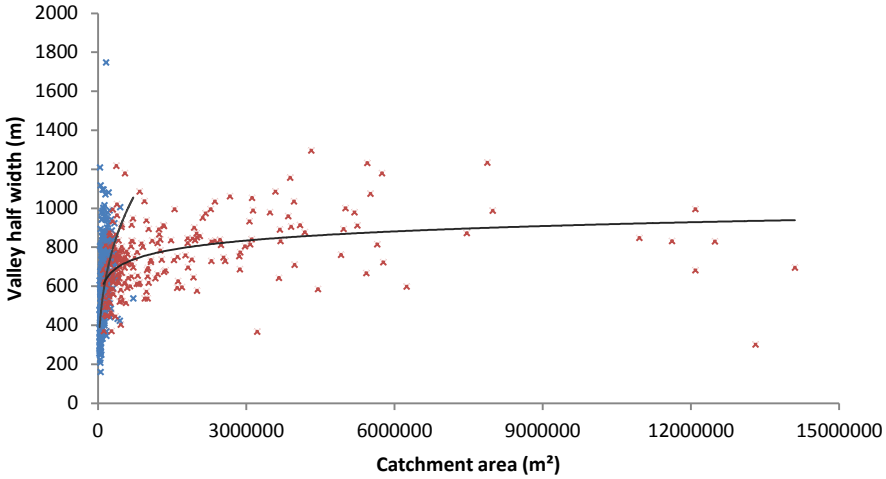

(b)

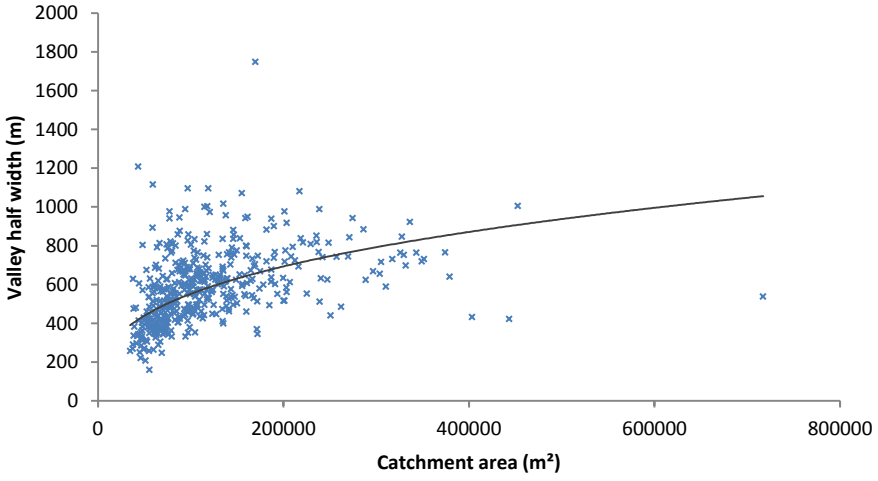

Figure 7.27 When analysing the entire glacial valley segments in the Pyrenees it can be seen (b) that correlation for the half width and catchment areas is positive for first order (blue) valley segments (R-squared value of 0.2797 for a power correlation, which for the 454 valley segments is significant beyond the 99.9% level) which have small catchment areas, whilst (a) second order and above (red) valley segments have a weaker but still positive correlation (R-squared value of 0.2008 for a logarithmic correlation, which for the 220 valley segments is significant beyond the 99.9% level).

(a)

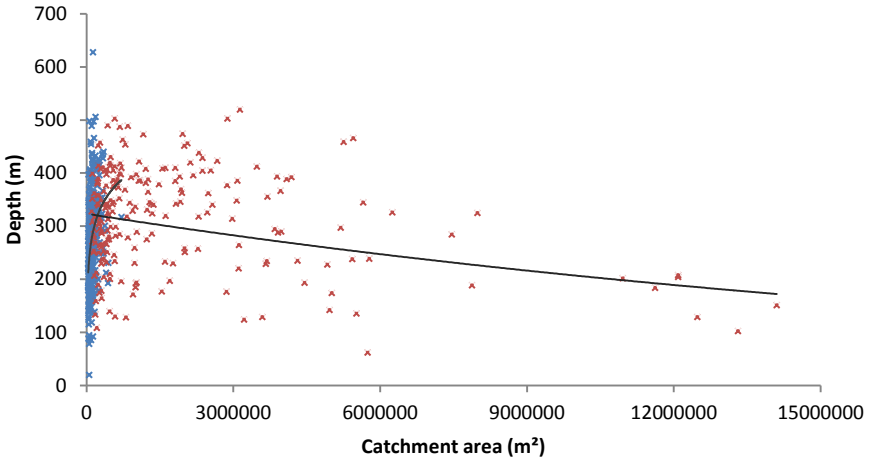

(b)

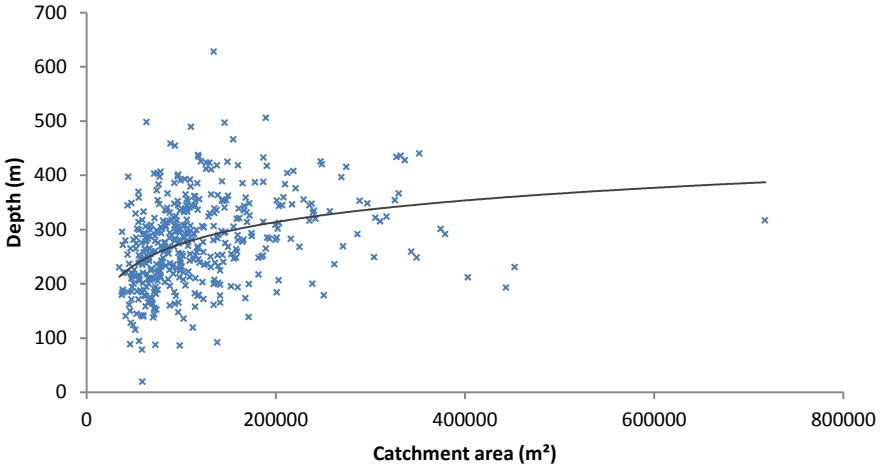

Figure 7.28 In the Pyrenees the first order (blue) valley segments relationship between depth and catchment area is similar to that of width and catchment area (b), i.e. there is a strong positive correlation (R-squared value of 0.1368 for a logarithmic correlation, which for the 454 valley segments is significant to the 99.9% level and better). However, with the second order and higher (red) valley segments (a) there is a definite negative correlation between depth and catchment area (R-squared value of 0.1019 for a exponential correlation, which for the 220 valley segments is significant to the 99.9% level and better).

7.4.4. Influence of valley floor slope on U-ness

There appears to be two types of glacial valley; the Rocky Mountain and Patagonia-Antarctica models, first recognised by Hirano and Aniya (1988), and identified in this research. The cross-sectional shape and proportions of glacial valleys is hypothesised to follow different evolutionary paths to maturity, where Rocky Mountain type valleys develop as narrow, deep valleys with increased maturity (and associated *b*-value) whilst Patagonia-Antarctica valleys become wider and relatively shallower with increased glaciation. Together with cross-sectional evolution of glacial valleys Montgomery (2002) found a longitudinal evolution of glacial valleys which was distinct from fluvial valleys. Glacial valleys were found to flatten their longitudinal profiles with maturity. It is therefore interesting to investigate whether down-valley floor slope can indicate valley maturity and can be linked to the cross-sectional evolution of valleys.

Mountain ranges such as the Southern Alps, New Zealand are strongly asymmetric with steep slopes to the west and gentle slopes east of the divide. It is suspected that valley floor slope could influence *U-ness* measures and this may be due to different glacial erosional processes responses to different valley floor slope angles. The influence of slope is investigated using GWR in the Southern Alps.

Valley floor slope for each valley segment was simply measured by finding the maximum and minimum valley floor elevation. This was done using the defined stream network within each valley segment, as it was given that the stream network defined the valley floor. In addition the length of the stream network within each valley segment was also found. With these three measurements the average valley floor slope for each valley segment was calculated.

When comparing individual regression models the GWR results (Table 7.2) show that slope has more significant valley segments (at the 99% level and better) when correlated with form ratio than either elevation or catchment area. For the *U-ness* measure of cross-sectional area correlations with slope provided more significant valley segments than for the proxy elevation but less than with the catchment area proxy, whilst *b*-values and slope had slightly fewer significant valley segments than for elevation or catchment area. When slope was included in local multiple regression models the number of significant valley segments increased suggesting that it is one of the variables which contributes to valley cross-section variability.

Table 7.2 showing the number of significant (at the 99% level) valley segments when *U-ness* measures and proxies are analysed as well as valley floor slope.

Sample area	**Total number of LGM valley segments**	**Explanatory variables used in regression model**	**Number of valley segments with a significance level of 99% or better**		
			Cross-sectional area	**Form Ratio**	***b*-value**
Southern Alps, New Zealand	1114	Elevation only	162	598	432
		Catchment area only	445	469	378
		Slope only	321	711	304
		Elevation and catchment area	603	898	676
		Elevation, catchment area and slope	781	1053	801

Coefficient surfaces show strong positive correlation between form ratio and slope whilst *b*-values and cross-sectional area have negative correlations. Interesting local trends are revealed in the intercept surfaces for *b*-values and form ratios when related to all proxies including slope. The Southern Alps is a strongly asymmetric mountain range, it is therefore assumed that when slope is introduced into the multiple regression, if no other factors influence *U-ness,* then intercept values will be the same across the mountain range. Results show a large variability of intercept *b*-values, the largest values still being found to the east (Figure 7.29), suggesting that other factors apart from slope, catchment area and elevation contribute to the large *b*-values found in this location. The intercept surface for the multiple regression of proxies, including slope, and form ratio (Figure 7.30) shows that small form ratios are still found to the east of the divide whilst large form ratios are found in the most mountainous regions.

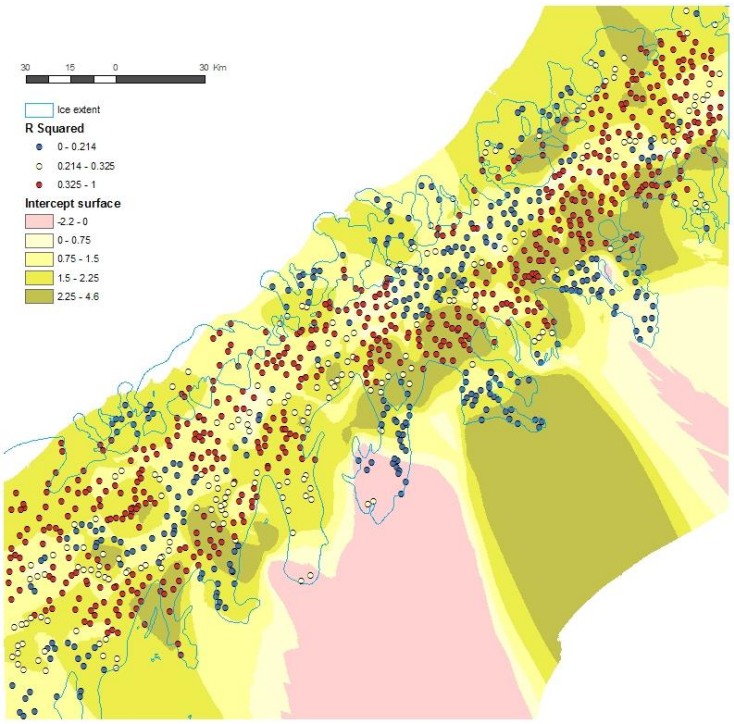

Figure 7.29 The intercept surface for local multiple regression models of catchment area, elevation and slope with *b*-values showing that after these explanatory variables have been taken into consideration *b*-values are still largest to the east of the mountain divide.

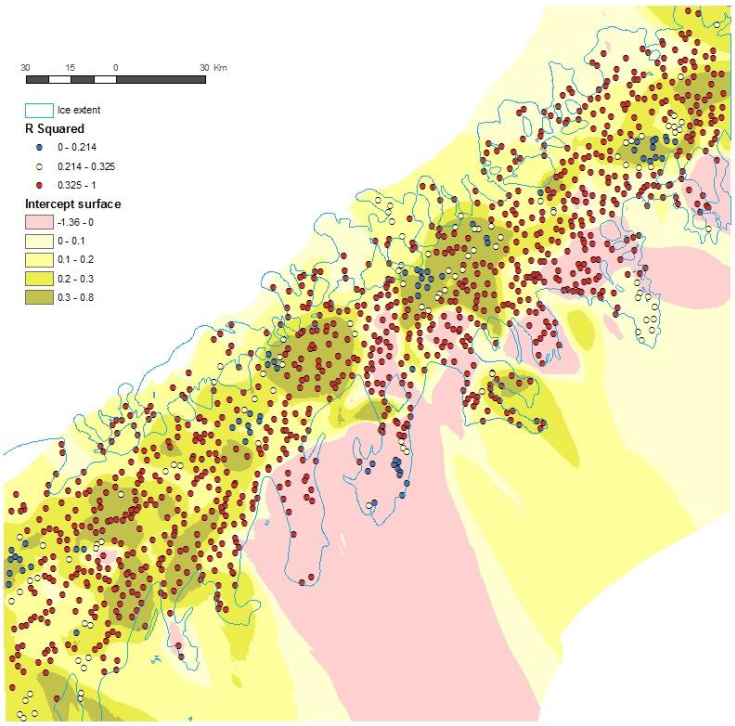

Figure 7.30 The intercept form ratio surface for local multiple regression models produced using all proxies, including valley floor slope, showing high form ratios around the mountain divide and the smallest form ratios to the east. Notice the very high amount of significant valley segments (above the 99.9% level shown as red points).

In conclusion, slope has also been found to be a factor in shaping glacial valley cross-section, especially with the *U-ness* measure of form ratio. This research shows that where mountain ranges are asymmetric, such as the Southern Alps, it is important to take slope into account when considering valley cross-sectional shape and size. However, catchment area, elevation and slope cannot fully explain *U-ness* variability.

7.4.5. Does climate explain variability?

In the whole sample area analysis in Section 6.5.4 there was some evidence that climate influenced the relationship between *U-ness* measures and proxies. When investigating *U-ness* measures with GWR analysis some interesting trends appear. These show a different response in *U-ness* between different climatic settings.

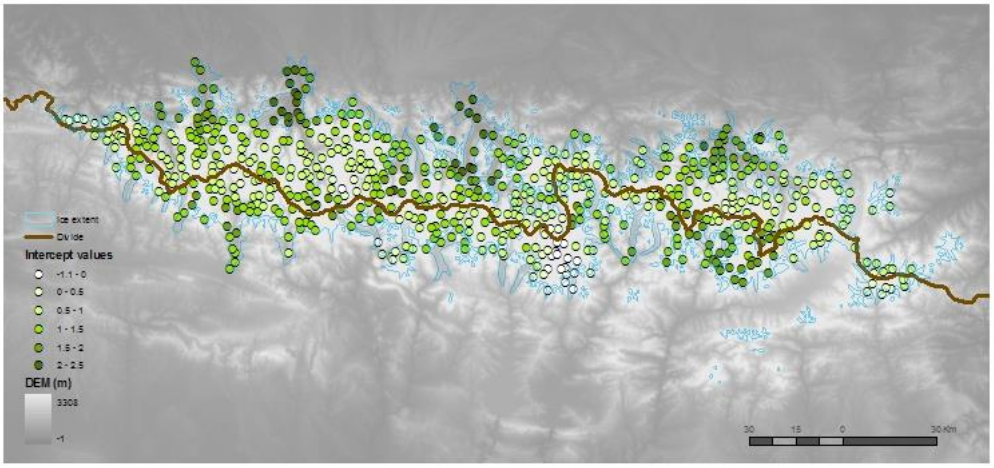

Figure 7.31 Intercept values for the multiple regression models of the Pyrenees show larger *b*-values north of the divide, in the trunk valleys and towards the LGM ice limit.

It can be seen from the LGM ice extent (Figure 7.31) that the northern region of the Pyrenees is more favourable for glacial conditions. This is evident by the fact that the ice limit is further away from the divide, indicating greater ice mass on the northern side of the range. However it is interesting to see whether this is reflected in *U-ness* measures. GWR analysis is a useful tool as the intercept surface can discount the influences of residence time (elevation) and ice flux (catchment area), and show the results of the local regression model for *U-ness* measures. The relationship between *b*-values and proxies was investigated (Figure 7.31) and showed that the highest *b*-values occurred towards the periphery of the LGM ice extent, whether the valley segments are north or

south. However, results show that north of the divide the greatest intercept *b*-values occur and in addition to this high intercept *b*-values are more widespread. This result contributes more evidence for climate influencing matters of glacial geomorphology (discussed further in Chapter 8).

7.4.6. Is cross-sectional area the best descriptor of U-ness?

In whole area analysis cross-sectional area was found to be the *U-ness* measure which was the most consistent with the hypotheses. Cross-sectional area is different from the other *U-ness* measures in that it is not a measure of shape but of size. In Section 6.5.2 and 6.5.3 cross-sectional area showed some interesting results with regard to ice flux and residence time proxies. It was thought then that cross-sectional area may reflect the confounding problem between proxies, even at an entire sample area scale, best when compared to other measures of *U-ness*. It is important to investigate whether this is also found locally with GWR analysis. As GWR is a technique which can tackle the confounding problem using multiple regression analysis it can take into account both proxies when analysing *U-ness* measures.

To assess which is the best descriptor of *U-ness*, when using the *mean valley profile method*, the GWR results for each *U-ness* measure were compiled and compared. The *U-ness* measure which has the greatest number of significantly correlated (better than 99% level) valley segments with proxies can be concluded to be the best *U-ness* measure for describing the valley development. GWR results (Table 7.3) show that, almost exclusively, cross-sectional area has the greatest number of significant valley segments, when compared to form ratio and *b*-value. This is with the exception of the Southern Alps, which may be a result of very large, wide, trunk valleys, which are altered by sedimentary fills, interfering with correlations.

Table 7.3 Each sample area showing the number of significant (to the 99% level) valley segments for each *U-ness* measure when multiple regression (with the proxies catchment area and elevation) is undertaken with GWR. It shows that valley segments have highest correlations for cross-sectional area with exception of the Southern Alps, New Zealand where form ratio has the best correlation.

Sample area	**Total number of LGM valley segments**	**Number of valley segments with a significance level of 99% or better**		
		Cross-sectional area	**Form Ratio**	***b*-value**
Pyrenees	674	446	304	300
North Patagonia	1745	973	815	742
Central Patagonia	2606	1169	886	1069
South Patagonia	1866	1619	1363	1592
Southern Alps	1114	603	898	676

Despite the summary of GWR results (Table 7.3) showing clear results concerning cross-sectional area and the confounding problem when GWR results are examined spatially the picture is less clear. When the GWR coefficient surfaces are mapped, for example, it is difficult to identify meaningful spatial patterns; surfaces appear to show high variability within mountain ranges. The only consistent result both within and across sample areas is that cross-sectional area has a positive correlation with catchment area (Figure 7.32).

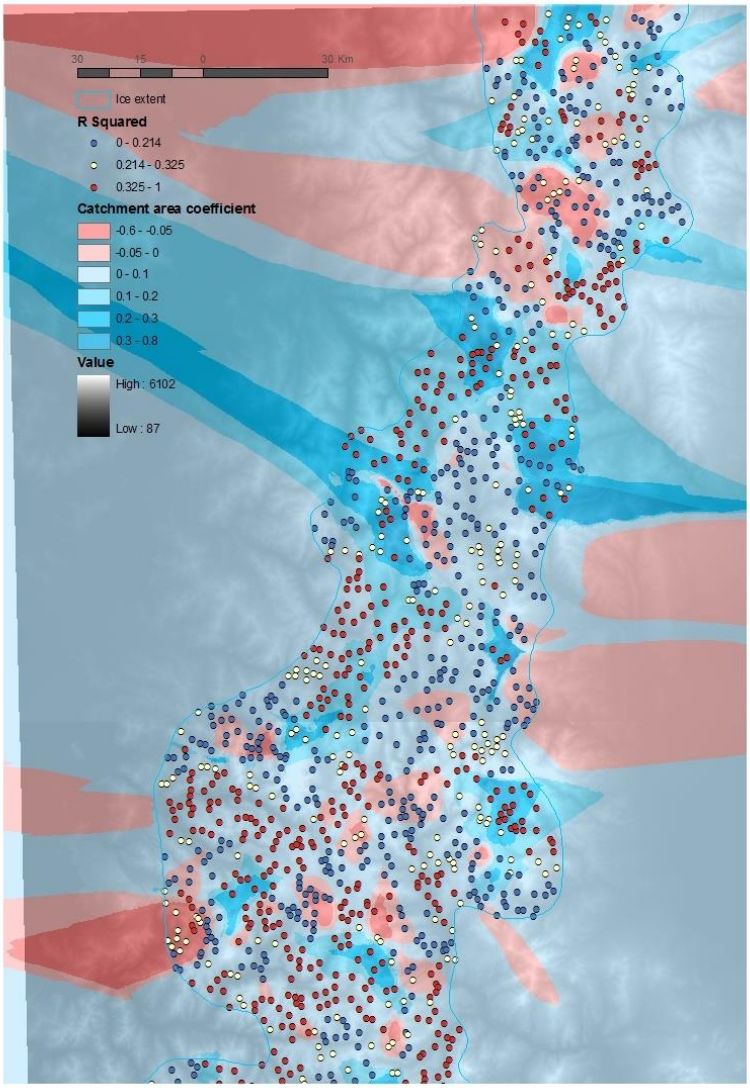

Figure 7.32 The catchment area coefficient surface for the GWR results for cross-sectional area in north Patagonia. It shows that the local relationships between cross-sectional area and catchment area are almost exclusively positive.

7.5. Summary

GWR provides not only regression models which allow for examination of spatial variability but also permits multiple regression analysis. By understanding how regression relationships vary in space, insight has been gained with regard to the impact of ice residence time and flux, as well as tectonics and climate, on valley cross-section shape and size and from which valley development can be inferred. GWR analysis in this

chapter increased understanding of the relationship between *U-ness* measures and proxies. The main conclusions for this can be summarised as;

1. GWR analysis confirms that the confounding problem between catchment area (proxy for ice flux) and elevation (proxy for residence time) does exist and that they appear to combine yielding enhanced *U-ness* measures mid-way along trunk valleys.
2. When valley floor slope is also taken into account the multiple regression models for all *U-ness* measures are further improved, implying that slope is also a factor in valley shaping.
3. Local regression models are best within valley systems rather than between them and across the mountain divides.
4. As expected, *b*-values were predicted by the model to be greatest along the major trunk valleys where there is the potential for the greatest ice flux.
5. Form ratios, on the other hand, decreased with increased catchment area and this was attributed to widening over deepening in these valleys. Infill may also play a part.
6. Although cross-sectional area showed the greatest correlation with proxies in the local multiple regression analysis, coefficient surfaces did not show clear patterns.
7. Conversely, *b*-values and form ratio coefficient surfaces appeared to be influenced by variation in climate.

By developing this sort of knowledge of valley cross-sections and their spatial variability, spatial scenarios can be used to infer temporal scenarios (Kirkbride & Matthews, 1997). Therefore, not only can valley cross-sections seen today be used to test numerical model outputs, they can also enlighten modellers regarding the development of valleys and consequently the evolution of valley form. This could prove useful for both landscape evolution models, as well as process knowledge understanding.

8. Discussion of valley cross-section results

8.1. Introduction

This chapter examines the results presented in Chapters 6 and 7 in relation to the literature. It begins by looking at how successful the mean valley method was compared to other methods used in valley cross-section analysis and includes the spatial techniques used in this thesis. An overview of the results are summarised before the results from each *U-ness* measure (form ratio, *b*-value and cross-sectional area) are discussed with reference to previous literature. The influence of the degree of glaciation, climate, lithology and tectonics on *U-ness* measures is examined. Lastly, valley evolution is considered, firstly by looking at the results from *b*-value/form ratio relationships before relating findings to process knowledge, valley scale evolution and, finally, landscape evolution models.

The success of the method

Developments in GIS and the advent of freely available DEMs have provided an opportunity in geomorphology to investigate large areas and generate considerable volumes of data. More than ever the raw data needed for examining landscape shape is now available, however, beyond mapping where features occur, glacial geomorphologists have been slow to use the full capacity of GIS software in landform analysis as noted by Napieralski *et al.* (2007). The mean valley cross-section method, developed in this thesis, goes some way to redressing this and enabling a step forward in valley cross-section development and understanding.

The mean valley cross-sectional method was used on five large sample areas, three in the Patagonian, Southern Andes, as well as the Southern Alps of New Zealand and the Pyrenees. The method was able to compute all valleys in small mountain ranges, such as the Pyrenees, large sample areas which crossed mountain divides, as in the case of the Southern Alps, New Zealand and the Patagonian sample areas. A total of 21,412 average valley segment profiles were produced, 8005 of which were within LGM ice extent limits. This number of average profiles was estimated to be the equivalent of 857,781

individually selected transects (334,086 within the LGM limits) and is compared to the 696 individually selected profiles analysed in all the previous literature.

As demonstrated above, the mean valley profile method can generate results for many more profiles than the individually selected transect method, allowing researchers to analyse valleys over large areas. There are, however, several other advantages to using the mean valley method over traditional methods. Firstly, it eliminates ambiguity of the position of transects with both the transect location and the orientation at which the transect crosses the valley. Secondly, it enables the entire valley segment cross-sectional shape to be taken into account, rather than just showing a snapshot, which the individually selected transect method is only capable of doing. Finally, it allows consistency in selecting the extent to which the profile spans the valley (i.e. the valley width).

The literature with results from individually selected transects inadequately discusses the influence of using different transect extents on measures of valley shape and size. In some investigations the transect spans the valley from ridge top to ridge top (Montgomery, 2002), whilst others use the trimline to delineate the transect extent (Graf, 1970; Pattyn & Decleir, 1995; Li *et al.*, 2001b). Tests showed that this influenced values traditionally used for describing valley shape (form ratio and *b*-values) and thus is not an inconsequential detail. An investigation into the extent to which mean valley profiles span valley segments showed that using the bottom half of the valley was most appropriate, as this part of the valley has had the most glacial modification. The mean valley profile method allows the lower half of the valley to be easily selected for investigation, as the sampling framework divides the valley into percentages of the total valley depth.

Apart from the lower half of the valley being selected to be measured, another conscious adaptation of the method to gain more useful results was to divide valley segments at tributaries and find the mean valley shape and size for each for these segments (Section 4.5.4). There is a good reason for selecting valley segments in this way, instead of simply selecting them at equal intervals along the valley. This is because at tributaries ice flux is increased, impacting on the erosional power of the glacier at this point. Overdeepenings at tributaries where convergent flow occurs are well documented (i.e. Shoemaker, 1986) where the sudden change in ice flux is reflected in the geomorphology of the valley. Jamieson *et al.* (2008) suggests that overdeepenings in

ice sheets may aid the stabilisation of the thermal regime and are therefore key to ice flow. It follows that dividing valleys at tributaries is logical when examining valley shape and size. Therefore within each segment the ice flux is likely to be more constant. This is important as the mean shape and size is being found for each segment and segments then compared. If segments had hugely differing ice fluxes within them then this could skew the resultant mean shape and size and be unrepresentative.

The power-law has been widely used to define valley shape and estimate the extent of glacial modification from a fluvial valley (Svensson, 1959). However, several limitations of the power-law have been identified. Firstly, the fact that the power-law only fits the power-curve to each side of the valley individually (Wheeler, 1984; Harbor, 1992) and secondly, when logarithmic transformation is used there is a bias to points closest to the valley centre (Harbor, 1992). The mean valley profile method circumvents these problems by creating a mean profile which encompasses both sides of the valley to create a single mean half-valley profile to which the power-curve can be fitted. The advantage of doing this, and not using the quadratic equation, which was the suggested solution by Harbor and Wheeler (1992), is that the variables in the quadratic equation are more difficult to interpret and could not be compared to other results in the literature, as the power-law curve is most widely used. In response to the problem with logarithmic transformation, by only using the bottom half of the valley, the focus for measurement is on the most glacially eroded part of the valley. In addition, the power-curve is fitted directly to the profile and no logarithmic transformation is used.

In addition to the limitations of the power-law detailed above the literature also questioned whether the power-law (Pattyn & Van Huele, 1998) is in fact an appropriate measure at all in defining valley shape. The use of an alternative power-law, the General Power-Law (GPL), suggested by Pattyn and Van Huele (1998), was investigated for use with the mean valley profiles. The GPL was designed to allow the power-curve to be extrapolated below the original valley floor to compensate for valley modification such as fill. The conclusion of using the GPL with the mean valley profile was that it had little effect on the power-curve; this was partly due to the mean profile having already smoothed out valley profile inconsistencies (another advantage of this method) but also that the GPL does not significantly adapt the power-law to allow for glacial fill. Therefore the original power-law (Svensson, 1959) was used in interpreting the valley shape of mean valley profiles.

Phillips (2009) conceived the major concepts behind the mean valley cross-sectional method used in this thesis. In particular the process used to create the sampling framework, which involves de-trending of valleys and allows a systematic sampling technique of valleys with different scales, was a critical aspect. The research in this thesis develops this method further, making it more user friendly and enabling it to handle much larger geographical areas (i.e. whole mountain ranges). The mean valley cross-sectional method is now fully integrated into ArcGIS. The method can now produce measurements for individual valley segments, rather than only valley measurements within a defined area (25 km by 25 km in the case of Phillips' (2009) research) or when valleys are defined by stream order. In addition to this, the problem of valley heads is also tackled. If valley heads are included in analysis they can interfere with the mean valley cross-section result, as valley heads are a separate feature to the valley sides, having undergone different glacial processes. Therefore a GIS technique was developed to eliminate valley heads from the valley segments used to create mean valley profiles.

The mean valley profile method has provided consistent data for comparing sample areas, for example when examining how *U-ness* changed with latitude. In Section 6.5.1, (a proxy for intensity of glacial erosion) the results showed that generally all measures increased with latitude. When whole area analysis was undertaken, exploring relationships between *U-ness* measures and proxies, some interesting results emerged. Sometimes, when *U-ness* measures associated with individual valley segments were plotted in their location within a mountain range, patterns were initially difficult to understand. However, once Geographically Weighted Regression (GWR) analysis was performed, and where local regression relationships were established, the picture became clearer and regression relationships became evident.

Local multiple regression analysis was carried out using GWR, a newly available tool in ArcGIS. Although widely used in social sciences (i.e. Brunsdon *et al.*, 1998), the potential for GWR has not been realised in geomorphology. This research uses GWR to understand spatial relationships and valley cross-sectional shape evolution.

8.3. Overview of valley cross-section results

Multiple regression analysis showed that when both elevation (proxy for ice residence time) and catchment area (proxy for ice flux) were included in the model for *U-ness* measures it was improved. This, together with the fact that the model predicts the largest *U-ness* measures part-way down trunk valleys (Figure 8.1), confirms that ice residence time and flux work against each other and is consistent with the literature, which states that ice thickness and velocity is generally greatest at the ELA (McCall, 1960) and this is where the greatest erosion occurs. By extension, over several glacial cycles, the point in the valley where the average ELA has occurred should be indicated through landform shape by having the greatest *U-ness* measures. This will always be the case in all but the most exceptional circumstances as glacial landscapes have nearly always been subjected to more than one glacial cycle. The analysis presented here provides a strong demonstration that a signal of average ELA position can be found in the landscape.

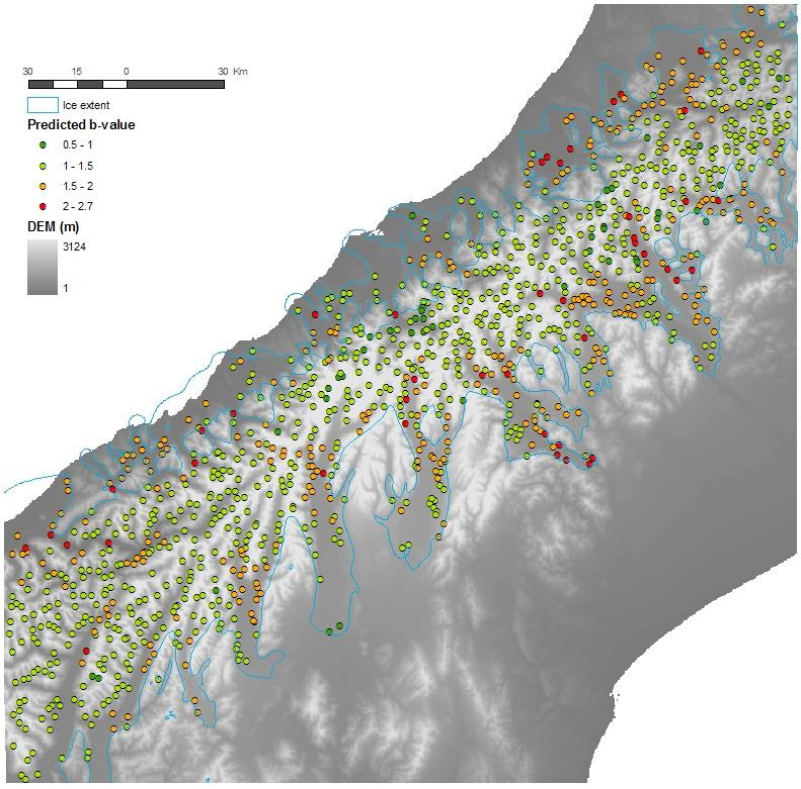

Figure 8.1 An example of how a predicted *U-ness* measure, in this case *b*-values, in the Southern Alps, New Zealand, from GWR can guide where the Average ELA is located. Note that high *b*-values are mostly positioned midway down trunk glaciers.

The best regression models occurred within valley systems (Figure 8.2), rather than between them, suggesting that valley systems have their own regimes, in that adjacent glaciers can have different influences on their accumulation and ablation. Local factors on ice mass, identified by Derbyshire and Evans (1976) for cirque development, such as a leeward aspect for maximum snow accumulation, poleward or easterly aspect for reduced ablation, could also affect valley cross-sectional shape and size. Brocklehurst and Whipple (2006) also recognised local factors could influence glacial geomorphology and included factors such as valley floor shading by the orientation of significant mountains or steep valley sides, as well as the contribution of avalanche material to accumulation and freeze/thaw rock material which, if thick enough, can insulate the glacier from significant ablation. Another consideration is subtle changes in rock structure between valley systems. A slight change in RMS or different orientation of foliation could influence the bedrock's resistance to erosion. Again evidence for this comes from research on cirques, which found that the orientation of bedrock layers could lead to different cirque forms (Haynes, 1968). In this thesis the Southern Alps provided some interesting results. Differences in the lithology between the schists to the west and greywacke to the east have led to differences in the evolution of the valley cross-section. The weather systems blow in from the west, producing large amounts of precipitation to the west of the mountain divide combined with the asymmetry of the range from the active fault where there are very steep slopes on the west, all of which create conditions of high ice flux on the west coast. The valley systems to the east of the divide receive the weaker morning sun (Derbyshire & Evans, 1976) which has less of an impact on ablation. In fact, the mountain divide is not directly north/south but instead more northeast/southwest, which means the valley systems to the east not only receive less solar radiation as they are more likely to face towards the pole, but are also protected by shading from valley sides and mountains to the north.

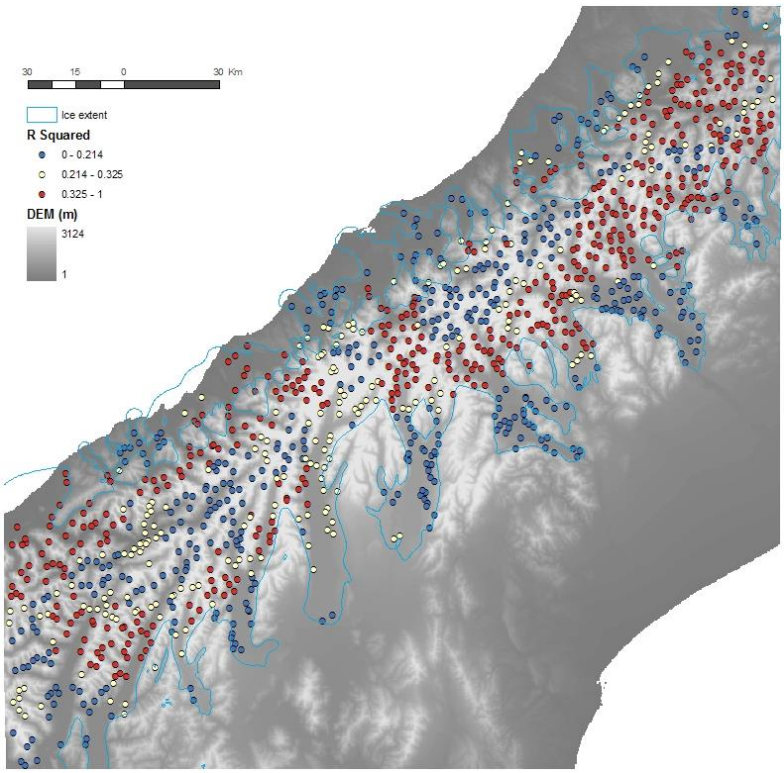

Figure 8.2 The GWR analysis of proxies (elevation and catchment area) against *b*-values shows high correlations *within* individual valley systems. Poor correlations are however found between valleys, which are shown by the low correlations at the mountain divide.

Although difficult to assess without detailed field measurements or literature which has researched the same area and produces the exact data required, it is thought that valley system level rock structure variation is not as important as the influences on accumulation and ablation in the Southern Alps. This is because different rock structures are likely to transcend valley systems and yet, valley local multiple regression models are strongest within valley systems. Therefore, it is concluded that the ice flux and residence time within valley systems can be very different, e.g. adjacent valleys can have different flux and residence times. The variability is created by influences on accumulation and ablation and therefore causes valley systems to have their own regimes which contribute to ice extent and valley evolution.

8.4. Interpretation of *U-ness* measure results

8.4.1. Form ratio indicates erosion processes

Form ratio was conceived as a measure for glacial valleys by Graf (1970) as a solution for constraining the infinite parabolic curve. It is a dimensionless measure which uses the valley depth and width (either from the trimline or from the valley top, and in the case of the mean cross-sectional valley method from halfway up the valley side). High form ratios signify deep, narrow valleys; whilst low form ratios denote wide, relatively shallow valleys.

Analysis of relationships between form ratio and proxies in whole mountain ranges showed that form ratio and elevation had the best correlation of any *U-ness* measure with a proxy (Figure 8.3). The positive relationship supports the hypothesis that form ratio increases with residence time. However, when fluvial and glacial valleys were analysed independently it was found that the fluvial valleys had a strong positive correlation whilst the glacial valleys much less so (Figure 8.3). As form ratio is a dimensionless representation between width and depth of a valley cross-section, a disproportionate change in width with respect to depth, or vice versa, will affect the measure. So, how is it possible for glaciers to either increase or decrease their form ratios? Form ratio could become greater if depth was to be increased by glacial erosion downcutting of the valley floor or isostatic rebound enhancing relief by uplifting ridges and peaks. It is not possible for glaciers to narrow valleys, so therefore deepening is the only way valleys can increase their form ratio. Conversely, if depth is reduced compared to width, the form ratio will decrease. This could occur due to sediment fill or erosion of the peaks and ridges. An additional plausible factor which could result in a decrease in form ratio is valley widening in relation to valley depth.

Erosion of the peaks and ridges has been identified as a process that limits relief as suggested in the glacial buzzsaw theory (Brozović *et al.*, 1997). The theory states that glacial erosion limits relief in terrain above the snowline (such as mountain peaks and ridges), or in this case the average snowline since the LGM. If width increases with respect to depth, form ratio will also decrease. In Harbor's (1992) model of valley evolution, widening initially occurs in the lower portion of a valley before deepening which, if the case, in reality this stage of evolution would be seen in relatively lightly glaciated areas, such as the Pyrenees. However, widening in Harbor's (1992) model occurs at the valley floor to create the parabolic shape of a valley, rather than at the

trimline or near the top of the valley where the form ratio width measurement is taken, and thus may only contribute marginally to valley widening. A much more significant contribution to valley widening is that alluded to by Hirano and Aniya (1988) in which two different models of glacial evolution were identified; the Patagonia-Antarctica and the Rocky Mountain model. The Patagonia-Antarctica valley cross-sections were defined by wide, relatively shallow valleys compared to the deep, narrow Rocky Mountain-type valleys. In this research, wide relatively shallow valleys with low form ratios and high b-values were found in the southernmost Patagonia sample area compared to other sample areas which suggests support for Hirano and Aniya's (1988) findings.

When form ratio is examined in the Pyrenees a positive correlation between form ratio and elevation (ice residence time) can initially be seen, but when the dataset is divided into glacial and fluvial valleys, glacial valleys show less correlation than fluvial valleys (Figure 8.3). This is unexpected as in a more alpine region like the Pyrenees, compared to Patagonia for example, a Rocky Mountain model of deep, narrow valleys, and therefore high form ratios, with increased residence time are hypothesised. To fully understand these results the form ratio measure was broken down into its two components; width and depth, and their relationship to elevation was examined separately. When this was carried out a marginally negative relationship occurs with width and elevation in both glacial and fluvial valleys (Figure 8.4), whilst depth had a poor positive relationship to elevation in glacial valleys (Figure 8.5), which was similar to the form ratio/elevation correlation (Figure 8.3), although maybe slightly more exaggerated. This is compared to fluvial valleys which have a stronger positive correlation between both depth and form ratio with elevation (Figure 8.3 and Figure 8.5). The difference between the relationship in fluvial and glacial valleys suggests that glacial valleys undergo different processes, which alter the valley depth and form ratio, which fluvial valleys do not undergo. The lack of correlation for depth and form ratio with elevation in glacial valleys suggests that there are processes which stop valleys getting deeper, despite longer residence times. An explanation for glacial valleys being less deep than expected could be attributed to the limiting of local relief (i.e. downwearing of peaks and ridges), which is in accord with the glacial buzzsaw theory. Another explanation is that there is greater potential for sediment fill in glacial valleys, compared to fluvial systems in mountainous areas, preventing downcutting as well as reducing valley depth. In contrast, fluvial erosion appears to be driven by incision towards the base level producing a strong relationship between elevation and form ratio

and depth. Due to the large amount of available relief at higher elevations, fluvial valleys create deep, narrow valleys which have a high form ratio. It is important to note that although glacial valleys do not show the strong positive relationship with elevation as fluvial valleys, they do have a larger mean form ratio. This suggests that glacial erosion still involves downcutting and that valleys in lightly glaciated areas, such as the Pyrenees, may exploit and enhance pre-eroded fluvial valleys.

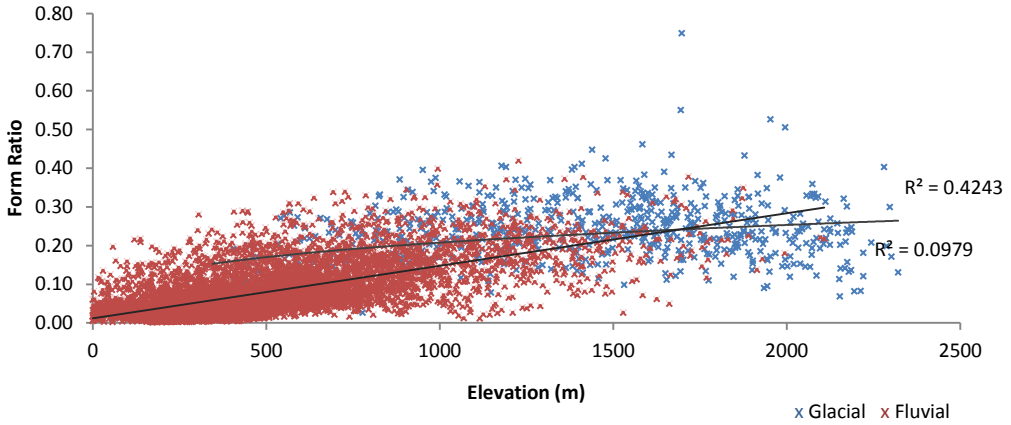

Figure 8.3 Values for form ratio plotted against elevation for fluvial and glacial valleys in the Pyrenees, showing a medium correlation for fluvial valleys whilst glacial valleys lack this correlation.

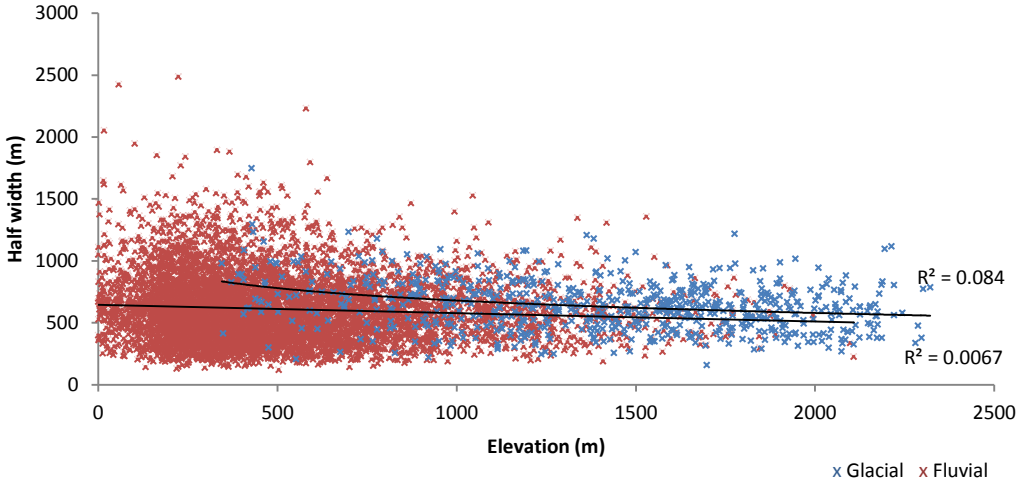

Figure 8.4 When width and mean valley floor elevations of Pyrenean valleys are plotted the correlation is less clear. Glacial valleys show a very slight decrease in width with elevation (R squared -0.084) whilst fluvial valleys show little correlation (R-squared -0.0067).

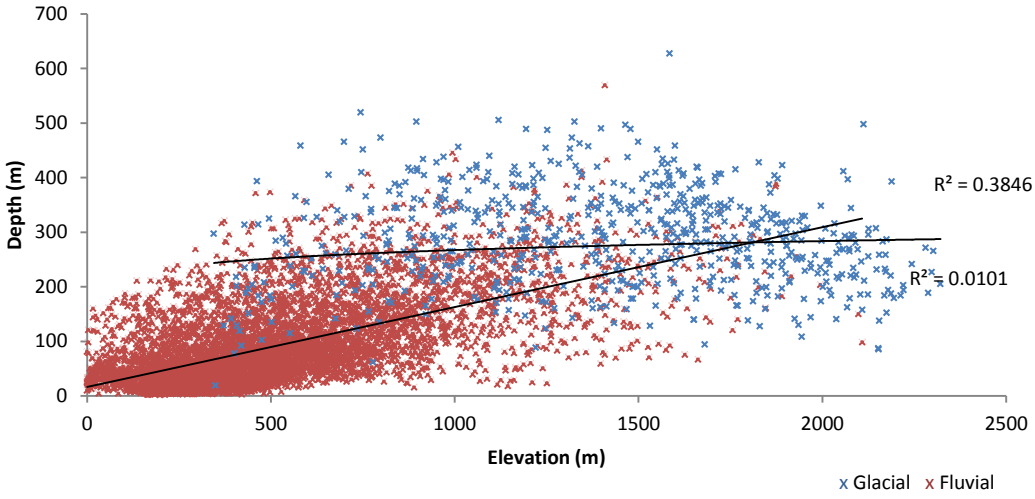

Figure 8.5 In the Pyrenees the depth relationship with elevation show that fluvial valleys have a positive correlation (R-squared 0.3846) whilst glacial valleys have a marginally positive, but generally poor correlation (R-squared 0.0101), similar to Figure 8.3.

When areas like the South Patagonia sample area are considered, which has undergone intense glacial erosion, no correlation is found between form ratio and elevation. This leads to the conclusion that fluvial erosion is highly dependent on available relief to create valleys with high form ratios (deep, narrow valleys). However, glacial erosion, when intense and for prolonged periods, creates valleys where the form ratio has no relationship with elevation. The intensity of the glacial erosion has destroyed the fluvial signal where form ratio is correlated to elevation. The lack of correlation with elevation could be due to the limiting of relief by the buzzsaw theory whereby the downwearing of mountain peaks and ridges occurs. It is suggested, therefore, that glacial valleys exploit fluvial valleys and continue to erode downwards whilst the peaks, ridges and mountain divides are also eroded which causes relief to be limited. An example of this is the destruction of mountain divides by glacial erosion (Oskin & Burbank, 2005) which cannot be achieved through fluvial erosion. Therefore less mature glacial erosion settings, such as the Pyrenees, are at the beginning of altering the fluvial trend of creating deep, narrow valleys where there is available relief. However in mature glacial landscapes, such as South Patagonia, the valleys have created flat longitudinal profiles and here the fluvial trend has been eliminated.

Other explanations for the lack of correlation between form ratio and elevation include the influence of sediment fill on the valley depth, and that downcutting at high elevations is not as intense because, despite longer residence times, there is reduced ice flux as per the confounding problem. It is suspected, however, that sediment fill in most cases is not significant enough to greatly alter the form ratio of a valley and this is investigated in detail in Section 8.4.5 in conjunction with the influence of fill on *b*-values.

Graf (1970) hypothesised that form ratio should increase with the intensity of glacial erosion, which, amongst other factors, would increase with stream order. His research showed that 2nd order valleys had larger mean form ratios than 1st order valleys. 3rd order valleys, however, had smaller mean form ratios than 2nd order valleys. Research in this thesis found similar results, but instead of comparing valley orders, catchment area was plotted against form ratio and in this case form ratio decreased with catchment area (Figure 8.6). In explanation of this Graf (1970) suggests that deposition is more likely to occur and in greater quantities in 3rd order valleys and this affects form ratio. It is known that where shear stress is low and normal stress is high deposition occurs and downward erosion ceases to take place. It does not, however, seem a satisfactory explanation that fill is solely causing a significant decrease in form ratio. In some situations glaciers have the ability to erode below their base levels (unlike fluvial systems) (MacGregor *et al.*, 2000), therefore downcutting should not be limited by available relief, and overdeepenings have been observed. So why do all glaciers not continue to erode downwards, increasing their form ratios? It is also possible that either due to the structure of the mountain range and/or pre-glacial wide fluvial valleys, valleys are naturally shallower and wider the further the distance from the divide. This would result in a decrease in form ratio with increasing catchment area, as larger catchment areas are further away from mountain divides, even without erosion altering the valleys. However, if this was the case, fluvial and glacial valleys would show a similar relationship between form ratio and catchment area which they do not (Figure 8.6).

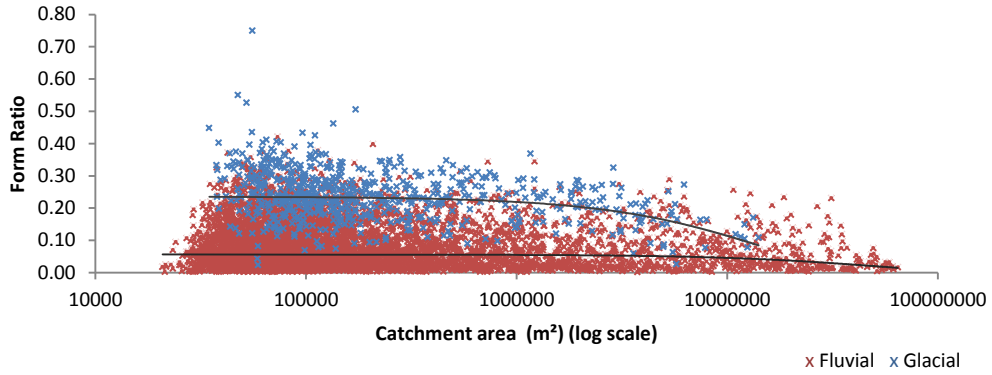

Figure 8.6 Form ratio plotted against contributing catchment area in the Pyrenees showing a slight decrease in form ratio for the largest catchments for glacial valleys.

Whole sample area analysis showed a slight decrease in form ratio with increased catchment area for glacial valleys (Figure 8.6). Further analysis showed that differences between valleys with small catchment areas and those with large catchment areas exist. Both valleys with large and small catchment areas have valley widths which increase with catchment area, albeit at a lot slower rate for large catchments (Figure 8.7). However, a different relationship emerges for valley depth (Figure 8.8). Here depth increases with catchment area for small catchments but decreases for large catchments, a result also found by Montgomery (2002). Different results were found in various fjord and outlet valley geometry research (Haynes, 1972; Roberts & Rood, 1984; Augustinus, 1992b; Brook *et al.*, 2003). Results in these papers indicate an increase in depth. However, the depth measurement used was the maximum depth of fjords below sea level, therefore not incorporating relief limiting effects, and also the longitudinal profile of the valley. Regarding the width measurements taken, there is no indication of whether these were made at the same point as the depth measurements, hence making a comparison and therefore inferring valley evolution difficult. Findings in this thesis show small form ratios occur in valleys with large potential ice flux which is attributed to a lessening of valley deepening rather than an increase in width, although widening does still occur. This still leaves the question of why glaciers stop incising unanswered; however, from the results in this thesis, there is evidence that they continue to widen their valleys. This question will be tackled in Section 8.5.

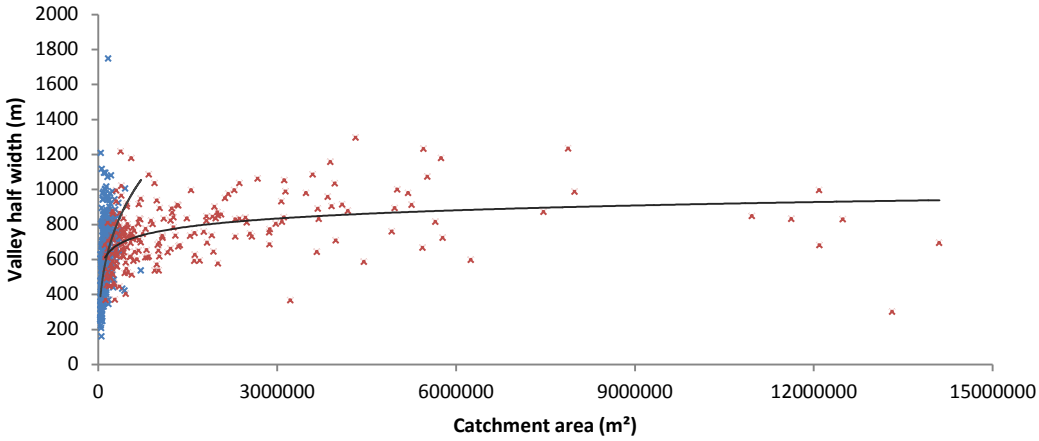

Figure 8.7 Width measurements of glacial valleys are examined with respect to catchment area in the Pyrenees. First order glacial valleys (blue) have small catchment areas and show a strong positive correlation, whilst second order and above valleys (red) have a weaker but still positive correlation.

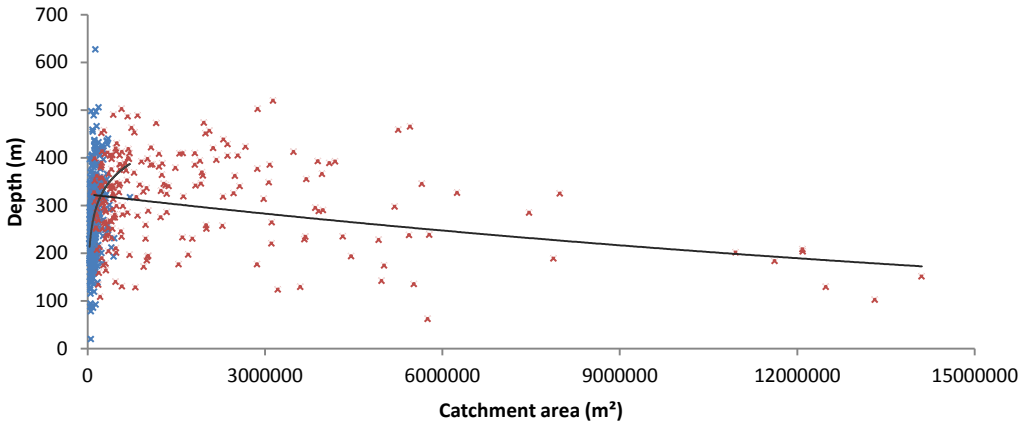

Figure 8.8 The same plot as Figure 8.7 but showing depth measurements of valleys. Here first order valleys (blue) still have a positive correlation but second order valleys (red) show a negative correlation.

Alpine mountain valleys at high elevations are often associated with steep valley floor slopes, whilst valleys at lower elevations have shallower slopes. Valley floor slope showed a strong positive correlation with form ratio, signifying deep, relatively narrow valley cross-sections where there are steep valley floors and wide, relatively shallow valleys where there are valley floors with gentle gradients (Figure 8.9). It is possible that there is a process link between the valley floor gradient and the valley cross-section shape which may be linked to ice velocity.

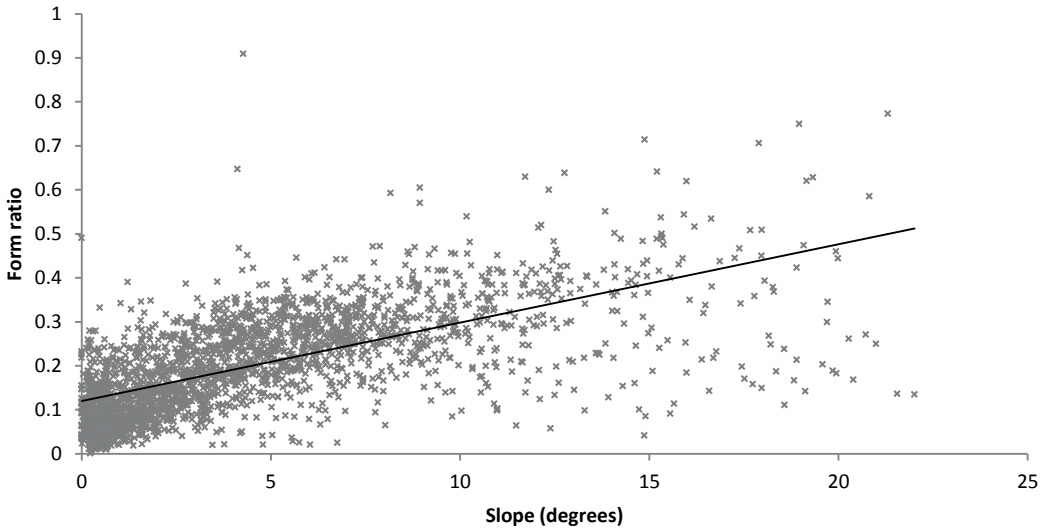

Figure 8.9 A form ratio/slope plot for glacial valleys in the Southern Alps, shows a strong positive correlation (R squared 0.4269) indicating that form ratio is closely linked to the valley floor slope.

When single regression GWR analysis was undertaken, form ratio had more significant valley segments with elevation than catchment area in all samples except for South Patagonia. This can be interpreted as all sample areas, with the exception of South Patagonia where glaciation extended well beyond the mountain range, still have a fluvial signature at lower elevations and more glacial erosion is needed to eliminate this. In South Patagonia glacial erosion has lowered longitudinal profiles and ice flux (catchment area) appears to be the dominant control on form ratio. In the Southern Alps of New Zealand, GWR analysis shows a positive relationship between form ratio and elevation, with the exception of valleys at the divide (Figure 8.10); this result supports Graf's (1970) view that the very highest valleys, which have the least ice flux but the greatest residence time, have smaller form ratios than the valleys downstream of them which Graf (1970) deems to have greater glacial erosion intensity. It also supports the confounding problem indicated by Graf (1970), although not explicitly defined in previous literature. Form ratio and catchment area have a nearly exclusively negative relationship although overall it is quite weak (Figure 8.11). This is because as catchment area increases down valley, the form ratios decrease. This could be from either or both a decrease in valley depth and an increase in valley width. In the case of the Southern Alps and at the furthest extent of the LGM, the decrease in valley depth and the increase

in valley width could be due to the mountain structure or a preglacial fluvially eroded landscape at the point the valleys are exiting the mountain range, and consequently the valleys are shallower and wider due to other processes rather than any modification from glacial erosion. Due to this it may be justified to discard the measurements of valley segments at the margins of the mountain range, however, it is important to note that form ratios within the mountain range still show a negative correlation between form ratio and catchment area (ice flux) and therefore it is still an interesting trend to investigate with regards to valley evolution.

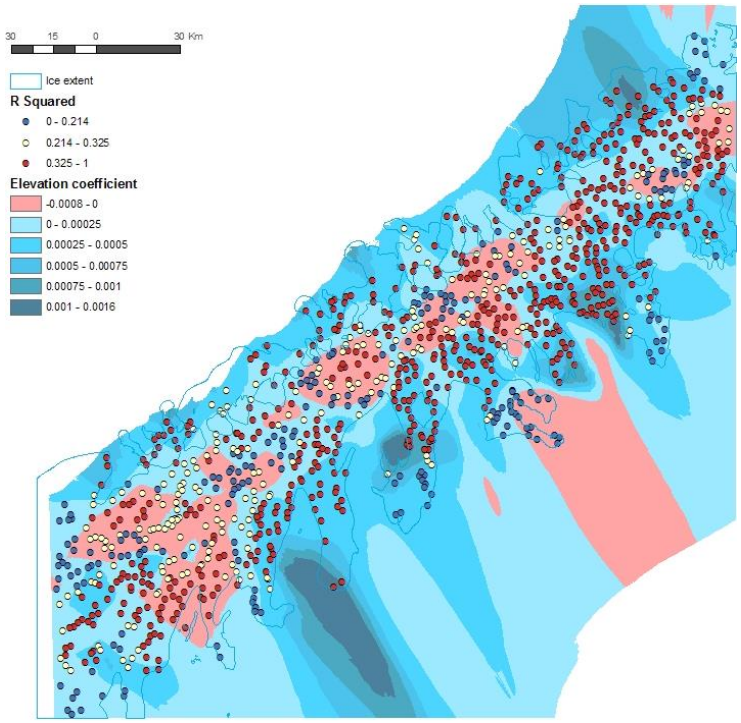

Figure 8.10 Elevation coefficient surface (slope of regression line) for GWR analysis between form ratio and proxies. It shows that form ratio and elevation generally have a positive relationship which is steepest near the LGM ice extent limit, especially to the east of the divide but also in the northwest. Weak negative correlations are found at the divide. A small area of negative correlation is found at the ice extent east of the divide but this is not reliable due to low R-squared values.

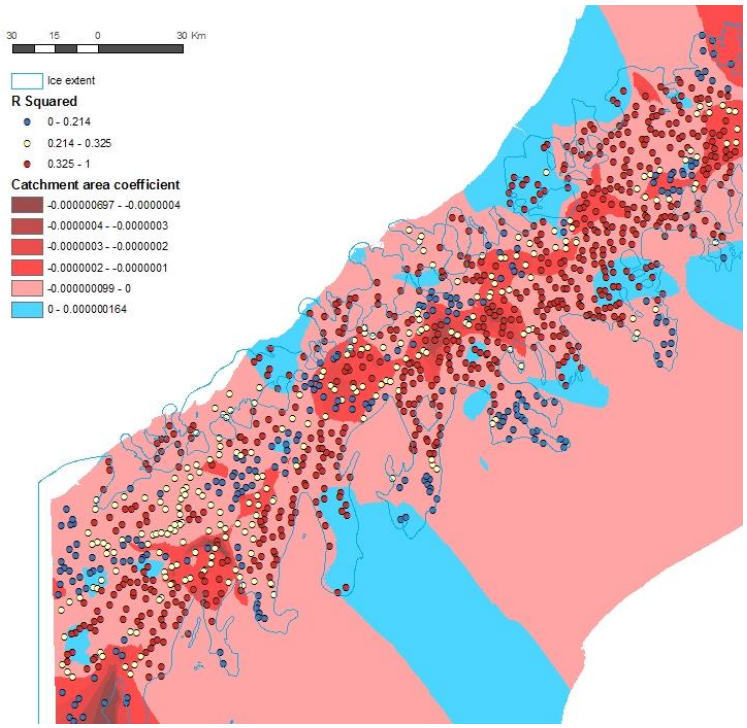

Figure 8.11 Local correlation between form ratio and catchment area are the opposite of that of elevation (Figure 7.19) in that they are mainly negative with the strongest negative correlations being at the divide.

When catchment area and elevation are both included in local multiple regression models, the number of significant valleys increases for all catchment areas, suggesting that by including both proxies in the model it is improved. Therefore both contribute to the form ratio of valleys, even in South Patagonia.

When valley floor slope and form ratio was investigated in the Southern Alps of New Zealand, the local regression models show the greatest amount of significant valleys, much more than the regressions for catchment area and elevation. It is possible that the focus of glacial erosion alters according to valley floor slopes; steep gradients causing downcutting, whilst gentle gradients create conditions for widening. Evidence in the Southern Alps showed that glacial erosion removes the fluvial signal of steep slopes by first eroding downwards, reducing valley floor elevation and flattening the valley longitudinal profile. As the valley floor gradient is reduced the tendency for valley widening over deepening occurs, concentrating erosion on the valley sides. In South Patagonia, where intense and persistent glacial erosion has taken place, valleys of all orders have developed flattened longitudinal profiles and low valley floor slopes have evolved and here widening prevails over deepening.

In conclusion, analysis of form ratio in this research has been able to indicate several elements of valley cross-section evolution. Firstly, it shows that fluvial valleys develop deep, narrow valleys where there is available relief. Glacial erosion then exploits the fluvial landscape by developing valleys into a parabolic form and then enlarging and widening them. Where the fluvial signal can still be seen in LGM landscapes it is thought that the landscape has been lightly glaciated, which is the case in the Pyrenees, whilst in South Patagonia, an intensely glaciated landscape, the fluvial signal has been eliminated. Valley depth is shown to reduce with catchment area and several reasons have been suggested. These are the reduction in depth due to sediment fill, a limiting of relief due to the glacial buzzsaw theory (Brozović *et al.*, 1997), as well as the influence of the mountain range structure where previously glaciated valleys, at the extremities of the LGM margins, exit the mountain range. It is fair to assume that all of these explanations may play a part, but finding whether there is a first order control on valley depth with catchment area is of interest. When valley floor slope is investigated a strong link between form ratio and slope emerges. As the valley floor slope decreases, arising from flattening longitudinal profiles caused by intense glacial erosion, valley widening is observed. Again, at the LGM margin, widening could be due to the fact that ice is exiting the mountain range or fluvially widened valleys and the valley statistics here should be treated with caution; however this trend is seen in valleys located well inside mountain ranges and in regions such as South Patagonia where glaciation extended well beyond the mountain ranges.

This research agreed with Graf's (1970) conclusion that form ratio increased with stream order; to a point. GWR analysis here showed an initial increase in form ratio down valley, which is identified as evidence of the confounding problem where the combination of favourable ice flux and residence time allows for the most well-developed glacial valleys cross-sections. This was also a point raised by Porter (1989), who concluded that the average location of the ELA was an important consideration and had been neglected in the literature to date. The interplay between residence time (ice occupancy) and flux (glacial erosive power) was also recognised by Andrews (1972), in that both were of importance for the cumulative impact of erosion over time. A study of corries showed that despite the lower flux in Arctic regions due to a much lower mass balance gradient, the length of occupancy compared to alpine regions meant that corries were greater in size due to the overall greater denudation (Andrews, 1972). Translating this to the cross-section of valleys, Andrews (1972) recognised that valleys

were wider and shallower in Arctic regions compared to Alpine ones, and commented on the importance of ice residence time to create conditions for shallow, wide valleys compared to deep, narrow valleys. This is consistent with Hirano and Aniya's (1988) Patagonia-Antarctica/Rocky Mountain model of glacial valleys, but neither gave further explanation of these observations in differing valley shape and dimensions. Downstream of the maximum form ratio location the form ratio decreases as catchment area increases. After investigation it was found that this was due to valley depth decreasing whilst valley widths continued to increase therefore generating lower form ratios. There may be several explanations for this that are not related to glacial erosion, for example the fact that valleys are exiting the mountain range and wider and shallower valleys may simply be a consequence of the mountain range structure as suggested by Graf (1970), or formed by lowland fluvial processes, and therefore valley morphology statistics at the extremities of ice margins should be treated with caution. Sediment fill may also contribute to a decrease in valley depth, as well as a reduction in shear stress and an increase in normal stress causes a reduction in the ice's erosional power. It is interesting to note, however, that *b*-values still increase with valley width increases (the relationship to form ratios will be discussed in Section 8.4.5.), indicating that in many cases glacial erosion is still taking place, but there may be a shift in the erosional focus from down wearing to side wearing.

8.4.2. b-values as a measure of valley development

B-values have been used to suggest the level of glacial development from a fluvial valley to a glacial valley (e.g. Harbor, 1992) since Svensson (1959) proposed it as a useful descriptor of valley cross-sectional shape. Research in this thesis found, firstly, that *b*-values were a poor distinguisher for assessing fluvial-glacial valley shape, at least with the mean valley profile method. Fluvial valleys of the Pyrenees showed a high variability of *b*-values (Figure 8.12). *B-values* ranged from 3.2 to 0.15 for fluvial valleys, not simply the valley of 1 or less as is often suggested (Svensson, 1959). This wide variability is due to fluvial valleys having a less distinct form than glacial valleys, particularly out of upland areas. Fluvial valleys are not just V-shaped, instead they have meandering or canyon forms, for example. It is also true that fluvial valleys are less straight, taking a sinuous line around protruding spurs. This characteristic of fluvial valleys means that within any valley segment there is high variability of cross-sectional shape making it difficult for the mean valley cross-sectional method to define a mean cross-sectional shape. It is

therefore concluded that *b*-values are a poor discriminator between fluvial and glacial valleys when the mean valley cross-section method is used, also a conclusion found by Phillips (2009).

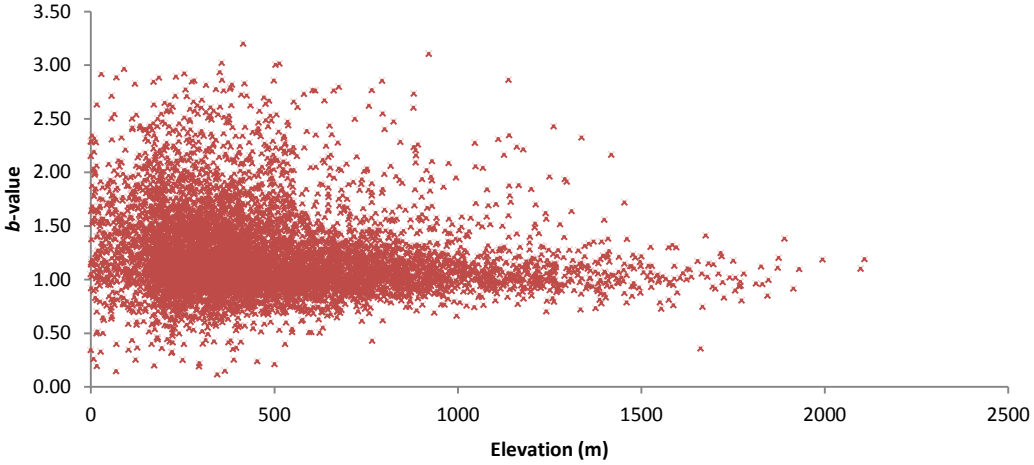

Figure 8.12 Fluvial valleys in the Pyrenees showing high variability of *b*-values, especially at the lower elevations.

Using the *b*-value measure for glacial valleys, on the other hand, has been seen in this thesis to be useful in understanding glacial valley development. Glacial valleys are shown over the whole research area to have a more consistent form, typically displaying *b*-values between 1 and 2 for valley segments (Figure 8.13). The glacial valley form lends itself to the mean valley cross-section method as glacial valleys are straighter than fluvial valleys, as well as having less steep longitudinal profiles and truncated spurs. Glacial valleys are also large features in the landscape which, at the 90 m resolution of the SRTM data used in this research, can adequately be analysed. Large *b*-values are found at the lowest elevations (Figure 8.14) of LGM ice extent and this is attributed to the broad and wide valleys which, at the LGM maximum, channelled ice from high accumulation zones (Figure 8.15). These valleys, however, are susceptible to large volumes of sediment fill. Therefore, the high *b*-values should be treated with caution here, as infilled valleys have artificially flat valley floors and higher a degree of curvature where the fill meets the valley sides, the combination of which results an artificially high *b*-value when a parabolic curve is fitted to the cross-section.

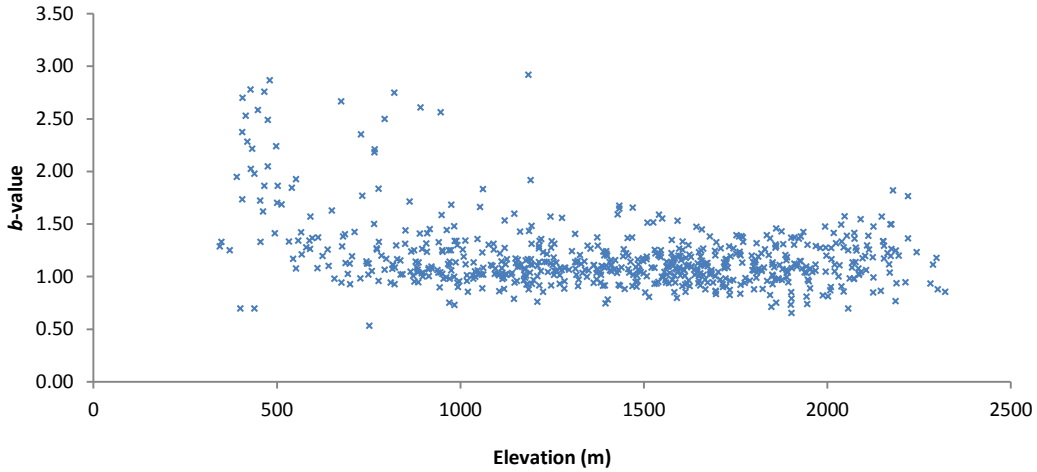

Figure 8.13 Glacial valleys show a reduction in the variability of *b*-values especially above 1250m. This is compared to fluvial valleys (Figure 8.12) where there is much less variability with a concentration of values between 1 and 2. It suggests that glacial valleys have a more consistent form when the mean valley profile is used.

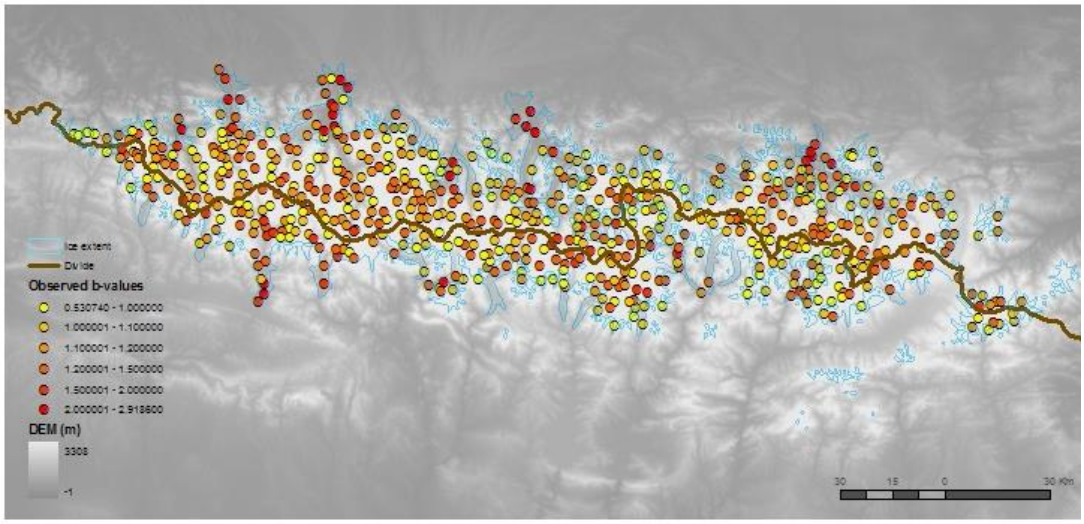

Figure 8.14 Observed *b*-values from GWR analysis for the Pyrenees show that the largest *b*-values are found in the trunk valleys at the limit of the LGM extent.

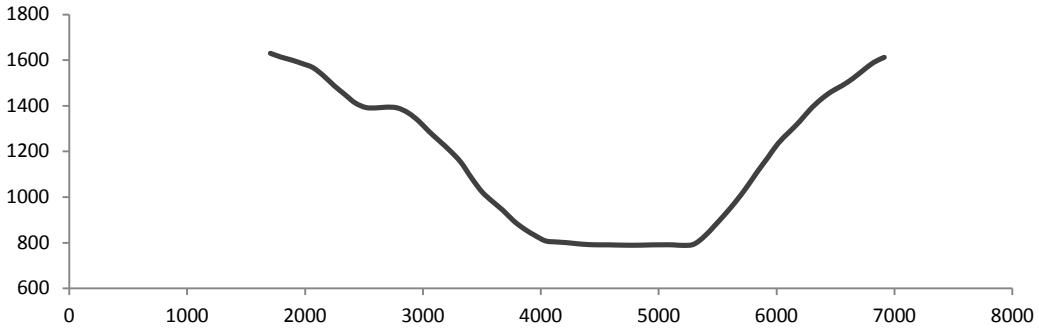

Figure 8.15 A transect of a trunk valley in the Pyrenees showing a very flat valley floor. This is due to sediment fill (units in metres).

Overall *b*-values are slightly smaller than would initially be expected in relation to the literature, but this is easily explained by the fact that the mean valley cross-section method encompasses the entire length of defined valley segments, meaning that all slope anomalies, created by rock structure for example, are included in the profile. Not only is the method non-selective in the location of profiles, as it encompasses the whole valley segment by averaging the width and depth measurements, but it also is non-selective in the sense that all useful valley segments are analysed. Although most valley segments within an area are analysed, some are discarded when the valley segment area is deemed too small or if a power-curve cannot be fitted to the profile. Therefore this method is unique in valley cross-sectional research, in that it is objective in nature. The trade-off for the objective nature of the method is that the dataset has the potential to be quite noisy which may mask trends. This is offset by the size of the dataset and the focus of the research to find first order trends in glacial valley development. From the results of the sample areas investigated it should be noted that, when using the mean valley profile method, slightly lower *b*-values should be expected.

When a comparison between sample areas with increasing latitude was undertaken, *b*-values also showed an increase, indicating that valleys are developed into better parabolas with the increasing degree of glaciation. Spatial analysis within sample areas showed that *b*-values and elevation, a proxy for residence time, were negatively correlated (Figure 8.16), contrary to the hypothesis which stated that increased residence time would lead to larger *b*-values. Catchment area (a proxy for ice flux), on the other hand, showed an almost exclusively positive relationship with *b*-values (Figure 8.17). GWR analysis showed that when individual regressions for *b*-values in relation to

elevation and catchment area were modelled, more valley segments were significant with respect to *b*-values and catchment area rather than elevation. This occurred in all sample areas apart from the Southern Alps of New Zealand. The conclusion from this result is that ice flux is more important in developing a valley with a parabolic form than residence time. However, when both are considered in multiple regression analysis the local regression models are improved, suggesting that ice residence time does contribute to the development of *b*-values; this is probably because the negative correlation between elevation and *b*-values is related in itself to catchment area, as the lowest elevations are found in the trunk valley segments which have the greatest contributing catchment areas. An explanation for the Southern Alps not having better local regression models for *b*-values and catchment area, unlike the other sample areas, is that the eastern trunk valley cross-sections have been modified by a large degree of fill, disrupting the correlation between catchment area and *b*-values.

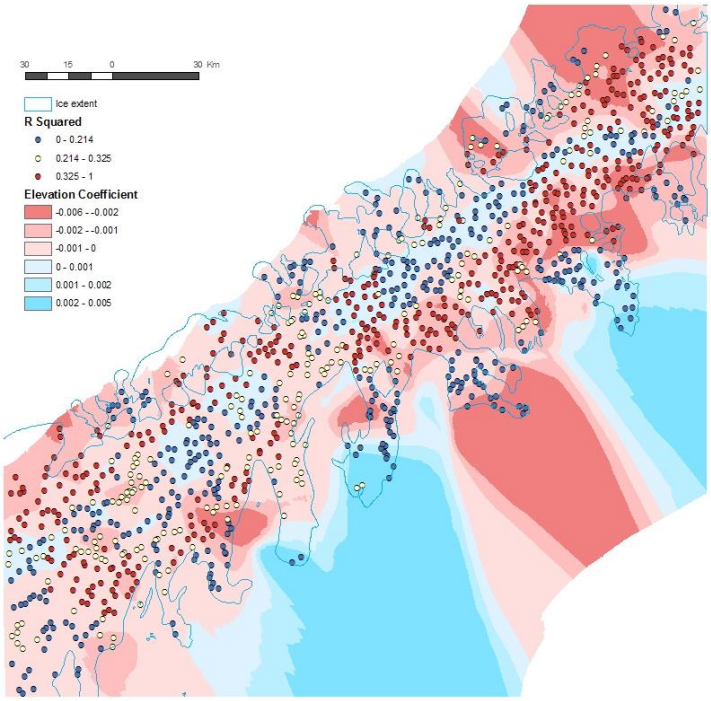

Figure 8.16 The elevation coefficient (slope of the regression line) surface for *b*-values shows a mainly negative correlation between the variables, meaning that as the elevation decreases valleys become more parabolic.

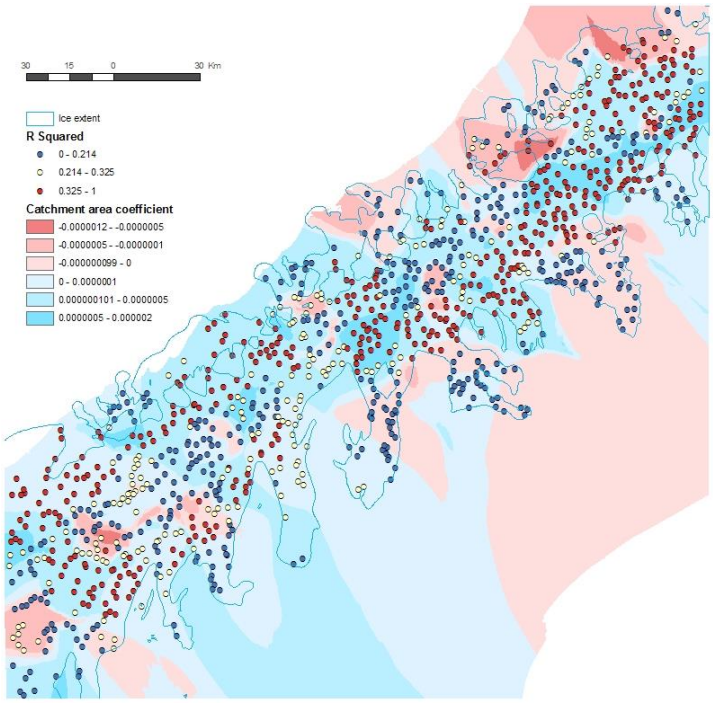

Figure 8.17 In contrast to Figure 8.16 the catchment area coefficient surface for *b*-values shows mainly positive correlation showing that as the catchment increases the valley becomes more parabolic.

In conclusion, *b*-values are highly variable for fluvial valleys but largely conform to a parabola between 1 and 2 in glacial valleys. Due to the mean valley cross-section method being objective in nature, so that all slope anomalies are included, as well as measurements from all valleys in an entire mountain range, the resultant mean profile has marginally smaller values than produced using the transect method. Evidence that ice flux, over residence time, is the major control on the parabolic form of valleys is apparent, although large amounts of fill can disrupt this trend.

8.4.3. Using Cross-sectional area as a U-ness measure

Cross-sectional area for valleys has been used as a measure for the degree of glaciation when comparing valley size to contributing catchment area (Haynes, 1972; Roberts & Rood, 1984; Augustinus, 1992b; Montgomery, 2002; Amerson *et al.*, 2008) and Phillips (2009) found it to be the best discriminating measure between fluvial and glacial valleys. Other than this, cross-sectional area is not commonly used when assessing glacial valley evolution. Not only do glacial valleys generally have greater width and depths than fluvial valleys making for valleys with greater cross-sectional areas, but given the same

width and depth, the 'U-shape' of glacial valleys have approximately a 50% greater cross-sectional area than the 'V-shape' of fluvial valleys (Roberts & Rood, 1984). Therefore the greater the parabolic form of a valley (the higher the *b*-value) the greater the cross-sectional area tends to be.

It was hypothesised that cross-sectional area will increase with the degree of glaciation and also in regions more favourable for glacial erosion (less resistant lithology, high precipitation and low temperatures as well as high tectonic uplift). Results for valley segment cross-sectional area when comparing whole sample areas supported these hypotheses in that cross-sectional area increased with latitude in the three sample areas in the Andes. When relationships with proxies are considered, results show an increase in cross-sectional area with elevation, however when only LGM valleys are graphed, results are similar to the relationship between form ratio and elevation, in that glacial valleys show little correlation (Figure 8.18). This is attributed both to the relief limiting nature of glacial environments (Brozović *et al.*, 1997), identified in form ratio relationship with elevation, as well as the confounding factor between elevation and catchment area .

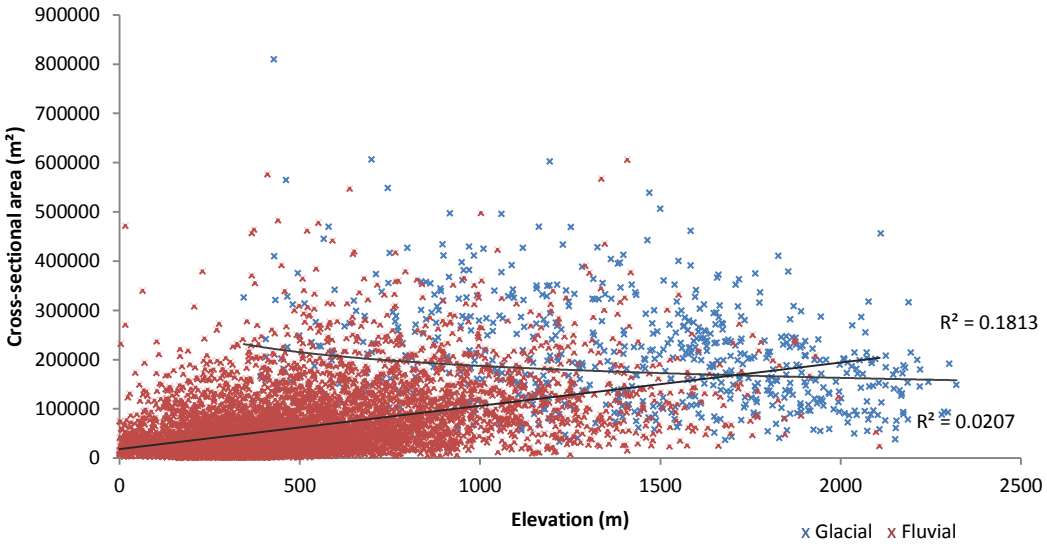

Figure 8.18 The relationship between elevation and cross-sectional area for the Pyrenees is plotted here for glacial (blue) and fluvial (red) valleys. Similar to the relationships seen for form ratio and depth with elevation in Figure 8.3 and 8.5.

When the relationship with catchment area is considered, fluvial valleys show no correlation whilst glacial valleys have a positive relationship with catchment area (Figure 8.19). This concurs with the hypothesis that cross-sectional area will increase with ice flux. Research studying fjords has observed similar relationships (Haynes, 1972; Roberts & Rood, 1984; Augustinus, 1992b) as well as in alpine settings (Montgomery, 2002; Amerson *et al.*, 2008). This, combined with the fact that local regression analysis showed that all sample areas have more valleys with significant relationships for catchment area and cross-sectional area than with elevation, confirms that ice flux is more important in creating large valleys than ice residence time in alpine settings. Analysis, therefore, suggests that the most cumulative erosion occurs when ice mass is greatest and fastest flowing rather than simply having existed for longest as is the case in highest alpine valleys.

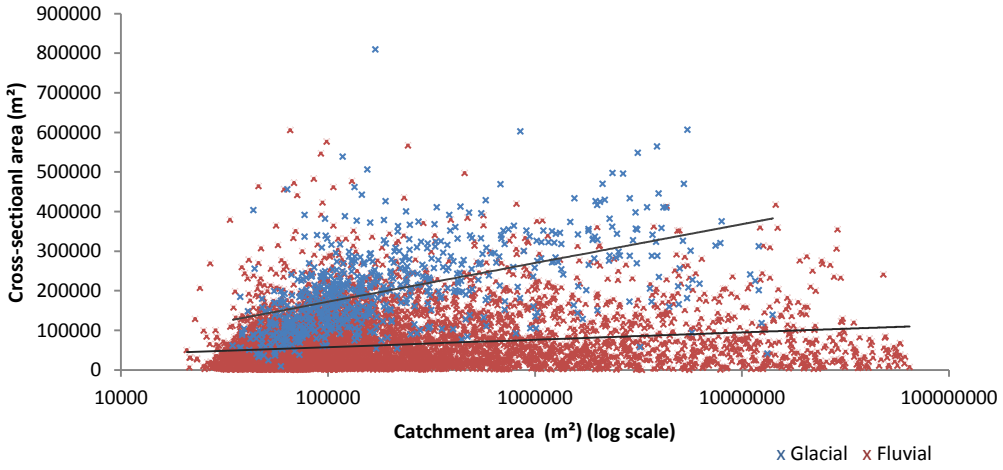

Figure 8.19 Data for glacial (blue) and fluvial (red) valleys in the Pyrenees showing a strong positive correlation for glacial valleys whilst fluvial valleys do not show any correlation.

GWR local multiple regression analysis shows that the relationship between proxies and cross-sectional area produces the greatest number of significant valleys when compared to other *U-ness* measures. This gives the impression that cross-sectional area accounts for valley development on a local level the best. However, when coefficient surfaces are analysed, the only major pattern which emerges is that cross-sectional area and catchment area has a positive relationship, although this relationship is weak. It is suggested that the high variability and difficulty in identifying local relationships with cross-sectional area is due to cross-sectional area being highly sensitive to local relief

and this is demonstrated in Figure 8.20. Changes in local relief are partly attributed to relief limiting effects (Brozović *et al.*, 1997), as well as variation in the ridge line heights. Both effects vary local relief which greatly alters the valley cross-sectional area (Figure 8.20).

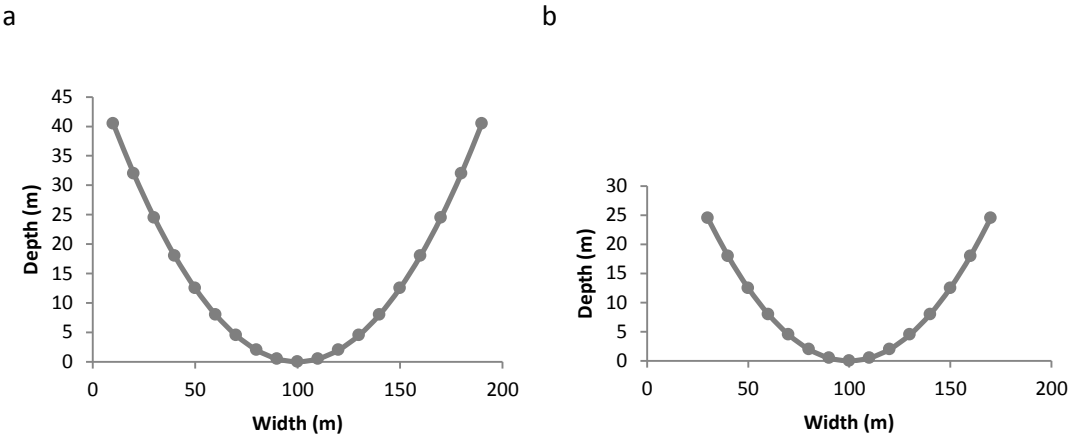

Figure 8.20 Shows a representation of two different valleys with the same *b*-value of 2 (and a variable of 0.005). As relief is reduced so is the form ratio, which is 0.225 in (a) and 0.175 in (b). However it is the cross-sectional area which is altered most (proportional) (a) having a cross-sectional area of 4860, whilst (b) has a value of less than half that at 2286.7.

This research concurs with Phillips (2009), finding that valley cross-sectional areas are greater for glacial valleys when compared to fluvial valleys when using the mean valley cross-section method. In this research cross-sectional area has been shown to be useful in examining the degree of glaciation of whole mountain ranges, showing that highly glaciated regions such as South Patagonia had larger valleys than less glaciated regions such as North Patagonia, however it was not so useful in valley system level analysis, as when GWR was performed no clear trend emerged within sample areas. Therefore cross-sectional area was not useful for investigating individual valley development.

8.4.4. Influence of tectonics, lithology, climate and the degree of glaciation on U-ness

The influence of tectonics, lithology, climate and the degree of glaciation has been touched on in previous sections in this chapter when discussing *U-ness* measures. This section reinforces these findings, examining them in more detail with reference to the literature.

Tectonic uplift builds mountain ranges. Some mountain ranges experience uplift during glaciation whilst others are glaciated post-uplift. Research has shown that higher erosion rates occur where there are higher uplift rates (Schlunegger & Hinderer, 2001). From research in this thesis a link between valley floor slope and valley form is evident. Steep valley floors were associated with narrow, deep valleys which had high form ratios as per the Rocky Mountain type model (Hirano & Aniya, 1988), whilst lower valley floor gradients were more likely to have wide, shallow valleys with low form ratios and typical of the Patagonia-Antarctica model (Hirano & Aniya, 1988). As the longitudinal evolution of glacial valleys trends towards a flattening of the valley floor (MacGregor *et al.*, 2000) over time valleys will evolve to have wide, shallow valleys unless there is a process which steepens mountain range slopes. Tectonic uplift is one process which can maintain steep valley floor slopes, and therefore preserves a pattern of erosion identified with steep slopes, i.e. high form ratios, and preventing the flattening of longitudinal profiles. Some evidence of this occurs in the Southern Alps, New Zealand. This mountain range is strongly asymmetric with the alpine fault to the west of the divide maintaining steep slopes to the west whilst low gradients are found to the east of the divide. However, as is often the case when using real landscapes in experiments, other factors such as the contrasting lithologies and differing climate influences either side of the divide make a robust conclusion solely on the results from this sample area difficult. Valleys with a low valley floor gradient, especially if they are in regions of less resistant lithology, may be subject to large amounts of sediment fill where shear stress is low and normal stress is high. Sediment fill is thought to artificially increase *b*-values and will reduce valley depth to some extent (Section 8.4.2).

The Pyrenees was a sample area where the effects of climate on valleys could be studied, due to the North/South aspects of the range as well as the strong precipitation gradient across the divide. It was evident from this study that more mature glacial valleys existed north of the divide where conditions for glaciation were more favourable (much higher precipitation and a poleward aspect). This supported the hypothesis that climate influences valley form.

Southern Patagonia was used to ascertain how *U-ness* changed with latitude, a proxy for the degree of glaciation. Results from glacial valleys in the whole sample areas show a clear increase in the *U-ness* measures of cross-sectional area and *b*-values with latitude (glacial intensity) and is therefore thought to be a first order control on these measures. Form ratio, on the other hand, decreases with the intensity of glaciation; this will be discussed in more depth in the following section (Section 8.4.5).

The research on the characteristics of glaciation in this thesis shows the difficulty in choosing real world examples for studies due to the complexity of landscapes. It is extremely difficult to isolate one influence in order to study and compare valley form. It is felt that the investigations into the intensity of glaciation using the three sample sites in Southern Patagonia, and the investigation into climate in the Pyrenees, were particularly successful, but the Southern Alps, New Zealand was a complex environment to try to understand the influence of tectonics and lithology on valley cross-sections. Many researchers overcome this problem by using synthetic landscapes constructed in modelling experiments; this is a valid approach but comes with disadvantages, the main one being that real landscape processes and feedbacks have not been fully defined and therefore any results must acknowledge this limitation. By using both real landscapes and modelling experiments to explore landscape evolution the results and conclusion from both forms of research can help to further understand in this field of research and therefore collaboration between these two approaches is important.

8.4.5. Relationships between form ratio and b-values

Graf (1970) found that the mean *b*-value increased with the stream order, however form ratio did not follow this relationship, instead increasing between 1st order and 2nd order valleys but decreasing between 2nd order and 3rd order valleys. He attributed this to 3rd order valleys emerging from the mountain ranges. Hirano and Aniya (1988) studied the relationship between *b*-values and form ratio, finding that in some areas there was a negative correlation between form ratios and *b*-values, whilst in other areas there was a positive relationship. The negative relationship between form ratio and *b*-values was termed a 'Patagonia and Antarctica' type of glaciation whilst the positive relationship was identified in alpine areas and therefore described as a 'Rocky mountain' glacial model. These models suggest that wide, relatively shallow valleys develop in areas which have undergone intense and prolonged, even ice sheet, glaciation, whilst deep,

relatively narrow, valleys occur in alpine areas where glaciation has neither been persistent nor enduring. Several studies have investigated this relationship (Pattyn & Decleir, 1995; Li *et al.*, 2001a; Seddik *et al.*, 2009), finding mixed results. In the Tien Shan Li *et al*. (2001a) found that, overall, the dataset revealed a weak negative correlation between *b*-values and form ratio associated with a 'Patagonia-Antarctic' type glacial model, although Li *et al.* (2001a) were tentative about concluding this. When more localised analysis was undertaken both 'Patagonia-Antarctic' and 'Rocky Mountain' type models could be found. In particular, a deepening trend was identified in tributary valleys, whilst widening was identified in the main trunk valleys (Li *et al.*, 2001a). Li *et al*. (2001a) recognised that the *b*-value/form ratio relationship was complex and instead favoured using the quadratic equation c coefficient. Li *et al.*'s (2001a) research is more comprehensive in terms of the number of transects analysed, 49, when compared to Hirano and Aniya's (1988), six 'Rocky Mountain' transects and six 'Patagonia-Antarctica' transects (Aniya & Welch, 1985, unpublished, cited in Hirano & Aniya, 1988).

In an attempt to find where there were different local relationships between *b*-values and form ratios, GWR analysis was carried out. It showed a mainly negative relationship between *b*-values and form ratios, although some positive relationships occurred at the divide and the LGM ice limits (Figure 8.21). This confirms that in most cases form ratios decrease as *b*-values increase.

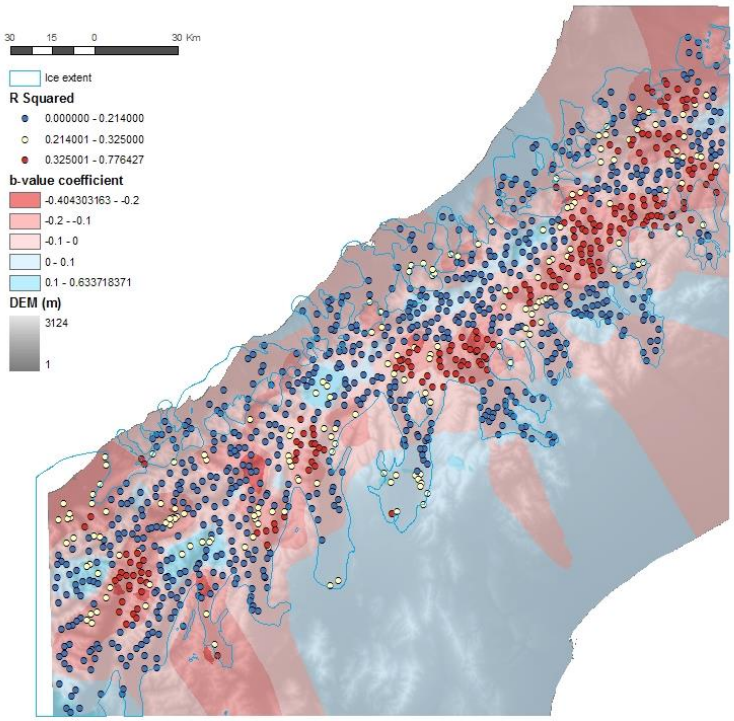

Figure 8.21 GWR analysis using form ratio as the dependent variable and *b*-values as the explanatory value it shows a mainly negative relationship, where form ratios decrease *b*-values increase, i.e. valleys become shallower and wider and they get more parabolic.

The *b-FR* diagrams produced in this thesis concur with Li *et al.* (2001a), in that a predominately negative trend was found and that the relationship showed complexity. The majority of valleys were found to have a 'Patagonia-Antarctica' type relationship even in strongly alpine type regions, such as the Pyrenees. However, an interesting pattern was found from the graph and is shown in Figure 8.22 and 8.23. Here there is some evidence that when valleys are divided into those with a form ratio of 0.4 and less and those with a form ratio of 0.4 and greater, the valleys display a 'Patagonia-Antarctica' and 'Rocky Mountain' model respectively. The transects collected in Li *et al*.'s (2001a) research did not exceed a form ratio of 0.4 and it can be seen in Figure 8.24 that they showed a very similar relationship to those with a form ratio of 0.4 and less.

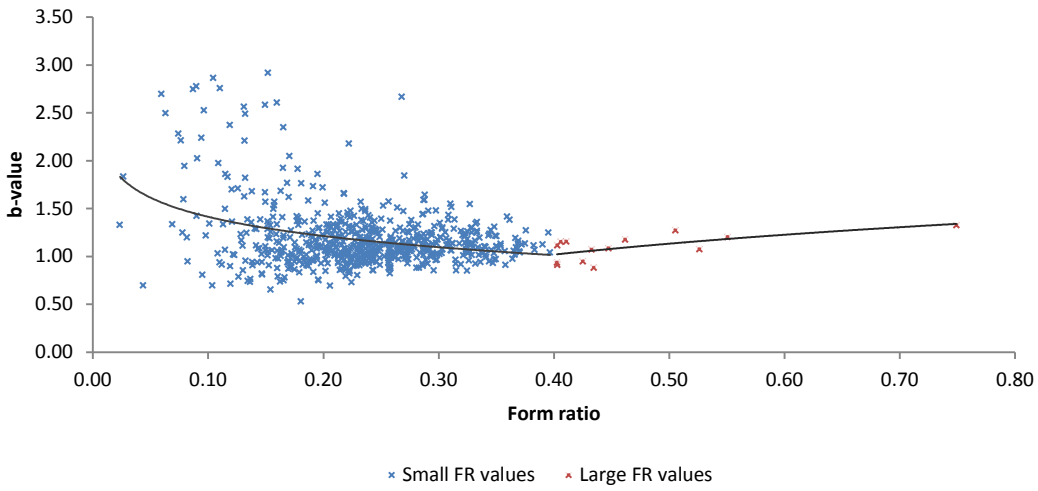

Figure 8.22 A *b-FR* diagram for glacial valleys in the Pyrenees showing the majority of valleys have a negative correlation (R-squared = -0.1007) (blue) whilst only a few valleys have a positive correlation (R-squared = 0.4319) (red). The threshold for the change is at a form ratio of 0.4.

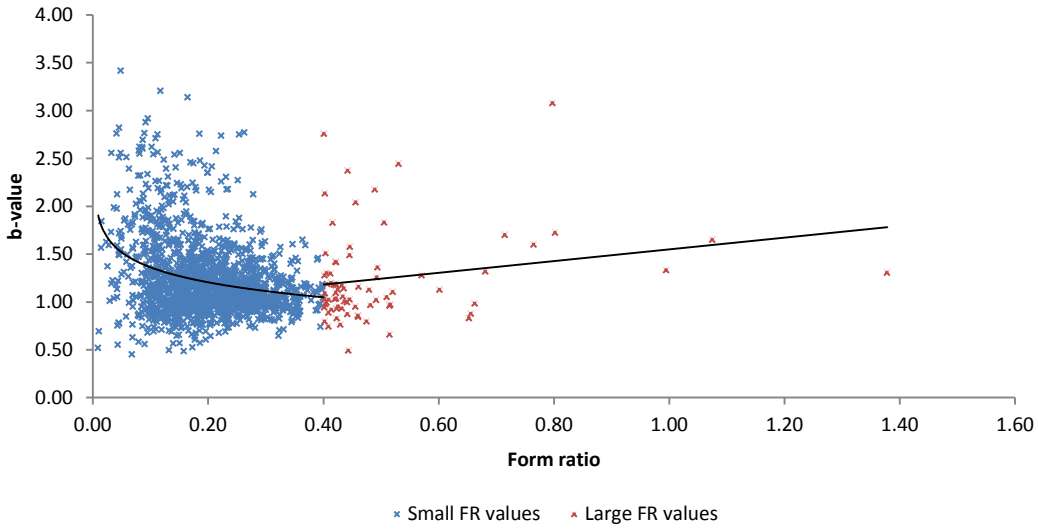

Figure 8.23 In North Patagonia the same pattern occurs as in the Pyrenees (Figure 8.22), albeit much weaker. A negative correlation (R-squared = -0.0752) is evident for valleys (blue) with a form ratio of less than 0.4 and a positive correlation (R-squared = 0.0462) is seen for valleys (red) with a form ratio of 0.4 or greater.

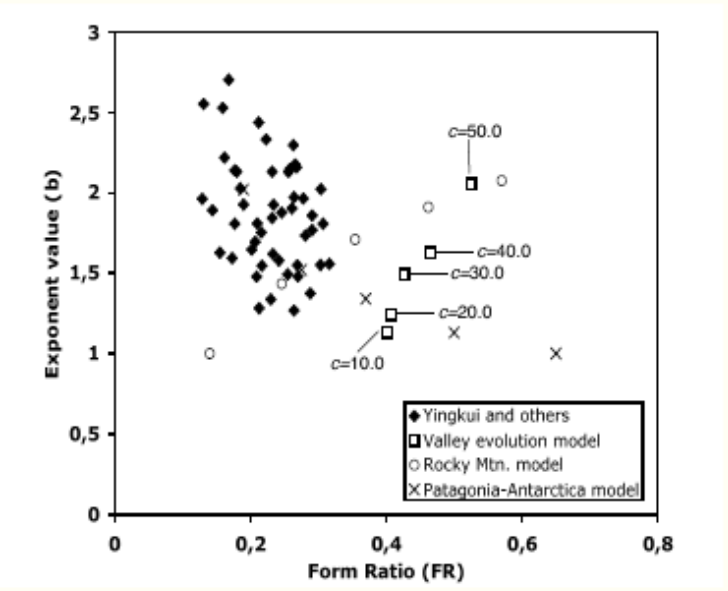

Figure 8.24 A *b-FR* diagram from Seddik *et al.* (2009) comparing field data and model data. Field data from Li *et al.*'s (2001a) research (shown in black diamonds as Yingkui and others) is plotted with Hirano and Aniya's (1988) 'Rocky Mountain' (circles) and 'Patagonia-Antarctic' model data, as well as Seddik et.al's (2009) valley evolution model output. The field data (Li *et al.*, 2001a) shows a negative correlation. All form ratios are below 0.4 and compare closely with the data in this thesis. This contrasts to the Rocky Mountain and Seddik *et al.*'s (2009) model outputs which show a positive correlation.

When comparisons are made on a whole sample area scale, the relationship between the mean valley form ratios and *b*-values in the Patagonia sample areas show a transition from a 'Rocky Mountain' type glaciation to a 'Patagonia-Antarctic' type glaciation. When the Central Patagonia sample area was compared to the Northern Patagonia sample area, both form ratio and *b*-values increased, whilst when the Central Patagonia sample was compared to the Southern Patagonia sample area, *b*-values increased as form ratios remained unchanged or, in the case of the 1st order valleys, decreased.

The geomorphological data shows that deep well-developed valleys are actually quite rare and instead valleys tend to widen with greater glacial erosion. This may be partly due to the sample areas which were chosen not having the combination of highly resistant lithology, such as granite, and intense glaciation. In such cases, a highly resistant lithology may mean that steep valley walls can be maintained. Within the areas sampled several factors could explain the trend towards valleys with low form ratios, firstly the 'buzzsaw' theory (Brozović *et al.*, 1997) of glaciation limiting relief means that

glacial erosion reduces local relief, decreasing the potential depth of valleys by the erosion of divides which reduces peak and ridge height (Oskin & Burbank, 2005) (Figure 8.20). Secondly, whilst the form ratio is affected by limiting of local relief, *b*-values can be affected by sediment fill at the valley floor. Sediment fill creates a flatter valley floor causing a power curve to have greater curvature when fitted to the cross-section and thus exaggerating the resultant *b*-value. Large amounts of fill are most noticeable in the widest valleys (i.e. valleys with low form ratios). Wide valleys are located at the lowest elevations where ice residence times are lowest. These areas are more likely to have been within the ablation zone of former glacial extent and thus have the potential to deposit large amounts of debris, and evidence of this can be seen in the large trunk valleys of the Southern Alps, New Zealand. These two factors, combined with the fact that these valleys are emerging from the mountain range resulting in less available relief, means that the *b*-value and form ratio relationship may well be exaggerated. However, if the form ratio value itself is ignored, therefore eliminating the influence of relief on valleys, valleys exhibit a widening trend, where valleys widen proportionally more than they deepen, which causes the lower form ratios observed. Lower form ratios could not be solely caused by the effects on artificially smaller depth measurements caused by glacial erosion destroying local relief (glacial buzzsaw theory) or any relief reduction from sediment fill. For form ratios to not become lower, and instead stay constant or increase, the discharge required to create such wide (and to maintain the form ratio proportional deep) valleys would be improbably large. This is because discharge scales with approximately the fifth power of ice depth (Paterson, 1994). And, under certain conditions, such as convergent flow, glaciers are able to erode below their base levels so deepening should not necessarily be related to available relief. This is a finding which has generally been ignored by process theory and modelling.

8.5. Understanding *U-ness* results through process theory

One of the key overall results is that in most glacial valleys widening is the dominant process and exceeds downcutting in well-developed (high *b*-values) valleys, which have flat longitudinal profiles and consequently low valley floor slopes. Conversely, deepening occurs in less well-developed glacial landscapes where glaciers have not had the time or intensity to eliminate the fluvial signal, so steep longitudinal profiles still prevail. Although the ice velocity is directly linked to the ice surface slope, the valley floor slope

also contributes to ice velocity, for example, it has been shown that ice velocity reduces directly below a rock step (Fabel *et al.*, 2004). Therefore, in general, steep slopes create fast moving ice. Other factors which create faster moving ice include: temperate glacier regimes; the location of ice within the glacier cross-section, as ice in the centre of the glacier has higher velocities compared to the edges; as well as where the ice is thickest in the longitudinal profile of the glacier which generally occurs at the ELA (Sugden & John, 1976). Evidence for this includes that where sudden increases in ice thickness occur, such as immediately downstream of ice confluences, especially if immediately followed by divergent flow (Shoemaker, 1986), and steps in the valley longitudinal profile which can cause overdeepenings to develop (MacGregor *et al.*, 2000). Many glacial erosion models scale erosion with basal ice velocity (e.g. Harbor, 1992), discussed further in Section 8.6.

Boulton's (1974) abrasion model incorporates several variables including sliding velocity, effective normal pressure (which is a function of gravitational acceleration, density and thickness of ice, less the value of water pressure existing at the ice/bed interface) and a lodgement index. He identified that as effective normal pressure increases so does the abrasion rate up to a threshold, but thereafter increased effective normal pressure actually decreases the abrasion rate and particle lodgement occurs. Hallet (1979) challenged Boulton's (1974) interpretation of effective normal pressure which results in lodgement being predicted for relatively thick glaciers unless basal ice velocity is high. Hallet (1979) suggests that effective contact force between rock particles and the bed is independent of the effective normal pressure due to the rock fragment behaving as a buoyant mass in the ice. Instead, the movement of the rock fragment depends on the viscous drag it experiences which, in turn, depends on the particle properties and the ice velocity normal to the bed. Due to the use of a contact force function, which allows for debris concentration, as in the Boulton (1974) model, lodgement may still occur, but only when basal sliding velocity is extremely low and equivalent to the basal melt rate which could be caused by ice being impeded by very high debris concentrations in ice. Hallet (1979) also noted a difference of the quantity of rock debris entrained in ice from observations in subglacial cavities and after recent ice retreat, and he acknowledged that his model reflected a glacier with scarce rock debris whilst Boulton's (1974) model reflected a debris rich glacier.

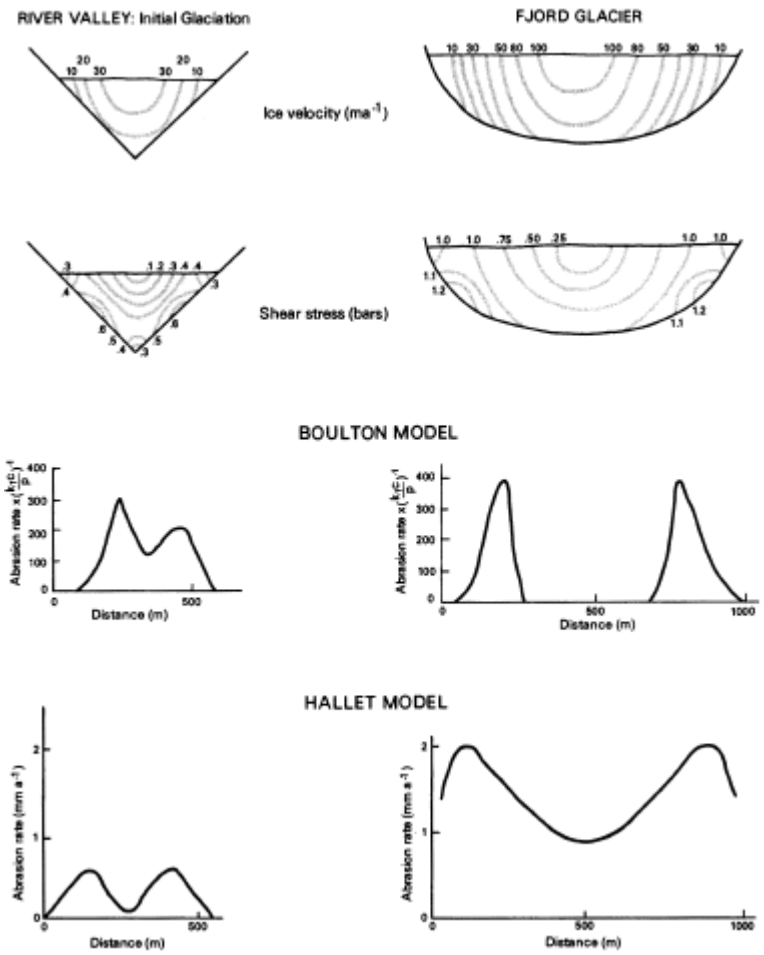

Figure 8.25 Ice velocity, shear stress and predicted rates of abrasion in a fjord glacier using the Boulton (1974) and Hallet (1979) model in research by Roberts and Rood (1984). The figures show that erosion is concentrated on the valley sides over the valley bottom in both the initial and latter stages of trough evolution.

Roberts and Rood (1984) were surprised to find that, when both the Boulton (1974) and Hallet (1979) models were used to derive abrasion rates for the fjord glaciers studied, the models produced valley widening over deepening in both the initial and latter stages of trough evolution (Figure 8.25). When ice occupies a valley, which is a V-shape, erosion is shown to concentrate either side of the valley centre, in order to alter the valley form into a U-shape. This is compared to a wide valley trough where erosion is concentrated much closer to the valley sides due to the increases in shear stress here, and so widening of the valley occurs from greater wearing away of the valley sides compared to downcutting. In the Boulton (1974) model, deposition occurs at the valley bottom by lodgement, whilst the Hallet (1979) model shows that widening is dominant but some deepening still occurs (Figure 8.25). Hallet (1979) argues that the velocities at which

lodgement occurs in Boulton's (1974) model are unrealistically high and Roberts and Rood (1984) agree that the scenario where no erosion occurs is improbable. Nonetheless, the Hallet (1979) model still shows widening dominating over deepening (Roberts and Rood, 1984) and is supported by the geomorphological evidence found in this thesis (Figure 8.9).

The results presented in this thesis show a link between valley floor gradient and valley cross-sectional shape, particularly form ratio, *b*-values and the relationship between them (*b-FR* diagram). It is therefore proposed that the longitudinal profile of valleys is intrinsically linked to the valley cross-section evolution and/or vice versa. The glacial processes described in Boulton (1974) and Hallet's (1974) models could help to identify the reason behind the development of valleys, however, before explanations are proposed, the use of these models in a valley evolution context will be investigated.

8.6. Implications for glacial models

Analysis of valley cross-sectional shape in this thesis has suggested a strong link between glacial valley cross-section and longitudinal development; deep, narrow valleys being found where valley floor slopes are steeper, and wide shallow valleys are found where valley floor gradients are gentler. Numerical models have initially dealt with valley cross-section evolution (Harbor, 1992) and longitudinal evolution (MacGregor *et al.*, 2000) separately. MacGregor *et al.* (2000) constructed a numerical model that created a flattening of longitudinal valley profiles which corresponded well with the profiles seen in real landscapes. Harbor (1992) modelled the evolution of valley cross-sections, successfully creating a U-shape from an initial V-shape. When an ice-discharge constraint is used the active channel reaches a steady state shape. It is interesting to note that the steady state shape has a *b*-value of 2.26 and form ratio of 0.41 which is the form ratio threshold identified in the analysis *b-FR* diagram analysis in Section 8.4.5., however this is not further explored and may well be a coincidence of the constants used in the Harbor (1992) model. After a steady state shape is achieved in the Harbor (1992) model, downcutting is dominant (Figure 2.10) creating deep, narrow valleys. However when Roberts and Roods (1984) applied Boulton (1974) and Hallet's (1979) abrasion models to a wide valley, they found that widening occurred (Figure 8.25). This was due to the valley shape being outside the stable state recognised by Harbor's (1992) model, therefore, similar to when a valley is a V-shape, higher shear stresses occur on

the valley sides where the high curvature is located compared to the centre of the valley. So, once a wide valley occurs, it continues to widen from relatively greater shear stresses (Roberts & Rood, 1984) on the valley sides, but when a valley evolves from an initial V-shape it creates a steady state active channel form which then erodes downwards creating deep valleys. So how does the transition from a deepening valley to a widening valley occur? How is widening initiated? Evidence from the sample areas in this thesis has shown that that widening does occur but so far models have failed to recreate it.

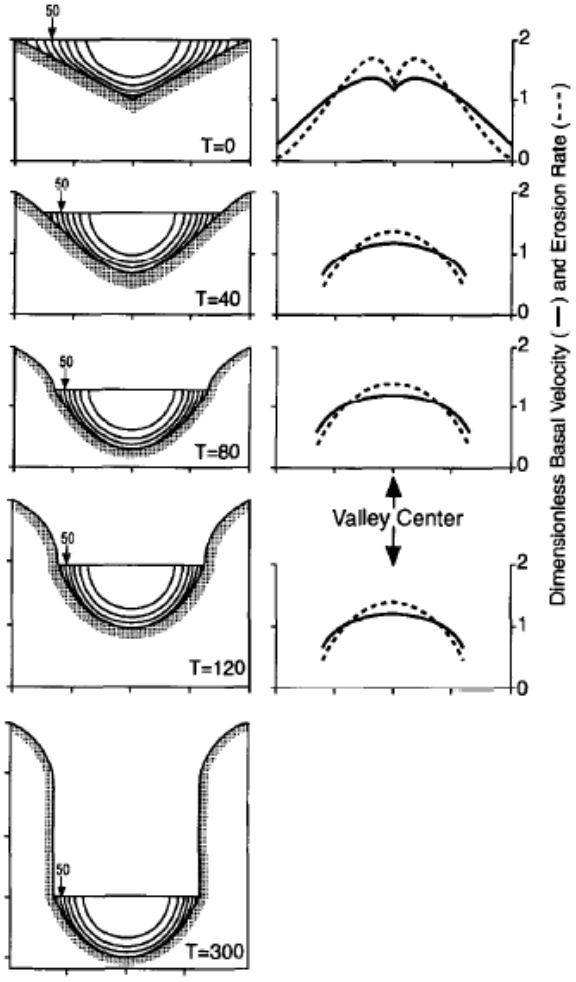

Figure 8.26 Harbor's (1992) model results where erosion is scaled with basal velocity squared. Progressive time steps (T) in valley cross-section evolution show the development of a 'U-shape'. A steady state form is reached in T = 194 after which downcutting occurs.

Seddik *et al.* (2009) recognised that models failed to account for the widening observed in real landscapes. He noted that Harbor (1992) provided little information on the computation of basal shear stress and attempted to develop the model by including lateral drag (Seddik *et al.*, 2005; Seddik *et al.*, 2009) and improving the definition of basal shear stress (Seddik *et al.*, 2009). However when the model results were compared to empirical data by Li *et al.* (2001a) it still failed to create widening from an initial V-shape (Figure 8.27).

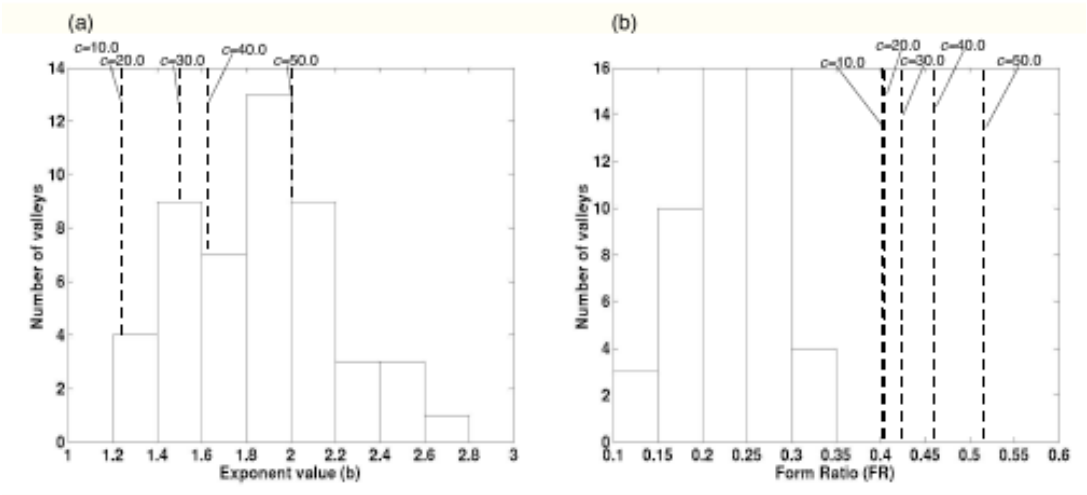

Figure 8.27 Results from Seddik *et al*.'s (2009) model experiment showing that model runs, *c*, conformed well with *b*-values (a) from Li *et al*.'s (2001a) geomorphological results, however model form ratios were far higher than observed values (b). Therefore the model creates valleys which are too deep and narrow.

Harbor's (1992) model adapted and simplified Hallet's (1979) abrasion model so that erosion scaled with basal sliding velocity, which increases proportionally with effective normal stress and towards the centre of the cross-section, despite Hallet (1979) stating that abrasion rates could not be assumed to monotonically increase with particle / bed contact forces (effective normal stress). In fact high contact forces could result in low abrasion or even lodgement. High contact forces can be created by high concentrations of fragments and/or increased bed roughness (amplitude/wavelength), and the interaction between the two (Hallet, 1981), as this reduces ice basal velocity (Figure 8.28 and 8.29). The results in Harbor's (1992) model only show widening either side of the centre line during the initial stages of valley development from a V-shape to a U-shape,

after which the dimensions of the active channel remain the same, and it simply translates vertically, as downcutting is the dominant erosion process (Figure 8.26).

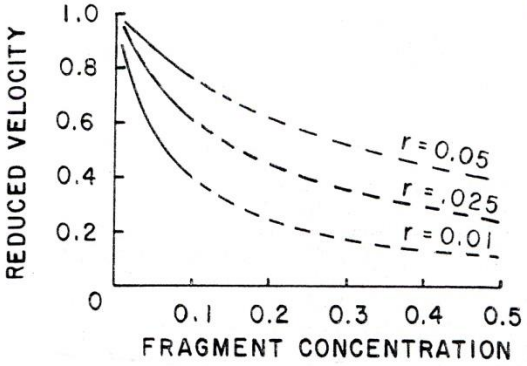

Figure 8.28 When using the Hallet (1981) model of abrasion the effect of debris on sliding rate shown. *r* refers to various bed roughness. It shows reduced velocity with increased debris concentrations.

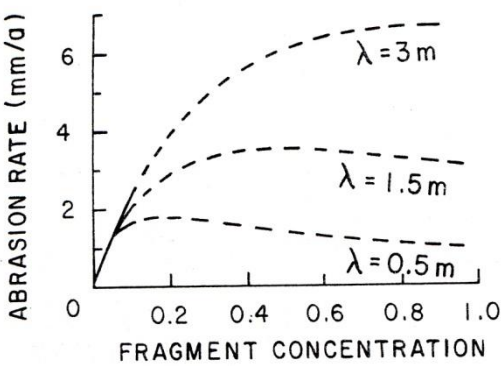

Figure 8.29 This shows the abrasion rate for 200 mm in diameter fragments as a function of the proportion of the bed effectively covered by debris. Bed roughness was given a value of 0.05 and λ defines the wavelengths of bed undulations. It shows that low wavelengths cause a reduction in abrasion rate with increased fragment concentration (Hallet, 1981).

In spite of Harbor's (1992) assertion that valleys only deepen, his research does hint to a widening trend in a low velocity ice flow setting. No comment was made on this result, beyond mentioning that steady state was not reached. In fact the results clearly show that, when the velocity component in Harbor's (1992) model is low, the valley form initially increases, as both form ratio and *b*-value increase, but after 100 time steps the model produces a gradual decrease in form ratio whilst *b*-values still increase (Figure 8.30).

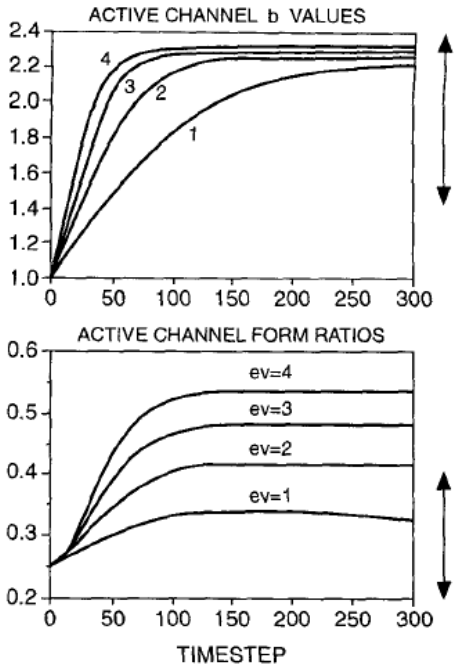

Figure 8.30 A sensitivity test by Harbour (1992) for the *ev* exponent of basal ice velocity. It shows that when *ev* is given a value of 1 form ratios decrease after time step 100, whilst *b*-values continue to increase and, unlike for higher *ev* values, no steady state is achieved. *ev* = 2 was used in the main model runs (Harbor, 1992).

Evidence from geomorphological data in this chapter shows that form ratio is linked to valley floor slope, with wide, relatively shallow valleys occurring at low slope gradients and therefore the change in valley floor slope may well initiate valley widening i.e. slope controls width. It has been demonstrated that once widening has occurred it is enhanced (Roberts & Rood, 1984)(Figure 8.25), but it is not understood how this is initiated. To find an explanation for valley widening initiation, the literature from process studies and modelling research is examined. Slope changes in the valley floor could have several changes in a number of glacial processes. For example it could change ice velocity. Hallet (1979) states that a particle embedded in ice will move when the viscous drag due to the ice flowing past it and the down-slope component of its buoyant weight exceeds the frictional drag of the fragment against the bed. Therefore slower ice velocities can prevent the frictional drag being exceeded and thus causing debris lodgement (Boulton *et al.*, 1974; Hallet, 1979). When ice and debris is not moving against the bed then erosion does not occur as there is no vehicle for abrasion or plucking. No erosion at the bed means that there cannot be any downward denudation and valleys are not deepened.

From research in this thesis it is known that wide glacial valleys occur in landscapes and that these valleys occur where the valley floor slope flattens. In order for widening to occur, erosion has to switch from a proportionally greater amount at the centre of the valley, which causes deepening, to proportionally more erosion on the valley sides to create a widening effect. The process explanation for the initiation of valley widening is unknown and therefore requires further research which is outside the scope of this thesis.

What is known is that once the valley form is widened beyond the 'steady state', condition widening will continue by increased shear stress from the deviation of the stable state valley form (Roberts & Rood, 1984). As such, understanding the initiation of valley widening is key to modelling realistic valley formation. Current models generally scale erosion with cross-sectional basal ice velocity (Harbor, 1992). Research in this thesis has shown that this might not be appropriate. By scaling erosion with ice velocity, erosion is always concentrated at the valley centre, meaning that valley formation is always caused by downcutting and widening cannot occur. Therefore to improve valley-scale models such as by Harbor (1992), these should be linked to valley longitudinal profile models (MacGregor *et al.*, 2000) with a widening initiation threshold.

Modelling has advanced from valley-scale models to modelling of whole landscapes. The physics used in landscape evolution models reflects process knowledge and valley-scale modelling but is forced to simplify glacial processes even further, for example by using the shallow ice approximation (Braun *et al.*, 1999; Tomkin & Braun, 2002; Egholm *et al.*, 2009; Tomkin, 2009) to define glacial erosion. The shallow ice approximation computes shear stress parallel to the bed which is dependent on ice thickness and has been shown to replicate ice sheet erosion well (Mangeney & Califano, 1998), however it is less suited to alpine settings where it struggles to create U-shaped valleys from an initial V-shape (Figure 8.31) (Seddik *et al.*, 2009). Modellers justify its use due to the coarseness of model grid-scales (Tomkin, 2009). With this model, erosion is concentrated in the centre of the valley, where ice thickness is greatest, and the effect of valley sides on ice flow are ignored (Seddik *et al.*, 2009) (Figure 8.31) and effectively creating a similar problem to that in Harbor (1992). With the addition of the finding that, in some circumstances, valleys widen rather than deepen, the shallow ice approximation appears even less appropriate in attempting to reconstruct glacial landscapes.

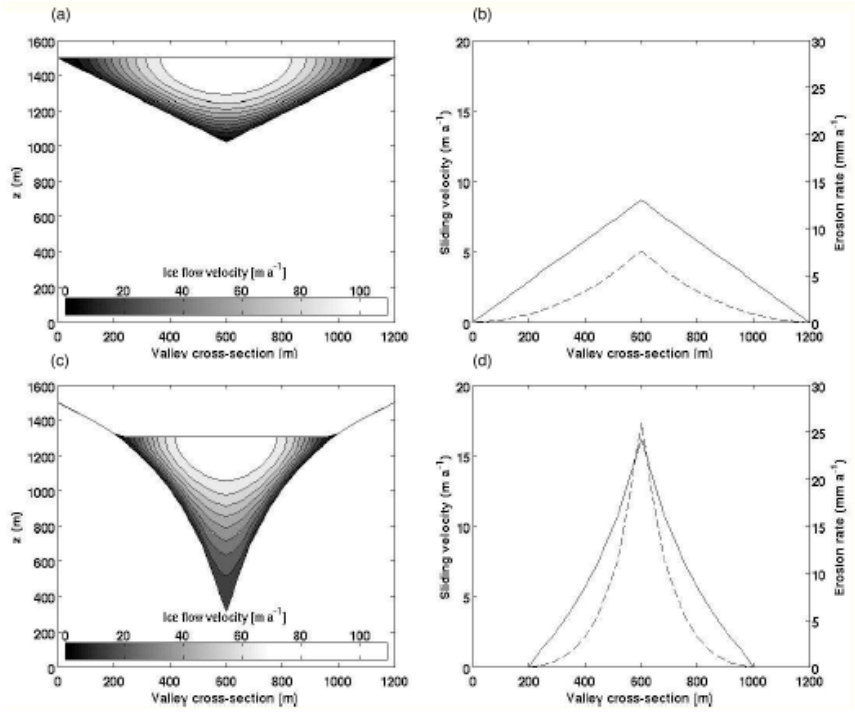

Figure 8.31 Modelling experiment by Seddik *et al.* (2009) showing initial V-shape valleys (a) and the resultant valley after the shallow-ice approximation is used (c). (b) and (d) show the corresponding valley cross-section variation in sliding velocity (solid line) and erosion rates(dashed line). The experiment shows the inability of the shallow-ice approximation to form U-shaped valleys.

In combination with the shallow ice approximation and similar to Harbor's (1992) research, landscape evolution models often incorporate generalised glacial erosion laws such as Hallet's (1979) abrasion model, where glacial erosion is set as proportional to sliding (Braun *et al.*, 1999; Tomkin & Braun, 2002; Tomkin, 2009). From research in this thesis it is suggested that landscape evolution models need to incorporate a slope dependent ice erosion threshold which initiates widening over deepening. This would mean that valleys evolve by first altering a V-shape cross-section into a U-shape before eroding downwards. Downcutting then results in the flattening of the longitudinal profile which in turn initiates widening.

To conclude, both valley-scale and landscape-scale models do not recreate the widening initiation in valley development seen in real landscapes, thought to be triggered by a decrease in valley floor slope from the flattening of the glacial valley longitudinal profile. Once widening has occurred from the stable state form it has been shown that it continues (Roberts & Rood, 1984). This provides a process explanation for 'Patagonia-Antarctica' and 'Rocky Mountain' type glacial models (Hirano & Aniya, 1988).

Landscapes which have undergone the longest and most intense glaciation have a ‘Patagonia-Antarctica’ type glacial landscape featuring wide, relatively shallow valleys as well as flat longitudinal profiles, whilst a ‘Rocky Mountain’ type landscape, which has deep, relatively narrow type valleys, develops in less intense glacial scenarios (this can be due to being in an area which has been exposed to lighter glaciations or less within a section of a valley system which has had less ice flux, and therefore both types of valleys can be found in a single mountain range). As the valley evolves downcutting flattens the longitudinal profile which then initiates widening.

8.7. Summary

By providing a large dataset of valley cross-sections, over several differing sample areas, a much more comprehensive overview of real valley shapes and sizes has provided a resource for examining the evolution of valley cross-sections. By studying the spatial variability of these valleys within mountain ranges has given additional insight into valley evolution, in particular the finding that valley cross-section evolution is linked to the development of the valley longitudinal profile. The key findings in this thesis will be summarised in the following chapter (Chapter 9).

9. Conclusion

9.1. Introduction

In this thesis a method was developed which generated large volumes of valley cross-section data. This provided an opportunity to better quantify valley shapes and to explore how glacial valley shape and sizes vary within mountain ranges and differ between areas. Trends with ice flux and residence time proxies, as well as spatial patterns, have given insight into valley development and the glacial processes which create the distinct glacial valley cross-sectional form. The key findings in this thesis are summarised in the following sections. The final section makes suggestions for further research.

9.2. Advancement in valley cross-section profile methodology

Glacial process theorists, as well as glacial landscape modellers, have expressed frustration at the lack of empirical data to test their research against (e.g. Seddik *et al.*, 2005). The advancements in GIS software combined with the increasing availability of datasets on topography have the potential to be a powerful tool to analyse glacial geomorphology. Despite this GIS science has not sufficiently developed to provide solutions which produce the quantity of empirical data other researchers require to progress with their work. In support of this view Napieralski *et al.* (2007) noted that GIS has presently been underutilised, particularly in glacial geomorphology. The GIS methods developed in this thesis aimed to overcome some of the current data limitations.

The GIS-based method in Chapter 4 enables a consistent means for producing large quantities of data on cross-sectional topography across whole mountain ranges. This method is a different approach to the more commonly used individually selected transect method and is meant as an alternative which can be used to complement other research on valley cross-sectional form. As the method used in this thesis is non-

selective it overcomes several problems associated with fitting power-curves to transects. The method in this thesis also improves on the GIS-based method developed by Phillips (2009) as it is fully integrated into one piece of software, ArcGIS, as well as allowing for analysis of individual valley segments, and also eliminates the head of the valley from the first order valley segments.

In this thesis the method was used to generate the equivalent of 1,000 times more data than that produced in all the previous reported investigations. Measures of valley shape and size were obtained from applying the method to the sample areas chosen for this research. Trends both within mountain ranges and between ranges revealed relationships between variables which are both interesting in their own right as well as providing yet more data for comparison with model results. In Chapter 7 Geographical Weighted Regression (GWR) was used to analyse spatial trends and proved a useful statistical technique from the respect of understanding multiple regression as well as trends within sample areas. Although GWR has been used to detect spatial trends in human geography, it is not currently used widely in physical geography applications, but this research shows how valuable the technique can be in untangling spatial trends.

9.3. Measures of glacial valley cross-sectional shape and size and dataset use in modelling

Results from the five sample areas were arranged in a single dataset to ascertain the range of glacial valley shapes and sizes. This dataset is useful in understanding the spread and distribution of *U-ness* measures (Table 9.1 and Figure 9.1). It is now possible for glacial modellers to compare model outputs with the range of shapes and sizes found in real world examples. If the model outputs do not fall within the real world values, and the distributions of measures are not similar, then it can be inferred that the processes in the model are not formulated satisfactorily. It is possible for the dataset in this thesis to be used directly for comparisons with model outputs, or the method could be used to generate data from specific sample areas for model experiments.

Table 9.1 A summary of the *U-ness* statistics for valley segments within LGM limits, a total of 8005 valley segments are included which results in 334,068 equivalent individually selected transects.

	Minimum	Mean	Median	Mode	Maximum
***b*-value**	0.003	1.38	1.24	1.13	3.56
Form ratio	0.0009	0.20	0.19	0.20	1.74
Cross-sectional area (m²)	301	206,058	171,460	102,550	1,736,100

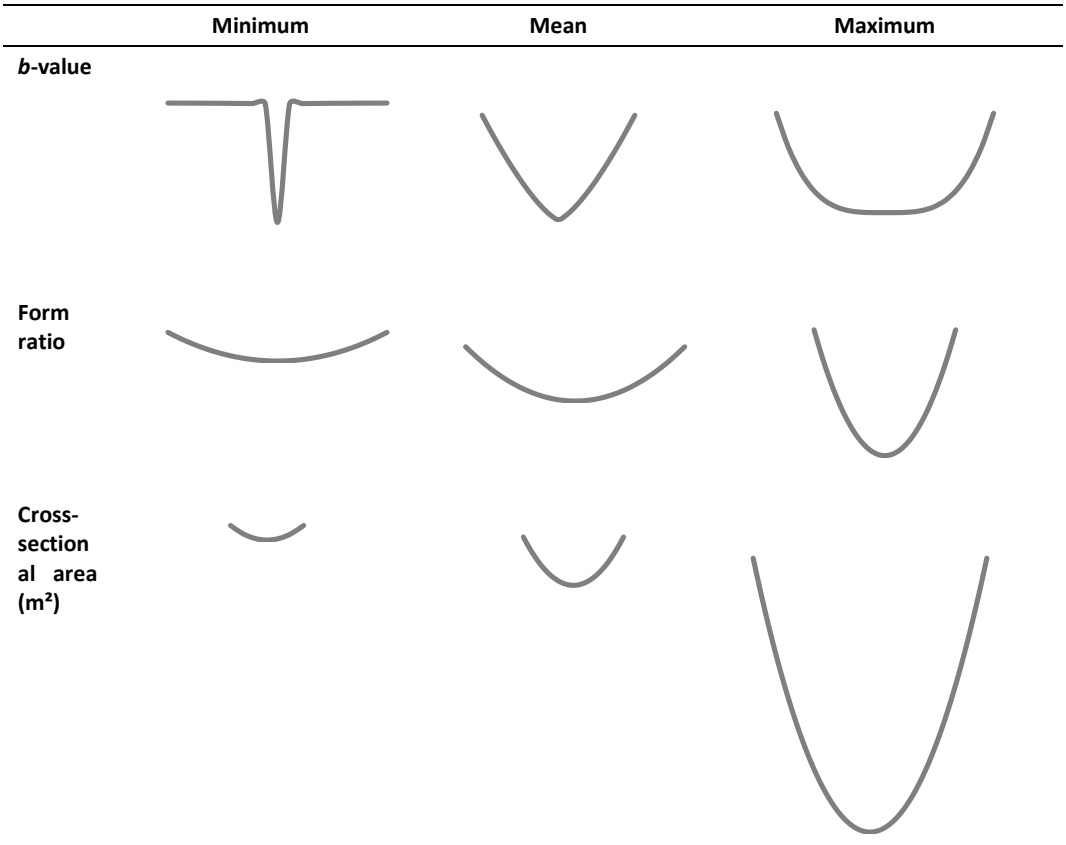

Figure 9.1 The minimum, mean and maximum *U-ness* statistics for the entire dataset of LGM valleys represented schematically. If model outputs do not replicate this spread of values then it can be inferred that the model is not adequately representing the real world.

Results, particularly those for form ratio, indicated that valleys tended to became wider and shallower both down valley and in areas which had been intensely glaciated, like South Patagonia. Although form ratios taken from valley cross-sections at LGM margins need to be treated with caution as mountain structure and former fluvial erosion could have created wide valleys, valleys tend to decrease in depth and widen; a reduction in valley depth is consistent with the glacial buzzsaw theory (Brozović *et al.*, 1997) which suggested that glaciation limits mountain relief. The same result parallels with previous research on valley development, for example the 'Rocky Mountain' verses 'Patagonia-Antarctica' models of glaciation (Hirano & Aniya, 1988). Here the 'Rocky Mountain' model was found to be much rarer than suggested and the 'Patagonia-Antarctica' model prevails, even in areas not associated with intense and prolonged glaciations such as the Southern Alps of New Zealand, (although a region of very resistant lithology, which is associated with deep, narrow valleys (Augustinus, 1992a), was not investigated in this research). Results also give insight regarding valley evolution, as mentioned above, it was found that although deep, narrow valleys occur, wide, relatively shallow, valleys were predominant. This jars with the valley development model created by Harbor (1992) where downcutting is concluded to be the dominant process. Seddik *et al.* (2009) recognised the lack of widening in current models but have yet to create a mechanism for valley widening in a modelling context.

Investigations into understanding valley widening in this thesis reached several conclusions. Firstly, that lack of available local relief in parts of mountain ranges can mean that valleys are proportionally wider than deeper. In alignment with this, limiting of relief in glacial landscapes by the glacial buzzsaw theory could cause a similar result, in that valleys are proportionally wider than deeper. These, however, are side issues resulting from using form ratio to understanding valley development. When the actual width and depth of valleys are compared a trend for widening, especially in large trunk valleys (i.e. those which have had a large ice flux), is evident. As of yet this is not replicated in any valley or landscape-scale model. Current models have successfully developed U-shaped valleys from initial V-shapes (Harbor, 1992), followed by a valley cross-section achieving a steady state form (Harbor, 1992), whilst the only model of valley widening occurs when a valley has a wider shape than the steady state form and here widening continues from positive feedback mechanisms (Roberts & Rood, 1984). Therefore the missing link is how widening is initiated. Once this is understood in a process context then models can be improved.

9.4. Valley morphology data demonstrates ice flux and residence time both influence valley characteristics

The results (Chapter 6 and 7) proved that a confounding problem between ice residence time and flux is evident in the valley geomorphology. Where large ice flux occurred in a valley (usually in downstream valley segments at low elevations), ice is likely to have had a short residence time. This creates a combined effect imprinted on the valley geomorphology over multiple glaciations, as ice waxes and wanes. The confounding problem has rarely been articulated by researchers. An exception is Porter (1989), where he expressed that glacial erosion would be greatest at the average ELA (defined as the average point the ELA was situated through the cumulative effects of all glaciations) and Andrews (1972). It is suggested that the confounding problem concept is given more attention within glacial geomorphology and that further research gives more precedence to the combination of effects of glaciations, as well as their intensity and duration, rather than treating geomorphology as a snapshot of a single episode, which is of course a simplifying temptation. This research found that valleys displayed the greatest adaptation to ice mid-way down their trunk valleys suggesting that this is where most reshaping occurred and likely records the position of the average ELA.

It was observed that valleys in lightly glaciated regions, such as the Pyrenees, still showed evidence of a fluvial signature whilst intensely glaciated regions, like south Patagonia, had eliminated this. This supports views that glaciers exploit any existing fluvial valleys, adapting valleys into a glacial form.

In general, greater potential ice flux (deduced from larger contributing catchment areas), rather than ice residence time, had a greater influence on the glacial valley cross-sectional shape and size. For the *U-ness* measures of *b*-value and cross-sectional area large values are found in valleys with larger potential ice flux. However, high form ratios (deep, narrow valleys) were found where high ice residence times occur. Lower form ratios (wide, relatively shallow valleys) were found to occur in valleys with the largest potential ice flux. GWR analysis confirmed this finding spatially within sample areas. It was therefore concluded that the more ice flux is available, rather than the amount of time the ice has existed in a valley, the greater the intensity of glacial erosion which forms large, wide, parabolic valleys. This indicates that most glacial erosion occurs where the ice flux is greatest and not where it has persisted for longest.

9.5. Acknowledging the importance of local effects on geomorphology

Spatial analysis (Chapter 7) of the variability in valley cross-sections identified the impact of local effects on glacial erosion. Local effects could be valley floor shading, accumulation of windblown snow or the addition of avalanche debris on the glacier, for example. Evidence, in the Southern Alps for example, revealed different valley *U-ness* measures, even in valleys which are adjacent and had similar, lithologies, climate, elevation and catchment areas. Although some researchers recognise the effect of local effects on glacial accumulation areas (e.g. Brocklehurst & Whipple, 2006), most research on local effects concerns cirque development (Haynes, 1968; Evans, 1977) rather than valley geomorphology. The importance of local effects on glaciers should be incorporated into geomorphological understanding. It is proposed that local factors can influence ice extent and erosion intensity, including valley orientation and shading, as well as the influence of avalanche debris and leeward slopes on snow accumulation and ablation. It was also concluded that such local effects on valleys were more important than variations in rock structure.

9.6. Understanding valley cross-sectional shape and size

9.6.1. V to U shaped valley paradigm

Valleys change from a V-shape to a U-shape, indicating the transition from a fluvially dominated landscape to a glacially dominated one, which has long been employed in thinking about the evolution of valleys. Although in this thesis a progression towards a parabolic form was identified in glacial valley development, fluvial valleys did not develop to a single distinct form. In fact fluvial valleys occupied a wide range of valley shapes, not simply the V-shape referred to in previous, particularly glacial orientated, literature. This means these idealised forms cannot be solely used to distinguish between glacial and fluvial valleys, a result also found by Phillips (2009). For modellers this finding also means that an initial fluvial landscape, before glaciations occurs, should consist of a wide range of valley shapes not simply a V-shape.

9.6.2. Glacial valleys are less parabolic than previously thought

It has long been accepted that the *b*-value of a power curve is a good representation of the development of glacial valleys (Svensson, 1959). Analysis of *b*-values here showed that they represent fluvial valley form poorly. This is because fluvial valleys have many valley shape types, other than parabolic, as well as having more irregular shapes. However, when using the power curve for glacial valleys, *b*-values mostly conformed to a parabolic shape between values of 1 and 2, although it was found they have smaller *b*-values than expected from the literature (Figure 9.2). Such smaller *b*-values were attributed to the nature of the method including all slope anomalies. It is also thought that when transects are individually selected the profiles which best represent the U might be selected, thus creating a bias in the data.

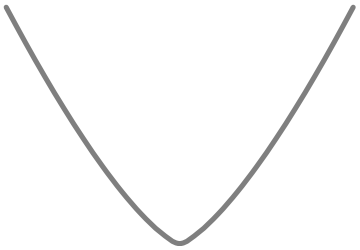

Figure 9.2 The mean valley parabolic shape (*b*-value = 1.38) of all glacial valleys in all sample areas. This value compares with the often quoted *b*-value of 2 in the literature.

Despite valleys generally being found to be less parabolic than expected, some situations artificially increased the *b*-value. In particular the impact of sediment fill was found to increase *b*-values by creating flatter valley floors which causes higher curvature of the power curve. This was found in particular in the large valleys of the Southern Alps. It is therefore important that attention is paid to the affect of sediment fill on the power curve and caution used on results in regions with sizeable deposition at valley floors.

In spite of the limitations of using *b*-values to indicate the extent to which a valley has been altered into U-shaped valley, it still proved useful in ascertaining glacial erosion intensity. In Patagonia *b*-values showed a clear increase with latitude, which here is used as a proxy for the intensity of glaciation. In the Pyrenees more favourable conditions for ice accumulation (higher precipitation and lower solar radiation) north of the divide

were also indicated by greater *b*-values. It is concluded that *b*-values are helpful in indicating the intensity of glacial erosion.

9.6.3. Valley cross-sectional area discriminates between fluvial and glacial valleys but does not inform understanding through spatial variability

Valley cross-sectional area is a measure of the valley size. It was shown by Phillips (2009) that valley cross-sectional size best discriminated between glacial and fluvial valleys, far outperforming *b*-values as a discriminator. This thesis concurred with Phillips (2009) in that glacial valleys were found to be much larger than fluvial valleys. Cross-sectional area, however, showed high variability within valley systems. Since cross-sectional area was good at discriminating between valley types (fluvial and glacial), it was surprising that good spatial trends were not evident. Further research showed that this could be attributed to the sensitivity of the measure to local relief and ridge height. As such it is concluded that the valley cross-sectional area is only useful when comparing glacial and fluvial valleys and not a good measure in understanding spatial trends within glacial valley systems.

9.6.4. Form ratio alludes to valley development

The highest form ratios (deep, narrow valleys) were found near the mountain divide whilst lower form ratios (wide, relatively shallow valleys) were identified towards the LGM extents. As a consequence of this, when form ratio was analysed with respect to ice flux (catchment area), a negative relationship emerged. The amount of available relief for downcutting was no doubt a factor here; however when form ratio was examined in terms of width and depth, and explored using scatter plots, it was seen that glaciers switch the focus of erosion from a valley deepening to a widening trend. This is an important finding when understanding how valleys develop.

9.7. The extent to which favourable conditions for glacial erosion are expressed in valley morphology

It was hypothesised that more favourable conditions for ice accumulation would result in valley cross-sections showing a greater degree of glacial erosion as reflected in the *U-ness* measures. Results from Patagonia showed a clear increase in *U-ness* with latitude. More mature glacial valleys (i.e. higher *b*-values) were observed further south. When climate variations were observed within the Pyrenees, valleys which had more precipitation and a more northerly aspect had greater *U-ness* values, which is consistent with the idea that these valleys experienced more intense glacial erosion.

Previous literature had suggested that higher tectonic uplift rates promoted greater erosion. In this thesis higher form ratios (deep, narrow valleys) were found in areas which had undergone high uplift during glaciation. This was inferred to be due to uplift maintaining steep valley floor slopes, thus causing a downcutting erosional tendency rather than a widening trend.

Other influences on *U-ness* measures include the impact of valley floor fill particularly on *b*-value results. Fill was found to artificially increase *b*-values and therefore b-values calculated in areas which have significant valley fill should be treated with caution. Fill had less of an impact on overall valley depth but still needs to be considered. The GPL solution to valley floor fill was not found to be effective in forcing the parabolic curve much below the profile's valley floor and more work is required to find a mathematical solution to this problem.

9.8. Valley cross-section development linked to longitudinal profile evolution

A close relationship was found between valley floor slope and form ratio. Steep valley floor slopes were associated with deep and narrow valleys whilst wide and shallow valleys had low valley floor slopes. This finding suggests that feedbacks exist between the focus of glacier cross-sectional erosion (downcutting versus widening) and the development of valley longitudinal profiles. More mature glacial valleys have been shown to have flatter longitudinal profiles (MacGregor *et al.*, 2000). In this thesis, and

implied in the 'Rocky Mountain' / 'Patagonia-Antarctica' type glacial models (Hirano & Aniya, 1988), more mature valleys have cross-sectional profiles which are wider and relatively shallower i.e. those found in south Patagonia.

Although valley cross-section and longitudinal development has been studied and modelled separately (Harbor, 1992; MacGregor *et al.*, 2000) they have not been linked before. Following the empirical investigations in this thesis, a feedback mechanism between the valley longitudinal profile and cross-sectional area is suggested, whereby underdeveloped glacial valleys have steep valley floor profiles which promote erosional downcutting. As downcutting continues it flattens the longitudinal profile of the valley until the valley floor slope reaches a point where the erosional focus switches to widening.

9.9. Further research suggestions

The benefits of continuing research in this area of glacial geomorphology include increasing knowledge of how landforms are created in order to inform the understanding of how processes operate. Incorporating better process knowledge into modelling, including landscape evolution models, improves model outputs and the robustness of conclusions drawn from these experiments. Landscape change over long timescales (several glaciations) cannot be observed, consequently a modelling approach, in the form of landscape evolution models, is relied upon to understand landscape development. A contribution to the correct formulation of these models enables further research to be undertaken. Within this thesis, several areas in need of additional research have been highlighted. These areas are summarised below;

1. Improve understanding of local effects on glacial valley development (e.g. valley shading).
2. Find the actual process reason for valley widening initiation, which satisfies the identified link between valley cross-sectional development and valley longitudinal profile.
3. Once known, valley widening should be incorporated into valley and landscape scale evolution models.

4. Further investigation into the form ratio threshold, identified in this thesis as 0.4, where a transition between the 'Patagonia-Antarctica' and 'Rocky Mountain' type glaciation appears to occur.

9.10. Summary

This thesis has taken a step towards the production of large quantities of consistently measured, valley cross-sectional statistics; a method which complements the alternative method of individually selected valley profiles. It answers the call from modellers for more real world data to test and verify model outputs against. The results produced by this method in this thesis have given insight into valley development and glacial erosion processes. In this chapter the major findings of the thesis have been concluded and suggestions have been made for improvements to models, as well as areas in which further research should take place.

10. Bibliography

Amerson, B. E., Montgomery, D. R. & Meyer, G. (2008) Relative size of fluvial and glaciated valleys in central Idaho. Geomorphology 93, 537-547.

Anderton, P. W. & Chinn, T. J. (1978) Ivory Glacier, New Zealand, an IHD representative basin study. Journal of Glaciology 20, 67-84.

Andrews, J. T. (1972) Glacier power, mass balance, velocities and erosion potential. Zeitschrift für Geomorphologie 13, 1-17.

Andrews, J. T. & Miller, G. H. (1972) Quaternary history of the northern Cumberland Peninsula, Baffin Island, N.W.T., Canada. Part IV: Maps of the present glaciation limits and lowest equilibrium line altitude for north and south Baffin Island. Arctic and Alpine Research 4, 45-59.

Aniya, M. & Welch, R. (1981) Morphological analyses of glacial valleys and estimates of sediment thickness on the valley floor: Victoria valley system, Antarctica. Antarctic Record 71, 76-95.

Ariztegui, D., Bösch, P. & Davaud, E. (2007) Dominant ENSO frequencies during the Little Ice Age in Northern Patagonia: The varved record of proglacial Lago Frías, Argentina. Quaternary International 161, 46-55.

Augustinus, P. C. (1992a) The influence of the rock mass strength on glacial valley cross-profile morphometry: A case study from the Southern Alps, New Zealand. Earth Surface Processes and Landforms 17, 39-51.

Augustinus, P. C. (1992b) Outlet glacier trough size-drainage area relationships, Fiordland, New Zealand. Geomorphology 4, 347-361.

Augustinus, P. C. (1995a) Glacial valley cross-profile development: the influence of in situ rock stress and rock mass strength, with examples from the Southern Alps, New Zealand. Geomorphology 14, 87-97.

Augustinus, P. C. (1995b) Rock mass strength and the stability of some glacial valley slopes. Zeitschrift für Geomorphologie 39, 55-68.

Batt, G. E. & Braun, J. (1999) The tectonic evolution of the Southern Alps, New Zealand: Insights from fully thermally coupled models dynamical modeling. Geophysical Journal International 136, 403–420.

Beavan, J., Samsonov, S., Motagh, M., Wallace, L., Ellis, S. & Palmer, N. (2010) The M*w* 7.1 Darfield (Canterbury) earthquake: Geodetic observations and preliminary source model. Bulletin New Zealand Society of Earthquake Engineering 5, 392–409.

Beighley, R. E., Dunne, T. & Melack, J. M. (2005) Understanding and modeling basin hydrology: interpreting the hydrogeological signature. Hydrological processes 19, 1333-1353.

Bennett, M. (1990). The Cwms of Snowdonia: A Morphometric Analysis, London: Department of Geography, Queen Mary and Westfield College.

Bieniawski, Z. T. (1984) The design process in rock engineering. Rock Mechanics and Rock Engineering 17, 183-190.

Blisniuk, P. M., Stern, L. A., Chamberlain, C. P., Idleman, B. & Zeitler, P. K. (2005) Climatic and ecologic changes during Miocene surface uplift in the Southern Patagonian Andes. Earth and Planetary Science Letters 230, 125–142.

Boulton, G. S., Dent, D. L. & Morris, E. M. (1974) Subglacial Shearing and Crushing, and the Role of Water Pressures in tills from South-East Iceland. Geografiska Annaler. Series A, Physical Geography 56, 135-145.

Braun, J. & Sambridge, M. (1997) Modelling landscape evolution on geological timscales: a new method based on irregular spatial discretization. Basin Research 9, 27-52.

Braun, J., Zwartz, D. & Tomkin, J. H. (1999) A new surface-processes model combining glacial and fluvial erosion. Annuals of Glaciology 28, 282-290.

Brocklehurst, S. H. & Whipple, K. X. (2006) Assessing the relative efficiency of fluvial and glacial erosion through simulation of fluvial landscapes. Geomorphology 75, 283-299.

Brook, M. S., Brock, B. W. & Kirkbride, M. P. (2003) Glacial outlet valley size - drainage area relationships:some considerations. Earth Surface Processes and Landforms 28, 645-653.

Brook, M. S., Kirkbride, M. & Brock, B. W. (2004a) Rock strength and development of glacial valley morphology in the Scottish Highlands and Northwest Iceland. Geografiska Annaler 86A, 225-234.

Brook, M. S., Kirkbride, M. & Brock, B. W. (2004b) Rock Strength and Development of Glacial Valley Morphology in the Scottish Highlands and Northwest Iceland. Geografiska Annaler: Series A, Physical Geography 86, 225-234.

Brook, M. S., Kirkbride, M. & Brock, B. W. (2008) Temporal constraints on glacial valley cross-profile evolution: Two Thumb Range, central Southern Alps, New Zealand. Geomorphology 27, 24-34.

Brook, M. S., Kirkbride, M. P. & Brock, B. W. (2006) Quantified time scale for glacial valley cross-profile evolution in alpine mountains. Geology 34, 637-640.

Brook, M. S. & Tippett, J. M. (2002) The influence of rock mass strength on the form and evolution of deglaciated valley slopes in the English Lake District. Scottish Journal of Geology 38, 15-20.

Brown, E. T. (1981). Rock characterization, testing & monitoring: ISRM suggested methods Oxford: International Society for Rock Mechanics.

Brozović, N., Burbank, D. W. & Meigs, A. J. (1997) Climatic limits on landscape development in the Northwestern Himalaya. Science 276, 571-574.

Brunsdon, C., Fotheringham, S. & Charlton, M. (1998) Geographically weighted regression - modelling spatial non-stationarity. The Statistician 47, 431-443.

Brunsdon, C., McClatchey, J. & Unwin, D. J. (2001) Spatial variations in the average rainfall - altitude relationship in Great Britain: An approach using geographically weighted regression. International Journal of Climatology 21, 455-466.

Burbank, D. W., Leland, J., Fielding, E., Anderson, R. S., Brozović, N., Reid, M. R. & Duncan, C. (1996) Bedrock incision, rock uplift and threshold hillslopes in the northwestern Himalayas. Nature 379, 505-510.

Calvet, M. (2004). The Quaternary glaciation of the Pyrenees., In Quaternary Glaciations - Extent and Chronology. Part I: Europe., edited by J. Ehlers & P. L. Gibbard, London: Elsevier.

Campbell, J. F. (1865). Frost and Fire. Edinburgh: Edmonston and Douglas.

Chinn, T. J. & Whitehouse, I. E. (1978). *Actes de l'Atelier de Riederalp*. Riederalp: IAHS-AISH.

Choukroune, P. (1992) Tectonic evolution of the Pyrenees. Annual Review of Earth Planetary Science 20, 143-158.

Chueca, J. & Julián, A. (1996). Datación de depósitos morrénicos de la Pequeña Edad del Hielo: macizo de la Maladeta, In Dinámica y Evolución de Medios Cuaternarios, edited by A. Pérez Alberti, P. Martini, W. Chesworth & W. Martínez Cortizas, pp. 171–182. Santiago de Compostela: Xunta de Galicia.

Clayton, K. (1996) Quantification of the impact of glacial erosion on the British Isles. Transactions of the Institute of British Geographers 21, 124-140.

Climate change, impacts and vulnerability in Europe 2012 (2012). European Environment Agency.

Colombo, R., Vogt, R. V., Soille, P., Paracchini, M. L. & de Jager, A. (2007) Deriving river networks and catchments at the European scale from medium resolution digital elevation data. Catena 70, 296-305.

Copons, R. & Bordonau, J. (1994). La Pequeña Edad del Hielo en el Macizo de la Maladeta (alta cuenca del Esera, Pirineos Centrales), In El Glaciarismo surpirenaico: nuevas aportaciones, Geoforma Ediciones, edited by C. Martí-Bono & J. García-Ruíz, pp. 111–124. Logroño.

Coronato, A., coronato, F., Mazzoni, E. & Vázquez, M. (2008). Physical geography of Patagonia and Tierra del Fuego, Vol. 11, In Late Cenozoic of Patagonia and Tierra del Fuego. Development in Quaternary Sciences, edited by J. Rabassa, pp. 13–56. Amsterdam: Elsevier.

Coronato, A., Martínez, O. & Rabassa, J. (2004). Glaciations in Argentine Patagonia, southern South America. In Quaternary Glaciations - Extent and Chronology.

Part III: South America, Asia, Africa, Australasia, Antarctica., edited by J. Ehlers & P. L. Gibbard, London: Elsevier.

Davis, W. M. (1899) The Geographical Cycle. The Geographical Journal 14, 481-501.

Davis, W. M. (1906) The Sculpture of mountain glaciers. Scottish Geographical Journal 22, 76-89.

Davis, W. M. (1916) The Mission Range, Montana Geographical Review 2, 267-288.

De Mets, C., Gordon, R. G., Argus, D. F. & Stein, F. (1990) Current plate motions. Geophysical Journal 101, 425-478.

Derbyshire, E. & Evans, I. S. (1976). The climatic factor in cirque variation, In Geomorphology and Climate, edited by E. Derbyshire, pp. 447-494. London: Wiley.

Dietrich, R., Ivins, E. R., Casassa, G., Lange, H., Wendt, J. & Fritsche, M. (2010) Rapid crustal uplift in Patagonia due to enhanced ice loss. Earth and Planetary Science Letters 289, 22–29.

Doornkamp, J. C. & King, C. A. M. (1971). Numerical analysis in geomorphology: An introduction. London: Arnold.

Egholm, D. L., Nielsen, S. B., Pedersen, V. K. & Lesemann, J.-E. (2009) Glacial effects limiting mountain height. Nature 460, 884-888.

Ehlers, T. A. & Farley, K. A. (2003) Apatite (U-Th)/He thermochronometry: methods and applications to problems in tectonic and surface processes. Earth and Planetary Science Letters 206, 1-14.

Evans, I. S. (1972). General geomorphometry, derivatives of altitude, and descriptive statistics. In Spatial Analysis in Geomorphology, edited by R. J. Chorley, pp. 17-90. London: Methuen.

Evans, I. S. (1977) World-wide variations in the direction and concentration of cirque and glacier aspects. Geografiska Annaler 59, 151-175.

Fabel, D., Harbor, J., Dahms, D., James, A., Elmore, D., Horn, L., Daley, K. & Steele, C. (2004) Spatial patterns of glacial erosion at a valley scale derived from terrestial cosmogenic ^{10}Be and ^{26}Al concentrations in rock. Annals of the Association of American Geographers 94, 241-255.

Farr, T. G., Rosen, P. A., Caro, E., Crippen, R., Duren, R., Hensley, S., Kobrick, M., Paller, M., Rodriguez, E., Roth, L., Seal, D., Shaffer, S., Shimada, J., Umland, J., Werner, M., Oskin, M., Burbank, D. & Alsdorf, D. (2007) The Shuttle Radar Topography Mission. Rev. Geophys. 45, RG2004.

Flint, S. S., Prior, D. J., Agar, S. M. & Turner, P. (1994) Stratigraphic and structural evolution of the Tertiary Cosmelli basin and its relationship to the Chile triple junction. Journal of the Geological Society 151, 251–268.

Fortheringham, A. S., Brunsdon, C. & Charlton, M. (2002). Geographically weighted regression: the analysis of spatially varying relationships. Chichester: Wiley.

Fortheringham, A. S. & Zhan, F. B. (1996) A comparison of three explanatory methods for cluster detection in spatial point data. Geographical Analysis 28, 200-217.

Franzén, L. G. & Olvmo, M. (1991) Small Scale Glacial Erosion Forms and Their Possible Relation to Post-Glacial Weathering Geografiska Annaler. Series A, Physical Geography 73, 1-7.

Garcìa-Ruiz, J. M. & Martì-Bono, C. (1994). Rasgos fundamentales del glaciarismo cuaternario en el Pirineo aragonés. In El glaciarismo surpirenaico: Nuevas aportaciones, edited by C. Martì-Bono & J. M. Garcìa-Ruiz, pp. 17-32. Logroño: Geoforma Ediciones.

Ginot, P., Schwikowski, M., Schotterer, U., Stichler, W., Gaggeler, H. W., Francou, B., Gallaire, R. & Pouyaud, B. (2002) Potential for climate variability reconstruction from Andean glaciochemical records. Annals of Glaciology 35, 443-450.

Golledge, N. R., Mackintosh, A. N., Anderson, B. N., Buckley, K. M., Doughty, A. M., Barrell, D. J. A., Denton, G. H., Vandergoes, M. J., Andersan, B. G. & Schaefer, J. M. (2012) Last Glacial Maximum climate in New Zealand inferred from a modelled Southern Alps icefield. Quaternary Science Reviews 46, 30–45.

Graf, W. L. (1970) The geomorphology of the glacial valley cross section. Arctic and Alpine Research 2, 303-312.

Griffiths, G. A. & McSaveney, M. J. (1983) Distribution of mean annual precipitation across some steepland regions of New Zealand. New Zealand Journal of Science 26, 197-209.

Hack, J. T. (1960) Interpretation of erosional topography in humid temperate regions. American Journal of Science 258A, 80-97.

Hallet, B. (1979) A theoretical model of glacial abrasion. Journal of Glaciology 23, 39-50.

Hallet, B. (1981) Glacial abrasion and sliding: Their dependence on debris concentration in basal ice. Annals of Glaciology 2, 23-28.

Hallet, B. (1996) Glacial quarrying: a simple theoretical model. Annals of Glaciology 22, 1-8.

Hallet, B., Hunter, L. & Bogen, J. (1996) Rates of erosion and sediment evacuation by glaciers: A review of field data and their implications. Global and Planetary Change 12, 213-235.

Harbor, J. (1989) Early Discoverers XXXVI: W.J. McGee on glacial erosion laws and the development of glacial valleys. Journal of Glaciology 35, 419-425.

Harbor, J. & Warburton, J. (1993) Relative rates of glacial and nonglacial erosion in alpine environments. Arctic and Alpine Research 25, 1-7.

Harbor, J. M. (1992) Numerical modeling of the development of U-shaped valleys by glacial erosion. Geological Society of America 104, 1364-1375.

Haynes, V. M. (1968) The influence of glacial erosion and rock structure on corries in Scotland. Geografiska Annaler 50, 221-234.

Haynes, V. M. (1972) The relationship between the drainage areas and sizes of outlet troughs of the Sukkertoppen Ice Cap, West Greenland. Geografiska Annaler 54, 66-74.

Hervé, F., Pankhurst, R. J., Fanning, C. M., Calderón, M. & Yaxley, G. M. (2007) The South Patagonian batholith: 150 my of granite magmatism on a plate margin. Lithos 97, 373–394.

Hickley-Vargas, R. L., Moreno, H., Lopez-Escobar, L. & Frey, F. A. (1989) Geochemical variations in Andean basaltic and silicic lavas from Villarica-Lanin volcanic chain (39.5°S): an evaluation of source heterogeneity, fractional crystallization and crustal assimilation. Contributions to Mineralogy and Petrology 103, 361-386.

Hickley, R. L., Frey, F. A., Gerlach, D. C. & Lopez-Escobar, L. (1986) Multiple sources for basaltic arc rocks from the southern volcanic zone of the Andes (34°-41°S): trace element and isotopic evidence for contributions from subducted oceanic crust, mantle, and continental crust. Journal of Geophysical Research 91, 5963-5983.

Hicks, D. M., McSaveney, M. J. & Chinn, T. J. H. (1990) Sedimentation in proglacial Ivory Lake, Southern Alps, New Zealand. Arctic and Alpine Research 22, 26-42.

Hirano, M. & Aniya, M. (1988) A rational explanation of cross-profile morphology for glacial valleys and of glacial valley development. Earth Surface Processes and Landforms 13, 707-716.

Hoek, E. (1983) Strength of jointed rock masses. Géotechnique 33, 187-223.

Hoek, E. (1994) Strength of rock and rock masses. ISRM News Journal 2, 4-16.

Hoek, E. (2001). Rock Mass Properties for Underground Mines., In Underground mining methods: Engineering fundamentals and international case studies, edited by W. A. Hustrulid & R. L. Bullock, Litleton, Colorado: Society for Mining, Metallurgy and Exploration.

Hoek, E. & Brown, E. T. (1997) Practical estimates of rock mass strength. International Journal of Rock Mechanics and Mining Science 34, 1165-1186.

Hulton, N. R. J., Sugden, D. E., Payne, A. & Clapperton, C. M. (1994) Glacier modeling and the climate of Patagonia during the Last Glacial Maximum. Quaternary Research 42, 1-19.

Iverson, N. R. (1995). Processes of glacial erosion. In Modern glacial environments: Processes, dynamics and sediments, edited by J. Menzies, pp. 241-260. Oxford: Butterworth-Heinemann.

Iverson, N. R., Hooyer, T. S., Fischer, U. H., Cohen, D., Moore, P. L., Jackson, M., Lappegard, G. & Kohler, J. (2007) Soft-bed experiments beneath Engabreen, Norway: regelation infiltration, basal slip and bed deformation. Journal of Glaciology 53, 323-340.

James, L. A. (1996) Polynomial and power functions for glacial valley cross-section morphology. Earth Surface Processes and Landforms 21, 413-432.

Jamieson, S. S. R., Hulton, N. R. J. & Hagdorn, M. (2008) Modelling landscape evolution under ice sheets. Geomorphology 97, 91-108.

Jansson, M. (1985) A Comparison of Detransformed Logarithmic Regressions and Power Function Regressions. Geografiska Annaler. Series A, Physical Geography 67, 61-70.

Jenson, S. K. & Domingue, J. O. (1988) Extracting Topographic Structure from Digital Elevation Data for Geographical Information System Analysis. Photogrammetric Engineering and Remote Sensing 54, 1593-1600.

Johnson, A. M. (1970). Physical processes in geology : a method for interpretation of natural phenomena-intrusions in igneous rocks, fractures and folds, flow of debris and ice. San Francisco, California: Freeman, Cooper.

Kaeding, M., Forsythe, R. D. & Nelson, E. P. (1990) Geochemistry of the Taitao ophiolite and near-trench intrusions from the Chile Margin Triple Junction. Journal of South American Earth Sciences 3, 161–177.

Kamp, P. J. J. & Tippett, J. M. (1993) Dynamics of Pacific plate crust in the South Island (New Zealand) zone of oblique continent-continent collision. Journal of Geophysical Research 98, 105–116.

Kanasewich, E. R. (1963) Gravity measurements on the Athabaska glacier, Alberta, Canada. Journal of Glaciology 4, 617-631.

Kaplan, M. R., Fogwill, C. J., Sugden, D. E., Hulton, N. R. J., Kubik, P. W. & Freeman, S. (2008) Southern Patagonian and Southern Ocean climate during the last glacial period. Quaternary Science Reviews 27, 284–294.

Kaplan, M. R., Hein, A. S., Hubbard, A. & Lax, S. M. (2009) Can glacial erosion limit the extent of glaciation? Geomorphology 103, 172-179.

Kaplan, M. R., Hulton, N. R. J., Coronato, A., Rabassa, J. O., Stone, J. O., Kubik, P. W. & Freeman, S. (2007) Cosmogenic nuclide measurements in southernmost South America and implications for landscape change. Geomorphology 87, 284–301.

Kennan, L. (2000). Large-scale geomorphology of the Andes: interrelationships of tectonics, magmatism and climate, Vol. 167–199. In Geomorphology and Global Tectonics, edited by M. A. Summerfield, Chichester: Wiley.

King, L. C. (1953) Canons of landscape evolution. Geological Society of America Bulletin 64, 721-752.

Kirkbride, M. & Matthews, D. (1997) The role of fluvial and glacial erosion in landscape evolution: The Ben Ohau Range, New Zealand. Earth Surface Processes and Landforms 22, 317-327.

Knap, W. H., Oerlemans, J. & Cadee, M. (1996) Climate sensitivity of the ice cap of King George Island, South Shetland Islands, Antarctica. Annals of Glaciology 23, 154-159.

Kooi, H. & Beaumont, C. (1994) Escarpment evolution on high-elevation rifted margins: Insights derived from a surface processes model that combines diffusion, advection and reaction. Journal of Geophysical Research 99, 12191-12209.

Kooi, H. & Beaumont, C. (1996) Large-scale geomorphology: Classical concepts reconciled and integrated with contemporary ideas via a surface processes model. Journal of Geophysical Research 101, 3361-3386.

Kump, L. R., Brantley, S. L. & Arthur, M. A. (2000) Chemical, weathering, atmospheric CO2, and climate. Annual Review of Earth and Planetary Sciences 28, 611-667.

Kutzbach, J. E., Prell, W. L. & Ruddiman, W. F. (1993) Sensitivity of Eurasian climate to surface uplift of the Tibetan Plateau. The Journal of Geology 101, 177-190.

Leathwick, J. R., Wilson, G. & Stephens, R. T. T. (2002) Climate Surfaces of New Zealand. Landcare Research: Hamilton, New Zealand.

Legates, D. R. & Willmott, C. J. (1990) Mean seasonal and spatial variability in gauge-corrected, global precipitation International. Journal of Climatology 10, 111-127.

Li, Y., Liu, G. & Cui, Z. (2001a) Glacial valley cross-profile morphology, Tian Shan Mountains, China. Geomorphology 38, 153-166.

Li, Y., Liu, G. & Cui, Z. (2001b) Longitudinal variations in cross-section morpholohy along a glacial valley: a case-study from the Tian Shan, China. Journal of Glaciology 47, 243-250.

Lòpez-Morneo, J. I. & Beniston, M. (2009) Daily precipitation intensity projected for the 21st century: seasonal changes over the Pyrenees. Theoretical and Applied Climatology 95, 375-384.

MacGregor, K. R., Anderson, R. S., Anderson, S. P. & Waddington, E. D. (2000) Numerical simulations of glacial-valley longitudinal profile evolution. Geology 28, 1031-1034.

Manabe, S. & Terpstra, T. B. (1974) Effects of mountain on general circulation of atmosphere as identified by numerical experiments. Journal of the Atmospheric Sciences 31, 3-42.

Mangeney, A. & Califano, F. (1998) The shallow ice approximation for anisotropic ice: Formulation and limits. Journal of Geophysical Research 103, 691-705.

Martz, L. W. & Garbecht, J. (1992) Numerical definition of drainage network and the sub-catchment areas from digital elevation models. Computers & Geosciences 18, 747-761.

McCall, J. G. (1960). The flow characteristics of a cirque glacier and their effect on glacier structure and cirque formation. In Norwegian Cirque Glaciers. R.G.S Research Series. No. 4., edited by W. V. Lewis.

McGee, W. J. (1883) Glacial canons. Science 2, 315-316.

McGee, W. J. (1894) Glacial canons. Journal of Geology 2, 350-364.

Miller, A. (1976). The climate of Chile, In World survey of climatology, Vol. 12, Climates of Central Chile and South America, edited by W. Schwerdtferger, pp. 113-145. Amsterdam: Elsevier.

Mix, A. C., Bard, E. & Schneider, R. (2001) Environmental processes of the ice age: land, oceans, glaciers (EPILOG). Quaternary Science Reviews 20, 627–657.

Molnar, P. & England, P. (1990) Late Cenozoic uplift of mountain ranges and global climate change: chicken or egg? Nature 346, 29-34.

Montgomery, D. R. (2002) Valley formation by fluvial and glacial erosion. Geology 30, 1047-1050.

Moon, B. P. (1984) Refinement of a technique for determining rock mass strength for geomorphological purposes. Earth Surface Processes and Landforms 9, 189-193.

Moores, E. & Twiss, R. J. (1995). Tectonics. New York: W.H. Freeman.

Morisawa, M. E. (1968). Streams: Their dynamics and morphology. New York: McGraw-Hill.

Napieralski, J., Harbor, J. & Li, Y. (2007) Glacial geomorphology and geographic information systems. Earth-Science Reviews 85, 1-22.

Naylor, S. & Gabet, E. J. (2007) Valley asymmetry and glacial versus nonglacial erosion in the Bitteroot Range, Montana, USA. Geology 35, 375-378.

Nelson, E. P. (1982) Post-tectonic uplift of the Cordillera de Darwin orogenic core complex: evidence for fission track geochronology and closing temperature–time relationship Journal of the Geological Society 130, 755–762.

Neukom, R., Luterbacher, J., Villalba, R., Küttel, M., Frank, D., Jones, P. D., Grosjean, M., Esper, J., Lopez, L. & Wanner, H. (2010) Multi-centennial summer and winter precipitation variability in southern South America. Geophysical Research Letters 37, 1-6.

Nye, J. F. & Martin, P. C. S. (1967) Glacial erosion. International Association of Hydrological Sciences Publication 79, 78-85.

Oerlemans, J. (1989) A projection of future sea level. Climatic Change 15, 151-174.

Oskin, M. & Burbank, D. W. (2005) Alpine landscape evolution dominated by cirque retreat. Geological Society of America 33, 933-936.

Pallàs, R., Rhodés, Á., Braucher, R., Bourlès, D., Delmas, M., Calvet, M. & Gunnell, Y. (2010) Small, isolated glacial catchments as priority targets for cosmogenic surface exposure dating of Pleistocene climate fluctuations, southeastern Pyrenees. Geology 38, 891-894.

Paterson, W. S. B. (1994). The Physics of Glaciers, 3rd ed. Oxford: Elesevier Science Ltd.

Pattyn, F. & Decleir, H. (1995) Subglacial topography in the Central Sør Rondane Mountains, East Antarctica: Configuration and morphometric analysis of valley cross profiles. Antarctic Record 39, 1-24.

Pattyn, F. & Van Huele, W. (1998) Power law or power flaw? Earth Surface Processes and Landforms 23, 761-767.

Penck, W. (1972). Morphological analysis of land forms, a contribution to physical geography. New York: Hafner.

Phillips, A. (2009) Development of geomorphologically significant measures of landform. Thesis, University of Sheffield.

Pillans, B. (1986) A late Quaternary uplift map for North Island, New Zealand The Royal Society of New Zealand bulletin 24, 409–417.

Porter, S. C. (1975) Glaciation Limit in New Zealand's Southern Alps. Arctic and Alpine Research 7, 33-37.

Porter, S. C. (1989) Some geological implications of average Quaternary glacial conditions. Quaternary Research 32, 245-261.

Ramos, V. A. (1989) Foothills structure in Northern Magallanes Basin, Argentina. American Association Petroleum Geologists Bulletin 73, 887–903.

Rapalini, A. E., López de Luchi, M., Croce, F., Lince Klinger, F., Tomezzoli, R. & Gímenez, M. (2008). *5° Simposio Argentino del Paleozoico Superior, Resúmenes*, p. 34. Buenos Aires

Reynaud, L. (1973) Flow of a valley glacier with a solid friction law. Journal of Glaciology 12, 251-258.

Riveria, A., Benham, T., Casassa, G., Bamber, J. & Dowdeswell, J. (2007) Ice elevation and areal changes of glaciers from the Northern Patagonia Icefield Chilean. Global Planetary Change 59, 126–137.

Roberts, M. C. & Rood, K. M. (1984) The Role of the ice contributing area in the morphology of transverse fjords, British Columbia. Geografiska Annaler. Series A, Physical Geography. 66, 381-393.

Röthlisberger, H. & Iken, A. (1981) Plucking as an effect of water-pressure variations at the glacier bed. Annals of Glaciology 2, 57-62.

Schellart, W. (2002) Alpine deformation at the western termination of the Axial Zone, Southern Pyrenees. Journal of the Virtual Explorer 8, 35-55.

Schlunegger, F. & Hinderer, M. (2001) Crustal uplift in the Alps: why the drainage pattern matters. Terra Nova 13, 425-432.

Seddik, H., Greve, R., Sugiyama, S. & Naruse, R. (2009) Numerical simulation of the evolution of glacial valley cross sections. eprint arXiv:0901.1177

Seddik, H., Sugiyama, S. & Naruse, R. (2005) Numerical simulation of glacial-valley cross-section evolution. Bulletin of Glaciological Research 22, 75-79.

Selby, M. J. (1980) A rock mass strength classification for geomorphic purposes: with tests from Antarctica and New Zealand. Zeitschrift für Geomorphologie 26, 1-15.

Serrat, D. & Ventura, A. (1993) Glaciers of the Pyrenees, Spain and France. U.S. Geological Survey Professional, 1386, 49-61.

Shoemaker, E. M. (1986) The formation of fjord thresholds. Journal of Glaciology 32, 65-71.

Silverman, B. W. (1986). Density estimation for statistics and data analysis. London: Chapman and Hall.

Small, E. E. & Anderson, R. S. (1998) Pleistocene relief production in Laramide mountain ranges, western United States. Geology 26, 123-126.

Stern, C. H. R., Frey, F. A., Zartman, R. E., Peng, Z. & Kyser, T. K. (1990) Trace element and Sr, Nd, Pb and O isotopic composition of Pliocene and Quaternary alkalic basalts of the Patagonian Plateau lavas of southernmost South America. Contributions to Mineralogy and Petrology 104, 94–308.

Stern, C. H. R., Futa, K., Saul, S. & Skewes, M. A. (1986) Nature and evolution of the subcontinental mantle lithosphere below southern South America and implications for Andean magma genesis. Reviews of Geology Chile 27, 41-53.

Stern, C. H. R. & Kilian, R. (1996) Role of the subducted slab, mantle wedge and continental crust in the generation of adakites from the Andean Austral Volcanic Zone. Contributions to Mineralogy and Petrology 123, 263-281.

Stock, J. & Molnar, P. (1982) Uncertainties in the relative positions of the Australia, Antarctica, Lord Howe, and Pacific plates since the late Cretaceous Journal of Geophysical Research 87, 4697–4714.

Sugden, D. E., Glasser, N. & Clapperton, C. M. (1992) Evolution of Large Roches Moutonnees Geografiska Annaler. Series A, Physical Geography 74, 253-264.

Sugden, D. E. & John, B. S. (1976). Glaciers and Landscape. London: Arnold.

Suggate, R. P. (2004). South Island, New Zealand; ice advances and marine shorelines., In Quaternary Glaciations - Extent and Chronology. Part III: South America, Asia, Africa, Australasia, Antarctica, edited by J. Ehlers & P. L. Gibbard, London: Elsevier.

Sutherland, R. (1995) The Australia–Pacific boundary and Cenozoic plate motions in the southwest Pacific: some constraints from GEOSAT data. Tectonics 14, 819–831.

Sutherland, R. (1996) Magnetic anomalies in the New Zealand region, 1 : 4,000,000 Institute of Geological and Nuclear Sciences, Lower Hutt, Geophysical Map 9.

Svensson, H. (1959) Is the cross section of a glacial valley a parabola? Journal of Glaciology 3, 362 - 363.

Swift, D. A., Persano, C., Stuart, F. M., Gallagher, K. & Whitham, A. (2008) A reassessment of the role of ice sheet glaciation in the long-term evolution of the East Greenland fjord region. Geomorphology 97, 109-125.

Taillefer, F. (1969). *Études franc-aises sur le Quaternaire presentées à l'occasion du VIIIe Congrés International de l'INQUA*, pp. 19-32. Paris

Tarboton, D. G. (1997) A new method for the determination of flow directions and contributing areas in grid digital elevation models. Water Resource Research 33, 309-319.

Tarboton, D. G., Bras, R. L. & Rodriguez-Iturbe, I. (1991) On the extraction of channel networks from digital elevation data. Hydrological processes 5, 81-100.

Thomson, S. N., Hervé, F. & Stöckhert, B. (2001) Mesozoic–Cenozoic denudation history of the Patagonian Andes (southern Chile) and its correlation to different subduction processes Tectonics 20, 693–711.

Tippett, J. M. & Hovius, N. (2000). Geodynamic processes in the Southern Alps, New Zealand, In Geomorphology and Global Tectonics, edited by M. A. Summerfield, pp. 109–134. Chichester: Wiley.

Tippett, J. M. & Kamp, P. J. J. (1993) The role of faulting in rock uplift in the Southern Alps, New Zealand. New Zealand Journal of Geology and Geophysics 36, 497—504.

Tomkin, J. H. (2009) Numerically simulating alpine landscapes: The geomorphic consequences of incorporating glacial erosion in surface process models. Geomorphology 103, 180-188.

Tomkin, J. H. & Braun, J. (1999) Simple models of drainage reorganisation on a tectonically active ridge system New Zealand Journal of Geology and Geophysics 42, 1-10.

Tomkin, J. H. & Braun, J. (2002) The influence of alpine glaciation on the relief of tectonically active mountain belts. American Journal of Science 302, 169-190.

Tucker, G. E. & Slingerland, R. (1996) Predicting sediment flux from fold and trust belts. Basin Research 8, 329-349.

Vogt, E. V., Colombo, R. & Bertolo, F. (2003) Deriving drainage networks and catchment boundaries: a new methodology combining digital elevation data and environmental characteristics. Geomorphology 53, 281-298.

Wellman, H. W. (1979) An uplift map for the South Island of New Zealand and a model for uplift of the Southern Alps The Royal Society of New Zealand bulletin 18, 13-20.

Wheeler, D. A. (1984) Using parabolas to describe the cross-sections of glaciated valleys. Earth Surface Processes and Landforms 9, 391-394.

Whipple, K. X. & Tucker, G. E. (1999) Dynamics of the stream-power river incision model: Implications for height limits of mountain ranges, landscape response timescales, and research needs. Journal of Geophysical Research 104, 17661-17674.

Winslow, M. A. (1981). Mechanisms for basement shortening in the Andean foreland fold belt of southern South America, Vol. 9, In Thrust and Nappe Tectonics, edited by K. R. McClay & N. J. Price, pp. 513–528. London: Geological Society Special Publication

Wohl, E. & Legleiter, C. L. (2003) Controls on pool characteristics along a resistant-boundary channel. The Journal of Geology 111, 103-114.